Managing the twilight

A comprehensive forecast and analysis of PV End of Life at a Global, Regional and National scale

Luca Allione

TU Delft

Managing the twilight

A comprehensive forecast and analysis of PV End of Life at a Global, Regional and National scale

by

Luca Allione

Project Duration:	December, 2023 - July, 2024
Faculty:	EEMCS

TU Delft

Abstract

The rapid adoption of photovoltaics (PV) is crucial for meeting global climate goals, yet it presents significant challenges related to PV waste management. This research aims to project PV end-of-life (EoL) streams globally, regionally, and nationally, with some focus on the effects that an aging PV fleet will have on demand for PV modules. Utilizing the PV ICE software developed by NREL, this study models the degradation, failure, and EoL processes of PV modules, accounting for new installation rates and technological advancements. The methodology involves three key components: PV capacity installation forecasts, module technology characteristics, and EoL determination. Historical and projected PV installation data were sourced from IRENA, IEA, and LUT University. These data were interpolated and modeled using polynomial and sigmoid functions to predict capacity growth. Module aging was simulated through degradation rates, random failures modeled by Weibull distribution, and economic lifetimes. The PV ICE tool facilitated these simulations, converting capacity forecasts into material flows, from installation to removal.

Global PV EoL volumes are expected to increase significantly starting from 2040, reaching 42 million tons of cumulative material by 2050, and potentially surging to 432 million tons in the low scenario and 1 billion tons in the high scenario by 2070. Simultaneously, the PV market will see increased demand, with projections indicating a 62% rise in the low scenario (from 14.7 TW to 23.8 TW) and a 28% rise in the high scenario (from 95.8 TW to 122.8 TW). Regionally, Asia & Oceania is the region forecasted to generate the most EoL material, with 274 million tons in the low scenario and 539 million tons in the high scenario by 2070. Europe and North America will also see significant volumes, with Europe reaching 57 million tons and North America 65 million tons in the low scenario, rising to 141 million tons and 107 million tons, respectively, in the high scenario. The high scenario also forecasts Africa to become the secondary global hub for PV EoL volumes and for demand of new modules. Nationally, China is projected to accumulate the largest volume of EoL material, with 197 million tons by 2070, followed by the USA (49 million tons) and India (33 million tons).

The findings highlight a substantial increase in PV waste volumes, necessitating the development of large-scale recycling infrastructure, Regional and national disparities underscore the need for specific and potentially collaborative waste management strategies. The impact of modules reaching End of Life not only emphasizes the need for the development of effective collection and recycling policies but will also allow the solar manufacturing industry to keep producing at high output levels. The industry in fact will need to scale up considerably in the next few decades and modules intended for the replacement of aging capacity will allow for continuous production, enabling investments in manufacturing capacity fundamental for the global energy present and future.

Acknowledgments

This work is the culmination of my studies at the Technical University of Delft. The path has not always been easy, but it has always been inspiring and a source of real personal growth.

First, I would like to sincerely thank my TU Delft supervisor, Malte Vogt, for always being able to dedicate his time to me, giving never banal feedback, i would like to thank him for his ability to push me to always do better in the university and in private life. I can really feel the passion and dedication that Malte puts in his work, something I admire. I would like to thank Silvana Ovaitt and Garvin Heath, the two experts from NREL that followed and guided me through this project, thanks for your time and insight, being able to work with you taught me a lot about how to handle hard tasks, influencing significantly to my personal and professional growth.

I would like to thank all the friends I made in these two years, with you I was able to share experiences, dreams, and fears; these two years were very intense inside the university walls. but all the fun had outside of them makes it look like nothing in comparison. These two years I spent almost every day with some of you, building a second family that supported and pushed me to become a better student and person. Even if our futures might take us apart, the memories we made will never be erased.

Finally I would like to thank my mum, my dad, my brother, and my two amazing grandmas; without the support and reassurance that you always gave me everything would have been much harder. Grazie per aver sempre creduto in me.

Luca Allione Delft 4-7-2024

Contents

List of Figures

List of Tables

1 Introduction

The adoption of photovoltaics (PV) is happening at a pace that few could have anticipated. This incredible development, key to humanity's race towards its climate goals, introduces an obvious but easy to forget issue: PV waste. The risks and opportunities of this novel challenge are unclear and still rather far in the future. Mass deployment of PV has, by no means, reached its maximum potential. As of 2024, the global deployed capacity was 1.5 TWp with an annual installation rate of about 380 GW/year, these numbers are projected to grow to about 500-1000 GW/year by 2030 and stabilize at a total installed capacity of around 16-75TW by 2050 [2] [3] [4]. Considering different authors and scenarios, installed PV capacity might stabilize by 2060, with new installations being balanced out by modules entering the waste cycle [4]. Other scenarios project that energy demand and PV installations will continue to grow well beyond 2050 [5], while some papers limit their scope and predictions to 2050 [6]. Regardless of different models and assumptions, given the timeline at which PV modules are being deployed and their lifetime of around 30 years, the management of decommissioned PV modules will become a more tangible issue by the second part of the century. Nevertheless, significant analysis and investments need to be made well before then to ensure a smooth transition to effective recycling and disposal processes [7].

Before analyzing opportunities and risks related to PV waste material, the scale, regional implications, and foreseen technological advancements need to be assessed and understood. Before beginning with a deeper analysis and forecast, is necessary to point out that making predictions is always risky, especially when referring to such fast-changing technologies. Still, it is essential to prepare and be aware by envisioning the policies, resources, and technologies necessary once the problem presents itself.

This research aims to develop updated global, regional and national projections of PV End of Life (EoL) mass streams, underlying the materials that can be obtained from decommissioned modules undergoing recycling, and the impacts that this could have. This research in fact will try to analyze the impact that an aging fleet of PV will have on waste volumes, but also on new demand, given that lost photovoltaic capacity will have to be replaced once lost.

This work leverages *PV ICE*, a Python-based open-source software developed at the National Renewable Energy Laboratory (NREL), which facilitates the modelling of mass flows in the photovoltaic industry. Given PV development projections, degradation rates, and other technology-dependent inputs, the software models the aging and failure processes of modules, determining the amount of panels reaching their End of Life each year and the resulting waste material flow.

Chapter 2 provides an overview of the current literature perspective, focusing on four main topics. Section 2.1 delves into PV installation forecasts at national and regional levels. Section 2.2 discusses the current state and evolution of PV technology. Section 2.3 offers an overview of the current state of PV waste, circularity, and materials. Finally, section 2.4 examines PV reliability, failure, and degradation due to environmental influences.

Chapter 3 outlines the methodology followed in modeling PV installations and End of Life processes.
Chapter 4 provides results at the global level. This chapter presents the expected waste volumes from photovoltaics before 2070 for a high and a low installation scenario. The chapter also investigates the reasons why

modules will reach the end of their operational lifetime and the implications to global PV markets that this will have. This chapter, other that confronting ts results with previous literature, also introduces two additional scenarios to the baseline results: a scenario on degradation and a scenario on the use extension of modules past their project lifetime (merchant tail), and a scenario on reduced reliability of modules.

Chapter 5 presents the results obtained at the regional level, confronting different regions, such as Europe and North America, to understand the evolution of PV end of life in different regions of the globe. This analysis will also be presented for one high and one low installation scenarios and will try to understand, other than the region-specific levels of end of life material and their evolution, how these volumes compare among different regions and with other sources of waste.

Finally chapter 6 details the results found for some selected nations. These include cumulative and annual End of Life flows, together with the expected demand of photovoltaics in the future, understanding the impact that lost capacity will have on national PV demand. For the different countries, the economical impact of recycling will be also analyzed, understanding if and when different countries should start domestic PV recycling plants, together with the expected profits of such operations.

2
Literature review

Photovoltaics is among the most revolutionary industries of our time. It has reached the threshold of 1 TWp installed in late 2022 and at the beginning of 2024 the total cumulative installed capacity reached 1.5 TWp [8]. In 2014, only 10 years before, the total installed capacity was of 180 GWp; a growth of 730% in installed capacity in a decade [9]. Given the enormous change and the rapid pace at which this is happening, it is fundamental to stay updated on the latest version of every paper and report that predicts the future of the industry.
To introduce the main body of this work, four aspects were researched in the literature:

- **Installation projections:** How much PV power will be deployed from now to 2050? How will it be divided by country and region?
- **Technology and trends:** What is a PV panel today and how will it change? How will the material usage change?
- **End of Life and circularity:** What is the current understanding of circularity and recyclability of PV? Is there any value in pursuing recycling in photovoltaics?
- **Failure, degradation, and reliability:** When does a PV panel enter its End Of Life? What influences it?

2.1. PV installation projections

Many research centers and institutions published predicions the future of PV, regarding its technological evolution and penetration into tomorrow's energy landscape. The findings often differ quite significantly, installation forecast to 2050 vary in recent literature from 9 TWp [3] to 117 TWp [5]. Later in this research the difference between these numbers will be analyzed.
This section presents three updated projections from some of the most regarded institutions. Forecasts from the International Energy Agency (IEA), the International Renewable Energy Agency(IRENA), and LUT University will be shown and discussed in this section.

2.1.1. International Energy Agency, IEA

The IEA has a yearly release on the current trend and future forecast for renewables and fossil energy, called the World Energy Outlook [2]. In this report, three different scenarios for the evolution of the energy mix are presented. The **Stated Policies Scenario**, **STEPS** is based on current policy settings and considers the implications of industrial policies that support clean energy supply chains as well as measures related to energy and climate. The **Announced Pledges Scenario, APS** gives governments the *benefit of the doubt* and explores what the full and timely implementation of national energy and climate goals, including net zero emissions targets, would mean for the energy sector. The **Net Zero Emissions by 2050 Scenario**, **NZE** maps out a transition pathway that would limit global warming to 1.5 °C.

Methodology

The IEA uses a *hybrid modeling approach*, a combination between the *World Energy Model* (WEM) – a large-scale simulation model designed to replicate how energy markets function and the *Energy Technology Perspectives model* (ETP) – a technology-rich bottom-up model. This model is called *Global Energy and Climate model*

	2030			2050		
	STEPS	**APS**	**NZE**	**STEPS**	**APS**	**NZE**
Total Final Consumption (of which electricity)	402 EJ (108 EJ)	451 EJ (109 EJ)	406 EJ (113 EJ)	536 EJ (159 EJ)	429 EJ (176 EJ)	343 EJ (183 EJ)
Yearly PV yield	19 EJ	23 EJ	29 EJ	62 EJ	87 EJ	112 EJ
Cumulative PV capacity	4.70 TWp	5.38 TWp	6.10 TWp	12.64 TWp	16.04 TWp	18.75 TWp
Yearly PV installations	0.50 TWp	0.64 TWp	0.82 TWp	0.58 TWp	0.77 TWp	0.82 TWp

Table 2.1: IEA World Energy Outlook 2023 Global PV forecast

(GEC) and is now the principal tool used to generate detailed sector-by-sector and region-by-region long-term scenarios across IEA publications. The model is fully private and its data or assumptions can't be accessed. The model is primarily based on the idea of finding the solution that is more economically viable for each of the 29 regions considered. It is explained that: *while the model aims to identify an economical way for society to reach the desired scenario outcomes, the results do not necessarily reflect the least-cost way of doing so. This is because an unconstrained least-cost approach may fail to take account of all the issues that need to be considered in practice, such as political or individual preferences, feasible ramp-up rates, capital constraints and public acceptance*[10].

PV forecast

On a global scale, the IEA forecasts the numbers seen in table 2.1 for its three scenarios.
It is interesting to note that in the Net Zero Emissions scenario, global energy demand is the lowest. This is due to higher energy efficiency brought by a greater electrification of the energy mix. In such an electrified energy mix, PV will have much more space to grow, producing about 62% of the total electricity and 32% of the total energy demand. It is easy to see that these numbers are much lower than the ones described in the introduction. In subsection 2.1.4 these discrepancies are considered and explained. The report also gives installation forecasts for some selected countries and regions, the details on these figures can be seen in the respective chapters; chapter 5 for the regional forecast and chapter 6 for the national ones.

2.1.2. International Renewable Energy Agency, IRENA

IRENA publishes a similar report to the one released by the IEA, called World Energy *Transitions* Outlook [3]. The report, according to the official description, provides an overview of progress by tracking implementation and gaps across all energy sectors, identifying priority areas and actions based on available technologies. The focus of the report is, also, outlining the steps needed to take to achieve carbon neutrality and the 1.5° goal. In this report two scenarios are presented, the **1.5° Scenario** (limiting global warming to 1.5°C by 2050), and the **Planned Energy Scenario**, **PES** based on current countries plans and ideas for the future of the energy mix. No methodology for the modeling process is provided by IRENA, nor a dataset is presented in correlation to the report.

PV Forecast

For its two scenarios, IRENA forecasts the figures that can be seen in table 2.2

	2030		2050	
	PES	**1.5°**	**PES**	**1.5°**
Total Final Energy Consumption (of which electricity)	-	370 EJ (170 EJ)	-	353 EJ (180 EJ)
Yearly PV yield	15 EJ	30 EJ	49 EJ	109 EJ
Cumulative PV installed	3.10 TWp	5.47 TWp	8.66 TWp	18.20 TWp
Yearly PV installations	-	0.55 TWp	-	0.62 TWp

Table 2.2: IRENA World Energy Transitions Outlook 2023 Global PV forecast

The numbers provided by IRENA are in line with the ones from the IEA. The scale of PV installations is similar to the one proposed by the IEA, just like the yearly installations of PV. The Total Final Energy Consumption (TFEC) and its share of electricity are comparable with the results in section subsection 2.1.1. The trend of lower energy consumption with a greater share of electricity is confirmed in this study as well. The discrepancies with the numbers presented in the introduction are treated in subsection 2.1.4.

	2030			2050		
	LEES	**DEES**	**EEES**	**LEES**	**DEES**	**EEES**
TFEC (of which electricity)	543 EJ (330 EJ)	565 EJ (347 EJ)	586 EJ (364 EJ)	585 EJ (546 EJ)	677 EJ (660 EJ)	813 EJ (833 EJ)
Yearly PV yield	182 EJ	192 EJ	202 EJ	430 EJ	526 EJ	676 EJ
Cumulative PV installed	31.83 TWp	33.54 TWp	33.25 TWp	75.43 TWp	91.99 TWp	117.45 TWp
Yearly PV installations	5.49 TWp	6.05 TWp	6.69 TWp	1.27 TWp	2.06 TWp	3.37 TWp

Table 2.3: LUT-Demand Global PV forecast, TFEC indicates Total Final Energy Consumption

2.1.3. LUT university

LUT University *(Lappeenranta-Lahti University of Technology)* is a Finnish technological university that has risen to international fame in the PV world for its numerous studies in energy systems forecasting, both at a global and regional/national level. The group led by professor Christian Breyer published more than 200 papers describing scenarios and possibilities for countries and regions to reach a fully sustainable energy system.

Methodology

The software used by the group is *"LUT Demand"*, an open-source model able to predict the energy demand of the future. Based on baselines and inputs, the model assumes the future energy demand and mix based on population and economic growth. The main assumption of the scenarios is that countries will eventually reach a shared economic condition, with every country having the same GDP per capita. In particular, three scenarios were proposed. The Early Economic Equality Scenario (EEES), the Delay Economic Equality Scenario (DEES), and the Late Economic Equality Scenario (LEES). The three scenarios assume, respectively, equality by 2100, 2175, and 2300. The software allows for modeling up to 2100. LUT-Deamand has been regarded as one of the best energy systems models in multiple studies [11, 12] for its precision and high temporal definition. After outlining the energy demand for the coming years, the model calculates what mix of sustainable energy sources could suit better the specific characteristics of each world region and country. With the constraint of keeping emissions in line with the 1.5°C scenario, the software then outputs the cost-optimal energy mix for every country/region and the pathway from today's situation. The model is fully open-source.

PV Forecast

From the research of LUT University, the data in table 2.3 can be extracted.
The data presented is considerably higher than the projections of IRENA and the IEA. Firstly, the Total Final Energy Consumption (TFEC) proposed by LUT University is more than double the previously shown numbers. Greater demand coincides with greater electricity needs. This study models differently the electrification rates as well. While the IEA and IRENA foresee that electricity will account for around 30% of total energy in 2030, and for slightly more than 50% in 2050, LUT University foresees an energy demand made of 64% by electricity in 2030 and 96% of electricity in 2050. PV installation numbers vary greatly as well. According to LUT University in 2030 global installed PV capacity will surpass the 30 TWp mark, to then grow to 75-117 TWp by 2050. The growth numbers are remarkable as well. According to the model, PV installations will ramp up greatly already before 2030, to then slow down before 2050. The model predicts 5.8 TWp in 2025 and 33.5 TWp in 2030, almost 28 TWp of capacity in only 5 years! In the discussion of this section, these numbers will be analyzed with the previously exposed results.

2.1.4. Discordant Outlooks, discussion of PV projections in literature

Understanding the nature of these conflicting projections is necessary to build a baseline projection for the model. Luckily this issue has already received attention in literature. Plenty of publications have expressed doubts and criticisms towards models that foresee low shares of PV in the future energy mix [4, 13, 14, 15, 16, 17, 18]. In particular, Haegel et al. [4] and Breyer et al. [13, 14] will be further explained and analyzed in this section. Nancy Haegel, director of the Materials Science Centre at NREL, coauthored by many leading figures of the photovoltaic industry [4], supports the projection of 75 TWp installed by 2050. The authors stress how recognizing too late the authentic scale of PV demand would mean needing to ramp up manufacturing and deployment to unrealistic and unsustainable levels. This could potentially jeopardize the chances of completing the energy transition [19, 20]. Haegel also adds that PV is a "no regret" option and does not see why this technology is sometimes not considered the best solution in projection papers even if it is the cheapest and risk-free energy solution. Both authors express a common doubt about the figures reported in the IEA and IRENA projections: the global south. These

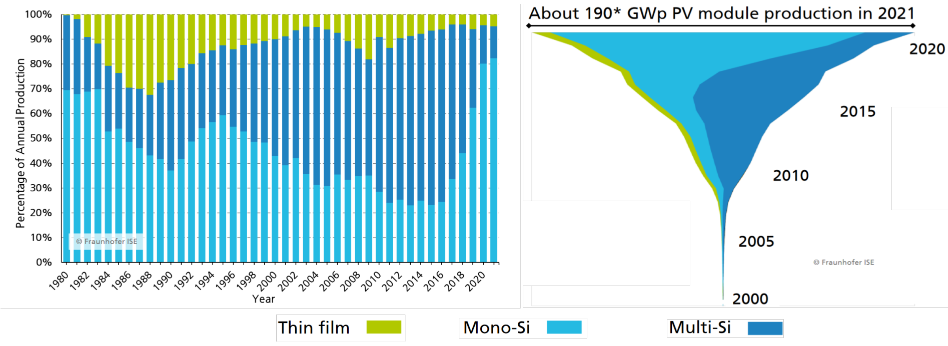

Figure 2.1: Market share and absolute installation comparison of Si-based and thin film PVs [26], the share of thin film gas been reducing, while mono-si is taking more than 80% of the marketshare.

more conservative projections seemingly imply low demographic and economic growth in those countries, today characterized by low energy per capita consumption. If they were to grow to levels similar or even comparable to the ones of Europe and North America, worldwide energy demand would skyrocket, a scenario not considered by conservative publications. Another point that both authors bring forward is cost assumptions for energy sources. Distorted cost projections for PV and its competing technologies play a fundamental role in the definition of the future energy mix. Conservative projections from the IEA and IRENA, frequently cited alongside the IPCC report [21], have faced criticism for employing too pessimistic, if not unrealistic, cost projection assumptions regarding photovoltaics and over-optimistic assumptions for technologies that today show no path towards lower prices, such as fossil Carbon Capture and Storage (CCS), nuclear and hydrogen. The rapid growth projected for these latter technologies, and the consequent believed price reduction, still needs to be realized. Conservative PV forecasts often disregard PV in favor of more expensive solutions altogether, citing regional-specific reasons for this decision. Breyer highlights that even if these higher-cost solutions might be justified, it is fundamental that these assumptions are made public and transparent, to ensure a smooth and realistic path towards a 100% renewable energy system.

2.2. PV technology and trends

To understand what to expect from the End of Life mass flows of PV, it is needed to know what elements and materials make a solar panel, what they used to be, and what the the industry thinks they will become. The feasibility and potential success of recycling heavily relies on the technological evolution of PV modules. A 2022 paper by Ovait et al. [22] explains how most existing studies on EoL waste flows don't capture the non-linear evolution of PV technologies and fail to foresee improvements in material efficiency and circularity, focusing instead on waste projections for one static module. Of particular interest in photovoltaics, as in many other renewable energy technologies, is the focus on critical materials; elements whose availability in today's known reserves does not align with the demand expected in a future characterized by multi-terawatt annual installations. In this section, the past present, and future of PV modules are presented.

2.2.1. The evolution of PV, from the '50s to today

PV technology was introduced in the 1950s, shortly after the first semiconductor diode was produced. From the beginning, silicon emerged as the chosen semiconductor for this technology; the first efficiency recorded from PV cells was 6%. In the 60s the industry introduced the product that started the deployment of PV as we know it today: the Aluminum Back Surface Field (Al-BSF). This technology used either mono or polycrystalline silicon cells and was initially employed in space applications. In the 80's the solar industry took a very important step towards mass production with the introduction of the Spectrola Block II cells and modules [23, 24]. At the end of the 80's another photovoltaic technology started taking a relevant part of the market share: thin film photovoltaics. These are semiconductor materials with significantly higher absorption coefficients that can be made into a photovoltaic device in only a few nanometers of thickness. Even if these modules are flexible, light, and easy to deploy, their penetration in the photovoltaic industry has been marginal and relegated to specific uses as can be seen in figure 2.1. While this is the case today, the share of thin films is expected to grow in the future, thanks to applications such as microelectronics, building integrated PV and floating PV [25].

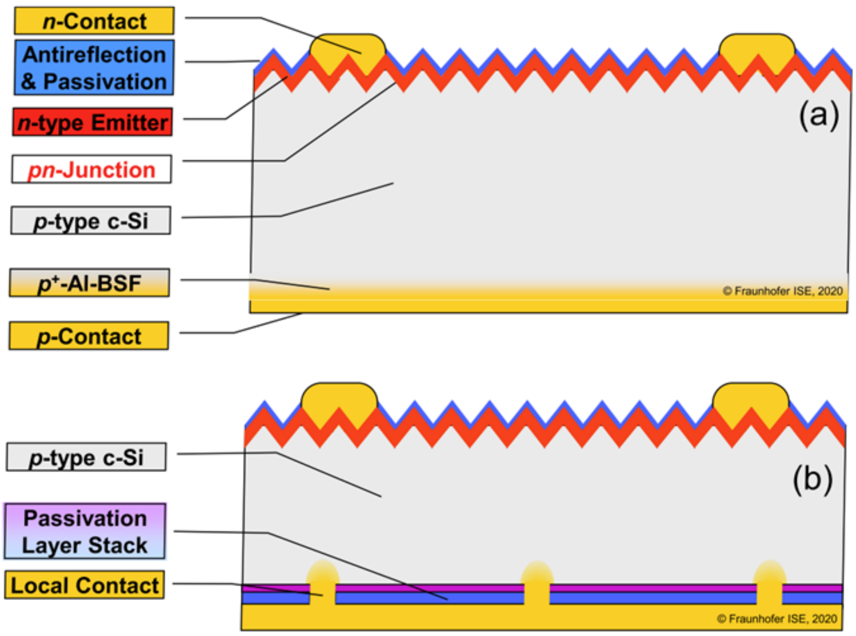

Figure 2.2: Al-BSF(a) and PERC(b) cells cross sections [23]. The two cell designs are very similar, allowing for an easy transformation of production lines.

Silicon technology in the form of Al-BSF dominated the market until the mid-2010s when progress over its efficiency plateaued, opening the way for new technologies. The Passivated Emitter and Rear Cell or PERC technology was came up as the natural evolution of Al-BSF and started gaining more and more marketshare. This cell technology required only two additional steps in the already well-known manufacturing line of Al-BSF and even if other technologies already looked promising, the similarity between Al-BSF and PERC, as can be seen in figure 2.2, allowed PERC to take over the industry. In 1999 a record PERC cell was built with an efficiency of 25.0%, while the best Al-BSF cell ever made, in 2017, could only reach 20.3% [23, 27]. PERC can be defined as the workhorse of the PV industry, its technology allowed for the explosion of photovoltaics as we know them today. In the decade between 2010 and 2020 the photovoltaic industry went through significant changes; manufacturing cost decreased at a rate of roughly 15% a year, with a yearly efficiency improvement of 2%. The cost of producing photovoltaics dropped by about 30% for every doubling of cumulative production [23]. As of 2024 PERC modules represent the vast majority of installed photovoltaic capacity but are now projected to slowly leave the market for better technologies, as presented in subsection 2.2.2 [28].

2.2.2. Expected evolution of PV technologies

Photovoltaics went through great change in the last decade and the consensus is that the next decades will bring similar disruption. The International Technology Roadmap for PhotoVoltaic, or ITRPV, is a biannual publication that forecasts and keeps track of technological change in the photovoltaic industry. It is an anonymous collection of data from multiple parties of the PV environment (researchers, manufacturers, sellers). The data is collected, processed, and evaluated by a team of researchers and a report is published. It is considered the reference point for technological forecasting in the PV industry. In the latest ITRPV report [28], the following projections for the PV industry were outlined:

- PERC will exit the market, going from a market share of around 80% in 2023 to around 10% in 2032
- Three new cell technologies will enter mass production and distribution: SHJ (Silicon HeteroJunctions), IBC (Interdigitated Back Contact) and TOPCon (Tunnel Oxide Passivated Contact). These are all Silicon-based technologies with better performances than PERC. In figure 2.3 the latest numbers of ITRPV predictions are presented, up to 2033. It is clear to see how TOPCon will be the dominant technology while SHJ and IBC will represent a minor part of the market. While these upcoming technologies are distinguished by higher efficiencies, manufacturing know-how will play a major factor in PV market shares; tandem cells would be the ideal solution but the industry's inexperience will slow down their introduction.

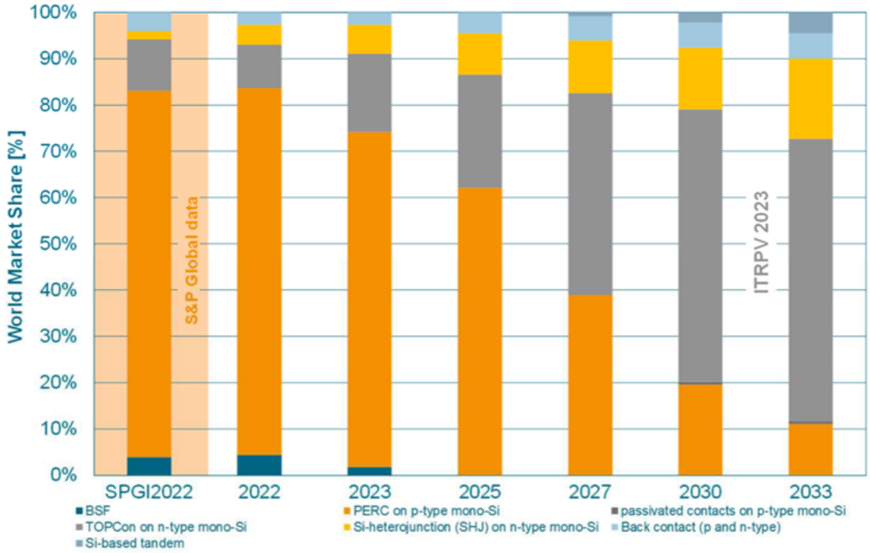

Figure 2.3: Technological evolution forecast to 2033 [28]

- Bifacial PV modules will represent the majority the installed capacity. These are modules that have similar cell technology used in conventional panels, but encapsulated by two sheets of glass, therefore able to absorb light from the both top and rear side. These modules will represent the vast majority of installations in large scale PV farms. The ITRPV projects that 70% of the marketshare will go to bifacial modules in 2033, and that 25% of the marketshare will be composed by monofacial modules, with bifacial cells.
- While promising great performance, the presence of persovskite modules withing the PV market is still zero, and will stay close to these levels for the foreseeable future (around 5% in 2033). The main issue with these modules today is performance degradation; today in fact perovskite modules have a 90% drop in performance within the fist 500 hours (20 days) of exposure to outdoor conditions [29], making them not suitable for any sort of application.

As already mentioned in the introduction of this work, making predictions in such a fast-paced industry is risky, and not always accurate. Vicari Stafani et al. [27] collected and analyzed the evolution and accuracy of the ITRPV report, compared with actual market evolution. The results can be seen in figure 2.4. The author explains how the speed at which the market moves is often unpredictable. For example, the adoption of PERC technology was much faster than anticipated, in opposition to the struggles that SHJ faced. The author emphasizes how the "business as usual"evo lution does not always describe the reality of the fast-moving PV industry and should therefore be approached with caution.

2.2.3. Materials in PV: current technology, trends, and challenges

Analyzing the material composition of each PV technology, combined with the prediction of their future market penetration, will provide a first glance at what the industry should focus on regarding material use and recycling. Fundamental to this analysis is the recognition of critical materials and trends in their use. In figure 2.5, the evolution in PV technology can be observed. The image shows what an average module looked like around 15 years ago compared to a modern module. Most elements remained the same, other than the presence of a back glass sheet in modern technological models.

Materials use and trends in different PV technologies

In a 2022 paper, Ovaitt et al. [22] explain how tracking down the historical evolution of material used in PV is not an easy task given the low availability and segmentation of data in the existing literature. Through a comprehensive study of industry data, publications, LCA datasets and projections, the authors were able to develop a mass composition baseline for PV modules, as can be seen in figure 2.6. This baseline tracks down the evolution of silicon-based technologies from 1995 to today and is extended to 2030 following ITRPV projections. The 2030 values are then assumed constant until 2050. The mass rate of glass, aluminum, silicon, silver, copper, encapsulant and backsheet are reported. The main observable trend is the constant reduction in silicon and alu-

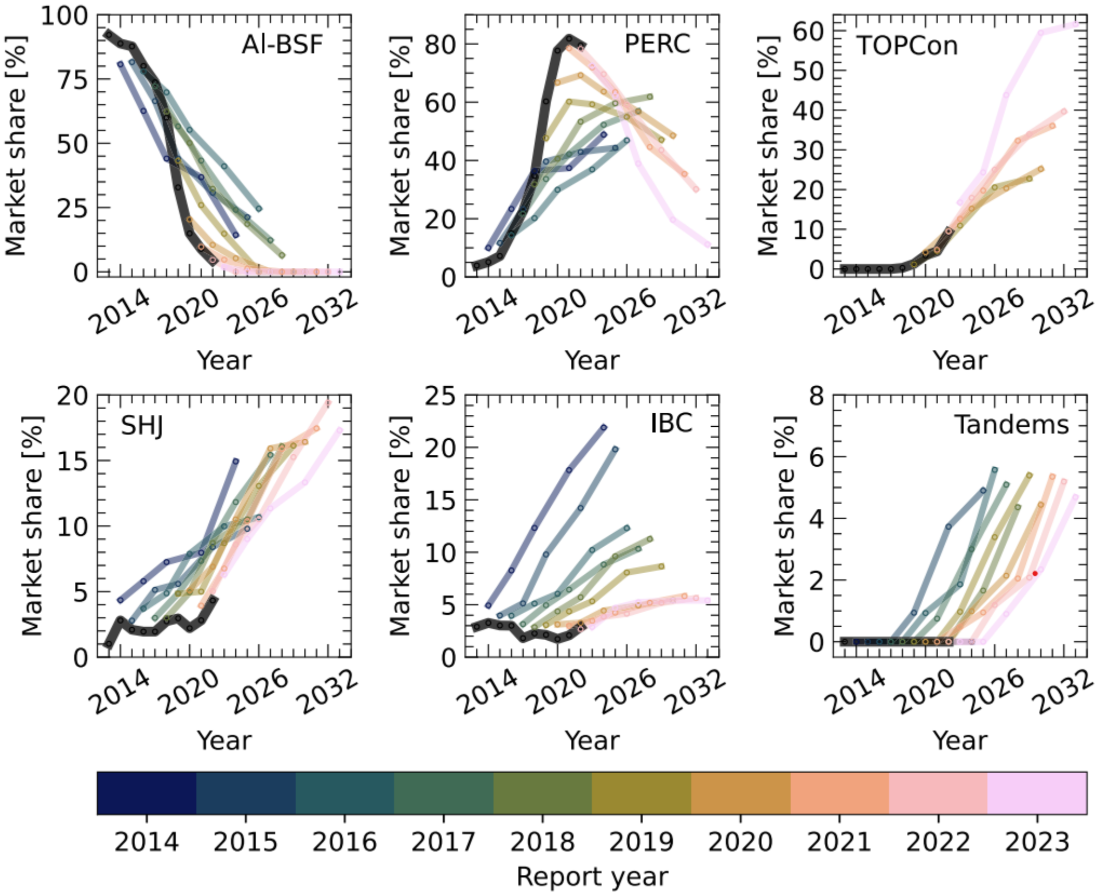

Figure 2.4: ITRPV projections compared with actual market evolution [27]

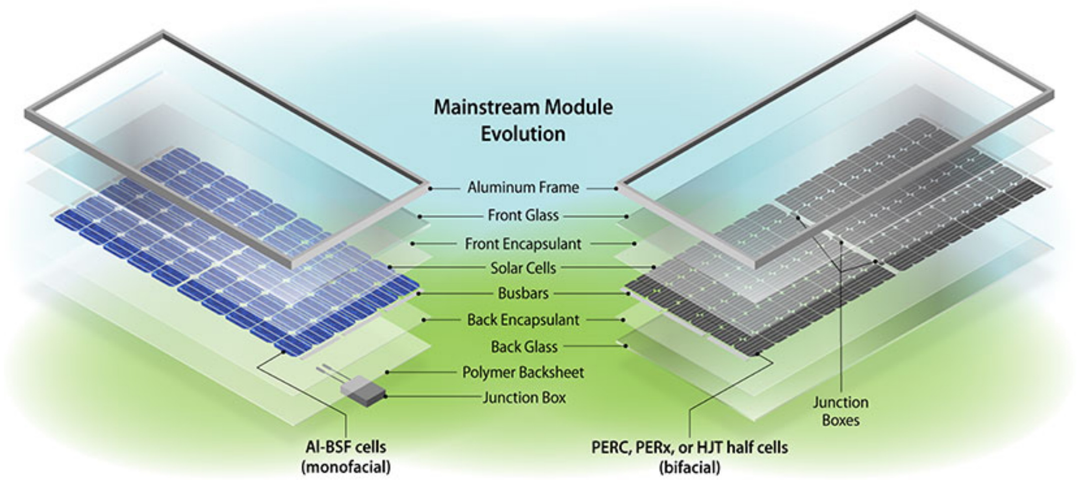

Figure 2.5: Schematic representation of common PV modules in 2010 (left) and in 2023 (right), [22]

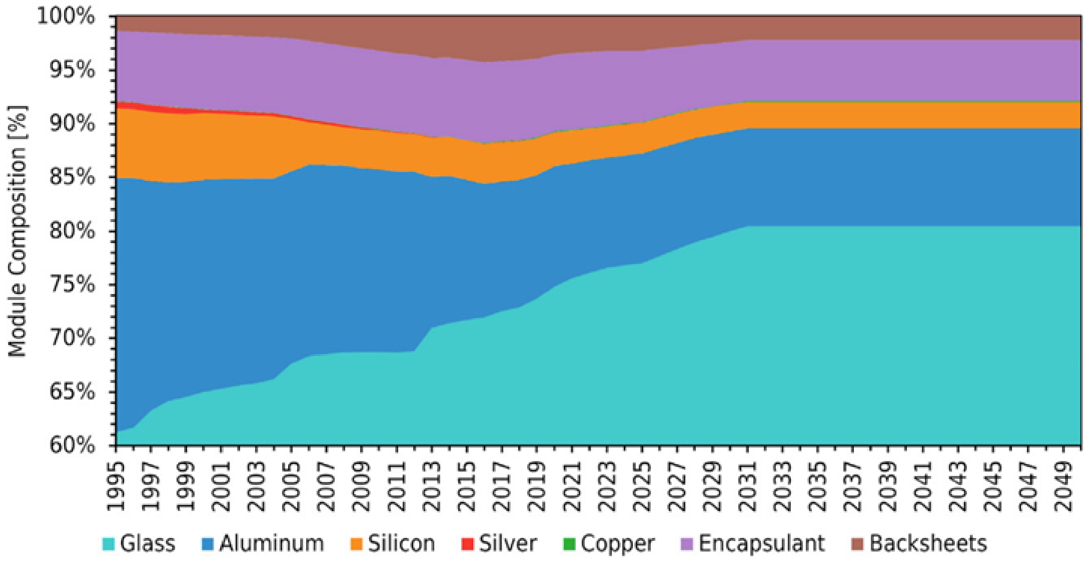

Figure 2.6: Average PV module composition mass shares [22]

minum contribution to the overall mass, in opposition to the growing percentage of glass. This trend is due to the increasing adoption of glass-glass configurations for monofacial and bifacial modules.

Glass is the main contributor to the weight of PV panels. Its contribution is not negligible in End of Life mass and energy flows. The ITRPV 2023 report gives projections for glass use in the coming years. The overall trend seems to be reducing glass thickness for both front and back side glass. Today around 10% of front glass enclosures have a thickness greater than 3mm while the rest 90% of marketshare has a thickness between 2 and 3 mm. The ITRPV projects that in 2033 around 85% of modules will have a thickness between 2 and 3 mm and 15% will have a thickness lower than 2mm. The trend is the same with the backside glass. Today, less than 5% of back glasses are > 3mm and the rest have a thickness in between 2 and 3mm. It is projected that by 2033 75% of market share will be between 2 and 3 mm while the remaining 25% will be thinner than 2mm.

Silicon is the second most abundant element in a PV module and the main contributor to the module's price. Most modules being produced today use monocrystalline silicon, a high-purity form of crystalline silicon composed of a single crystal structure.Si intensity has been going down and is projected to drop even further in the coming years; state-of-the-art modules in 2023 consume around 2.0 g/W, a number foreseen to drop to around 1.55 g/W by 2033.

The **frame** constitutes another essential component of a PV module, playing a pivotal role both during its operational phase and End of Life stage. The frame is usually made of **aluminum** (92% market share in 2023 per the ITRPV), an extremely well-recyclable material. By 2033 it's projected that aluminum will only have 75% of market share, in favor of frameless (10%), plastic (5%), and steel (10%). The steep increase of bifacial modules' market share will have a great impact on aluminum consumption. The ITRPV reports that bifacial configurations need only around 25% of the aluminum needed in regular monofacial configurations.

The **backsheet** and the **encapsulant** are two fundamental components of a PV module as well. These are polymeric layers that allow for the protection of the solar cells from environmental stressors such as moisture, UV radiation, and mechanical damage. The backsheet serves as the outermost layer, providing electrical insulation and structural support, while the encapsulant, typically made of ethylene-vinyl acetate (EVA), cushions the cells and binds them to the glass and backsheet. Together, they enhance the durability and longevity of the module, ensuring consistent performance over its lifespan. In bifacial modules, the backsheet will be substituted by a rear glass protection (as seen in figure 2.5).

Silver and **Copper** are the elements present in the smallest share in a module, but they serve a fundamental role. Both silver and copper are essential for conducting electricity. Silver is used in conductive pastes for creating electrical contacts on the solar cells, while copper is used for interconnecting the cells with ribbons or busbars. In the next paragraph, the presence of silver in PV modules will be discussed, focusing on the availability of silver for the projected demand coming from photovoltaics.

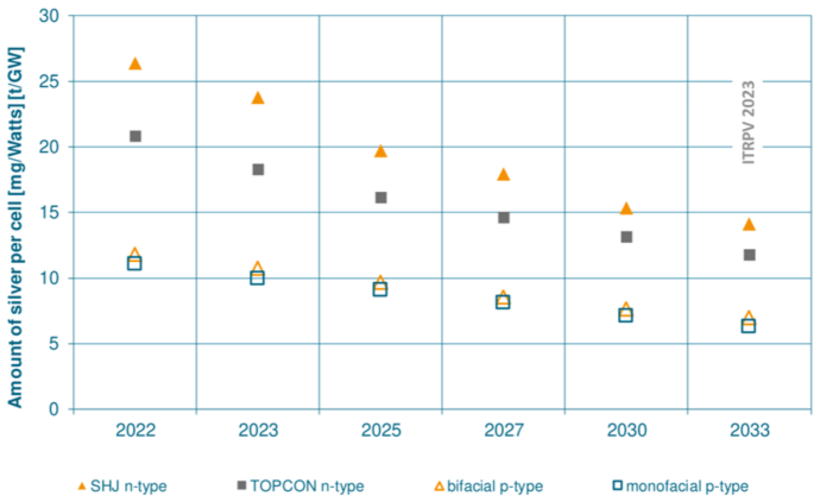

Figure 2.7: Silver use projections for the main solar cell technologies [28]

Materials scarcity in Photovoltaics

The photovoltaic industry, as many other industries in the energy field, is regarded as likely to suffer from material shortages[30, 31]. This section will consider materials potentially able to disrupt the regular evolution of the technology's supply chain. Understanding the role of scarce materials in photovoltaics could push technological development towards the preservation of the industry's market potential by, for example, shifting material use to more available resources.

Silver is the main element worth mentioning for PV applications. Silver is used as a conducting paste in silicon-based cells and is key to high module efficiencies. As per the Global Silver Institute, PV is now responsible for 11-12.7% of global silver demand [32, 33] and for 30% of silver going into the industry sector. Silver consumption in modules experienced a remarkable reduction in the past decade: in 2010 consumption was of 52-65 mg/W while in 2023 the average Ag consumption was of 11 mg/W [34, 33]. figure 2.7 shows the ITRPV forecast for silver consumption in the leading crystalline silicon cells technologies. A downward trend is evident for all technologies but there is another crucial factor fundamental to analyze. SHJ and TOPCon technologies, expected to fully replace PERC (figure 2.3), are projected to have in 2033 higher silver consumption than commercial 2023 PERC. a In particular, by 2033 TOPCon is expected to consume 12 mg/W, SHJ is projected to use around 14 mg/W while PERC technologies, almost phased out by then, would reach a consumption of 6.5 mg/W. The ITRPV reports that if in 2022 10% of the world supply went into producing PERC cells, for SHJ and TOPCon this number would have been double (at current consumption levels). Copper has, already for a long time, been considered a possible replacement for silver, being a cheaper and more abundant material. The ITRPV though excludes a rapid shift towards it citing technological issues that still make silver so much more appealing. In the latest report modules with copper are expected to only capture 7.5% of the 2033 market share. Material intensity is closely correlated with technology; higher efficiencies and bifaciality might increase the material need for a single module, but reduce the intensity per unit of produced energy.

The available literature is discordant on the future impact that silver will have on PV deployment. The main source of disagreement comes from conflicting predictions for PV installation forecasts. Papers that consider lower-end numbers (table 2.1, table 2.2) come to more reassuring conclusions for silver's role in the energy transition [35], while research that forecast over 60 TWp of installations show concerns for Ag availability. A 2022 review by Hallam et al. [33] takes into account the possibility of 63,4 TWp cumulative installations by 2050 and explains how, even if taking into account technological reduction in Ag use or learning rates (LRs), the required silver would account for 89-93% or current known global silver reserves. The report adds that if Ag availability for PV was limited to 20% of reserves, then the maximum installable capacity would be 6.7 TW, less than the lowest IEA or IRENA scenarios. A concerning remark is made towards the rapid adoption of SHJ and TOPCon technologies, a quick and immediate transition, as currently forecast by the ITRPV, would increase silver demands to 554-599 kt, meaning 101-109% of global silver reserves known in 2023 (550 kton) [36], as can be seen in figure 2.8. In order to maintain silver demand within 10 kt/year (43% annual silver supply), the silver learning curve must accelerate to rates of 30-40%; as mentioned before, it looks like the learning curve right now is around 0% given the technological changes. The author ends its paper by strongly recommending that the PV industry shift its

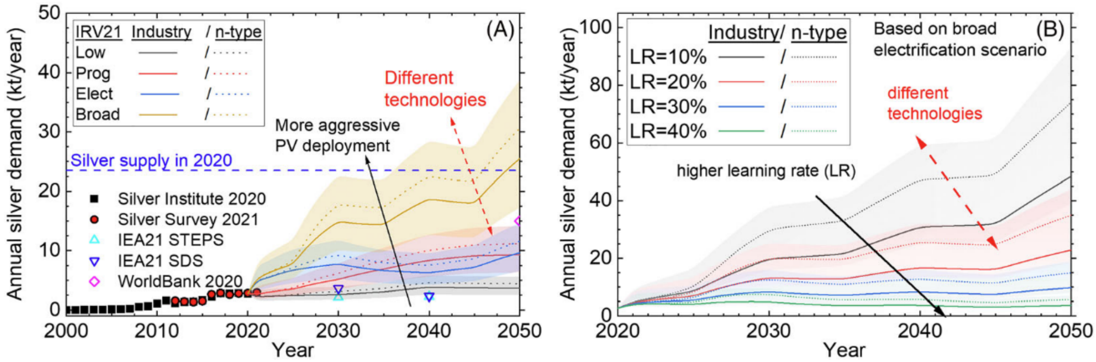

Figure 2.8: Global projected silver consumption for PV applications [33]

practices and developments from the pursuit of the highest possible efficiency to material use considerations. Having Ag consumption close to the limit capacity would mean needing to use caves with poor concentrations or with very deep ores, two extremely energy-intensive practices that would significantly higher modules' carbon footprint and prices. Other than reducing silver intensity, the authors indicate recycling and silver recovery as the solution to ensure stable long-term- capacity of PV production.

Other than silver, the main other materials worries are to be found in CdTe thin-film technologies. CdTe plus c-Si technologies make up almost 100% of the current and future photovoltaic market share [37] and will therefore be the only other technology considered. In particular, tellurium is the metal that could cause supply chain disruptions. Heath et al. [38] reports that in a high electrification scenario (with more than 60 TWp of PV in 2050), Te would require 600% of the current annual market demand. Contrary to c-Si, CdTe technologies already have well-established recycling and circularity paths [39] and therefore constitute a lower interest in EoL mass flows [22].

2.2.4. Final use of PV

PV modules are, by definition, modular, meaning that they can be installed in infinite configurations, sizes, and installation purposes. Understanding the final destination of a PV module means understanding the conditions under which the panel will operate and degrade. The size of modules installed for different uses also differs and is relevant in the projections of end-of-life mass flows. The ITRPV reports projections for deployment characteristics up to 2033 as can be seen in figure 2.9. The share of rooftop PV is assumed to stay constant, right above 30% of installed capacity. Power plant installations, now covering almost 70% of installed capacity are supposed to share their market share with emerging technologies such as floating PV and agrivoltaics. Regarding size,power plant installations, almost uniquely bifacial, are today between 2.5 m^2 and 3.0 m^2 while rooftops are between 1.8 m^2 and 2 m^2.

2.3. PV waste and circularity

The current growth in PV installations is highlighting the need for sustainable and circular practices in the photovoltaic industry. Many studies have investigated challenges and strategies for doing so. In 2016 a highly influential paper on photovoltaic end-of-life was published in a cooperation between the IRENA and IEA-PVPS [40]; the agencies collaborated to shine a light on what to expect from waste flows of photovoltaics. The paper presented a methodology on how to model the dynamics of panels reaching their end of life through a Weibull curve and two loss scenarios (regular and early), a practice still used today. In the 2016 study around a range of 60 to 72 million tonnes of worldwide cumulative PV modules were projected to reach their end of life by 2050. The research gave a first glance at the scale of the challenge ahead but today, in 2024, it can be said that those numbers are profoundly outdated. The 2016 paper was based on installation projections that saw PV reaching 4.5TWp by 2050; a figure that the conservative IEA and IRENA projections now expect around 2030. Even if the numbers and scale are outdated, the ideas behind PV recycling and circularity presented in the paper are today more relevant than ever.

The authors of the 2016 paper outlined that when recycling processes are efficient, they offer energy and emission reductions compared to virgin material extraction and treatment. Energy saving is today the biggest push

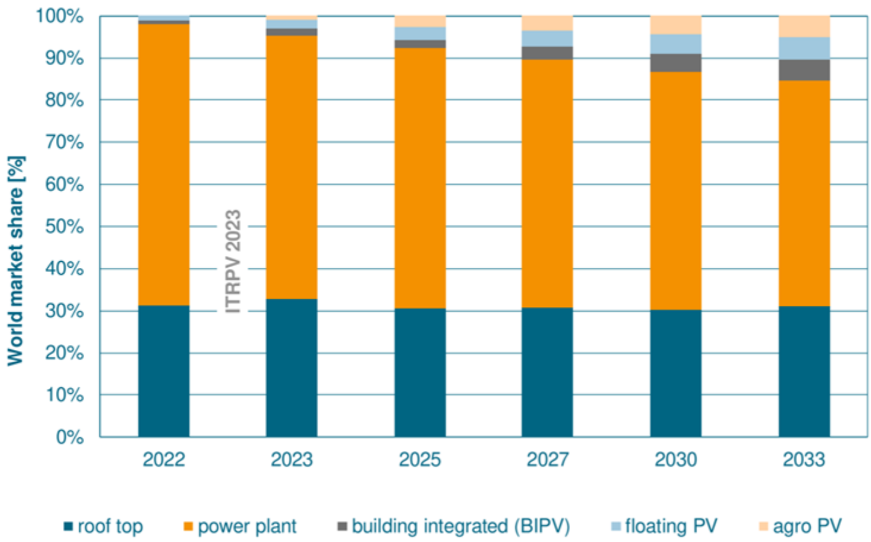

Figure 2.9: Projections of market share for different PV end-uses [28]

for recycling given that the low volumes would not yet make critical materials replenishment relevant enough [41]. In photovoltaics, energy and carbon savings are particularly applicable to silicon which requires highly intensive processes to reach low impurity concentrations. These necessary steps cause it to be responsible for half the energy content of a module [42]. Bartie et al. [43] modeled the entire manufacturing process of a crystalline silicon photovoltaic module and explained how recycling would reduce power consumption significantly, from 116 kWh/m^2 to $75kWh/m^2$. The noted 35% reduction, achieved through the use of silicon from old wafers, is attributed to avoiding the Siemens process, a purification step aimed at obtaining solar-grade silicon. More energy could by saved by reintroducing in the manufacturing line kerf material as well. Kerf is the byproduct of cell slicing and is today considered waste material. Kerf would need to go through the Siemens process again but would allow omitting the fist purification step. The mass flows of virgin and recycled silicon can be seen in figure 2.10.

Another element that is often overlooked but that could be an important driver for PV recycling is carbon savings, especially in countries with net zero goals or financial mechanisms around carbon [44]. CO_2 emissions decrease thanks to the recycling process, in particular avoiding silicon purification would on average save 14% of the usual carbon emissions (from 146 $kgCO_2/m^2$ to 125 $kgCO_2/m^2$) and kerf residues could support another 1% of carbon emissions [43]. Even if energy and carbon savings represent evident reasons to pursue recycling and EoL management, these process will never happen without profitability. What makes the recyclability of a module financially advantageous is the presence of valuable materials such as silver and copper[45]. A recent analysis from Granata et al. [1] dived into the economical feasibility of c-Si recycling and found that the price and amount of silver in modules combined with the quantity of panels entering the waste stream can alone indicate the profitability of recycling. The study indicates that with great possibilities some sort of fee will be required to allow recycling plant to offer interesting ($\geq 20\%$) Return Of Investment (ROI). The trend of higher silver consumption in newer cell technologies could prove fundamental for the feasibility of recycling and high collection rates of Ag from dismissed modules could help on the long run to solve availability issues described in subsection 2.2.3. This is particularly relevant for regions such as the EU that will have ample capacity demand but don't have the natural resources to partly self-sustain the manufacturing process. Material streams coming from European recycling facilities might prove necessary and fundamental to the energy security and independence goals of the European area [46]. Literature is definitive that the path toward photovoltaic recycling will be turbulent and will require significant efforts from multiple stakeholders [7, 47, 48]. Other than economic feasibility, considered by far the main issue, the other obstacles to PV recycling are:

- Missing policy and unclear responsibilities of each stakeholder.
- Unwillingness to pay a recycling fees from customers.
- Uncertainty about waste volumes at a regional/national causing investment uncertainty.
- Unclear logistics and high transportation fees.
- Concerns about toxicity of modules

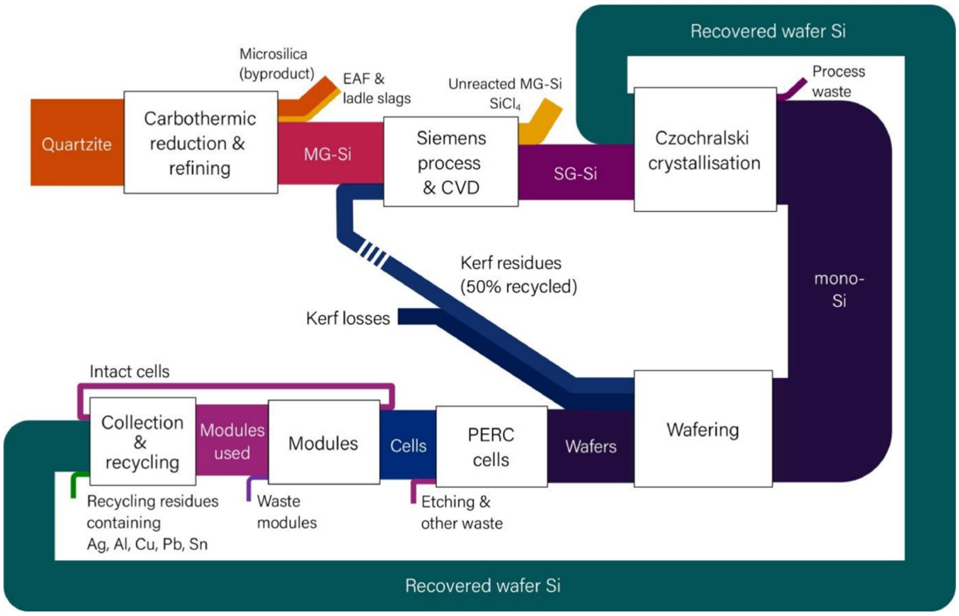

Figure 2.10: Silicon mass flows in a recycling process to scale, [43]

Heath et al. [42] emphasizes the necessity of publications that focus on a national or regional level and that consider interactions between different jurisdiction to provide investors with enough information to spark investments in circularity paths for PV. Regarding logistic issues, literature is unambiguous on the need for high recycling volumes to enable profitability, and therefore central, often international, recycling plants will be necessary, at least for the first half of the century [38, 48]. Chen et al. [48] points out how transporting heavy modules for long distances might cause high costs and cut already slim profits, the author suggests that modules should be first treated locally to remove the glass enclosure(s), responsible for around 75% of the weight (figure 2.6). By doing so cargo would be lighter and only high-value materials would be transported to central recycling plants while glass could be treated at local and already specialized facilities. Heath et al. [38] points out that even if most literature concerning circular economy in photovoltaics is focused on recycling, more space and attention should be given to other circular paths such as reduce, rethink, and reuse. These alternative strategies could overall improve the sustainability footprint of photovoltaics and at the same time cause waterfall effects for the whole chain. Reducing material use, for example, would make modules more affordable and less energy intensive to produce but at the same time would reduce recycling revenues. More research needs to be done for these strategies that could potentially prove fundamental for photovoltaics' circular economy. The authors point out how it is still more than unclear how well-recovered silicon can be inserted back in the manufacturing line; the recycling process would probably slightly contaminate the silicon, causing unknown effects on performance and making recycled silicon less appealing to producers than predictable virgin silicon.

2.4. Failure, degradation, and reliability

The previous section portrayed the "fate" of solar modules that entered their end-of-life phase. This section will provide a brief explanation on the process that leads a module to its failure. This can happen for three main reasons: **excessive degradation**,the **end of economic lifetime** and **random failures**.

During operation, modules go through steady and unavoidable degradation caused by multiple and simultaneous events, also potentially leading to failures due to excessive degradation. Jordan and Haegel [49] explain that a modules are considered failed due to excessive degradation when they operate below 80% of their rated capacity. When modules drop below this threshold they are considered failed and ready to enter the end-of-life stream. Literature is well documented on causes and effects of degradation [50, 51], but the pace at which photovoltaic technologies are evolving is making it harder to predict exactly the lifetime of new installations. Most photovoltaics will be installed and operated without the three year of performance data that has been usually required to estimate long term performance [49]. Available publications have analyzed performance of moder photovoltaic systems and came to the common conclusion that the average degradation rate for a PV system is of -0.7% to -0.75% per year [49, 52, 53]. In literature, the value of -0.5% per year is found as well but it often refers to single modules, rather than to entire systems. Note that these values are to be considered as percentile changes and not as absolute changes (a 0.5% drop will make a 20% efficient module go to 19.9%, not to 19.5%). The ITRPV reports that degradation rates are projected to diminish in 2033, in particular by then modules would have a -0.4%/year drop while systems would degrade at a -0.5%/year rate [28]. Even if in reality degradation is often irregular, the industry and literature has decided to use a linear degradation rate to ease customer's understanding and expectations. Degradation values are influenced by a vast range of variables such as climate, size and maintenance standards [52, 54] but an average figure can give a good first glance at what to expect during the lifetime of a module. All the main cell technologies, Al-BSF, PERC, SHJ and IBC show similar degradation rates; CdTe as well degrades with a comparable rate [52].

Economical failure are something that needs to be considered as well. Photovoltaic manufacturers offer a warranty for their technologies, specifying the timespan during which a module is expected to maintain a production capacity deemed “acceptable”. This ensures that modules will operate at no less than 80% of their designated nameplate value throughout the warranty period. During the early stages of the PV industry, performance warranties were 10 to 15 years but steadily grew as technology progressed and are now at around 25 to 40 years [22]. The ITRPV projects that by 2033 warranty will be 35 years [28]. Warranty is a very good indication of a module's expected economical lifetime but these two are not always necessarily the same. When a module is economically failed, it indicates that its owner has a stronger business case in substituting the panels with new factory fresh pieces, even if its current fleet does is still properly working. This practice, defined as “on site re-powering”, makes the prediction of modules economic failure more complex and dynamic. The opposite phenomenon is possible as well: if a module exceeds its lifetime warranty and the owner does not have a clear economical reason tu replace the installed fleet, every W produced would be free for its operator. This phenomenon is referred to as ”Merchant tail”.

The third and final pathway through which modules can reach End of Life (EoL) are random failures. These failures result from one-time events that cause modules to perform below their acceptable range or cease functioning entirely. The causes of these failures are multiple and are usually related in imperfections in the module manufacturing process or in the installation and cabling procedures. Some examples are thermal stress leading to solder bonds failure [55], corrosion caused by moisture ingress [56], cracked cells [57], localized overheating (hot-spots) caused by manufacturing errors [58], bypass diode failures (more frequent in poor field configurations) [59] and many more. Failures connected to extreme weather such as hail or dust storms are also considered in this category.

To conclude, this paragraph explained that a PV module has three pathways for reaching End of Life: excessive degradation, the end of its economic lifetime and random failures. These considerations will be used in the simulation of the lifetime of a PV module

2.5. Methodology to simulate EoL: the past and the present

In 2016, a paper in collaboration between the IEA and IRENA laid the grounds for research of PV EoL modeling by proposing a methodology that would forecast PV waste volumes given installation forecasts and information about the module's technology [40]. While this methodology managed to spark the interest in research of PV waste flows and allowed for multiple researchers to simulate the evolution of PV EoL material in different countries, the assumptions used in 2016 do not apply anymore to the photovoltaic industry of 2024.

In the previous section of the report, we explained how a PV module can reach End of Life (EoL) through three pathways: excessive degradation, random failures, and the end of its economic lifetime. The most problematic aspect of the old methodology are its assumptions on random failures, not in line with today's standards. The 2016 paper in fact proposes a method to forecast PV random failures through two Weibull curves, two different distributions correlating the probability of failure with age. These two scenarios are presented under the names of “Early loss” and “Regular loss”. The two scenarios follow for the most part different distributions, but have a common point: the loss of 64% of the installed capacity within the first 30 years of operation due to random failures. This number is today profoundly outdated, leading to overestimating waste volumes. Today, system owners and financial models expect only around 10% of their fleet to fail within their economical lifetime as explained in section 2.4. This issue led to the creation of a the new methodology in 2022 by Ovaitt et al. [22], where only 10% of installed capacity is lost due to random failures. Furthermore, in the 2016 methodology economic lifetime was modeled by assuming that modules had a definite lifetime of 40 years, and that after the 40 years modules would be removed regardless. In the novel methodology, modules are removed after their economic lifetime expires. By doing so, the historical value of LCOE calculations is taken into account, evaluating investment considerations in End of Life. The last issue with the old methodology is that degradation was not considered. In the new proposed methodology, however, modules are removed when they degrade below 80% of their rated capacity.

2.6. Research Question and Aim

After the considerations summarized before, this section will outline the specific aim of this project. The objective of this research is to provide a projected estimation of PV EoL streams on three scopes: global, continental (regional), and national.

These results will be studied through two main lenses: analyzing the scale of module replacements and determining the amount of EoL materials available for recycling in different nations and regions. The first analysis will outline the share of installations aimed at replacing failed modules compared to the total yearly installation size. The second analysis will focus on illustrating the amount of materials available for recycling. These numbers could then be used to develop investment decisions for large-scale recycling infrastructure. As mentioned in previous sections, uncertainty about the scale of EoL material at national and regional levels is one of the main hurdles to the development of recycling plants. Literature offers research on EoL projections, but papers usually focus on single countries or regions, such as China [44, 60], the USA [22, 61], Thailand [62], Flanders [63], Spain [64], among others, or they focus on specific selections of countries such as OECD countries [65] or other arbitrary selections [66]. While these papers are fundamental contributions to the PV recycling landscape, their scope is different from this research. Country-specific studies might not provide a sufficient scale to facilitate large-scale PV recycling initiatives. Initially, recycling plants will likely need to be central international hubs to receive the necessary material inflow to prove a business case [1]. This will be particularly true in regions with multiple countries nearby, such as Europe or Southeast Asia. The role of transportations costs, now one of the major barriers to PV recycling economic viability, needs to be assessed before any central PV recycling center can start operating. The methodology used in these papers raises some concerns as well. Most of the publications use the outdated 2016 methodology better explained in section 2.5. It is therefore necessary for this research to implement the new methodology to the scopes shown above, and develop new and updated figures on photovoltaic End of Life. In the following chapter, the methodology followed to model PV EOL is shown and explained.

3
Methodology

This chapter of the report outlines the methodology followed in the simulation and modeling of this reaserch. All the assumptions regarding input data and model calculations are reported and justified in the following sections. The primary objective of this study is to forecast the volumes of photovoltaic waste worldwide, until 2070. After reporting the main findings, the study aims at exploring the implications and relations of these forecasts. The forecasts will be conducted at a global, continental (regional) and national scale, which each scope focusing on different issues. For the global analysis, chapter 4, a high and low installation forecast scenario will be compared. At the global level other scenarios, that don't entail different installation forecast but that differ for assumptions or methodology, will be run tested and analyzed as well. At the regional level, chapter 5, the similarities and differences of different world regions will be underlined and studied. Finally for the national level chapter 6, the different nations will be compared over the time evolution of the expected waste flows.

In order to develop the forecast for any of the three scopes outlined, three "ingredients" are necessary inputs to the model:

1. PV capacity installation forecasts
2. Module technology characteristics and expected evolution
3. Methodology on how to determine End of Life

All three aspects will be discussed in the following subsections. A deeper dive into PV installation forecast data selection and manipulation is presented in section 3.1, section 3.1 dives deeper into the baseline assumptions on module technology and section 3.3 describes the methodology used to model End of Life. Once all the required "ingredients" are ready, simulations about modules' operational lifetime, degradation, and failure can start. By simulating modules' operational lifetime, multiple parameters can be explored, starting from the expected amount of PV discarded material. The main instrument used to perform the waste flow calculation is PV ICE, a Python-based tool developed by NREL that provides functions to simulate PV lifetime.

3.1. Photovoltaic installation forecast

In section 2.1, the latest available information on PV installation forecasting are presented. In particular, it is emphasized how different research centers and universities present radically different outlooks for installed photovoltaic capacity. Given that the scope of this project is not to analyze and verify which forecast can be considered more reliable; both a high and a low installation scenario will be used. The findings of the two scenarios will then be analyzed and compared. For the **low scenario**, the IEA World Energy Outlook 2023 "Announced Pledges Scenario" (APS) forecast will be used [2]. Using the APS scenario comes from the unavailability of data for the Net Zero Emission (NZE) scenario in the full dataset. The IEA dataset provides installation forecasts for the following regions: Europe, Africa, North America, Central and South America, Eurasia, Middle East, Asia Pacific and Southest Asia. In figure 3.1 the regional divide can be seen. IEA datasets are highly regarded and widely used in policy-making. For the **high scenario**, data coming from LUT University is used. The projections are of 75TW of installed capacity by 2050. The LUT dataset contains projections for the following regions: Europe, Eurasia, Sub-Saharan Africa (SSA), Middle East and North Africa (MENA), South Asian Association for Regional Cooperation (SAARC), Northeast Asia, Southeast Asia, North America, and South America. The

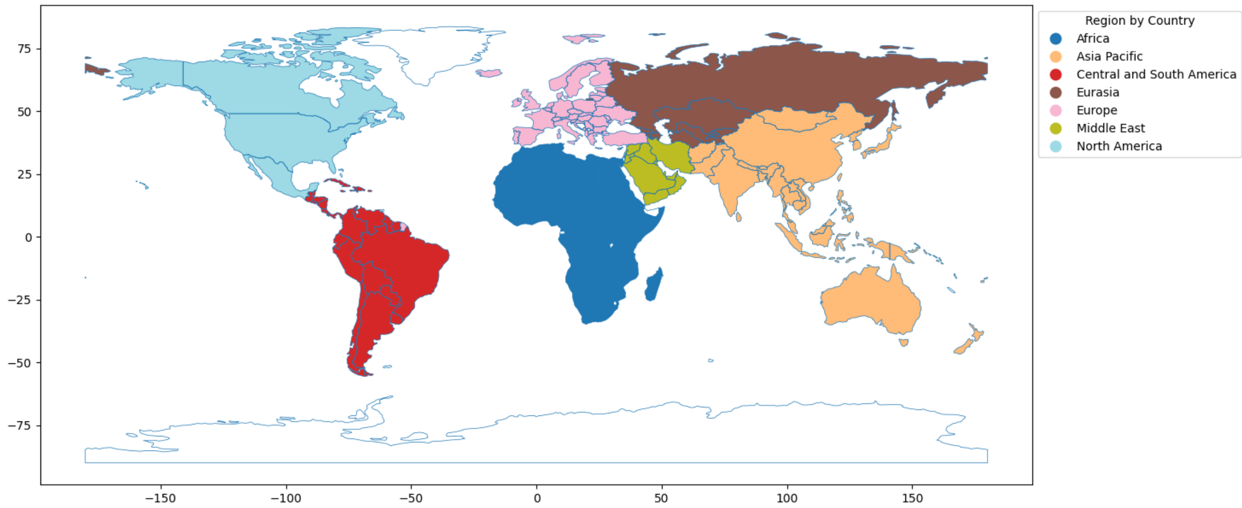

Figure 3.1: Regional divide IEA

regional divide can be seen in figure 3.2. The comparison between IEA and LUT data will be performed both at a global scale in chapter 4 and at a regional scale chapter 5. To compare the two projection scenarios, it is necessary to select a common regional division for the two forecasts. In the following lines, the main discrepancies between the regional divisions of the two datasets will be explained, as well as the choices made in order to build a common and comparable regional divide.

First of all, the IEA decided to divide Africa and the Middle East (using the Suez Canal). The forecast coming from LUT University, on the other, chose the Sahara Desert as point of separation between regions, defying the Sub-Saharan Africa (SSA) region, and the Middle East and North Africa (MENA) region. This discrepancy led to the necessity of merging the African continent and the Middle East into a common entity for regional confrontation, under the name of Africa & Middle East. The other major difference resides in the division of Asia and Oceania. While in teh LUT university forecast this region is divided in three separate entities, Southeast Asia, Northeast Asia and South Asian Association for Regional Cooperation (SAARC), the IEA forecast combines the whole region under the name od Asia Pacific. Given the lower amount of detail of the IEA's regional division, the latter had to used as the common regional division for the confrontation, leading to the merging of the three LUT regions under a new region defined as Asia & Oceania.

The regions chosen for the comparison are therefore **Asia & Oceania**, **Europe**, **Eurasia**, **Africa & Middle East**, **Central & South America**, and **North America**. The final regional division can be seen in figure 3.3.
In the final chapter of the report, chapter 6, forecasts for individual nations are also shown. Installation forecasts of individual nations come from multiple sources, given that the IEA World Energy Outlook dataset only provides data for 6 countries (India, China, USA, Russia, Japan, and Brazil).

3.1.1. Historical PV installation data

To generate accurate forecasts regarding end-of-life (EoL) material flows, it is crucial to include historical photovoltaic (PV) deployment data. However, neither the International Energy Agency (IEA) nor the LUT dataset provides this historical deployment data. To fill this gap, data from the 2024 IRENA Capacity Statistics report was utilized [67]. This report offers a dataset with detailed historical data on installed capacity for both countries and regions, divided under another unique regional scheme. In particular, the IRENA dataset divides historical installations among Asia, Oceania, North America, Central America and the Caribbean, South America, Europe, Eurasia, Africa and the Middle East. This new categorization led to the necessity of constructing a historical regional PV capacity dataset that accurately reflects the regional divisions used in this research, as delineated in figure 3.3. This involved aggregating the data for Central America and the Caribbean with South America for the South & Central America region and combining the figures for Africa with those for the Middle East to align with the regional breakdown used in this research of Africa & Middle East. Similarly, the installation figures for Asia and Oceania were summed to represent the Asia & Oceania region. Some minor adjustments had to be added as well, regarding the belonging of certain countries to particular regions. Turkey in the IRENA historical dataset

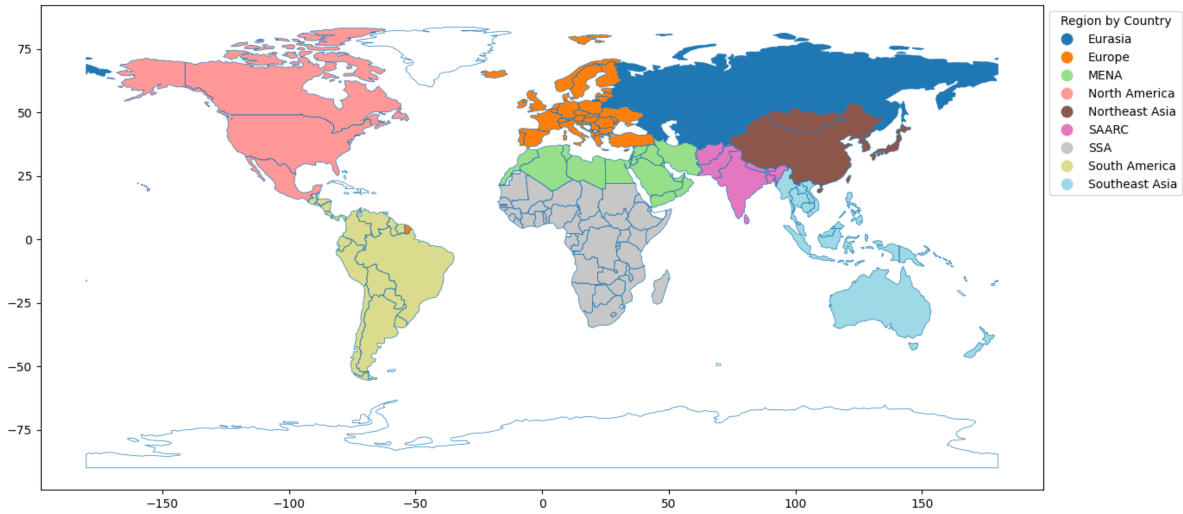

Figure 3.2: Regional divide LUT dataset

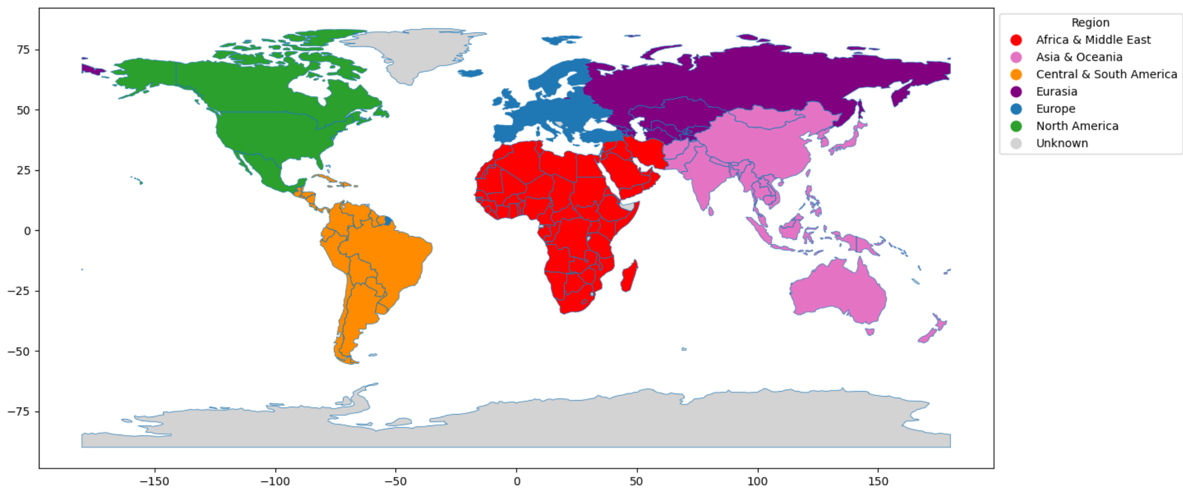

Figure 3.3: Final regional division

was considered as part of Eurasia, while in the final division used in this reaserch belonged to Europe. This meant subtracting Turkish historical installation numbers from the Eurasian total to add them to the European one. The same procedure was followed for Palestine-Israel which was moved from Europe to Africa & Middle East. Belarus was moved from Eurasia to Europe. These adjustments ensured that the input data for the modeling was as consistent as possible. The refined historical dataset was employed for both high and low scenario forecasts of this study, providing historical installation data from 2000 to 2023 fundamental for the calculation of waste flows.

3.1.2. Low installation scenario: IEA dataset

The IEA dataset used in this project comes from the full dataset of the 2023 World Energy Outlook report [2]. The database provides PV installation forecasts up to 2050 globally and for main world regions: Europe, Eurasia, Africa, the Middle East, North America, and Central & South America. It also forecasts six major countries: Russia, China, Japan, India, the United States and Brazil. The dataset provides regional installation forecasts for only the Stated Policies Scenario (STEPS) and the Announced Pledges Scenario (APS). The APS scenario was chosen and used in this project. The dataset provided projections for 2030, 2035, 2040, 2045 and 2050. To model PV EoL mass flow calculations, forecasts on a yearly base are required. This implied that the given data needed to be interpolated.

Data interpolation

Many techniques and algorithms are today available for data interpolation. After some trial and error, polynomial interpolation was chosen. The best results were obtained by fitting a grade 10 polynomial through the available data. The definition of "best" was based on two parameters: the Mean Relative Error (MRE) and visual inspection of the interpolated data. The Mean Relative Erroris calculated by averaging the absolute differences between the interpolated function values and the corresponding given data points.

$$\mathrm{MRE} = \frac{1}{n} \sum_{i=1}^{n} \left| \frac{f(x_i) - y_i}{y_i} \right| \tag{3.1}$$

where:

- $f(x_i)$ is the value of the interpolated function at point x_i,
- y_i is the given data value at point x_i,
- n is the number of data points.

The MRE was calculated between the interpolated data and the original dataset for the points present in both datasets (so the cumulative capacity in 2020, 2025, 2030, 2035, 2040, 2045, and 2050) for every region and summed up. Different MREs were calculated for different grades of fitted polynomials. By tracking the MRE relation with different polynomial grades, it was apparent that in general the higher the polynomial grade the lower the error. The majority of error reduction happens between the first 5 grades to then stay relatively constant until grade 10 to then drop from grade 11, for the low scenario, and from grande 12, for the high scenario, to then stay relatively constant until the highest grade tested (50). The polynomials with a grade higher than 10 were discarded because of visual inspections; the high grade polynomials would overfit the datapoints, leading to high swings on the capacity between years. It was therefore decided to use a grade 6 polynomial for the interpolation of both scenarios, given that it lead to sufficiently low error and had a lower level of complexity than a grade 10 polynomial. The curve was fitted using the data from 2020 onwards, but only "new" data points (from 2024 on) were used and appended to the historical data. The results fo the interpolation can be seen in figure 3.4. The value of the MRE based on different polynomial grades and the factors of the grade 6 polynomials used in the final interpolations are shown to allow for repeatability of the results: table A.1, table A.2, table A.3, table A.4 .

Data extension to 2070

After the interpolation for every year between 2023 and 2050 and the merging with the existing historical data, the forecast was extended to 2070. Given that modules have an economic lifetime of 30 - 35 years, ending the projection in 2050 would significantly limit the relevance and interest of the results. As shown in the projections of figure 3.4, most modules will be installed around 2040 - 2050; to observe the waste flow generated by those modules, or at least by a part of them, the timeline considered needs to be extended past 2050 (as further demonstrated in chapter 4). The choice of 2070 was a compromise between accuracy (forecasting too much into the future leads to excessive uncertainty) and the "appeal" of the obtainable results. With "appeal", it is intended the

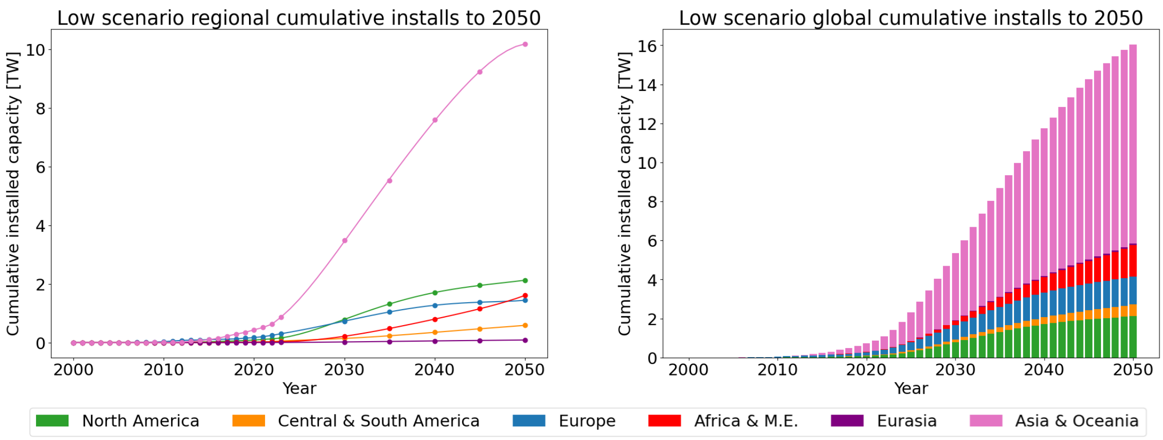

Figure 3.4: Regional and global interpolated IEA installation forecast for different region in the low scenario. On the left plot the dots represent given datapoints, while the line indicates the interpolation. The main hub of PV installations will be Asia and Oceania. North America is set to surpass Europe in cumulative installations around 2030 while Africa & Middle East will surpass Europe around 2050.

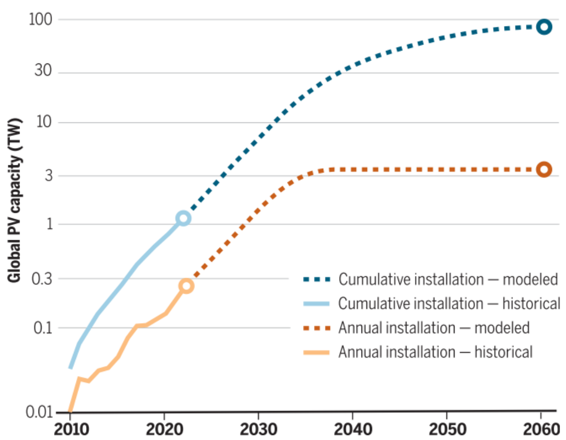

Figure 3.5: Predicted PV installation evolution globally [4]. This image allows for a perfect understanding of the expected evolution of the photovoltaic marker and will be the source for the methodology used in extending the installation forecast from 2050 to 2070.

quantity and interest of data that can be observed. Extending to 2070 allows for the inclusion of at least some of the major PV installations in the waste flow analysis, providing a more comprehensive and insightful assessment of future EoL material streams. Extending the scope further would call for excessive assumption on module material composition and PV installations. The temporal extension of the scope of the research demands for the extension of the input data, including PV forecast installations. While the extension of module-specific data will be presented in section 3.2, the extension of PV installation data will be explained in the following paragraphs. Figure 3.5 describes the current sentiment around PV installation evolution, estimations see the cumulative global PV capacity to grow steadily, reaching a stable figure around 2060. Annual installations are, on the other had, are projected to grow until 2040, to they stay constant. This particular shape of the installation evolution would allow the PV market to stay healthy. While the global capacity is expected to plateau, potentially signaling the end for PV modules demand, the role of replacements modules should allow demand to stay constant. If currently new modules are installed to add capacity, by the second part of the century replacements of old modules will represent most (if not all) of the demand for new modules. This idea will be further investigated in chapter 4; how will replacements of lost capacity influence annual demand for PV modules?

In order to extend PV capacity forecast data, a family of particular functions were used: sigmoid functions. Sigmoid functions are a class of mathematical functions that produce an S-shaped curve, in line with historical photovoltaic trends and the future projections just described.The typical behavior of a sigmoid function involves a gradual increase in the initial phase of its domain, followed by a more pronounced growth in the middle, and culminating in a slow, nearly plateau-like progression toward the end of its domain. In this research, sigmoid functions were specifically chosen for their ability to model the gradual uptake and eventual saturation of PV global installed capacity. These functions were fitted using data from 2000 to 2050 and were then extrapolated to extend up to 2070 to provide a comprehensive long-term forecast. The sigmoid function is given by:

$$S(t) = \frac{K}{1 + e^{-b(t-t_0)}} \tag{3.2}$$

In this formula:

- K represents the maximum value that the function can reach.
- b determines how steep or flat the curve is.
- t_0 shifts the midpoint of the curve along the time axis.

Given the project's scope, which involves analyzing multiple regions to obtain global installed PV capacity, it was necessary to develop a sigmoidal extension function tailored for each region by adjusting the above listed parameters. The optimization of these parameters was accomplished using an algorithm designed to minimize the discrepancy between the sigmoid curve and the available data, meaning the interpolated installed capacity from 2000 to 2050. This optimization procedure was done through the use of the function *curve_fit()*. The curve_fit function comes from the *scipy.optimize* module, which is part of the *SciPy* library. The curve_fit function is used to find the optimal parameters of a specified function so that the function best fits a given set of data points. In this context, the sigmoidal function's parameters were fine-tuned to align closely with the interpolated data, providing a reliable model for projecting future installations based on historical trends. This method ensures that each regional model is accurately calibrated to reflect its unique growth dynamics.

The first calculation of the sigmoid extension curves led to some improbable behaviour, with predicted capacity in 2070 (from the sigmoidal curve) being lower than the 2050 capacity (provided as fitting point). This anomaly was attributed to the nature of the optimization problem which, while offering an overall better fit within the scope of the problem, did not align with the anticipated trends for the projection period, described in the previous paragraphs. The curve-fitting optimization problem was therefore constrained by the assumption that the 2070 cumulative capacity should have be higher than the 2050 capacity by at least 3%. This constrain led to satisfying and reasonable extension functions used for the extension to 2070 of PV capacity. In table A.5 the optimal parameters for both low and high scenarios in every region are presented. Figure 3.6 shows the application of the sigmoid functions to two different regions, Europe and Africa, regions that show a different evolution of their photovoltaics capacity and therefore underline the need for such an optimization problem. In particular, the figure shows how European capacity is set to star stagnating (according to the low scenario) around 2037 while Africa & M.E. capacity is set to keep its upwards growth until 2050. This means that the two sigmoidal function used need to have different shapes and upward trends to extend these two different regional evolution.

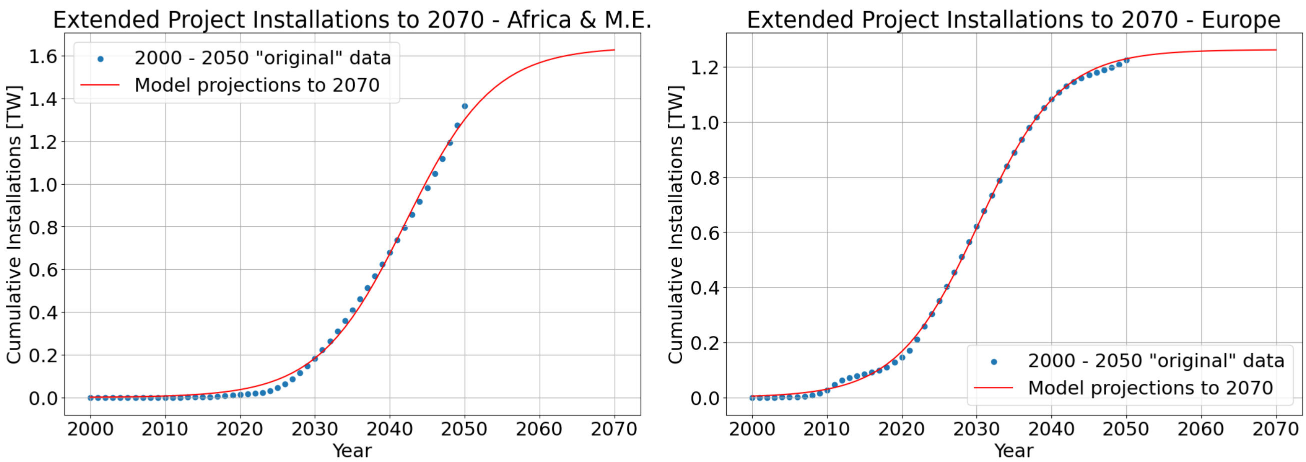

Figure 3.6: Example of sigmoid functions fitting for two different regions of the low scenario. The blue dots represent the points through which the sigmoid curve (red line) is fitted. This shows how some optimization is needed in order to find for each region the better curve given the different expected evolution of different regions.

Year	North America	C. & S. America	Europe	Africa & M.E.	Eurasia	Asia & Oceania	**Global**
2023	0.15	0.05	0.30	0.03	0.00	0.85	**1.39**
2025	0.28	0.08	0.40	0.05	0.01	1.44	**2.26**
2030	0.77	0.14	0.71	0.21	0.02	3.37	**5.23**
2035	1.29	0.23	1.02	0.47	0.04	5.45	**8.49**
2040	1.67	0.34	1.24	0.78	0.06	7.40	**11.49**
2045	1.90	0.46	1.35	1.13	0.07	9.04	**13.95**
2050	2.08	0.57	1.41	1.57	0.09	9.96	**15.68**
2055	2.13	0.64	1.44	1.80	0.09	10.27	**16.37**
2060	2.15	0.67	1.45	1.90	0.09	10.41	**16.67**
2065	2.16	0.69	1.45	1.95	0.09	10.46	**16.80**
2070	2.16	0.70	1.45	1.97	0.09	10.48	**16.85**

Table 3.1: Low installation scenario cumulative installations [TW]

The new data (form 2051 to 2070) was appended to the 2000 - 2050 previously interpolated data. Given that these two portions of the data come from different functions, a polynomial interpolation for the 2000 - 2050 period and a fitted sigmoidal function for the 2051 - 2070 portion, the juncture between the series had to be carefully analyzed. The approach of "gluing together" the two functions at 2050 - 2051 juncture led to a noticeable discontinuity, particularly in the year 2051, where capacity values were often observed to be lower than those for 2050 and 2052, suggesting an implausible scenario of negative installations for that year. This phenomenon was caused by the sigmoid function being too low for the 2051 value in some regions compared to the 2050 value, as could be observed in the left side of figure 3.6. This plot, confronting the sigmoid function with the beforehand calculated capacity until 2050, shows how the sigmoid function for Africa & the Middle East does not follow the data until the last point (2050) but starts to flatten out in 2049. This behavior makes the sigmoid function start from a value that is lower than what is expected after seeing the general trend in the final part of the 2000 - 2050 data series, leading to some misalignment in the years around the juncture. In case of misalignment, the 2051 capacity was changed to the average between the 2050 and the 2052 values. This operation lead to increasing the sigmoidal 2051 capacity by delta of extra added capacity. This offset was added to all the years after 2051 as well. By adding the offset to all the years after 2051 it was ensured that the growth trend described by the sigmoid function would follow the PV capacity evolution described in the 2000 - 2050 portion. The value of the added offset for every region (in both scenarios) can be seen in table A.6.

Once two portions of the dataset were attached together, the final PV installation data was considered ready to be used. The forecasted PV capacity is therefore represented by a function defined piece-wise as follows:

$$C(x) = \begin{cases} ax^6 + bx^5 + cx^4 + dx^3 + ex^2 + fx + g & \text{for } 2000 \leq x \leq 2050 \\ \frac{K}{1+e^{-b(x-x_0)}} + \Delta & \text{for } 2051 \leq x \leq 2070 \end{cases} \tag{3.3}$$

where:

- x is the time expressed in years
- a, b, c, d, e, f, g are coefficients of the polynomial fitted to data from 2000 to 2050.
- K is the maximum value of the sigmoid function.
- b is the steepness of the curve.
- x_0 is the midpoint of the sigmoid.
- Δ is the constant offset added to align the polynomial and sigmoid functions.

The values for all the parameters are reported in the appendix, from table A.1 to table A.6.

The plots reporting the final capacity evolution forecast used in the low scenario can be seen in figure 3.7 and are reported in 5 years intervals in table 3.1. On the left side of the figure, the dots represent the provided points of forecasted capacity for the different regions while the lines are product of the operations explained above and will be used in the remainder of this research.

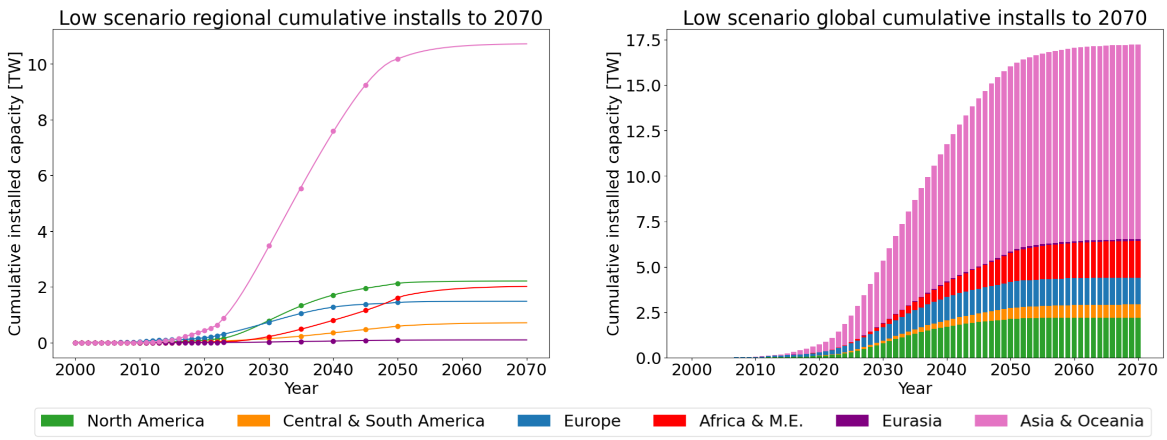

Figure 3.7: Low scenario 2070 PV installation forecast. The dots on the (left) figure represent the provided forecast, while the lines indicate the interpolation and data extension peculiar to this research.

3.1.3. High installation scenario: LUT University dataset

The high electrification scenario comes from projections done and published by LUT university researchers. More details about their work can be found in subsection 2.1.3. The data from LUT used in this work comes from two papers, a 2023 paper by D. Keiner et al. [5] and a 2021 paper by D.Bogdanov et al. [6]. A combination of the data provided in the two papers was used to develop the "high installation scenario" data for this project. In this section the motivations and methodology behind the choice and modifications of data are reported.

High scenario: PV data selection

In the literature review section, the results of the **2023 paper by Keiner et al.** [5] on forecasting the future energy mix are reported. The research in question provides PV installation forecast at the regional level using the *LUT-demand* model. The paper proposes three scenarios, different in terms of the pace and scale of the energy transition. For this research the slowest and lowest installation scenario proposed, the LEES scenario, is used. This scenario forecasts 75 TWp of cumulative global capacity by 2050 and this data could technically be used without further modifications. After detailed considerations, the particular shape of the installed capacity forecast raised some concerns. According to the data reported in the paper, the year 2030 would be the peak of annual added capacity, while, by 2050, annual added capacity would be almost zero. This would imply a ramp-up in installations in the coming few years that does not reflect current trends and expectations. In particular the model foresees 5.7 TWp of cumulative capacity by 2025; to put this into prospective 2023 global installed capacity was 1.6TWp, with 0.44TWp of new additions. This model foresees capacity to grow to 31.8 TWp by 2030 and 60.6 TWp by 2035, with average annual installations close to 5.5 TWp per year, something that is not likely to happen if compared to current growth rates. This indicated the need for some modification to the dataset.

As already described in the previous subsection, the Haegel et al. paper [4] forecasts installed capacity to reach a plateau around the year 2060. In a high installation scenario, this timeline would allow for a more realistic installation progression, with manufacturing able to keep up with demand. Given this, the data had to be modified to generate an installation curve similar to the one shown in Haegel et al. (figure 3.5). A very similar ramp-up scenario was proposed in another paper, the **2021 paper from Bogdanov et al.** [6]. In this paper, the authors provides a forecast for PV global installations until 2050, with an overall cumulative capacity predicted of 63.38 TWp by 2050. Even if this number is lower than what more modern literature points to, and even if this paper does not provide a regional division for this capacity, the shape of the capacity evolution matches what is expected. Combining the data coming from the 2023 Keiner et al. [5] and the 2021 Bogdanov et al.[6] papers, with the more qualitative ideas described by Haegel et al [4], led to the final high scenario forecast dataset used in this research. These ideas and concepts were combined, with the methodology explained in the next paragraph, in order to have the following characteristics:

- Installed capacity of 75 TWp in 2050
- Regional division
- A ramp-up similar to the one shown in figure 3.5

3.1.4. High scenario: PV Data Modification

Given the ideas and motivations described in the previous paragraph, this section aims at describing the methods followed to build the high scenario PV installation forecast for this research. First, in the new dataset, the 2050 global capacity should be 75 TWp. In order to obtain this result, the 63.38 TWp scenario from the 2021 Bogdanov paper was scaled up to 75 TWp. This scaling involved progressively increasing the 5-year interval capacity forecasts, with forecasts closer to the year 2050 receiving a larger adjustment than those projected for earlier years. This adjustment was implemented through a simple linear increase in the scaling factor over time, applied specifically to the years 2020, 2025, 2030, 2035, 2040, 2045, and 2050. The scale-up factors used and the results of this operation are reported in table A.7. The scaling factor $S(t)$ at year t can be expressed as:

$$S(t) = 1 + \left(\frac{75 - 63.38}{63.38}\right) \cdot \frac{t - 2020}{2050 - 2020} \tag{3.4}$$

Given a 75 TWp installation scenario, the model still needs a regional division of said capacity. This information was obtained from the 2023 Keiner paper by calculating the share of global capacity that each region was forecasted to have in the original provision. The regional share for region r at year t, denoted as $R_r(t)$, is calculated as:

$$R_r(t) = \frac{C_{r,\text{Keiner}}(t)}{C_{\text{global, Keiner}}(t)} \tag{3.5}$$

where $C_{r,\text{Keiner}}(t)$ is the capacity forecast for region r in the Keiner paper, and $C_{\text{global, Keiner}}(t)$ is the global capacity forecast in the Keiner paper.

Once both the new global installation forecast (scaled to 75 TWp) and the regional shares were calculated, these two figures were multiplied to obtain a scaled-up and regionally divided installation forecast to 2050. The regional capacity $C_r(t)$ at year t is given by:

$$C_r(t) = C_{\text{global}}(t) \cdot R_r(t) \cdot S(t) \tag{3.6}$$

The new installation forecast follows the growth path delineated in the 2021 Bogdanov paper and therefore follows the expected ramp-up described by Haegel, providing the new datasets with all the characteristics described before this paragraph. These results hold the same "shape" of both initial datasets, with forecasts every 5 years starting from 2020 to 2050. Given that the model needs yearly forecast figures, the next paragraph explains how this data was interpolated and extended past 2070.

High scenario: Data interpolation and extension

In the previous paragraph, the methode through which the initial data was calculated for the high scenario is reported; in this section the methodology through which this data is transformed from 5-year values from 2020 to 2050 into yearly values from 2000 to 2070 is explained. First, the high scenario was given the same historical values (2000 to 2023) as the low installation scenario, from the IRENA database mentioned above. In order to have yearly data for capacity forecast, the same procedure explained for the low scenario in subsection 3.1.2 was used. Briefly, this procedure consists of using polynomial interpolation for the data between the provided years (2023 - 2050) and of extending the dataset to 2070 with sigmoid equations, paying attention to the connection between the two functions (polynomial and sigmoid), adjusting the connection if needed.

The results can be seen in figure 3.8, with the plot of all regional installed capacity forecast, and in table 3.2, outlining for every five years the expected regional PV installed capacity. These are the final projections used for the high scenario forecast. Regarding the detail on data interpolation and extension. All the data is available in the tables from table A.1 to table A.6

3.2. PV modules technology model inputs

PV modules can be described by their **technological performances** and by their **material characteristics**. Both technological and material characteristics are necessary to explore and model waste projections. In this project, only crystalline silicon-based modules will be considered. Therefore **the installed capacity figures presented above are reduced by 15%**. This is assumed to be a valid balance between the historical share of thin films and the future projected market. In recent years the share of thin film, around 15% until 2010, started to decrease to roughly 5% of market share in more recent years. In this research, the figure of 15% is used for every year given

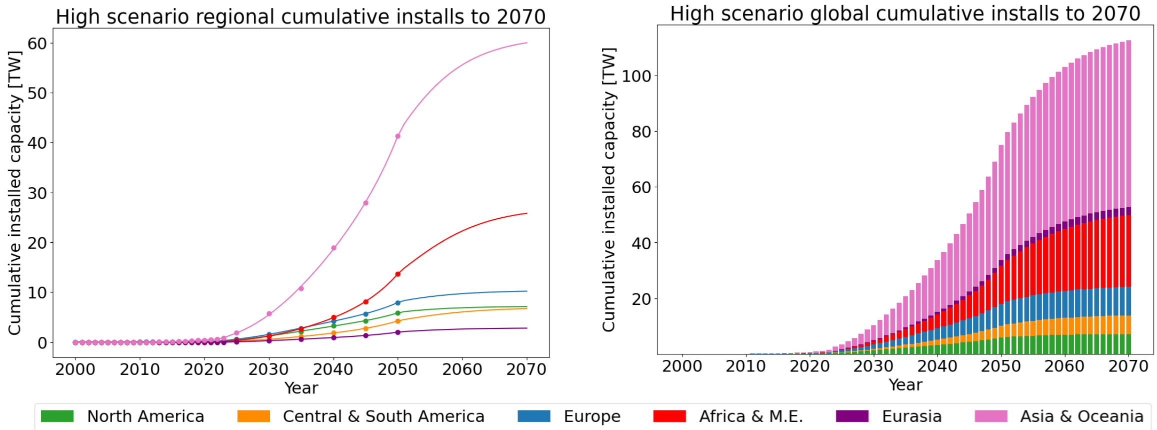

Figure 3.8: High scenario 2070 PV installation forecast. The dots on the (left) figure represent the provided forecast, while the lines indicate the interpolation and data extension peculiar to this research.

Year	North America	C. & S. America	Europe	Africa & M.E.	Eurasia	Asia & Oceania	**Global**
2023	0.16	0.05	0.30	0.03	0.00	0.87	**1.42**
2025	0.44	0.19	0.60	0.34	0.08	1.84	**3.49**
2030	1.23	0.59	1.56	1.23	0.30	5.50	**10.40**
2035	2.20	1.14	2.82	2.73	0.59	11.18	**20.67**
2040	3.22	1.83	4.20	4.91	0.92	18.60	**33.68**
2045	4.32	2.78	5.72	8.16	1.34	28.05	**50.37**
2050	5.85	4.24	7.94	13.66	2.00	41.27	**74.96**
2055	6.56	5.33	9.11	18.61	2.40	50.23	**92.24**
2060	6.88	6.05	9.72	22.27	2.62	55.56	**103.11**
2065	7.04	6.49	10.04	24.57	2.75	58.49	**109.38**
2070	7.12	6.73	10.20	25.82	2.81	59.98	**112.66**

Table 3.2: High installation scenario cumulative installations [TW]

that the ITRPV report foresees growth in the thin film market for applications like BIPV (Building Integrated PhotoVoltaics), floating PV, and other applications like cars, drones, and portable electronics.

Technological performance of a module incorporates all those characteristics that are necessary to describe the performance of a module and its evolution with time. This includes the module's efficiency, degradation rates, reliability, and the module's expected economical lifetime. The second fundamental list of characteristics needed to model a photovoltaic fleet are material characteristics. These include all of those elements that describe the physical side of the module, such as the year-specific material composition. In the introduction chapter, it was underlined how module technology has changed significantly since the beginning of PV and will do the same in the future. In this research different cell technologies are not explicitly considered, the figures used for material characteristics come from averaging out the features of different module technologies based on their past, current, and future market share. For this project, already existing datasets developed at NREL on technology and material characteristics are used. These datasets are only provided until 2050 and combine different historical data and forecasts, the datasets are characterized by a yearly evolution of PV technologies until 2030. The 2030 values are then repeated for every year until 2050; in this research, with a temporal scope that goes until 2070. the values are repeated for all the years between 2050 and 2070. This assumption should not have significant impact on the results given that later - installed modules will not show up in the end-of-life streams. All of the sources of these datasets were cited in section 2.2.In the GitHub repository of PV ICE (`https://github.com/NREL/PV_ICE/tree/main/PV_ICE/baselines`), all the material baselines used in this project can be found. In the next section of the report, the methodology used to transform capacity installations to mass are reported. This is the step that allows to keep track of all the materials deployed in the field for when they reach end of life.

Calculation of Material Mass from Installed Capacity

The following steps outline the process to calculate the total mass of materials used in photovoltaic modules based on the installed capacity in watts. The following operations are done every time new capacity is given in input, relative to a certain year. Given the year when the capacity is installed, the mass calculation takes into account the technological characteristics of that year.

Step 1: Calculate the Installed PV Area

The total installed PV area A in square meters (m^2) is calculated from the new installed capacity P , the module efficiency η in percent (%), and the standard irradiance I in watts per square meter (W/m^2). The formula is given by:

$$A = \frac{P \times 10^6}{\eta \times 0.01 \times I} \tag{3.7}$$

where:

- P is the new installed capacity in MW.
- η is the module efficiency in percent.
- I is the irradiance in W/m^2: 1000 W/m^2 for standard test conditions (STC).

Step 2: Calculate Total Material Consumption per Unit Area

To calculate the total mass of a specific material (e.g., glass) used in the PV modules, we use the material mass per unit area m_{material} in kilograms per square meter (kg/m^2). These are values given in input to the model, based on PV material consumption historical and forecasted trends. The total mass M of the material is then given by:

$$M_{\text{material}} = A \times m_{\text{material}} \tag{3.8}$$

where:

- A is the total installed area calculated from Step 1.
- m_{material} is the material mass per unit area in kg/m^2.

Example Calculation for Glass

Using the above formulas, the total mass of glass M_{glass} used in the PV modules is calculated as follows:

$$M_{\text{glass}} = \left(\frac{P \times 10^6}{\eta \times 0.01 \times 1000} \right) \times m_{\text{glass}} \tag{3.9}$$

Combination of All Materials

The total material consumption for the PV modules includes several different materials, each calculated using the same method as shown for glass. The total mass M_{total} is the sum of the masses of all individual materials:

$$M_{\text{total}} = M_{\text{glass}} + M_{\text{aluminum}} + M_{\text{silicon}} + M_{\text{silver}} + M_{\text{copper}} + M_{\text{backsheet}} \tag{3.10}$$

where:

- M_{glass} is the total mass of glass.
- M_{aluminum} is the total mass of aluminum.
- M_{silicon} is the total mass of silicon.
- M_{silver} is the total mass of silver.
- M_{copper} is the total mass of copper.
- $M_{\text{backsheet}}$ is the total mass of the backsheet material.

Each material mass is calculated using its specific mass per unit area as follows:

$$M_{\text{material}} = \left(\frac{P \times 10^6}{\eta \times 0.01 \times 1000} \right) \times m_{\text{material}} \tag{3.11}$$

This comprehensive method ensures that the total material consumption is accurately determined based on the installed PV capacity, module efficiency, irradiance, and specific material properties. In the following paragraphs, the calculation on how much capacity gets installed is explained.

3.2.1. Capacity input: new installed capacity

For how the modeling code was set up, in order to operate the simulation model requires the input of new installed capacity for each year. This figure is crucial as it is directly transformed into new installed area. The new installed capacity used in the global and regional simulations was determined by subtracting the cumulative installed capacity of a given year (as detailed in section 3.1) from the capacity of the previous year. The new annual capacity in year t, denoted as K_t, is calculated using the following formula:

$$K_t = C_t - C_{t-1} \tag{3.12}$$

where:

- K_t is the new annual capacity installed in year t,
- C_t is the cumulative installed capacity at the end of year t,
- C_{t-1} is the cumulative installed capacity at the end of the previous year $t - 1$.

This calculation yields the newly installed capacity as shown in figure 3.9. The two scenarios are reported with different y-axis in order to allow for a good visualization of the low scenario. It is important to emphasize that this "original" new installed capacity does not account for modules installed in order to replace capacity that reaches end-of-life or degrades; it solely represents the additional capacity required to achieve the targeted cumulative installed capacity. The significance of considering new installations prompted by failures and degradation is explored in the results-specific sections of this report.

3.3. Methodology on end of life

In this section, the ways in which the lifetime of modules is simulated is described. In particular with this section the intent is to show how modules can reach their end of life and how these different pathways are modeled. PV modules can reach their End of Life through three different pathways:

- **Excessive degradation**

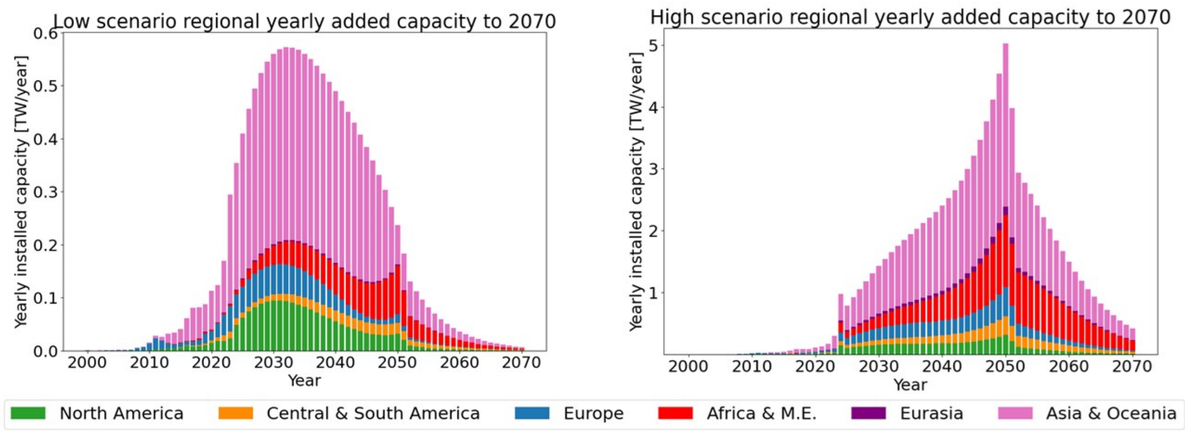

Figure 3.9: Low (left) and high (right) scenario annual new installed capacity to 2070. The two figures are reported with significantly different y-axis in order to clearly show the shape of forecasted installations in the low scenario as well. These plots only show crystalline-based PV yearly projections.

- **Random failures**
- **Economic lifetime**

When a module reaches EoL it is considered **failed**. In the first part of this section, the three pathways toward failure are explained. The theory and reasoning behind the definition of these three pathways was described in section 2.4; in this section, the formulas behind the simulations of the three pathways are reported and justified.

Excessive degradation

During their operation, modules are placed in outdoor conditions; the exposure to light, temperature swings and moisture causes materials to change their optical and electrical properties. This leads to the degradation of the module's ability to transform solar irradiation into electricity. Once the degradation causes the module's performance to drop below a certain threshold, the module is considered outdated and enters the End of Life stream. As already explained, even if module degradation has been found to follow a non-linear evolution, the industry decided to use as standard constant yearly value. This was done in this research as well. The formula that correlates degradation with capacity is the following:

$$C(t) = C_0 \cdot (1 - r)^t \tag{3.13}$$

Where:

- $P(t)$ is the production capacity time t (in years)
- P_0 is the initial capacity
- r is the annual degradation rate (as a decimal)
- t is the time (in years)

Random failures

The outdoor setting and the fragile nature of silicon cells can also lead to random failures during the module's lifetime. Random failures can be caused by multiple factors and stresses such as hail or electrical short circuits. In this reaserch they are modeled by a weibull curve that relates age with probability of failure of a module.

The Weibull distribution is a continuous probability distribution commonly used in reliability analysis and life data analysis. Its probability density function (PDF) is given by:

$$F(x; \alpha, \beta) = 1 - e^{-(x/\beta)^\alpha} \quad \text{for } x \geq 0. \tag{3.14}$$

where:

- α is the **shape parameter**, it influences the form of the Weibull distribution. If $\alpha < 1$, the distribution has a decreasing failure rate, useful for modeling products with higher likelihood of failing early, $\alpha > 1$ is suitable for modeling wear-out failures.

- β is the **scale parameter**; stretches or compresses the distribution along the x-axis. Larger values of β stretch the distribution, indicating a longer characteristic life.
- x is the time in years, starting from the installation year.

From Equation 3.14, it is evident how the Weibull distribution is dictated from the values of the shape (α) and scale (β) parameters. These values should therefore be related with the lifetime expectations of the modules. The main assumption is that only 10% of modules is lost through random failures within the economical lifetime. In order to do so, two figures are calculated and used to dictate the shape of the Weibull curves: T50 and T90. These are, respectively, the time in years at which 50% and 90% of modules have failed. The T50 and T90 figures are calculated for every year to ensure that changes on expected lifetime are reflected on the failure rate. In the following set of equations, the procedure that leads from t50 and t90 to α and β is shown.

The Cumulative Distribution Function (CDF) of the Weibull distribution, which describes the probability that a random variable X will take a value less than or equal to x,is given by:

$$F(t) = 1 - e^{-(t/\beta)^{\alpha}} \tag{3.15}$$

If we apply the definition of t_{50} and t_{90} to the concept of CDF we obtain that:
For t_{50}:

$$\begin{aligned} F(t_{50}) = 1 - e^{-(t_{50}/\beta)^{\alpha}} &= 0.50 \\ e^{-(t_{50}/\beta)^{\alpha}} = 0.50 \quad \Rightarrow \quad -(t_{50}/\beta)^{\alpha} &= \ln(0.50) \end{aligned}$$

For t_{90}:

$$\begin{aligned} F(t_{90}) = 1 - e^{-(t_{90}/\beta)^{\alpha}} &= 0.90 \\ e^{-(t_{90}/\beta)^{\alpha}} = 0.10 \quad \Rightarrow \quad -(t_{90}/\beta)^{\alpha} &= \ln(0.10) \end{aligned}$$

Taking the natural logarithm of both sides, we get:

$$\begin{aligned} (t_{50}/\beta)^{\alpha} &= -\ln(0.50) \\ (t_{90}/\beta)^{\alpha} &= -\ln(0.10) \end{aligned}$$

Dividing these equations, we obtain:

$$\left(\frac{t_{50}}{t_{90}}\right)^{\alpha} = \frac{\ln(0.50)}{\ln(0.10)} \tag{3.16}$$

Solving for α:

$$\alpha = \frac{\ln(\ln(0.10)) - \ln(\ln(0.50))}{\ln(t_{90}) - \ln(t_{50})} \tag{3.17}$$

Once α is found, β can be calculated using either t_{50} or t_{90}:

$$\beta = \frac{t_{50}}{(-\ln(0.50))^{1/\alpha}} = \frac{t_{90}}{(-\ln(0.10))^{1/\alpha}} \tag{3.18}$$

Therefore:

$$\begin{aligned} \alpha &= \frac{\ln(\ln(0.10)) - \ln(\ln(0.50))}{\ln(t_{90}) - \ln(t_{50})} \\ \beta &= \frac{t_{50}}{(-\ln(0.50))^{1/\alpha}} = \frac{t_{90}}{(-\ln(0.10))^{1/\alpha}} \end{aligned}$$

The process shown above relates the weibull curve to the t_{50} and t_{90} parameters. As stated above, these parameyers are closely related to the expected economical lifetime of modules; in particular the main assumption, as already stated, is that only 10% of modules will fail during the economic lifetime of a module. This means that the assumed economic lifetime of a modules coincides with an hypothetical t_{10}. From this value, t_{50} and t_{90} are calculated with the following formula:

For t_{50}:

$$t_{50} = t_{10}\left(\frac{-\ln(0.50)}{-\ln(0.90)}\right)^{1/\alpha} \tag{3.19}$$

For t_{90}:

$$t_{90} = t_{10}\left(\frac{-\ln(0.10)}{-\ln(0.90)}\right)^{1/\alpha} \tag{3.20}$$

As is clearly visible from the formulas above, both t_{50} and t_{90} are related to t_{10} through α. This calls for the need of an iteration between the formulas introduced thus far in order to find the values of t_{50} and t_{90} starting only from t_{10}. The steps to follow for this iterative calculation are:

1. **Initial Guess**: Start with an initial guess for the shape parameter α.

$$\alpha_0 = 1.5 \quad \text{(or any reasonable initial guess)} \tag{3.21}$$

2. **Calculate** β: Using the initial guess for α and the given t_{10}, compute β.

$$\beta = \frac{t_{10}}{(-\ln(0.90))^{1/\alpha}} \tag{3.22}$$

3. **Compute** t_{50} **and** t_{90}: Calculate t_{50} and t_{90} using α and β.

$$t_{50} = t_{10}\left(\frac{-\ln(0.50)}{-\ln(0.90)}\right)^{1/\alpha} \tag{3.23}$$

$$t_{90} = t_{10}\left(\frac{-\ln(0.10)}{-\ln(0.90)}\right)^{1/\alpha} \tag{3.24}$$

4. **Check Convergence**: Compare the calculated t_{10} with the given t_{10}. If they are sufficiently close, the process has converged. If not, adjust α and repeat the process.

Once this operation comes to convergence, the value for β can be calculated as well and used for the simulation of random failures.

Economical lifetime

The third and last cause of modules reaching End of Life are economical considerations. Owners of both large-scale and rooftop solar photovoltaic systems may consider replacing their modules before they fail unexpectedly or suffer excessive degradation. This decision is often influenced the cost-effectiveness of new modules, which offer improved performance and can justify the initial investment. The implementation of this pathway is straight forward; once modules installed reach the end of their economical lifetime, they get removed. Only the modules that have not failed through one of the other paths are removed at the end of the economic lifetime. This pathway might not reflect a real-world scenario where system owners extend the lifetime of their fleet past the economic lifetime. The effects of such considerations are tested and discussed in section 4.3.

Modeling End of Life; a summary

The overall capacity of PV modules over time, considering degradation, random failures, and economic lifetime, can be expressed as:

$$C_t(t) = \begin{cases} C_{t_0} \cdot (1-r)^t \cdot e^{-(t/\beta)^\alpha} & \text{if } t \leq \min(t_{econ}, t_{deg}) \\ 0 & \text{if } t > \min(t_{econ}, t_{deg}) \end{cases} \tag{3.25}$$

Where:

- C_t is the remaining capacity at year t, originating from the capacity installed at year t_0.

- C_{t_0} is the initial capacity installed in year t_0.
- r is the annual degradation rate.
- α and β represent the shape and scale parameters of the Weibull distribution, modeling the rate and pattern of failures.
- t_{econ} is the economic lifetime (in years)
- t_{deg} is the time at which the production capacity degrades to 80% of it's rated capacity due to degradation alone.
- t is the time in years passed from the year of installation t_0.

The degradation lifetime t_{deg} is defined as the time it takes for the module's capacity to degrade to 80% of its initial value:

$$t_{deg} = \frac{\log(0.8)}{\log(1-r)} \tag{3.26}$$

The combined equation provides a holistic view of the PV module's capacity over time, incorporating the effects of degradation, random failures, and economic considerations. The production capacity declines over time due to degradation, which is modeled by the factor $(1-r)^t$, and random failures are accounted for using the Weibull survival function $e^{-(t/\beta)^\alpha}$, representing the probability that a module will still be functioning at time t. The remaining capacity installed is then considered to reach EoL when t exceeds the minimum of the economic lifetime t_{econ} and the degradation lifetime t_{deg}, at which point the capacity $C_t(t)$ is set to zero. This approach must be applied annually to each new cohort of installed modules, as each group has their own lifetime characteristics. Tracking the evolution of each "annual" cohort individually allows for dynamic modeling, with lifetime characteristics adapting year over year based on the actual conditions experienced by the modules. This section analyzed how modules are modeled to reach their end of life. In the next section the need for substituting these modules is explained, specifying the procedure through which the amount of capacity to replace is calculated.

3.4. Replacing lost capacity

In section 3.3, the paths through which a module can reach EoL are explained and discussed. It is described how modules can fail through three pathways and the formulas that dictate these are reported. While excessive degradation is reported as one of these possible causes it is necessary to say that this pathway should theoretically happen with low frequency given that warrant times should take into account degradation, and not allow modules to degrade below 80% during the operational lifetime. While this is true, degradation will still occur and needs to be considered when discussing new installation and deployed capacity. The main assumption regarding installed capacity in this research is that both capacity lost through degradation (but still deployed) and capacity failed and removed needs to be re-powered, every year, to allow for adequate production capacity. The projections used in this research come from models that simulate future energy demand; these models usually operate by dividing the forecasted required energy production among different energy-producing technologies, such as PV, wind, nuclear, etc... . This means that provided forecasts for PV installations denote the installed photovoltaic capacity necessary to sustain a future energy system. If degradation and failures of modules were neglected, this would lead to an active capacity that is lower than anticipated. Consequently, PV would contribute less than expected to the grid, reducing the available energy in the system. It is, therefore, necessary to add extra capacity to make up for the lost capacity (degraded + reached EoL). This operation will be indicated in the remainder of this research as **replacing lost capacity**.

To accomplish this, we first calculate the capacity lost without any replacements by running simulations with only the "original" yearly installed capacity projected from new installations (figure 3.9). This simulation accounts for degradation and capacity loss that occurs naturally over time, as described in the previous section of the methodology; these results are stored and they indicate, for every year, how much capacity would be there if only the originally forecasted demand was installed; not considering any replacement to lost capacity. Subsequently, for the second year considered in the time domain, the first where degradation of capacity is visible, the effective cumulative capacity (without replacements) is compared against the planned cumulative installed capacity (original capacity planned). The difference between the expected and the actual capacity without replacements determines the necessary adjustments to the corresponding yearly new installed capacity. This operation then determines the necessary new installed capacity in year 2, made of the originally planned new capacity and the necessary adjustment. The simulation process is then run again, and the new cumulative capacity for year 3 is found. This capacity, will be lower than the expected one; a new extra addition to the yearly installations in year 3 will be calculated and added to the new installation figure of that year. This operation will allow that at the end of the year, cumulative capacity equals what is expected. This operation is then repeated for all the years considered.

The operation detailed above is necessary to ensure that the total capacity of the photovoltaic system meets the projected demand by compensating for both the decline in operational capacity due to aging and failures. This calculation incorporates both the expansion needs and the losses experienced by the system through modules degrading and through modules reaching End of Life. Itrepresents the real photovoltaic demand to be expected in the coming years. In the next section, the formulas behind this operation are listed and explained.

Components of the Calculation

1. **Projected Expansion (K_t)**: This is the forecasted new installation requirement for the year, based on the anticipated demand and system expansion plans.
2. **Degradation and End-of-Life Losses**: This accounts for the reduction in available capacity due to the natural aging of modules and modules reaching their lifespan end, either through physical degradation or economic obsolescence.

Calculating the Expected and Actual Capacities

The goal is to determine how much capacity has been lost between the end of the previous year ($t-1$) and the start of the current year (t), and to establish how much new capacity needs to be installed to not only fill this deficit but also meet the new capacity requirements.

Expected Capacity at the Start of Year t

$$\text{Expected Capacity at the start of } t = \sum_{i=0}^{t-1} C_i \cdot (1-r)^{t-1-i} \cdot e^{-((t-1-i)/\beta)^{\alpha}} \tag{3.27}$$

Actual Remaining Capacity at the Start of Year t

$$\text{Actual Remaining Capacity at the start of } t = \sum_{i=0}^{t-1} C_i \cdot (1-r)^{t-i} \cdot e^{-((t-i)/\beta)^{\alpha}} \tag{3.28}$$

Formula for Required Annual Installation (A_t)

The additional capacity needed each year, A_t, is calculated by adding the projected new capacity requirements to the net loss of capacity observed due to degradation and the end of operational life:

$$A_t = K_t + (\text{Expected Capacity at the start of } t - \text{Actual Remaining Capacity at the start of } t) \tag{3.29}$$

This calculation ensures that each year's installations are sufficient to maintain the system's operational effectiveness by replacing lost capacity and accommodating new growth.

$$A_t = K_t + \left(\left(\sum_{i=0}^{t-1} C_i \cdot (1-r)^{t-1-i} \cdot e^{-((t-1-i)/\beta)^{\alpha}} \right) - \left(\sum_{i=0}^{t-1} C_i \cdot (1-r)^{t-i} \cdot e^{-((t-i)/\beta)^{\alpha}} \right) \right) \tag{3.30}$$

Where:

- A_t is the capacity required to be installed in year t.
- K_t is the projected capacity expansion needed in year t.
- C_i is the capacity initially installed in year i.
- t_{econ} and t_{deg} represent the economic and degradation lifetimes, respectively.
- α and β are the Weibull distribution parameters affecting the probability of failure over time.
- $(1-r)^{t-i}$ models the remaining capacity after accounting for degradation.

For example, if initially in year X 500 MW of new installations were predicted to achieve 2 GW of cumulative installations but after the simulation it is found that, due to capacity loss, the total installed capacity in year X would only reach 1.8 GW, an additional 200 MW is needed, increasing the new installations in year X to 700 MW. This formulation ensures the accurate tracking and compensation of capacity loss due to degradation and end-of-life each year, facilitating effective and sustainable capacity management in PV systems.

By running the simulation annually and incorporating the additional capacity, we ensure that each year's new installations not only contribute to increasing the total cumulative capacity but also compensate for the lost capacity due to aging. This approach also ensures that any modules installed to replace old capacity undergo the same lifetime simulations, contributing to the overall End-of-Life (EoL) volumes. This methodology is consistently applied every year covered in the research. While it might not be extremely precise for the "historical" years, the real impact of replacements becomes evident in the later years of the century (figure 4.10). Choosing a different method for managing replacements before 2024 would add unnecessary complexity to the code without changing the results.

This section explored the methodology followed for determining replacement capacity and the need for including this particular aspect, in the next section the assumptions made on reselling and reusing of modules made in this research are explained.

Reselling and reusing

This section explores the assumptions reselling and reusing of PV modules in this research. Reselling and reusing are two concepts that can easily be linked with photovoltaics sustainability and EoL calculations. They refer to the possibility that modules that get dismounted because of economical considerations, can get deployed again somewhere else if their performance is still adequate. This can happen once expected lifetime is over or due to early terminations of projects, determined by economical calculations.

A general guideline for selecting modules that are suitable for reuse is that the production power available in the modules is greater than 90% when the economical end of life is triggered.

In this research, the possibility of reselling is not taken into account because of the following considerations:

- All the modules deployed in the same year are given one and steady degradation rate. These means that when modules reach the end of their economic lifetime, they will all have degraded past the 90% threshold. To put this number into perspective, modules would have to experience a degradation rate of 0.35% per year, something that is possible in real module applications but that is not foreseen by this research.
- This research does not consider the possibility of a dynamic economical lifetime. All the modules installed in a specific year will be dismantled at the end of their predicted lifetime, if they don't fail through one of the other two presented pathways. The idea that a system owner decides to change its fleet before the expiration of their economical lifetime because of other considerations (breakthrough in new photovoltaics modules leading to much higher efficiency for example).
- In recent years, the resale market for modules has been particularly volatile, with limited data available on resold units. Currently, the majority of modules entering the resale market are older units. These are primarily sought for replacing modules that have failed or degraded in systems, where such issues have led to a power output too low for the deployed inverter. This gives today's reselling market a marginal role and makes forecasting hard.

To some extent the concept of reselling could be associated with the concept of merchant tail explored in section 4.3. With merchant tail, it is indicated the possibility that modules were left on the field past their economical expected lifetime, in order to keep producing until excessive degradation or random failure. At first, one might think that modules that are interested by merchant tail could potentially be associated with modules that get removed from their original location and reused/resold at different locations, locations where performance is not valued as much. While this might be close to reality for some specific situations, merchant tail and reselling differ significantly for the absence of logistics in merchant tail. In merchant tail scenarios, modules keep being deployed in the same location where they were originally installed, with the same mounting and the same inverter. With reselling, modules need to be picked up, transported, installed and connected in a different location adding significant costs that would probably make the whole operation not economically viable. The potential for reselling is therefore not explored in this research.

The above sections outlined the steps and procedures followed in the calculation of PV installation forecasts and in the simulation of the lifetime of modules. In the following section, we introduce the tool that facilitated these calculations: PV ICE.

3.5. PV ICE and its functions

This paragraph explains and defines the python based model this research uses to model End of Life and waste flows: PV ICE. PhotoVoltaics In the Circular Economy or PV ICE is an open-source Python-based tool developed at the National Renewable Energy Laboratory (NREL) to study and assess mass and energy flows in the PV industry [68]. The complete model can be found here: *https://www.nrel.gov/pv/pv-ice-tool.html*.

The model provides built in functions that allow for two main things:

- Calculate the installed area from capacity.
- Simulate the lifetime and aging of modules, applying degradation and “killing” modules once they reach EoL through one of the three pathways.

In order to run, the model requires inputs on historical and forecasted characteristics of PV. This is done through two input files defined as “baselines”. Baselines are .csv files in the form of annual time series. The first baseline needed incorporates **technology-based data**. This includes, for every year scope of the modeling, newly installed PV capacity, module efficiency, degradation rates, end-of-life paths, and lifetime and reliability parameters. End-of-life paths indicate the share of modules that will follow each of the potential outcomes possible once they are dismounted; outcomes such as landfilling, recycling, and reusing, among others. The details regarding input lifetime and reliability parameters will be explained in the following chapters. As explained in previous sections of this research, these data are assumed to change year over year in line with literature consensus. For the sake of this research, all the circularity paths were set to zero, meaning that when a module reached EoL all of its materials were sent to landfill. This allows to see and analyze the total amount of PV material ready to be potentially recycled.

The second dataset and input relevant to PV ICE incorporates **material-specific data**. For every material discussed and analyzed, such as copper, silicon, and glass, manufacturing and processing data needs to be made explicit and fed to the model. This data contains material usage for photovoltaics in grams per square meter, material manufacturing efficiencies from virgin material to final product, and data on recycling efficiency. This information needs to be provided for every year included in the simulation. Once both files are given in input, the software converts newly installed capacity from capacity in watts to the equivalent photovoltaic area, in squared meters. For the sake of this reaserch, these parameters were taken from NREL research.

Once all the data is and processed, the **mass flow** or lifetime simulation calculation can start. This operation simulates the aging and failure of the installed fleet following the three EoL pathways explained above, and applying the formulas described in the previous sections. The simulation provides in output several parameters regarding PV End of Life, both regarding lost capacity and produced waste mass / volumes . In the following section the relation between PV ICE and the rest of the model can be observed.

3.6. Flowchart of the Model

figure 3.10 shows the flowchart behind the methodology explained thus far. The yellow boxes indicate what happens thanks to PV_ICE, following the details explained above and the formulas shown in this chapter.

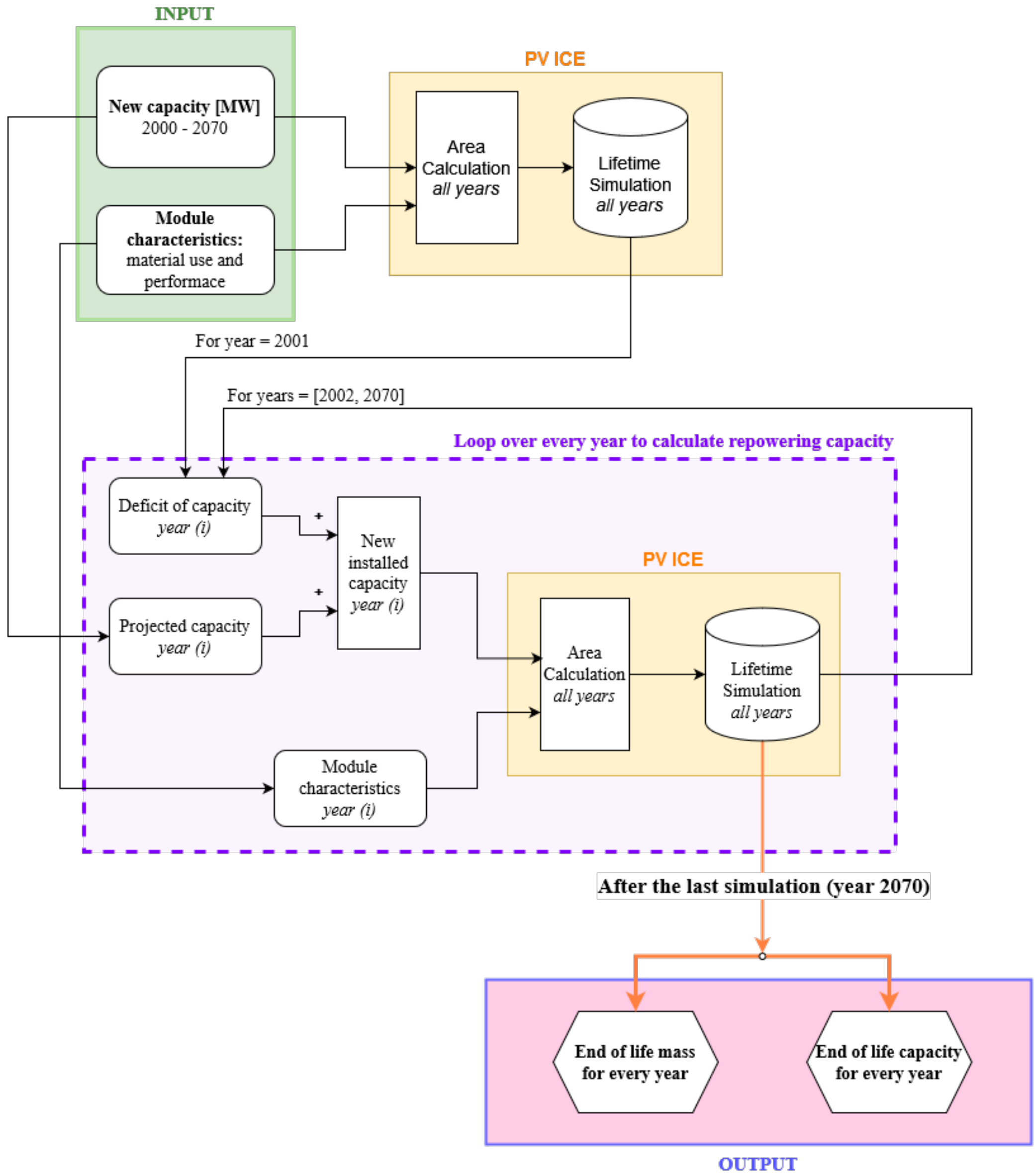

Figure 3.10: Flowchart of the research methodology

4

Global Projections

In this chapter, the findings regarding PV End of Life at the global level will be presented and analyzed. The analysis will be done for both the two installation scenarios presented in the previous chapter. First, a base scenario will be analyzed and compared with previous literature findings. The base results will then be compared with other scenarios, where particular aspects of the base inputs will be changed and the differences analyzed. In particular the scenarios will explore how changing the merchant tail, reliability and degradation rates affect the base global results. For the base analysis and for the scenario, both the high and low installation forecasts will be used. To better put into perspective the differences between the high and low installation scenario, fundamental to better reflect on the contrast of the results, figure 4.1 shows the two installation scenarios plotted with the same y-axis. The graphs only show the share of crystalline silicon in the total installed capacity (85%), given that this research only analyses crystalline silicon.

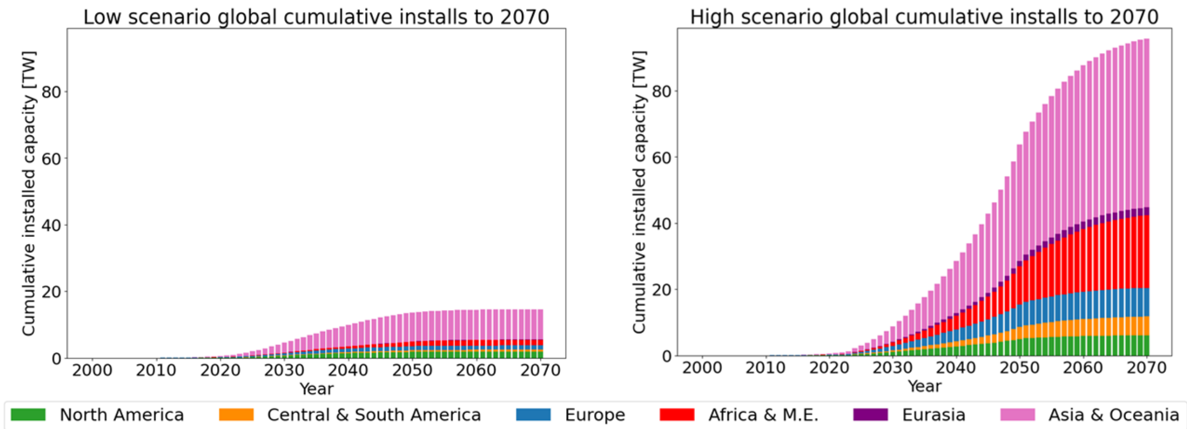

Figure 4.1: Comparison of forecasted crystalline silicon capacity in the two scenarios

Before analyzing the results, it is important to define what the figures that will be discussed actually represent. With End-of-Life volumes, it is intended the amount of photovoltaic material that is modeled to enter End of Life. It is important to note that this does not necessarily make it waste, this material could be collected and go through one of the sustainability pathways such as recycling or, if in good conditions, reusing. In the following graphs, the volumes represent the material that will be potentially available for recycling, therefore EoL volumes.

4.1. Base scenario

4.1.1. Assumptions and justifications of the base scenario

In this section of the report, the base scenario is explained and its results discussed. The results in this section should be considered as the base findings of this research and will be compared with previous literature. figure 4.2 shows the input degradation rates and project lifetime used in the base scenario. These evolution trajectories come from forecasts made at NREL. Lifetime projections come from a Lawrence Berkeley Laboratory study [69]. and

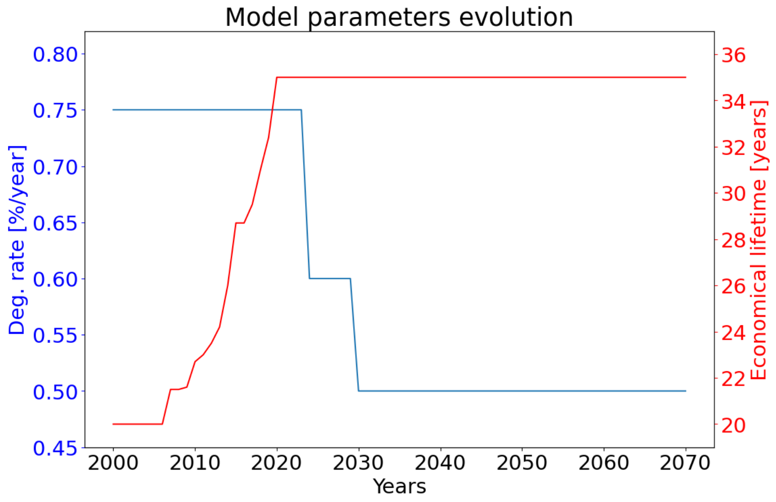

Figure 4.2: Base scenario parameter evolution; the left axis and the blue line indicate degradation rated considered, the red one together with the y axis show the economical lifetime considerations made in the base scenario of the global installation forecast.

indicate the values that is most often used in LCOE calculations, therefore the expected lifetime of a system. This value is not the warranty period given by module manufacturers, but the expected lifetime of systems. The projections are forecasted to stay at a constant level from 2020 to 2070 at 35 years, seen as a standard value today. In the base results, there is no possibility of life extension through merchant tail. Merchant tail indicates the possibility of extending a module's operations past its projected lifetime, even if the module is still in good condition. The effects of merchant tail will be explored in section 4.3.

Regarding degradation rates, in this research was decided to use the the -0.75%/year degradation rate for all the historical years, from 2000 to 2023. This decision came from the fact that papers that describe the state of degradation of PV modules in real installations, do not differentiate between the years of installations of modules. Since the 2016 ITRPV report, modules were reported to degrade at a rate below 0.7, with the latest ITRPV reporting degradation rates below 0.5% [25, 70]. Module manufacturers provide as well degradation rates in their warranty sheets, which go from -0.7 to -0.5 for different modules. The main issue with using the data provided from these sources is that modules degrade faster when installed in a system rather than when tested and degraded on their own [52, 53]. This led to the choice of using recorded field degradation data for modules installed in historical years (2000 - 2023). There is also a more nuanced consideration that can be made on this point; the degradation rates announced by module manufacturers are designed to assure consumers of the product's durability and reliability. However, these modules' actual lifespan and efficiency may not meet the optimistic projections set at the time of purchase. It is a real possibility that given the rapid economic returns of solar PV, especially if combined with financing schemes, manufacturers might anticipate that only a minority of consumers to actively pursue a warranty claim decades after installation, when modules potentially under-perform promises. On the other hand, module manufacturers might not support future insurance claims, indicating that the excessive degradation was caused by the mounting configuration, and not by the module itself. These possible practices raise important questions about the confidence in product longevity and the realistic expectations consumers should have regarding the performance of their solar installations over such extended periods. This is the reason why in the possibility that degradation rated will not improve is tested, discovering the impact of flat degradation rate (at -0.75%/year) would have on cumulative EoL volumes and on PV demand.

4.1.2. Global cumulative EoL volumes to 2050

In this section the global cumulative EoL volumes to 2050 will be shown and compared with the results found in the 2016 IRENA-IEA paper [40]. The 2016 figures are, as explained in section 3.3, product of a methodology that is not anymore suited for the standards of today's photovoltaics and are based on extremely low forecasts for PV (5TWp in 2016 compared to the 16-75 TWp of the low and high scenario). In the 2016 paper, only the waste coming from modules reaching end of life was considered. In this research as well, only the potential waste coming from modules reaching end of life is considered, ignoring the waste produced in the mining and manufacturing phases. This decision allows for the comparison with the 2016 figures but leaves out some impor-

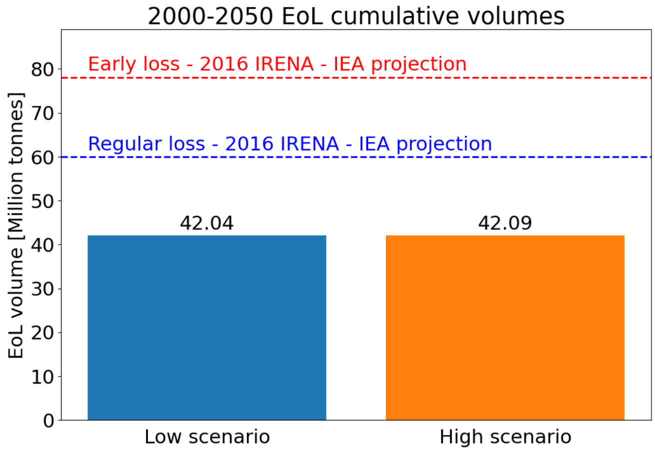

Figure 4.3: Low & high scenario global cumulative volumes to 2050 compare with the results from the 2016 Weckend et al. paper in the regular and early loss scenarios. While the new methodology considers higher installation volumes, higher quality and reliability of new modules leads to lower random failures, leading to lower cumulative volumes.

tant consideration on the circularity of photovoltaic modules. In figure 4.3 the cumulative results are shown and compared with the two scenarios from the 2016 paper.
The results reported in figure 4.3 can be analyzed through the two main aspects:

- The **similarity of results** between in the two scenarios.
- The **relation with the 2016 results**, with new estimations being lower than literature.

Similarity of the results of both scenarios in 2050

Even if the forecast installations for the two scenarios, shown in figure 4.1, are considerably different, the 2050 cumulative EoL volumes are very close. While it might seem counter-intuitive at first, after some considerations it is expected for the two scenarios to present similar cumulative volumes in 2050. Modern module technology is associated with an expected lifetime of around 30 to 35 years. This means that the cumulative 2050 volume is made up mainly of modules installed around 2020. Therefore, the modules that reach EoL are mainly made up of modules installed in years where the data used is historical and therefore the same in both scenarios. In subsection 4.1.3 the cumulative results for 2070 will be shown, exposing the true divergence of the two scenarios.

Comparison with 2016 results

The obtained results are smaller than both scenarios presented in the 2016 paper. This shows that, even though the installation forecast used in this research is much higher than what was expected in 2016, the influence of the End of Life methodology is greater. In order to better visualize the novelty of this methodology, figure 4.4 compares the above presented findings with 2050 cumulative EoL volumes calculated using the 2016 methodology and the new installation projections; for both scenarios. In the graph, low scenario results are darker while high scenario results are lighter; it is clear how using the old methodology not only produces much higher results, but underlines the difference between the two scenarios in terms of waste volumes. For the *regular loss* methodology 109 and 178 million tons are forecasted for the low and high scenario respectively. Using the early loss methodology, the difference with the new methodology grows even more, reaching 199 and 431 million tons in the low and high installation forecasts scenarios. This difference is justified by the more frequent early losses of modules in the old methodologies, a factor that significantly separates the two installation scenarios in terms of waste volumes already in 2050.

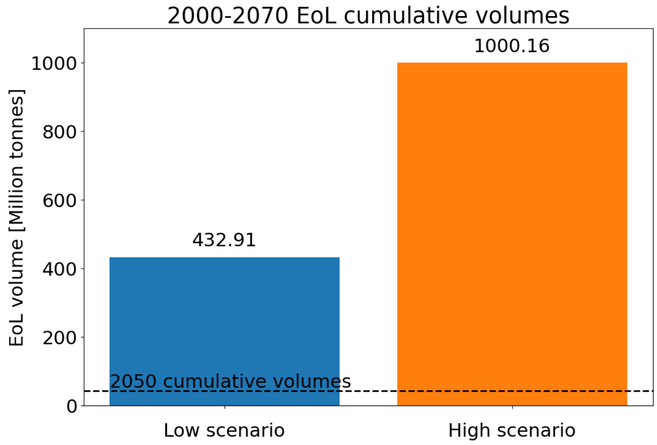

Figure 4.5: Low & high scenario global cumulative volumes to 2070, compared with the 2050 volumes found in this research. The 2050 volumes are common for both high and low scenarios, therefore only one line.

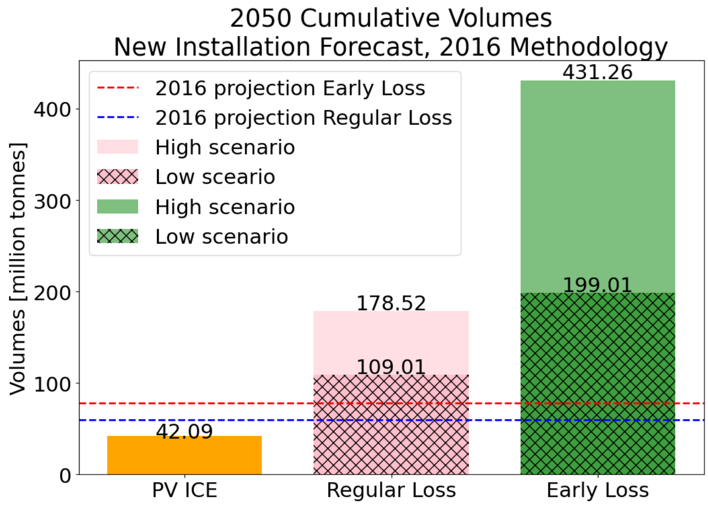

Figure 4.4: Old methodology applied to new installation forecasts: the orange bar represents the results obtained in this research, pink bar the results for high and low scenario using the "Regular loss" methodology from 2016 with today's projections, while the green bar applies today's projections to the 2016 "Early loss" methodology.

4.1.3. Global cumulative EoL volumes to 2070

In this section, the same figures shown above for 2050 are reported for the year 2070. In figure 4.5 the cumulative EoL volumes are shown.

The cumulative 2070, contrary to the 2050 results, clearly show the divergence between the two scenarios. The high scenario, with 1000 million tonnes of cumulative EoL material, is around 2.3 times higher than the 433 million tonnes forecasted for the low scenario. The results are validated by the ratio between the installed capacity forecast of the two scenarios for the year 2035, 35 years before 2070. In figure 4.5 the findings are as well compared with the 2050 results. The relation with the 2050 numbers is remarkable for both scenarios. Respectively for the low and high installation scenarios, the 2070 volumes are 10 and 24 times higher than the 2050 volumes. These differences make it clear that most volumes will come towards the end of the century. If the analysis was further extended past 2070, the difference between the two scenarios would further increase, given that the majority of the difference in cumulative capacity is recorded after 2035. In the next section of the report, the timeline of expected EoL flows is shown, together with the materials that will be potentially available for recycling.

4.1.4. Material streams & trends

In the previous section the total cumulative 2050 and 2070 volumes were shown. This section will present a deeper dive into the expected cumulative volumes of EoL material and their composition.

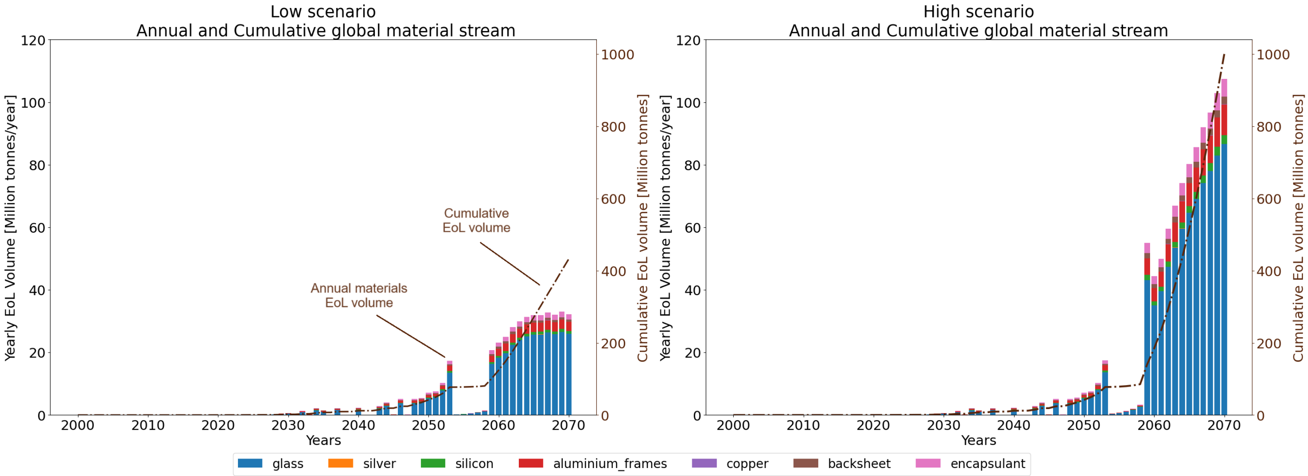

Figure 4.6: Low (left) & high (right) scenarios annual (bars - left axis) and cumulative (line - right axis) material streams to 2070. The two scenarios start to spread apart after 2060. The reason behind the draught in the years preceding 2060 will be explained in subsection 4.1.5

		Glass	Silver	Silicon	Aluminium	Copper	Backsheet	Encapsulant
EoL material [million tons]	Low scenario	342.49	0.09	12.20	41.80	0.25	11.52	24.56
	High scenario	797.55	0.17	27.47	93.98	0.57	25.16	55.22
Share of total weight		79.11%	0.02%	2.82%	9.65%	0.06%	2.67%	5.67%

Table 4.1: Cumulative 2070 EoL material composition, scenario comparison.

figure 4.6 shows the annual and cumulative modeled material flow for the two scenarios for every year between 2000 and 2070. Both scenarios have a similar evolution until around 2060, with volumes growing relatively constantly until 2053 then dropping between 2054 and 2058. After 2058 the two scenarios start to diverge significantly. The reason behind the drop in volumes between 2050 and 2060 resides in the End-of-Life causes which will be explained in the following section. The shape of both plots further demonstrates the comments made in the section above regarding the timing of waste volumes; these will rise significantly after 2060. Table 4.1 shows the cumulative 2070 materials volumes, together with the relative shares of each material in the total EoL material. Glass makes up the vast majority of the weight, contributing to around 80% of weight in both scenarios. Aluminium is the second biggest contributor with around 10% of share in the total weight. The encapsulant represents a bit more than 5% of weight while silicon and backsheet are responsible for around 3% of weight. Copper and silver are both below 0.1%. This means that only around 20% of the total waste stream will be composed of non-glass materials. The impact of this amount of glass waste will be analyzed for Europe in chapter 5.

4.1.5. Causes of End of Life

This section shows the causes that lead modules to failure. As mentioned in the methodology section, a module reaches failure (End of Life) through three possible pathways: random failures dictated by a Weibull function, degradation above 80% of rated capacity and economical lifetime dictated by project lifetime.

In figure 4.7 and figure 4.8 the amount of capacity lost through failures is shown, along with the respective shares of causes that led to failure. In both scenarios, economic lifetime is by far the biggest cause of failures, accounting for 85% of total failures in the low scenario and for 91% in the high scenario. In both scenarios, random failures account for around 4% of failed capacity while degradation accounts for 11% in the low scenario and for 5% in the high scenario. If the evolution of failures is taken into account, it is clear to see that the two scenarios present a very similar evolution until 2060, to then diverge. Random failures are dominant in the first years of the century (between 2000 and 2020), when overall volumes are too small to be visible in the plot. After 2020 modules begin to hit their lifetime projection, leading to economical failures in some years between 2020 and 2046. Economical failures disappear around 2050 to then “come back” in 2059 and stay until 2070. The years around 2050 are dominated by failures caused by degradation, a path that should technically not occur. Later in this paragraph, the causes of this effect are explained. What is also clearly visible is the minimal amount of failures in the years between 2054 and 2058. This “valley” is visible as well in figure 4.6 between the same years.

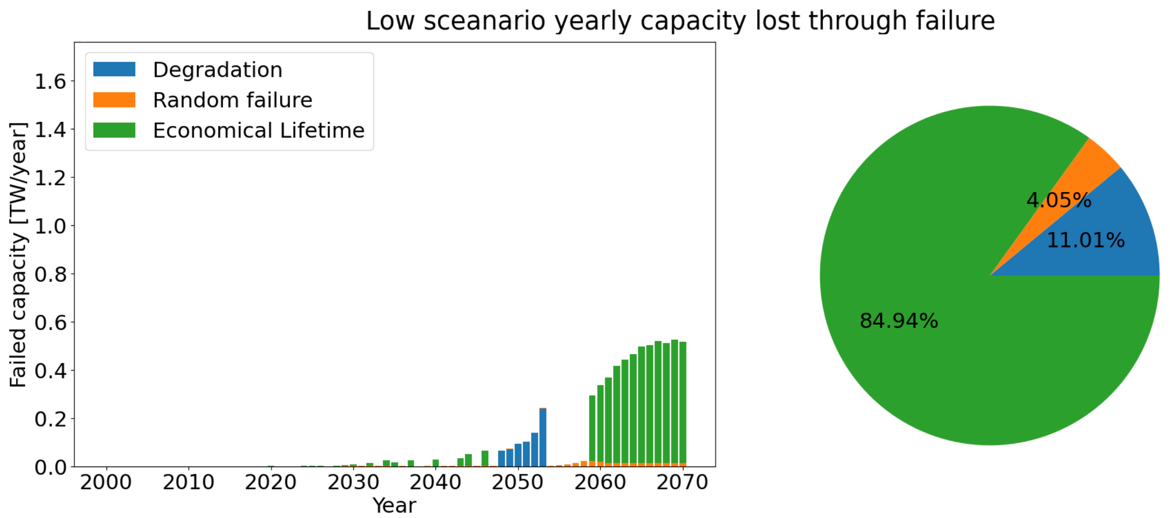

Figure 4.7: Low scenario causes of failure and share of each EoL path in the total. The main cause of EoL is economic lifetime. Followed by excessive degradation (found in the years around 2050) and random failure.

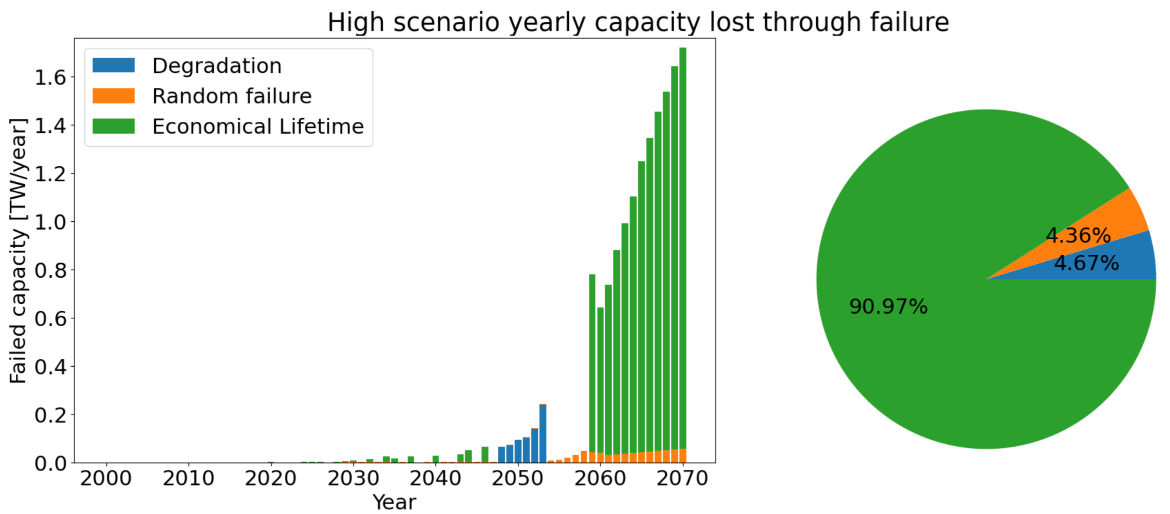

Figure 4.8: High scenario causes of failure and share of each EoL path in the total. The main cause of EoL is economic lifetime. Followed by excessive degradation (found in the years around 2050) and random failure.

The presence of degradation failures and of the failure "valley" have a common explanation: the misalignment of project lifetime with documented degradation rates. Modules that failed through degradation between 2048 and 2053 were installed in the years between 2017 and 2023. During these years the economic lifetime of modules was already considered too high compared to the documented degradation rate, leading to excessive degradation before the economic lifetime was reached.

4.1.6. Replacing lost capacity

As mentioned in the methodology section of this research (chapter 3), replacements are a fundamental aspect to consider when discussing PV EoL. By replacements, in this work, we indicate replacing lost capacity through the installation of new capacity. Capacity can be lost in two ways; through failures (EoL), as described in the section above, or through module degradation, with module performance degrading with time on the field. In this section the concept and effects of replacements will be explored, highlighting the impact of failures on replacements compared to degradation. The section will also explore how replacements will affect the future of PV module demand.
From table 4.2 the values of the impact of replacements can be seen. In the low scenario, if replacements were

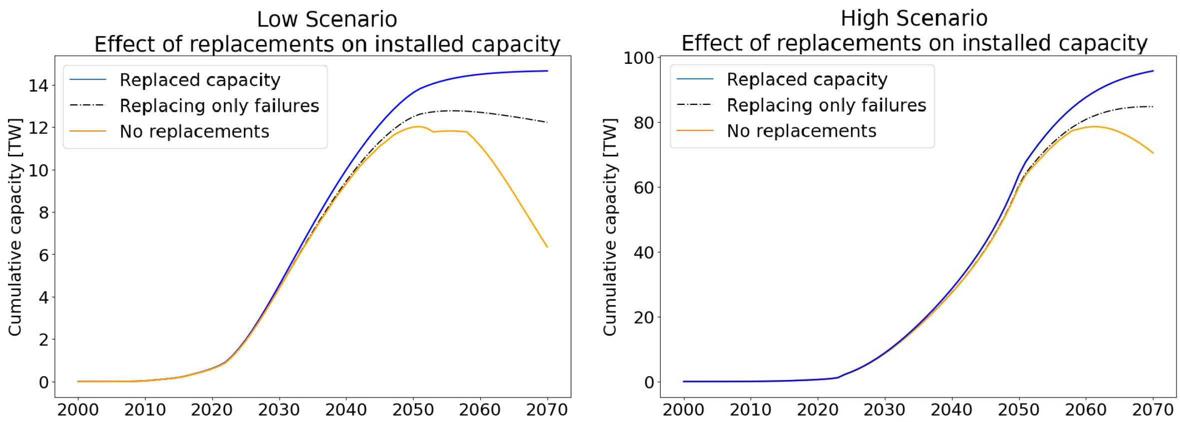

Figure 4.9: Effect of replacements on cumulative capacity in the low (left) and high (right) scenarios, presented with different y-axis to allow for better visualization. If only modules that fail are replaced, the producing capacity would be significantly lower than expected; capacity degradation in modules that are still installed needs to be taken into account and replaced

	Low scenario			**High scenario**		
	2070 capacity	Reduction		2070 capacity	Reduction	
	TW	*TW*	*%*	*TW*	*TW*	*%*
Fully replaced	14.65	-	-	95.76	-	-
Replacing only failures	12.23	-2.42	-17%	84.74	-11.02	-11%
No replacements	6.35	-8.3	-57%	70.50	-25.26	-26%

Table 4.2: Impact of replacements on cumulative installed capacity

not considered, 2070 capacity would be almost 60% lower than projections. In the high scenario, the share of reduction is lower compared to the low scenario, but the absolute values of capacity reduction are considerable. Not considering replacements would lead to a 25TW capacity deficit in 2070, a number that is hard to ignore, if put in the context that in 2023 the global cumulative capacity reached 1.3TW.

Impact of replacements on new installations

In this section, the effects of replacements on new installations will be explored. In both scenarios used in this research, total cumulative capacity is expected to flatten out towards the end of the century. This will come after years of constant capacity growth. To sustain such a growth, especially for the high scenario, production centers need to be built and operated at rates that will reach, according to the data used in the high scenario, 5TW/year of installed capacity in 2050. This will only be possible if companies are assured that even after 2050, when demand for new capacity will slow down, demand for modules will still be high enough to run the plants. In this section, the demand for new modules aimed at replacing lost capacity is shown.

Figure 4.10 shows the forecast yearly installations for the high and low scenarios, outlining the origin of new installation demand. For both scenarios, the same trend can be observed. Towards the end of the century, the shape of the replacements-driven demand, caused by both failures and degradation, (yellow and red bars) becomes the dominant source of PV demand. This new source of demand can also be closely correlated with the shape of new installations aimed at increasing cumulative capacity (green bars) in earlier years. If this analysis was extended further into the future, some sort of undulations in new installed capacity was to be expected, with peaks and valleys translated with multiples of 35 years from the original valley (around 2020) and the original peak (around 2035 for the low scenario and 2050 for the high scenario). The first peak of the low scenario is even visible in the further right side of its plot. in the high scenario, this undulatory effect was damped down by the still non-negligible presence of new added capacity in the latest part of the considered time domain, which makes the forecasted yearly new installations quite constant towards 2070. Once these installations aimed at highering capacity will disappear, an undulatory effect is expected for the high scenario as well. The expected waves of PV demand will have to be considered by PV manufacturers; these companies in fact will need to produce a constant output of modules, storing some of the production during periods of low demand to then sell it during periods of higher demand. These cycles of high and low demand periods might cause the price of modules to rise and fall based on the size of the demand (given that production will be likely constant) if there will be no cooperation

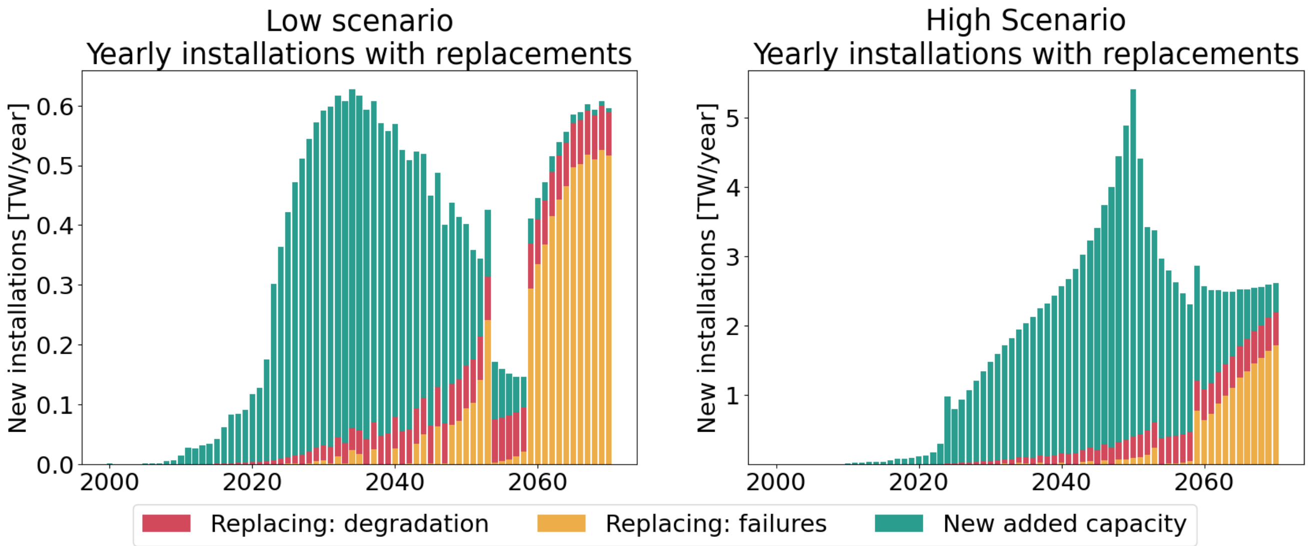

Figure 4.10: Effect of replacements on yearly added capacity for the low scenario (left) and the high scenario(right). Other than underling the greater tool on replacements caused by failures rather than degradation, the plot shows how global demand for PV will experience peaks and valleys, shifts of around 30-40 years from the "original" peak (2030 for the low scenario and 2050 for the high scenario) and the original valleys (around 2010)

between the major module manufacturers.

In the nest sections of this chapter, two scenarios are presented. In the first one the effects of a degradation rate that does not improve in the coming years is tested. The second scenario explores the impact that extending a module lifetime (after its economic lifetime) has on module's demand and on expected EoL volumes.

4.2. Scenario: flat degradation rate

This section will explore the effects that a stagnating degradation rate might have on the figures investigated in this research (End of Life volumes and moudule's demand). In the base scenario, the degradation rate of modules was based on the installation year: -0.75% from 2000 to 2023, -0.6%/year from 2024 to 2029, and -0.5%/year from 2030 to 2070. These values, chosen as baseline, have different origins. The -0.75% comes from the median value in field measurements [49], the most recent large-scale investigation on PV fleet degradation. For future values the assumption made is that module manufacturers improve the degradation performances of their modules, in line with what was reported in the ITRPV reports and in their warranty promises [25].
This methodology was selected because most new photovoltaic (PV) modules are installed before they undergo comprehensive aging tests. Consequently, the degradation rates provided by manufacturers often differ from actual field measurements [52]. In-lab tests try to emulate fast aging, leading to degradation rates that are not guaranteed to respect the actual in-site degradation [71]. Recent data collections indicate that PV system degradation rates are distributed, as shown in figure 4.11, with a median rate of -0.75%, the value used for the 2000-2023 values in this research and extended to all the other years in this scenario. This distribution does not clarify whether newer modules degrade slower than older ones, however, the rapid expansion in manufacturing might have decreased the consistency in module production, contributing to the variability in degradation rates and the possible stagnation or increase in these rates. The expected penetration of photovoltaics in regions where there is a lack of experience in PV installations might also lead to higher system degradation: modules in fact are susceptible to higher levels of degradation if mounted with poor electrical or mounting configurations [72, 73]. For these reasons, this section will explore a scenario in which the degradation rate for all modules will be fixed at -0.75% across all years covered by this study to examine the effects of a flat degradation performance.

4.2.1. No improvements in degradation: the effects of a flat degradation rate

Figure 4.12 shows the comparison in cumulative expected global EoL volume in 2070 for the base case and for the explored case with flat degradation at 0.75% in all the years considered. The results show a clear increase in

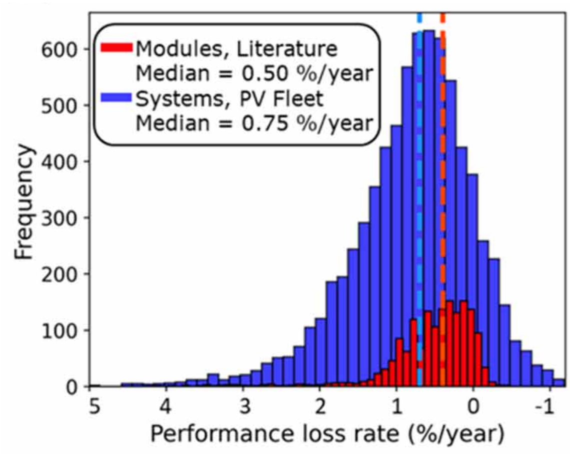

Figure 4.11: Recorded degradation rate distribution, the widely used figure of -0.75%/year comes from the median of a much wider distribution that starts from -5%/year and goes into, apparently impossible, positive degradation rates [49].

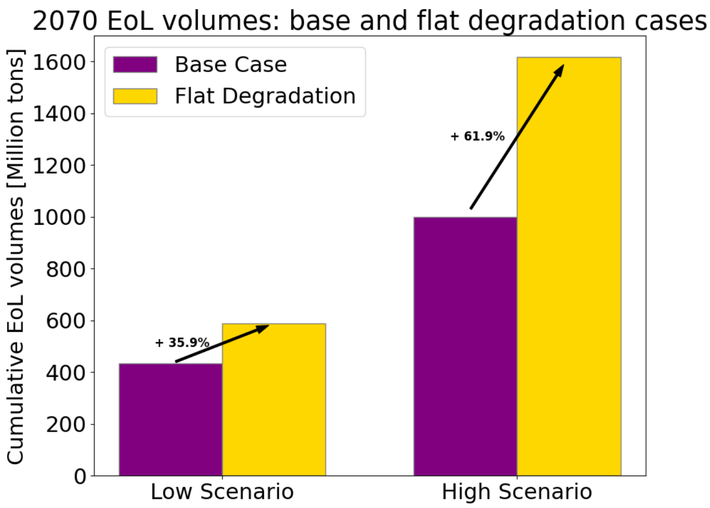

Figure 4.12: Cumulative 2070 EoL volumes, base (purple bars) and flat degradation (yellow bars) cases compared for both low (left bars) and high (right bars) scenarios. In the low scenario, the cumulative volumes grow by 36%, from 432 to 588 million tonnes. In the high scenario, there is a 62% growth, from 1000 to 1619 million tonnes.

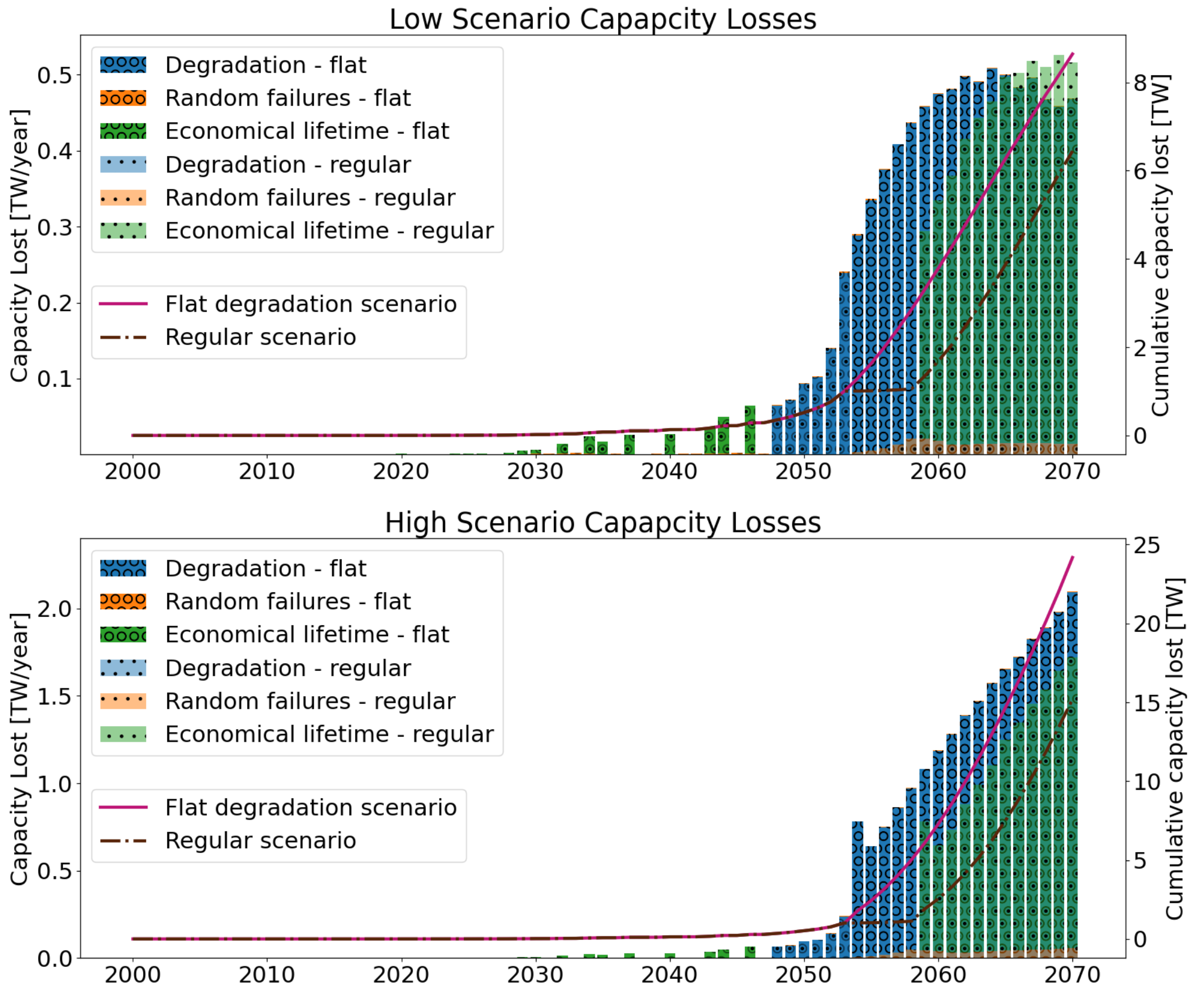

Figure 4.13: Flat and regular degradation; yearly (bars) and cumulative (lines) losses compared. The two cases differ in cumulative waste in 2070 for the absence of a period of almost no waste in the flat degradation case. In this scenario modules mainly fail through excessive degradation, continuing the trend of modules reaching EoL through this path in the years around 2050 seen in the base scenario.

volume, a 36% increase for the low scenario which goes from 432 to 588 million tonnes, and a 62% for the high scenario that goes from 1000 to 1619 million tons. These results are in line with expectations; for both scenarios, we see an increase in cumulative volumes. This increase is more present in the high scenario because of the effects that a higher degradation rate has on the specific timelines of expected EoL volumes of the two scenarios. These relations are described in the next paragraph.

Figure 4.13 shows the time distribution of modules reaching EoL, in both scenarios, for the base and flat degradation cases in terms of capacity lost. The losses are divided up in the three modes of failure (excessive degradation, random failures, and economic lifetime). The first main difference between the base and flat degradation case is the pathways through which modules enter EoL. For the base case, the majority of modules reaches End of Life through the end of their economic lifetime, as shown in figure 4.7 and figure 4.8. In the flat degradation scenario, modules reach their EoL mainly through excessive degradation between 2048 and 2070. This result is in line with expectations, given that modules with a -0.75% degradation rate are set to reach 80% of rated capacity 29 years after their installations, 6 years before the end of the 35-year module expected lifetime.

The second main difference between the base and flat degradation cases is that the flat degradation case does not show the ”valley” between 2054 and 2058 with almost no modules reaching EoL, as shown in in the base case (figure 4.8). This behavior was present in the base scenario because of the discrepancy between degradation rates and lifetime in modules installed between 2017 and 2023, when the expected lifetime was longer than the healthy lifetime of a module degrading with 0.75%/year. The discrepancy led modules installed in those years to

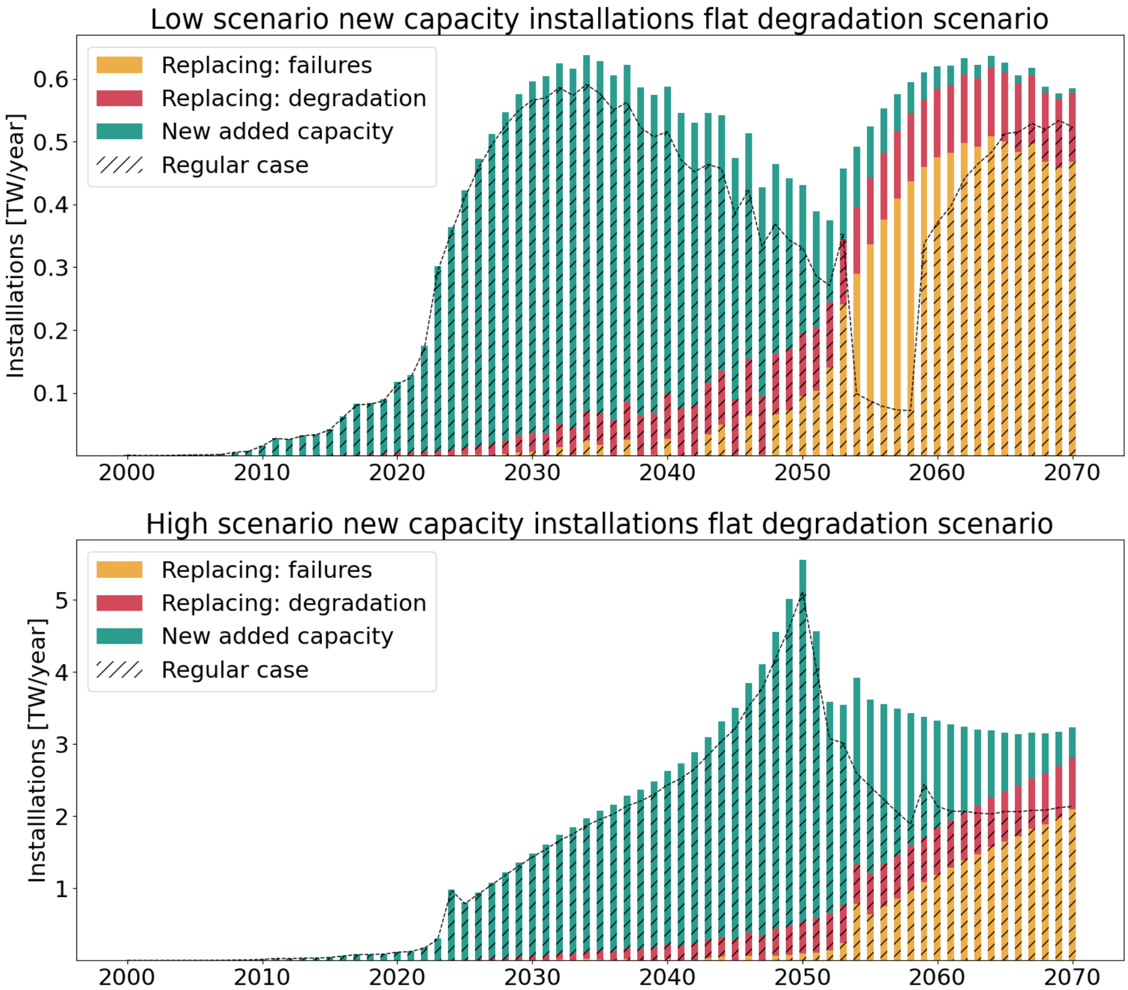

Figure 4.14: Flat degradation scenario capacity demand evolution. The bars are compared with the results obtained in the regular case (dashed line and dashed bars), to show the temporal divergence of the two cases regarding yearly installations.

be removed between 2048 and 2053 because of excessive degradation, rather than because of the end of economic lifetime. In the flat degradation scenario, this phenomenon does not stop in 2053, but continues until 2070. By following the pink and brown lines shown in figure 4.13, indicating cumulative EoL volumes, it is clear that the years without any economic or degradation failures in the base scenario are the cause of the difference in volumes with the flat degradation scenario. The flat degradation scenario appears in fact to be roughly a shift of five years from the regular scenario. This shift is the main reason for this increase in waste volumes. A parallelism can be done with what is discussed in table 4.1.6 and shown in figure 4.10 regarding global yearly demand. From what is shown in the above figure, also lost capacity (and therefore waste flows) appears to follow a cyclic pattern. This behavior is visible from the yearly lost capacity of the flat degradation scenario in the low scenario; towards 2060, the bars indicating the low scenario in the flat degradation case start to decrease, hinting that yearly capacity loss (and therefore yearly waste volumes) will have the same shape of new yearly installations and, therefore, will follow periods of highs and periods of lows.

To conclude this analysis, figure 4.14 together with table 4.3 show the impact that a flat degradation rate has on total module demand; demand that includes modules aimed at highering capacity and aimed at substituting lost capacity: both failed and degraded, as better explained in subsection 4.1.6. These results underline the importance of keeping degradation rates under control in order to contain the demand within reasonable limits. In the high scenario, total demand resulting from a flat degradation rate is 43% higher compared to the expected demand if modules had no degradation and did not have to be substituted, 43% that in TW translates to 41.5 TW, figure that can be lowered to 27.0 TW in the regular case. In the low scenario, the extra demand caused by replacements is forecast to make up a bigger share of the required production capacity; 62% and 84% for the base and flat

Table 4.3: Total demand in the regular and flat degradation case for the low and high scenarios

Scenario	Case	Demand New capacity [TW]	Extra Demand: Failures [TW]	Extra Demand: Degradations [TW]	Total Demand [TW]
Low Scenario	*Regular*	14.7	6.4	2.7	23.8 (+62%)
	Flat Degradation		8.6	3.7	27.0 (+84%)
High Scenario	*Regular*	95.8	11.8	15.2	122.8 (+28%)
	Flat Degradation		17.3	24.2	137.3 (+43%)

scenarios. The comparison with the regular case shows shown in the figures portrays a much smoother transition to the next cycle of module demand, lowering the decrease in module demand from the peak to lower demand periods, in both scenarios. Flat degradation therefore increases module demand and lowers the demand swings that would happen with a reducing degradation rate. This could play as an incentive to module manufacturers to keep degradation rates from decreasing as this would leat to an overall higher demand and to reduced alterations of the demand.

To conclude, this section showed the effects that a non-improvement of degradation rates would have on waste flow, capacity losses, and module demand. It underlines the necessity of keeping degradation lower to ensure significantly lower volumes of waste. A flat degradation rate was also found to significantly increase the demand for PV modules, lowering the swing in demand found in the regular scenario.

4.3. Scenario: Merchant tail variations

This section explores the effects that varying levels of merchant tail have on the cumulative expected EoL volumes. The term merchant tail indicates the possibility of keeping PV modules installed past the expiration of their warranty time, if the overall performance is still above the threshold of 50% of original capacity. In this section 11 scenarios were tested; each characterized by a different merchant tail percentage, going from 0% to 100% with 10% increases. The aim of these scenarios is to explore how much decisions of system owners on lifetime could influence EoL mass flows. As will be explored in chapter 6, merchant tail is expected to be closely related to two main parameters: land price and cost of capital. Where land is more expensive to rent or buy, merchant tail will probably play a very marginal role, given that system owners need to secure the highest revenue to ensure profitability. At the same time in countries where capital is more expensive, meaning that loans tend to have higher interest rates, merchant tail will play a more marginal role given that removing and substituting modules requires significant fixed costs. In the analysis done in the following paragraphs, the 0% scenario should be considered equal to the general case and serve as a reference.

Figure 4.15 shows the correlation between 2050 and 2070 cumulative EoL volumes with the different merchant tail scenarios. For both high and low installation forecasts, merchant tail is set to play a similar role; in both scenarios in fact an increase in merchant tail is correlated with a reduction of waste volumes. For the low scenario, 50% of merchant tail helps reduce 2070 cumulative volumes by 16%, while 100% merchant tail brings a total reduction of 45%. For the high scenario, a 50% merchant tail reduces volumes by 20% while 100% merchant tail lowers total volumes by 55%. It was therefore investigated what kind of function would better fit the data. In order to find a function to relate these figures, the correlation between merchant tail and total waste was tested fitted with multiple functions and the results evaluated through three primary data analysis metrics: Mean Squared Error (MSE), Akaike Information Criterion (AIC) and Bayesian Information Criterion (BIC). MSE assesses the difference between the expected value and the predicted quality, AIC and BIC help balance a model fit and complexity. After fitting the cumulative waste volumes shown in figure 4.15 with exponential, linear, quadratic, cubic and power law curves, the cubic curve resulted into the lowest MSE value. This gave the indication that polynomials would represent the better fit, therefore higher polynomials were tested to find the best function in terms of fit (MSE) and simplicity (AIC and BIC). Polynomial grade 4 was found to better fit the data for both high and low scenarios.

Figure 4.16 explores the correlation between the causes of End of Life and merchant tail. As expected merchant tail reduces, until complete elimination, the quote of modules lost through economical lifetime. Quite

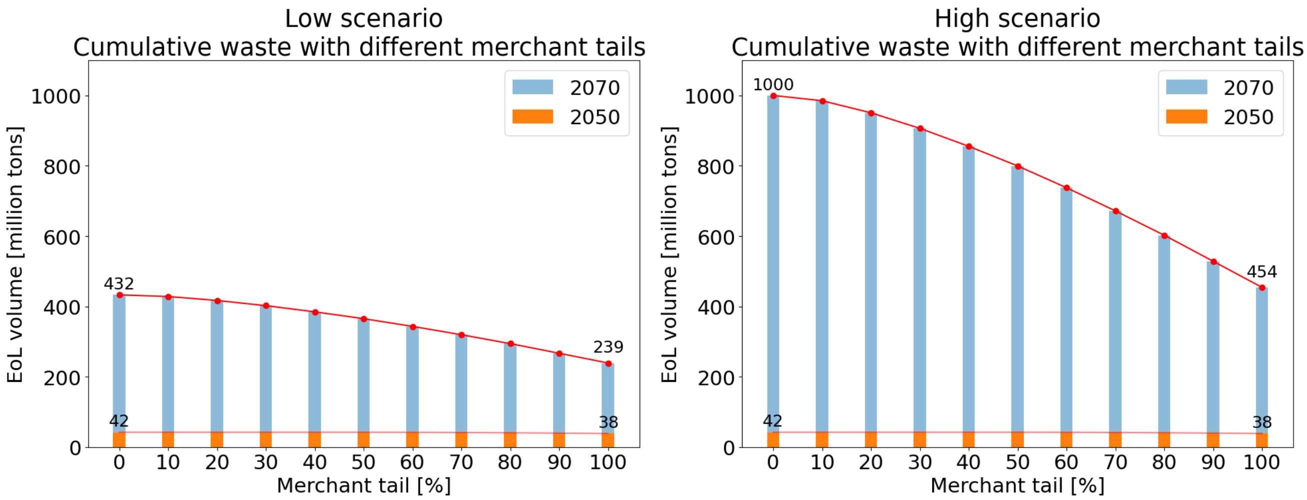

Figure 4.15: Effect of merchant tail on cumulative 2050 and 2070 EoL volumes, for both scenarios the 2070 cumulative waste volumes decrease significantly with higher percentages of merchant tail (x axis). The 2050 results are not subject to major differences considering different levels of merchant tail

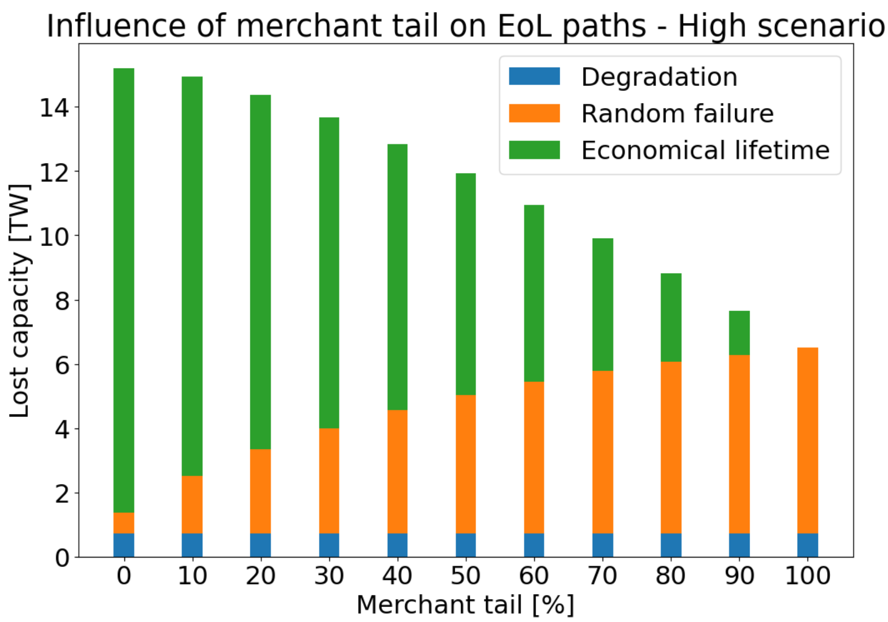

Figure 4.16: Effect of merchant tail on EoL paths; as expected an higher percentage of merchant tail increases the amount of modules that reach EoL through random failure, lowering the portion that reach EoL through the end of their economical lifetime.

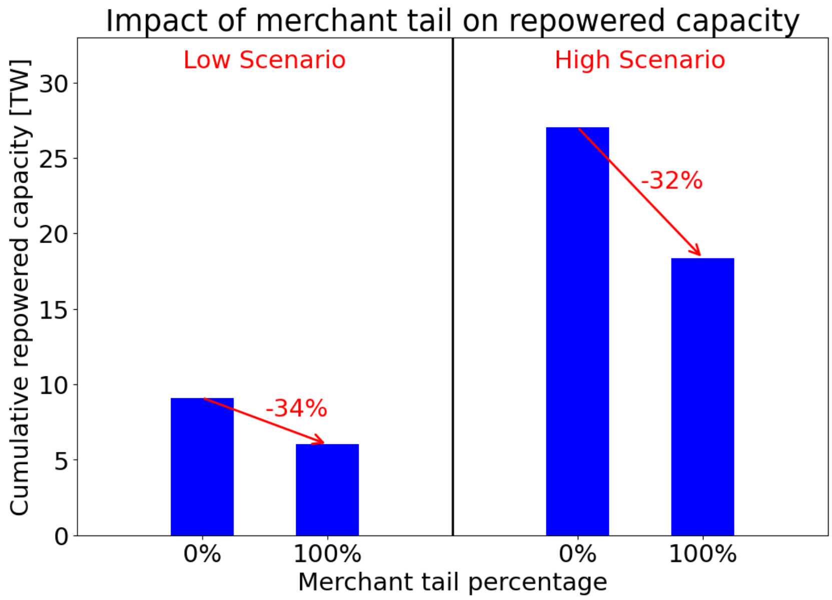

Figure 4.17: Effect of merchant tail on replacements; a 100% share of merchant tail reduces the need of replacements (and therefore the total installation demand) by more than 30% in both scenarios.

unexpectedly, most of the modules that are left on the field end up getting to EoL through random failures rather than degradation, a value that remains constant in all the tested scenarios. This results is acceptable given that the new threshold for modules reaching their EoL through excessive degradation is lowered at 50%, making this pathways less probable than random failure during the lifetime of modules. In order to fail because of excessive degradation, modules would have to degrade below 50% of their initial performance; with a degradation rate of -0.75/year, this would take 92 years. Both the high and low installation scenarios show the same trend, therefore only the high scenario was shown in the figure.

Figure 4.17 concludes this analysis on global merchant tail by showing the effects of different shares on the requirements of replacements. As expected, for both the high and low scenarios, a higher share of merchant tail leads to lower required levels of replacements. For the low installation scenario, no merchant tail leads to the extra installations of 9.1 TWp of capacity between 2000 and 2070, a number that drops by 34%, to 6.0 TWp if the merchant tail is set at 100%. For the high scenario, the original 0% merchant tail leads to a replacement demand of 27.0 TWp, while a 100% merchant tail lowers cumulative replacement demand to 18.5 TWp; a 32% decrease. Both for the low and high scenarios, the drop in replacement demand is lower than the drop in cumulative waste: 45% vs. 34% for the low scenario and 55% vs. 32% in the high scenario. This is because if merchant tail is very effective at reducing the number of modules reaching End of life (and therefore EoL volumes), the effect on replacements is smaller given the constant presence of degradation which lowers installed producing capacity. A significant part of replacements, in fact, is composed of the replacement of degraded and not failed capacity, a contribution to replacements that higher merchant tail increases. Merchant tail was shown to be a very important

factor to consider during the forecasting of future PV waste and of the PV market. A high share of merchant tail was found to decrease cumulative 2070 waste volumes by around 50% in both scenarios; modules in fact are left longer on the field and are mainly removed due to random failures in cases of high merchant tail shares. Higher merchant tail also reduces the need for modules aimed at replacing lost capacity (either failed or degraded but still installed) by around 30% in both scenarios. Extending the lifetime of modules therefore has a positive effect on the global impact of photovoltaics: it reduces both the waste volumes and the material impact of fabricating new photovoltaics. These considerations have the limitations of only considering results until 2070; extending the scope past this point would provide a better insight into the real impact of the lifetime extension of modules. The main question that an extension of the temporal scope would answer is if this reduction is maintained in years past 2070 or if the reduction experienced in the years simulated would appear after 2070.

4.4. Conclusions

This chapter gave a complete and broad investigation the effects that aging will have on the global PV fleet concerning waste and demand for new modules. Through a detailed comparative analysis of both high and low installation scenarios, this research has identified trends and variances that could significantly influence future policies and practices in photovoltaic energy systems.

Firstly, the base scenario provided an understanding of the current state of PV module degradation and failure rates, setting a benchmark for comparison against historically popular figures regarding volumes of expected PV waste. The results of cumulative PV waste for 2050 were found to be lower than previous projections developed with an outdated methodology. In particular, the novel results show a cumulative EoL volume in 2050 of 42 million tons (for both scenarios) compared to the literature numbers of 60 to 78 million tons. The divergence between the low and high scenarios was then highlighted in the cumulative waste volumes for 2070, showcasing the substantial impact that installation rates have on cumulative EoL volumes in an extended simulation period. In particular the 2070 cumulative EoL volumes add up to 432 million tons for the low scenario and to 1000 million tons for the high scenario.

Secondly, the analysis of various scenarios adjusting merchant tail, and degradation rates offered some insights into the potential to mitigate waste and extend the useful life of PV systems. The scenario variations underscore the sensitivity of EoL projections to these factors and suggest that improving module performance losses and system lifetime could substantially decrease waste volumes, while not improving the degradation rate would lead to higher waste flows, correlated with a higher but more constant demand for PV modules.

As the solar industry grows, the insights from this chapter emphasize the importance of developing strategies that address both the immediate need for more energy and the long-term sustainability challenges. Effective EoL management will require improvements in technology, regulatory approaches, and recycling processes to ensure that the expansion of solar power remains sustainable.

5

Regional Projections

This chapter of the report will delve deeper into the regional aspects of EoL projections, illuminating the differences and similarities of global regions. The methodology through which the regional division in this chapter was obtained is discussed in section 3.1, and the final regional division can be seen in figure 3.3.

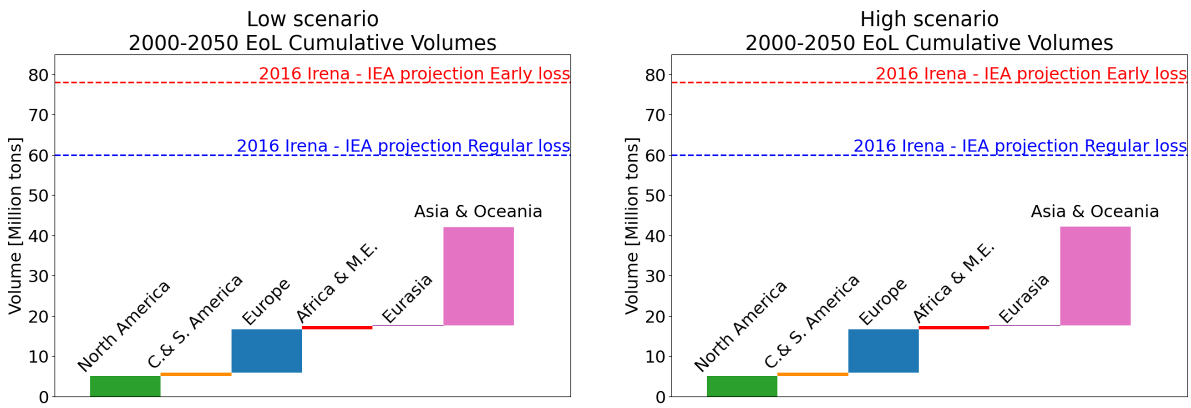

Figure 5.1: 2050 regional predicted EoL volumes, low (left) and high (right) scenarios. Asia & Oceania will be the biggest hub of PV recycling, followed by Europe and North America

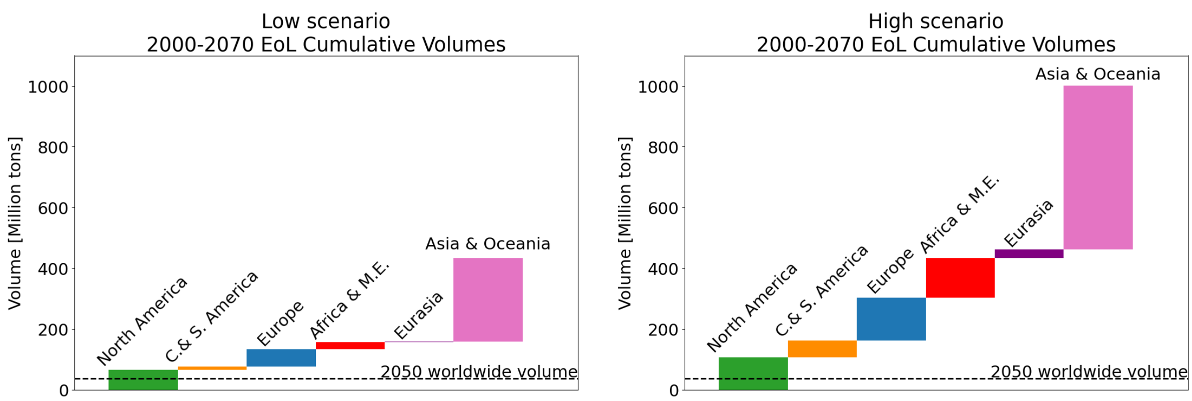

Figure 5.2: 2070 regional predicted EoL volumes, low (left) and high (right) scenarios. Asia & Oceania will remain the biggest hub in both scenarios, like in 2050. In the low scenario the apport of African EoL material is considered much lower than in the high scenario where cumulative African volumes are projected to be comparable with Europe and North America by 2070

In figure 5.1, figure 5.2 and in table 5.1 the regional expected EoL volumes forecasts are reported. It is clear to observe that 2050 volumes are almost exactly the same for both scenarios. As already discussed in figure 4.1.2,

Table 5.1: Forecast regional EoL volumes for low and high scenarios for 2050 and 2070. In parenthesis the share of total volumes represented by one region over the global one.

Region	2050 EoL Volumes (million tons) Low (share)	2050 EoL Volumes (million tons) High (share)	2070 EoL Volumes (million tons) Low (share)	2070 EoL Volumes (million tons) High (share)
North America	5.0 (12%)	5.0 (12%)	64.7 (15%)	107.1 (11%)
C. & S. America	0.9 (2%)	0.9 (2%)	11.5 (3%)	54.5 (5%)
Europe	10.7 (25%)	10.7 (25%)	56.9 (13%)	141.3 (14%)
Africa & M.E.	0.9 (2%)	0.9 (2%)	22.9 (5%)	129.8 (13%)
Eurasia	0.1 (1%)	0.1 (1%)	1.9 (1%)	28.2 (3%)
Asia & Oceania	24.4 (58%)	24.4 (58%)	274.8 (63%)	539.2 (54%)
Total	**42.1**	**42.1**	**432.9**	**1000.2**

volumes in 2050 are mainly made of installations that are today already deployed, a figure common in both scenarios. In 2050 Asia will already be the biggest hub for EoL volumes, with 24.4 million tons of material while Europe will be the second biggest hub with 10.7 million tons. If the analysis is shifted to 2070, the difference between the two scenarios becomes clear. In both scenarios Asia will remain by far the biggest contributor to global volumes, with 275 and 539 million tons for the low and high scenario. By 2070, the second biggest contributor becomes differs in the two scenarios, while in the low scenario North America takes second place with 59 million tons compared to Europe's 57, in the high scenario Europe's projected 141 million tons are more than North America's 107. For both scenarios, as can be seen in figure 5.2, the EoL volumes expected in North America alone, will be higher than the 2050 worldwide cumulative volumes. It is therefore fundamental that regions start to developed policy to ensure a smooth handling of the exponentially surging volumes of PV waste material.

All the high-scenario regional forecasts are higher than the low-scenario counterparts, but some differences are more remarked than others. This is the case for those regions that are today considered as "developing", such as Africa, Central-South America and Eurasia. These regions are characterized by the biggest gap between the two scenarios. In particular, C.& S. America's End of Life volumes in the low scenario are 80% lower than in the high scenario, a difference that grows to 82% for Africa and to 93% for Eurasia. To find the source of these misalignments, the focus needs to be shifted to installation projections for those regions. These regions are forecast to together represent in 2050 14% of installed capacity in the low scenario and 26% in the high scenario. This difference is responsible for 42% of the total difference between the two scenarios in 2050. The low scenario forecasts 16TWp in 2050, compared with the 75TWp of the high scenario, a difference of 59TWp. Of these 59TWp, 17.7TWp (42%) reside in the differences between the above-mentioned regions. It is challenging to justify this discrepancy, given that these regions are expected to experience significant population growth in this century [74], and that solar energy is projected to become the cheapest form of electricity (according to the IEA [2]), the IEA nevertheless appears to forecast other forms of energy to supply electricity to these developing regions.

5.1. Asia and Europe comparison

In this chapter the expected EoL volumes for Europe and Asia-Oceania will be discussed. In figure 5.3 the expected yearly EoL volumes for the two regions are put side by side. It is evident how Europe is expected to experience higher yearly volumes between 2000 and 2035, when Asia will start to grow exponentially, surpassing Europe's cumulative volumes around 2040. This trend increments after 2050, as can be seen in the right part of the figure. The two images were reported with different y-axis to allow for a visualization of the 2000-2050 period. In the picture showing the expected PV waste flow between 2051 and 2070, two extra values are reported, the 2022 European Union's WEEE waste (electrical waste); a category that contains PV modules, and the forecasted 2050 cumulative EoL volumes at the global scale. The bars seen in the image do not consider any recycling rate but only give a glimpse at the scale expected in the two regions and their evolution. As already said, only a small portion of these volumes will become waste; that portion will not get recycled.

WEEE in Europe and the EU's recycling goals

From the findings shown in figure 5.3, Europe is expected to encounter by 2060 annual PV waste flows similar to the combined electrical waste experienced today, and double that quantity in 2070. This number should be

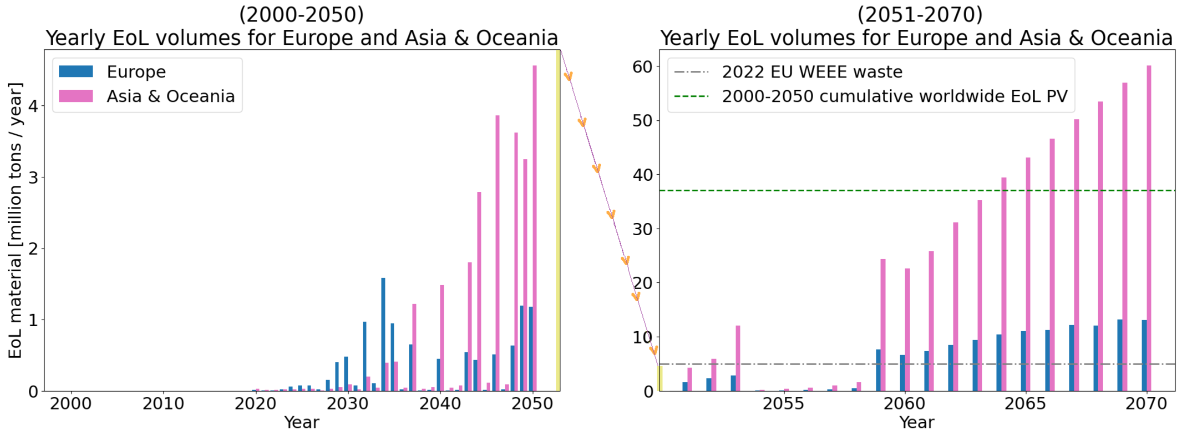

Figure 5.3: Yearly expected volumes in Europe and Asia-Oceania for two different periods - High scenario. The left plot indicates the time between 2000 and 2050, the right one from 2051 to 2070.

considered in the framework of the EU's current policies for PV recycling. Even if Europe and the EU are not the same combination of countries, in this section the two entities will be used interchangeably given that the difference resides mainly in smaller countries, not influential to the results. In 2018 the EU passed legislation to mandate that EU member states ensure a minimum recycling rate of 80% by weight for photovoltaic modules. This directive includes specific provisions for the collection, treatment, and recycling of PV panels to promote environmental sustainability and resource recovery. Therefore must collect 85% and recycle 80% of discarded modules by weight, which often translates to recycling the glass and some cables, leaving behind most of the valuable material, such as silver silicon, and copper then used as filling material for roads or construction works. The impact that the handling of glass coming from discarded PV modules is now investigated. In figure 5.4, the comparison between European glass waste in 2022 [Eurostat] and the projected yearly waste volume for PV glass in selected years in the future is shown, for the two scenarios. By PV glass waste, we assume 85% of all the glass produced in Europe from PV applications reaching EoL. This does not mean that this glass will automatically become waste, but this comparison provides an idea of the scale expected. The comparison is made with the EU's 2022 glass waste volumes given that this quantity has not changed significantly in the past decade, and is therefore projected to remain relatively constant in the coming years. What is set to change are glass' recycling rates, from today's 64% to 2035's 75%. The comparison, shown in the figure, shows how by 2050 PV glass could sum up to around 0.9 million tons in Europe (around 6% of 2022 EU glass waste), to then potentially grow to 10.5 million tons in 2070 for the high scenario or 2.7 million tons for the low scenario, 67% and 17% of currently handled glass waste volumes, a significant increase in both cases. Given the potential non-negligible impact of glass coming from PV modules in the future waste stream, it is important to reflect on the implementation of sustainable practices for the handling of End of Life PV glass. The glass used in PV modules is of extreme high quality, built with tempered or float glass, is highly durable, and is designed to be as transparent as possible to allow for the majority of incident light to go through. These characteristics make it ideal for re-purposing in other applications, such as windows for homes, vehicles, or greenhouses, rather than being relegated to mere glass fiber filler or lower-quality glass products. Reductions in glass consumption for PV modules could significantly impact the volume of glass waste anticipated in 2070. However, these changes need to be implemented more swiftly than currently projected. According to the ITRPV report, only a minimal reduction in glass consumption is expected for modules installed between today and 2033. Considering that the majority of the waste in 2070 will originate from modules installed around 2035, achieving a meaningful decrease in glass waste requires that glass consumption in modules should be reduced within the next decade, at a pace faster than what currently forecasted.

5.2. Replacements in regions

In this section the impact of replacements of old capacity on regional cumulative installations. A more in-depth explanation of what what replacements are and why they are necessary to consider when exploring End of Life can be found in section 3.4. Table 5.2 and table 5.3 illustrate the impact of replacements on cumulative 2070 installations for the low and high scenarios respectively. The table shows both projected capacity (original total capacity needed to meet solar installation goals) and real capacity installed, capacity that accounts for both ca-

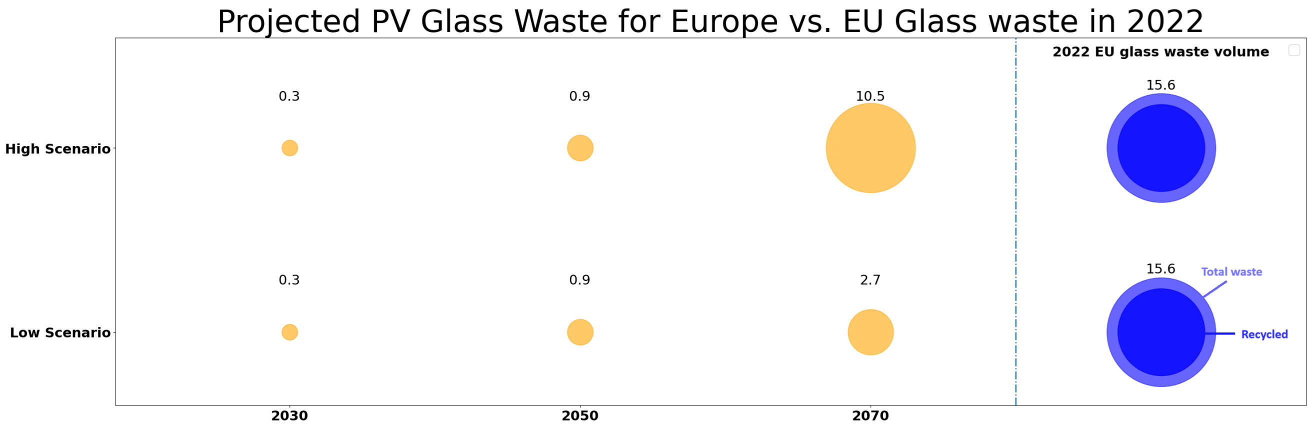

Figure 5.4: Comparison between 2022 EU glass waste and PV glass projected waste. With PV glass waste in eurpe we assume 85% of projected EoL PV glass; a figure in line with EU policies. This assumes that the glass from dismissed PV modules will not be reused or repurpoused.

pacity expansion and replacements. In the low scenario, the relative difference between forecasted and required installations is higher, with an extra 62% needed, compared to 28% of the high scenario. The low scenario anticipates new installations peaking around 2035, while the high scenario peaks in 2050. Thus, replacements have a greater relative impact in the low scenario. In absolute terms, the high scenario requires 27 TW of additional capacity, three times more than the 9.1 TW needed in the low scenario. In terms of regional impact, the regions subject to the greater relative difference between projected and real installations are Europe and North America for both scenarios. This result does not defy expectations, these two regions were historically the first two regions to implement photovoltaics at a larger scale, leading to an earlier need for replacements. The historical evolution of replacements in some selected regions is shown in the following subsection.

Table 5.2: 2070 Cumulative Installed Capacity - Low Scenario

Region	Projected Capacity	Total Capacity Installed	Increase Due to Lost Capacity
North America	1.9 TW	3.2 TW	1.3 TW (+71%)
C. & S. America	0.6 TW	0.9 TW	0.3 TW (+44%)
Europe	1.3 TW	2.3 TW	1.0 TW (+88%)
Africa & M.E.	1.7 TW	2.3 TW	0.6 TW (+34%)
Eurasia	0.08 TW	0.12 TW	0.04 TW (+51%)
Asia & Oceania	9.1 TW	14.9 TW	5.8 TW (+63%)
Total	14.7 TW	23.8 TW	9.1 TW (+62%)

Table 5.3: 2070 Cumulative Installed Capacity - High Scenario

Region	Projected Capacity	Total Capacity Installed	Increase Due to Lost Capacity
North America	6.0 TW	8.5 TW	2.5 TW (+41%)
C. & S. America	5.7 TW	7.2 TW	1.5 TW (+26%)
Europe	8.7 TW	12.0 TW	3.3 TW (+39%)
Africa & M.E.	21.9 TW	26.2 TW	4.3 TW (+19%)
Eurasia	2.4 TW	3.1 TW	0.7 TW (+31%)
Asia & Oceania	51.0 TW	65.6 TW	14.6 TW (+29%)
Total	95.8 TW	122.8 TW	27.0 TW (+28%)

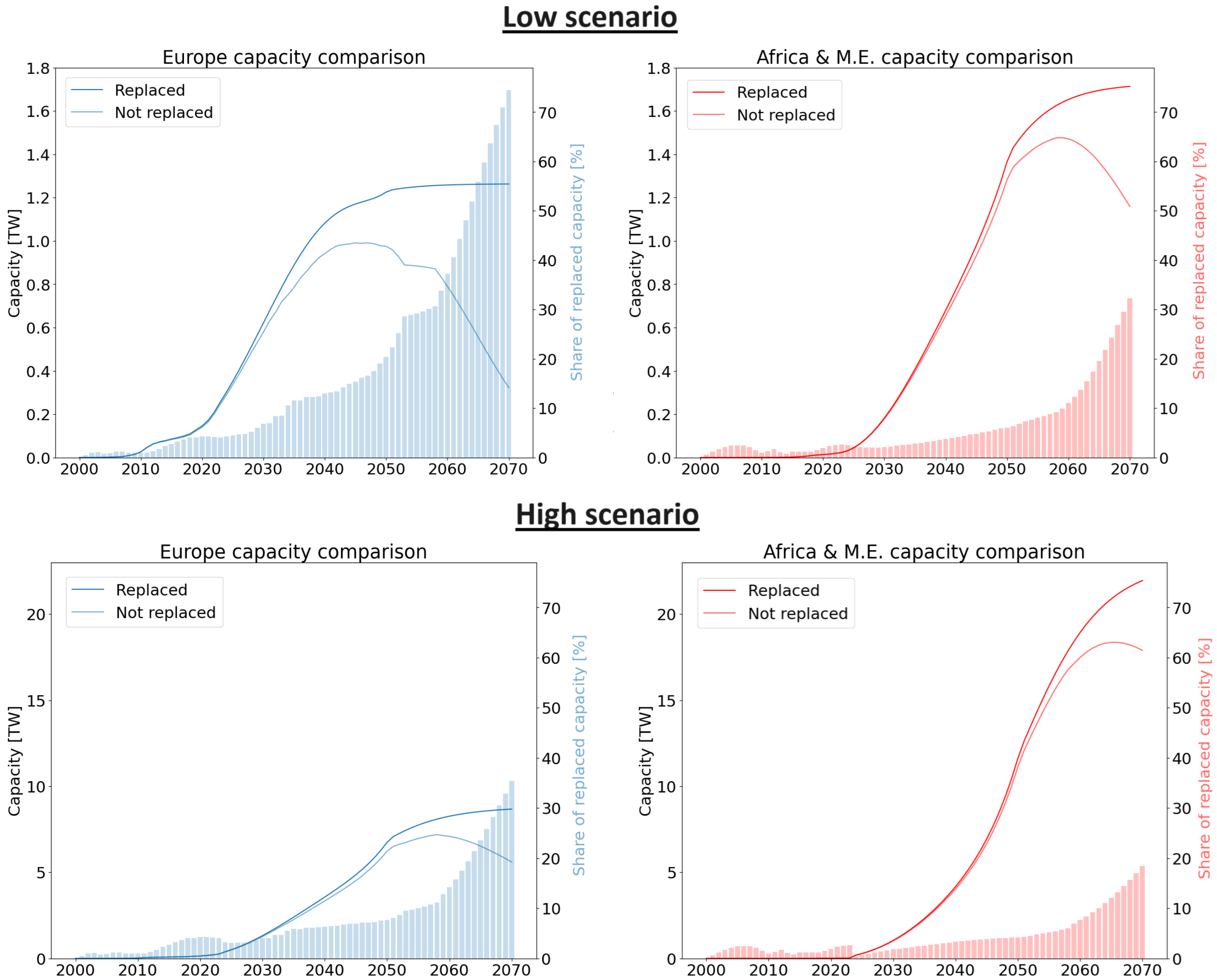

Figure 5.5: Effect and comparison of replacements in Europe and Africa & M.E. under high and low scenarios. The lines (left axis) indicate the cumulative capacity without (thin lines) and with (thick lines) replacements. The bars (right axis) indicate how much of the installed capacity comes from replacements. Given the different scales of installations between the two scenarios, replacement play a bigger role in the low installation scenario, even though they absolute replaced capacity is higher in the low scenario. In Europe replacements will influence installations and capacity more than in Africa & M.E. .

5.2.1. Replacements timeline for regions

This section of the report analyzes the temporal and quantitative impacts of replacements on selected regions. Figure figure 5.5 shows the comparison of cumulative capacity between Europe and Africa & the Middle East across the two scenarios considered in this research. The analysis assesses the implications of replacing lost capacity versus not doing so. These regions in particular were selected because although both are projected to have similar cumulative installed capacity in 2070, their paths toward this point differ significantly. The two scenarios in the figure are reported with different y-axis to allow for the visualization of the different developments If the same y-axis was used for both the low and high scenarios, the low scenario's curves would be indistinguishable given the scale difference with the high scenario. The figures also showcase the percentage of installed capacity every year that has been installed to replace lost capacity because of replacements. This is shown thanks to the vertical bars that refer to the right y-axis. By following the development of the bars, information on the temporal impact of replacements can be explored. The difference between Europe and Africa is evident in both scenarios, but it is particularly pronounced in the low scenario. Africa is expected to start mass deployment of PV modules only after 2030 making the impact of replacements modest before 2070; on the other hand, a significant portion of Europe's existing capacity was installed around 2010 and will reach end-of-life and begin to degrade before 2050. Europe's earlier adoption of photovoltaics necessitates substantial replacements compared to the installed capacity, particularly in scenarios predicting low capacity growth, where forecasts suggest that 74% of installed capacity in 2070 will consist of modules installed to replace lost capacity. Even under the high scenario, it is predicted that by 2070, about 35% of installed capacity will result from replacement efforts. Africa's percentages are lower at 32% in the low scenario and 18% in the high scenario. These percentages are also similar to the ones shown in table 5.2 and table 5.3 but not exactly. In the tables, the shares indicate extra demand exceeding forecasts installed to have enough production capacity, the figures shown above on the other hand indicate how much of the installed capacity comes from replacements. As a note, this analysis did not consider climate-dependent degradation; a factor that might significantly impact the results in certain regions subject to extreme weather, like Africa & the Middle East. Having discussed the temporal evolution of replacements for two regions expected to develop differently, the next section will offer a regional comparison of the evolution of new installations in all the regions considered. While this section was essential to demonstrate the impact of replacements on installed capacity fleets, highlighting the importance of replacing lost capacity to maintain sufficient production levels, the next section will discuss the evolution of annual installations, offering insights into the future demand for photovoltaic modules.

5.2.2. New installations: how much goes towards replacements?

In this section, yearly installations will be analyzed to understand the scale at which replacements will influence yearly installations, with the opportunity to understand how demand will fluctuate between today and 2070 in different regions. In figure 5.6, new installations forecasted for Europe and Africa & M.E. are shown. Both scenarios are reported and, again, the choice was to plot the two scenarios with different y-axis to allow for an immediate visual comparison between the two regions in the low scenario. Contrary to what was shown in the previous section of the report, this plot and the ones following show annual installations and not cumulative ones, offering an insight on the temporal evolution of the PV market. In the figures, two adjacent bars can be seen for every year; the darker bar represents the total yearly capacity demand for a region, the lighter bar indicates the amount of yearly demand that is caused by replacements, for the same year. This means that the difference between the darker and lighter bar is the amount of capacity installed for adding "new" capacity. The grey line on the plot, which refers to the right y-axis, shows the impact of replacements on total annual installations, underlining the temporal shift from installations aimed at highering capacity to modules installed to replace lost capacity.

The analysis of the result should start by comparing the scale of annual deployments, between the two scenarios and between the regions. In the low scenario, the scale of new installments between Africa and Europe is similar, averaging around 50 GW per year but with different developments. As hinted in the previous section and confirmed here, Europe's early adoption of PV, alongside modest growth projections in the low scenario, will lead to replacements accounting for over 50% of new installations by 2050—a figure that rises to 98% by 2060. Conversely, the African trajectory in the low scenario predicts that new installations will still dominate in 2050, with replacements contributing only 8% of new installations that year, increasing to 60% by 2060. By 2070, both Africa and Europe, along with all other regions analyzed under the low scenario data, are expected to see replacement installations comprise over 95% of total annual installations. Africa and South-Central America will have the lowest share at 95%, while Europe and North America will reach the highest at 99%. Before shifting the focus to comparing the two regions in the high scenario, it is crucial to emphasize once again the stark differences between the two scenarios considered. In the low scenario, around 50 GW of annual average installations are anticipated for both Africa and Europe. However, in the high scenario, this figure surges to 300 GW/year for Europe and approximately 500 GW /year for Africa, peaking at 1.2 TW/year in 2050 — a value that matches the cumulative capacity projected for Africa in the low scenario for the same year. In the high scenario the two regions show a similar evolution in terms of evolution, but not in terms of scale. The 2020 cumulative installation figure is not visible in the high scenario plot, contrary to the low scenario plot, underlying how much more "new" capacity (aimed at adding producing capacity) is expected in the high scenario. The presence of this demand for new capacity keeps the share of replacements below 10% for Europe and below 5% in Africa in 2050. For Europe, a similar share of replacements as seen in the low scenario is expected by 2070, reaching 93%. Africa's share of replacements in new installations for the high scenario in 2070 will reach 70%.

Replacing modules in Asia and in the rest of the world

In the previous sections, we focused on Europe and Africa because their similarities and differences led to some valuable insights. However a comprehensive regional analysis would be incomplete without considering Asia, the, expected, largest source of PV demand. Figure 5.7 presents, for both scenarios, the demand of Asia & Oceania

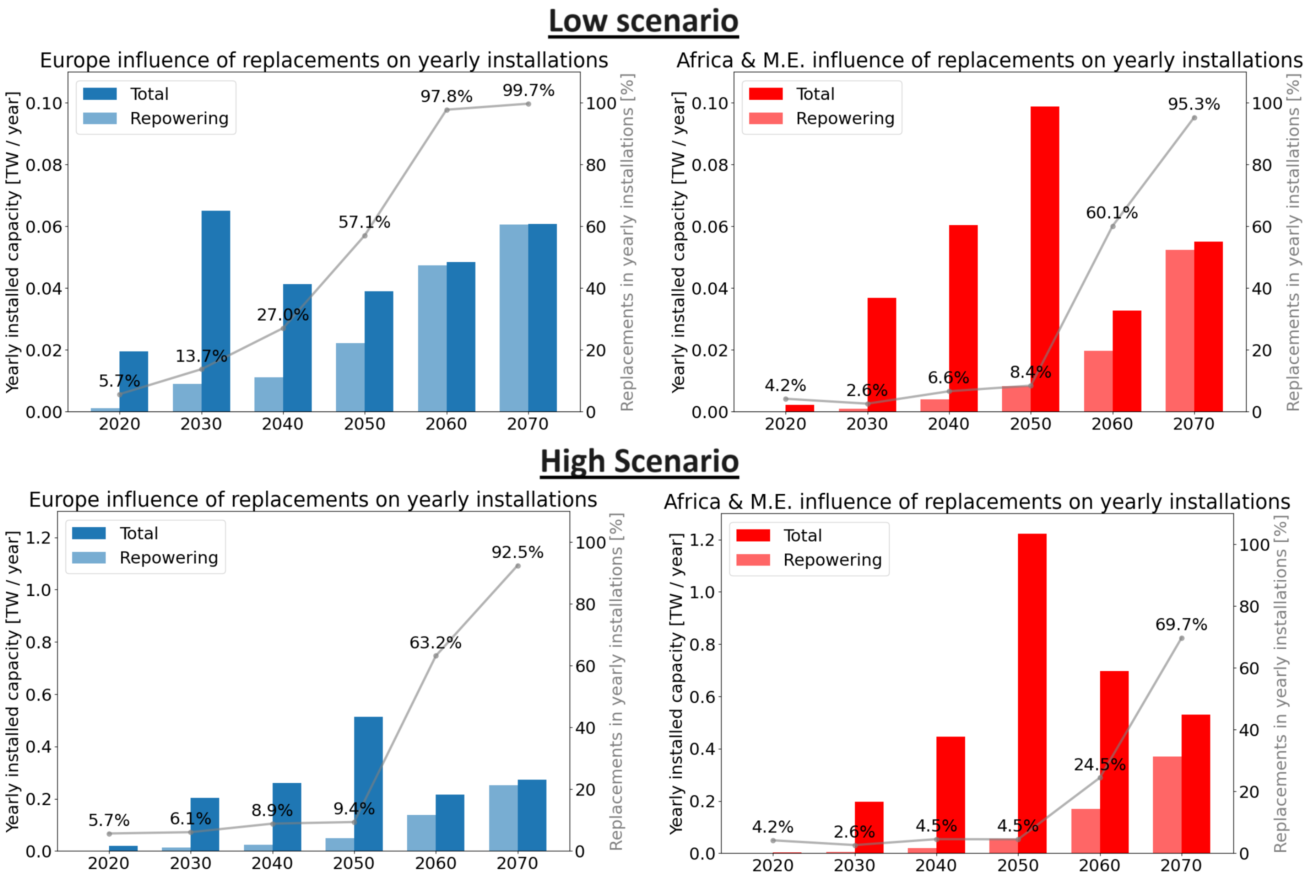

Figure 5.6: Influence of replacements on annual installations for Europe and Africa & M.E. under high and low scenarios. In both scenarios, the share or replacements in new installations is expected to reach above 90% by 2070 in Europe. The high scenario delays this figure in Africa, expected to still install a significant portion of new capacity by 2070

for 2020, 2030, 2040, 2050, 2060 and 2070. This is similar to what is reported in figure 5.6, where the annual demand for new PV modules is compared with the portion of it driven by replacements of lost capacity. The shares reported in the previous section with a grey line are not reported in this figure given the similarities to what is already discussed for Europe and Africa in for both scenarios. This novel representation is aimed at showing the scale of Asian photovoltaic demand, compared with the total annual demand of the rest of the world. For both scenarios, Asian demand is shown on the left of the image, and the projected demand for the rest of the globe is shown on the right of each scenario-specific plot. Also in this occasion, the y-axis used for representing the two scenarios in the respective plots is different to allow for a clear representation of the low scenario. To allow some degree of comparison between the two scenarios, a portion of the high scenario y-axis is highlighted, this is the interval of values shown in the low scenario y-axis: from 0 to 0.47 TW/year. In both scenarios the comparison between Asia's demand and the rest of the world is striking; for most of the years plotted Asian demand is higher or similar to the rest of the world combined. This is particularly evident in the low scenario where in 2060 Asian demand is forecasted to be 175% of global demand and 168% in 2070. In the high scenario this difference is damped down but still comparable with the rest of the world; in 2060 Asian demand will be 99% of what is expected for the rest of the world, and 116% of global demand in 2070. In this scenario Asian demand is closer to the rest of the world due to higher installations in general but mainly due to the more significant influence of Africa, the only market that is forecasted to be somewhat comparable to the Asian one in the high scenario. This analysis can lead to some other comments on the future of the photovoltaic industry and the role that Asia will play in it.

Regional implications of the future PV market on policy and trade

Today the vast majority of PV modules are produced in China and shipped to Europe and North America, markets that find in Chinese PV modules the ideal answer to a growing demand for renewable energy production. This ample availability of cheap modules is today at the center of the solar energy push in those markets; however,

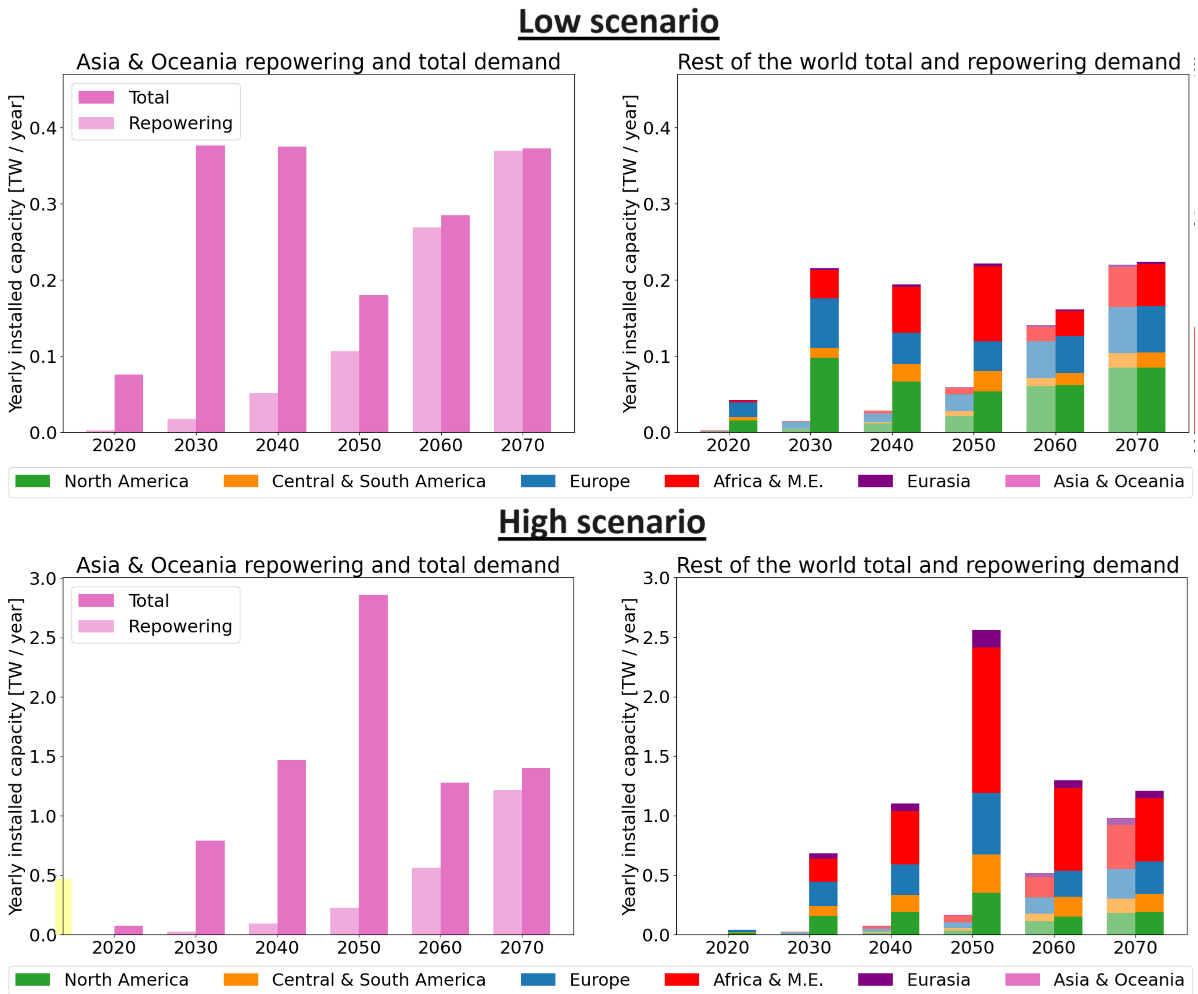

Figure 5.7: Comparison of Asia's demand for new installations with the rest of the world; in both scenarios, the role of Asia will be significant; if this is added to the role that Africa is expected to play, these two regions will represent almost the whole global demand for PV modules. The high scenario y-axis has a highlighted part which represents the full y-axis used in the low scenario.

European and American governments do not appreciate the centrality of China in such a strategic sector as energy, sector expected to go through major changes in the coming years and able to bring manufacturing jobs. Recently President Biden imposed a 50% fee on PV cells coming from China, to push for the commencement of a domestic PV manufacturing industry, a line that is being followed with other policies focused at reducing the dominance of China in the energy transition sector, such as a 100% fee on EV coming in the US from China. Even though these policies might have negative consequences on the immediate market share of Chinese manufacturers, focusing on a longer timeline, China will still be able to produce and satisfy the majority of the global demand for PV modules according to the outlined results. The majority of the demand will in fact be located in adjacent Asian countries and in Africa, a continent that is becoming progressively more intertwined with Beijing and that will probably turn to China for cheap and accessible modules as well as for other energy technologies. European and American policies, aimed at bringing manufacturing away from China, might yes spark internal manufacturing movements, but will not hurt China significantly, especially in the case of high installation scenarios.

5.3. Conclusions on Regional implications

In this chapter, we explored the dynamics of end-of-life photovoltaic projections across different global regions, underlying the similarities and differences between different locations. Key findings highlight Asia & Oceania's as the primary hub for PV EoL volumes, with significant growth anticipated through 2070. In particular, Asia is expected to handle around 60% of global end-of-life volumes, with Europe and North America representing the second potential hubs with around 13% of the volumes each. These results, especially in higher scenario projections, accentuate the need for robust EoL strategies tailored to handle increasing PV waste volumes efficiently. In particular, the levels of expected glass waste in Europe coming from photovoltaics were compared with today's volumes of glass waste, showing that by 2070 the amount of glass coming from photovoltaic waste could represent around 70% of all the glass waste processed today in the European union. The analysis also underlined the predominance that Asia & Oceania together with Africa & the Middle East will have on future PV demand.m The two regions combined will represent significantly more PV demand than the rest of the world together. As we move forward, the implications of these regional forecasts on global environmental policies and PV recycling initiatives become key, necessitating a clear understanding of regional capacities and developmental trajectories to ensure effective management of PV waste. Understanding the dynamics that will shape regional PV waste management is crucial for developing national policies. Countries within the same region, experiencing similar flows of EoL PV, may benefit from collaborations and common efforts. This regional approach can lead to more effective and harmonized waste management strategies.

6
National Projections

This chapter of the report will investigate EoL projections at the national level. The chapter will contain projections for installed capacity and expected end-of-life volumes for some selected countries. The analysis will also contain a brief economic analysis on the possibilities of recycling in the countries considered.

6.1. National PV projections data

The initial aim of this chapter was to investigate all countries worldwide, anticipating that the IEA would provide country-specific projections in its World Energy Outlook report. Although many countries are mentioned and discussed in the report, the full dataset included installation scenarios for only a few countries: China, the United States, Japan, Brazil, India, and Russia. Due to this data limitation, the scope of this chapter was modified, with the aim of only including few specific countries. The data for the remaining countries of this research was obtained through the IEA-PVPS Task 12 experts. I am grateful for their assistance and for providing the national projections for PV installations. In table 6.1 the table with the projected capacity in 2030 and 2050 for the countries analyzed in this research, with the sources of the forecast data.

Table 6.1: Country-specific projections used in this research, with source. The 2070 data is not derived from the reported sources but from interpolation and extension of forecasted data, with the methodology used in the global and regional scope (equations 3.1, 3.2 and 3.3)

Country	Capacity 2030 [GW]	Capacity 2050 [GW]	Capacity 2070* [GW]	Source
USA	744	1853	1926	[2]
China	2558	6749	7030	[2]
India	351	1716	1912	[2]
Brazil	78	197	233	[2]
Russia	6	33	38	[2]
Japan	156	208	208	[2]
Austria	21	61	69	[75]
Australia	76	405	704	[76]
France	35	117	138	[77]
Italy	80	250	294	[78]
Sweden	5	24	35	[79]
Netherlands	48	88	91	[80]
Germany	220	583	652	[81]

The capacity numbers reported in table 6.1 show the forecast for total PV capacity in 2030, 2050, and 2070 for the countries considered in this research. The sources cited in the last column of the table only provide forecasts until 2030. The 2070 numbers are product of the same data fit and extension already explained and discussed in subsection 3.1.2, previously applied to both the global and the regional scopes. Shortly, this procedure consists of fitting a polynomial through the points provided by the forecast source and extending the data past 2050 using a sigmoidal function fitted on the interpolated values. This research only includes projections for silicon-based PV modules, therefore the initial interpolated and extended capacity was multiplied by the share of silicon-based

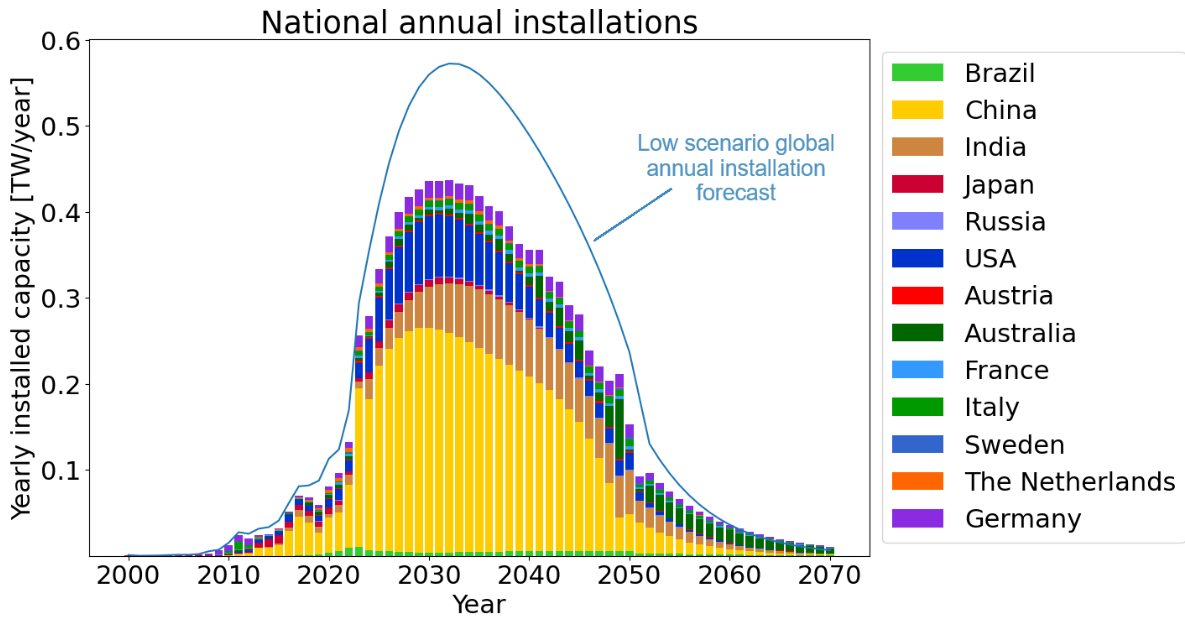

Figure 6.1: Annual installation forecast for the countries considered in this chapter. Comparison with the same figure for the global low scenario forecast analyzed in Chapter 4.

modules assumed to be in the PV market of each country. The full list with the thin film shares assumed for each country can be found in table A.8. In the same table, the effect that the share of thin film has on total capacity is shown as well; from this point on, the figures reported for this chapter will only include information about silicon-based modules. Also in the appendix, in table A.9, table **??** and in table A.11, the polynomial coefficients, the spline coefficients and the added delta for the countries considered is reported.
Figure 6.1 shows the annual installation forecast for the countries considered in this chapter. The figure indicates that China is, and will continue to be, the leading source of PV installations. India and the USA are the two countries contending for second place. The figure also compares the sum of the annual installations for these countries with the global annual installation forecast used in the low deployment scenario of chapter 4. The two projections are quite close to each other, prompting further considerations. While this analysis includes many of the largest energy-consuming countries, it omits numerous nations and regions that are likely to see significant PV deployment surges. Notably absent are countries from Africa and South-East Asia, as well as major countries such as Spain, South Korea, Canada, Mexico, and the rest of Central and South America excluding Brazil. It is difficult to believe that all these global regions will experience PV growth only to the extent of the difference between the country-specific bars and the global low scenario line. This skepticism is particularly valid when considering the anticipated growth in global energy demand driven by population increases in developing countries. Given that PV is currently the cheapest form of electricity, it is unlikely that these regions will opt for other forms of production capacity. This analysis casts doubt on the feasibility of the low scenario, putting some shade on the findings regarding waste and PV demand outlined in the previous chapters associated with the low scenario. Moreover, the fact that the main contributors to each bar representing yearly installed capacity are China, India, and the USA,countries whose forecasts come directly from the IEA dataset (used for the low scenario), further exacerbates the uncertainty about the capacity forecasts for the remaining countries in the IEA's model.

Figure 6.2 compares the capacity forecasts for India and the USA until 2070. The data used in this research shows the United States experiencing higher installed capacity until 2045, when India's cumulative capacity is projected to overtake that of the USA. The figure clearly shows that the United States is expected to reach its peak installation rate in 2030, around eight years before India's peak. Although India's peak installation rate (69 GW/year) is slightly lower than the American peak (73 GW/year), it is projected to decrease more gradually, leading to a higher overall installed capacity in India. It is important to note that this difference is particularly evident because this research focuses solely on silicon-based modules; when considering photovoltaic capacity as a whole, both countries are projected to have almost the same installed capacity by 2070 but the USA is assumed to have an higher share of thin film modules. In the country-specific sections (in the appendix), the expected installation evolution of each country is reported. Countries like Japan (figure A.8) or the Netherlands

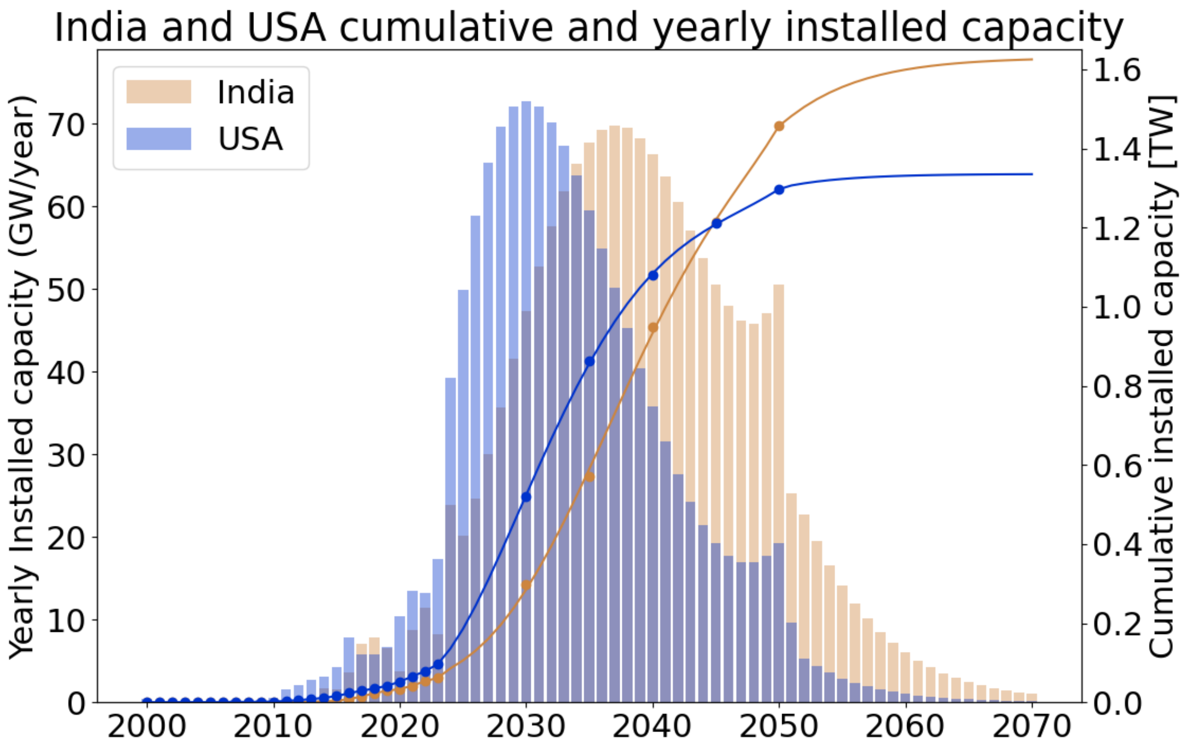

Figure 6.2: Comparison of cumulative (left axis) and new installed capacity (right axis) in India and in the USA. The dots represent forecasted points given from the source, the line is the interpolation and extension going through them.

(figure A.32) are forecasted to slow their installation rates between 2030 and 2040, with installations in 2050 projected to be minimal. In contrast, countries such as Austria, Italy, and Germany are forecasted to maintain a relatively stable growth rate from 2025 to 2050, before beginning a slower growth phase around 2050.

6.1.1. Merchant tail assumptions for the different countries

In this section of the report, the assumptions made regarding merchant tail in the countries considered are reported and justified. As already explored in section 4.3, merchant tail is the phenomenon that takes into consideration the possibility that modules are left in the field past the end of their expected economic lifetime. In this chapter, different levels of merchant tail were assumed and applied for each country; in the following paragraphs, the reasons and values of these assumptions are explained. The remainder of this chapter considers the merchant tail assumptions in the results, in order to see what different shares of merchant tail have on results, section 4.3 related merchant tail percentages with waste flows and its findings can be applied to the numbers presented here.

In determining the viability and financial sustainability of photovoltaic systems beyond their initial economic lifetime, two country-specific parameters were selected to indicate the potential share of the merchant tail: the Weighted Average Cost of Capital (WACC) and the share of total land area forecasted to be occupied by PV systems by 2070 in each country. The Weighted Average Cost of Capital (WACC) is a crucial metric in this analysis, as it encapsulates the overall cost of financing a project, including equity and debt. A higher WACC indicates more expensive financing, which could discourage investments in renovating PV fields at the end of their economic lifetime, thereby extending the use of existing systems. Conversely, a lower WACC suggests cheaper capital, which encourages investment in newer, more efficient technologies. In addition to WACC, the second parameter is the forecasted share of land that PV systems are expected to occupy by 2070. In countries where PV is expected to occupy only a minimal portion of the available land, land constraints are less of an issue, leading to the decision to implement new systems alongside existing ones rather than replacing them. By integrating WACC and projected land share, this research aims to establish a stable foundation for the assumptions regarding national merchant tail shares, an area where real data is not currently unavailable.

WACC in the Context of Merchant Tail

The Weighted Average Cost of Capital (WACC) is a critical financial metric used to assess the cost of financing for a company's investments, including projects in the energy sector such as photovoltaic (PV) systems. In the context of merchant tail analysis, which examines the financial viability of a project beyond the contracted period, WACC helps determine the attractiveness of extending the operational life of PV modules after their initial economic lifetime. The WACC represents the average rate of return required by all of the company's investors. It combines the cost of equity and the cost of debt, weighted by their respective proportions in the company's capital structure. The formula for WACC is:

$$\text{WACC} = \left(\frac{E}{V} \times \text{Re}\right) + \left(\frac{D}{V} \times \text{Rd} \times (1 - \text{Tc})\right)$$

where:

- E is the market value of equity
- D is the market value of debt
- V is the total market value of the company's financing (equity + debt)
- Re is the cost of equity
- Rd is the cost of debt
- Tc is the corporate tax rate

To understand and calculate the WACC, we need to break down its components and understand how each is derived.

Cost of Equity (Re)

The cost of equity represents the return required by equity investors. It is calculated with the following formula:

$$\text{Cost of Equity} = R_f + \beta \times ERP$$

where:

- R_f is the Risk-Free Rate, the return on an investment with zero risk, typically represented by government bond yields.
- β is the beta, representing the volatility of the stock relative to the market.
- ERP is the Total Equity Risk Premium, the additional return over the risk-free rate required by investors to compensate for the risk of investing in the stock market.

Cost of Debt (Rd)

The cost of debt is the effective rate that a company pays on its borrowed funds. It is calculated as:

$$\text{Cost of Debt} = R_f + \text{Country Default Spread}$$

where:

- R_f is the Risk-Free Rate.
- The Country Default Spread represents the additional risk associated with investing in a specific country, often derived from sovereign credit ratings.

After-Tax Cost of Debt

The cost of debt after accounting for tax savings due to interest payments being tax-deductible is:

$$\text{After-Tax Cost of Debt} = \text{Cost of Debt} \times (1 - \text{Tc})$$

where:

- Tc is the Corporate Tax Rate, the effective tax rate on corporate earnings.

Justification for Assumption of Equity and Debt Proportions (E/V and D/V)

In calculating the WACC, we assume the following proportions for equity and debt:

$$\frac{E}{V} = 0.7 \quad \text{and} \quad \frac{D}{V} = 0.3$$

These assumptions are based on industry norms. Companies in the renewable energy sector typically finance their projects with a higher proportion of equity. A capital structure involving around 60-80% equity and 20-40% debt is common. This higher equity proportion helps to reduce the financial risk associated with high leverage, providing a cushion against potential financial distress [82, 83].
Given these justifications, the assumed proportions of 70% equity and 30% debt are applied to our WACC calculations, reflecting realistic and prudent financial practices.

Provided Data for Calculation

We can now look at the specific data for each country, sources and used for this research. This data includes the Risk-Free Rate, Total Equity Risk Premium, Corporate Tax Rate, and Country Default Spread, which we will use to calculate the Cost of Debt, Cost of Equity, After-Tax Cost of Debt, and finally, the WACC for each country. The specific data for each country is reported in table 6.2, along with the source of each data point. In table A.12 the full intermediate results for every country are shown. The final results for WACC, as well as the merchant tail percentages chosen, can be seen in table 6.3.

Table 6.2: Financial parameters used in the calculation of the cost of capital for the countries considered in this research. * = the risk-free rate is the current yield of the 10-year bonds.

Country	Risk-Free Rate*	Total Equity Risk Premium	Corporate Tax Rate	Country Default Spread
China	2.3%	5.63%	25%	0.99%
United States	4.21%	4.60%	21%	0.58%
Japan	0.93%	5.63%	30%	0.43%
Italy	4.05%	7.81%	24%	1.34%
India	7.00%	7.81%	30%	0.99%
Australia	4.00%	4.60%	30%	0.26%
Austria	2.50%	5.18%	25%	0.27%
Germany	2.30%	4.60%	30%	0.29%
The Netherlands	2.50%	4.60%	25%	0.24%
Sweden	2.00%	4.60%	22%	0.28%
France	3.00%	5.32%	28%	0.43%
Brazil	11.30%	9.00%	34%	2.39%
Russia	15.15%	11.18%	25%	6.00%
Source	[84]	[85]	[85]	[85]

Example Calculation

Using the provided data, let's calculate the WACC for China.

China

- **Risk-Free Rate**: 2.3%
- **Total Equity Risk Premium**: 5.63%
- **Corporate Tax Rate**: 25%
- **Country Default Spread**: 0.99%
- **Beta**: 1.2

Cost of Debt:

$$\text{Cost of Debt} = 2.3\% + 0.99\% = 3.29\%$$

Cost of Equity:

$$\text{Cost of Equity} = 2.3\% + 1.2 \times 5.63\% = 9.06\%$$

After-Tax Cost of Debt:

$$\text{After-Tax Cost of Debt} = 3.29\% \times (1 - 0.25) = 2.47\%$$

WACC:

$$\text{WACC} = (0.7 \times 9.06\%) + (0.3 \times 2.47\%) = 6.34\% + 0.74\% = 7.08\%$$

Share of land area used for PV applications

Besides WACC, the other parameter used to determine a reasonable assumption for different merchant tails in the selected countries was the share of total land area that PV is expected to occupy by 2070. This measure aims to reflect the competition PV installations will face regarding access to land. Using the projected share of land occupied by PV rather than the total land area provides a more accurate picture of the scale at which PV needs to be implemented, highlighting the competition with other sectors for land and the subsequent challenges of obtaining new land. As mentioned at the beginning of this section on merchant tail, easy access to new land makes PV system owners more likely to extend the lifetime of their systems by building new installations in different locations rather than replacing the existing ones. However, this value does not capture other factors that might influence investment decisions, such as the suitability of empty land for PV installations (e.g., the Russian tundra or the Brazilian Amazon forest are not ideal locations) or the fact that suitable land might already be occupied by other uses.
For this calculation the same formula shown in section 3.2 (formula 3.7) for area calculation was applied and then divided by the land area of each country.

Final assumptions on merchant tail

Table 6.3: Merchant tail assumptions for different countries based on cost of capital and share of land occupied by PV in 2070

Country	Cost of capital (WACC)	PV land share	Merchant tail assumption
China	7%	0.01028%	10%
United States	8%	0.00250%	30%
Japan	6%	0.00674%	15%
Italy	10%	0.01317%	25%
India	13%	0.00836%	25%
Australia	8%	0.00089%	35%
Austria	7%	0.01088%	10%
Germany	6%	0.02663%	5%
The Netherlands	6%	0.03693%	0%
Sweden	6%	0.00097%	10%
France	8%	0.00397%	25%
Brazil	18%	0.00068%	50%
Russia	25%	0.00003%	50%

Table 6.3 shows the final values chosen for the merchant tail in different countries. The choice of the boundaries is arbitrary (instead of 0% - 50% the boundaries could have been set at 5% - 30%). Given that no literature is available on the topic, 50% gave the opportunity of clearly differentiate between countries that will reasonably experience significantly different shares of merchant tail, based on the data shown above. Silvana Ovaitt, an expert at NREL on photovoltaics sustainability and the supervisor of this research project, also approved the choices made. The highest values were chosen for Russia and Brazil, at 50%. These countries not only present the lowest shares of land use, but also have the highest cost of capital among all the countries considered. Conversely, the lowest merchant tail shares were assigned to the Netherlands, Germany, and Austria, at 0%, 5%, and 5%, respectively. These countries share both very favorable costs of capital and high shares of PV over the total land area.
In the next section, the country-specific expected levels of PV waste are reported and discussed.

6.2. Waste volumes

This section reports the main findings of global End of Life volumes expected for the countries considered in this research. By End of Life volumes, we consider the amount of weight from failed and removed modules. As already stated, this does not necessarily entail waste given that this material could potentially go through other end-of-life paths like reusing or re-purposing. The numbers that will be presented indicate how much material is forecasted to be available for recycling, with an ideal 100% collection rate.

Figure 6.3 illustrates the cumulative expected EoL volumes for all the countries considered, in the years 2050, 2060, and 2070. As expected, China is forecasted to be the main hub for PV waste handling, with 14.13 million tonnes in 2050, 56.07 million tonnes in 2060, and 197.46 million tonnes in 2070. These figures are remarkably higher than those of any other country considered in this research. The United States, the second-largest forecasted hub for PV waste management, is expected to experience 3.55 million tonnes in 2050, 11.73 million tonnes in 2060, and 46.51 million tonnes in 2070. India is projected to have the third-largest flow of PV EoL material by 2070, although by 2060 Germany and Japan are projected to have higher cumulative waste volumes.

In order to glimpse the temporal scale of the expected PV EoL flows, figure 6.4 shows the average expected volumes for the five decades between 2020 and 2070. The countries are divided into three groups, each with its unique scale of reference. All countries show a growth in EoL rates over the decades, with some minor exceptions. One such exception is Italy's 2030-2039 period, which is higher than the following two decades.Italy's installation history explains this anomaly. As shown in figure A.11, Italy experienced 9 GW of installations in 2010 alone (thanks to some favorable PV financing schemes [86]), a scale that is not forecasted to occur again in the country's future. Most of those modules installed in 2011, with a lifetime of 23 years, are expected to reach EoL around 2034 resulting in a higher average for that decade. For more detailed insights on the year-by-year breakdown of expected EoL flows in each country, each of the country-specific sections (in the appendix) contains a plot depicting the expected yearly volumes in comparison with the cumulative value. In the country-specific plots, each figure is presented with the most appropriate y-axis, allowing for a better visualization of the results.

This section compares waste volumes across countries, noting China's significantly larger expected end-of-life (EoL) flows compared to other major PV markets. It highlights the forecasted doubling of average annual volumes from 2060 to 2070 in nearly all studied countries. The following section will explore the effects of an aging PV fleet on demand and capacity replacement.

In the next, and final, section of this chapter, a brief "back of the envelope" consideration of the economic feasibility of recycling in the different countries is proposed, offering an idea on what to expect from the future of PV recycling in the countries considered above

6.3. Capacity demand

Table 6.4: National silicon-based PV demand - comparison between original forecasted demand and real demand, including the original forecast and the capacity aimed at replacing lost capacity

Country	Original Forecasted Demand 2070 (TW)	Total Demand 2070 (original + replacements) (TW)	Increase
USA	1.34	2.34	75%
China	5.98	10.07	69%
India	1.63	2.40	47%
Brazil	0.20	0.31	56%
Russia	0.03	0.05	45%
Japan	0.18	0.37	110%
Austria	0.07	0.11	57%
Australia	0.60	0.76	27%
France	0.13	0.20	56%
Italy	0.25	0.39	58%
Sweden	0.03	0.04	34%
Netherlands	0.09	0.16	86%
Germany	0.62	1.02	64%

Table 6.4, shows the increase in expected demand for silicon-based capacity caused by the replacement of lost

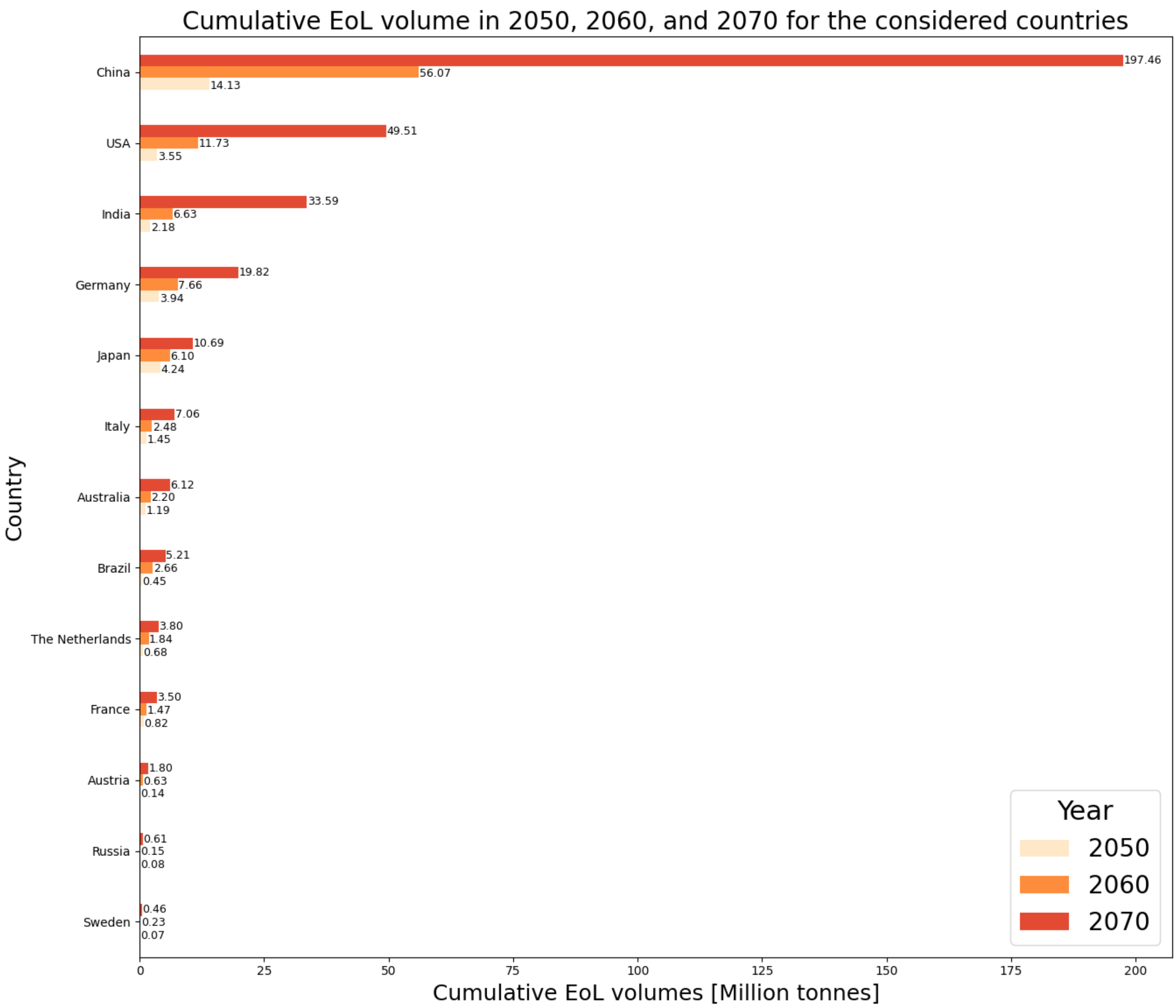

Figure 6.3: Cumulative EoL volumes for the countries considered in 2050, 2060, and 2070

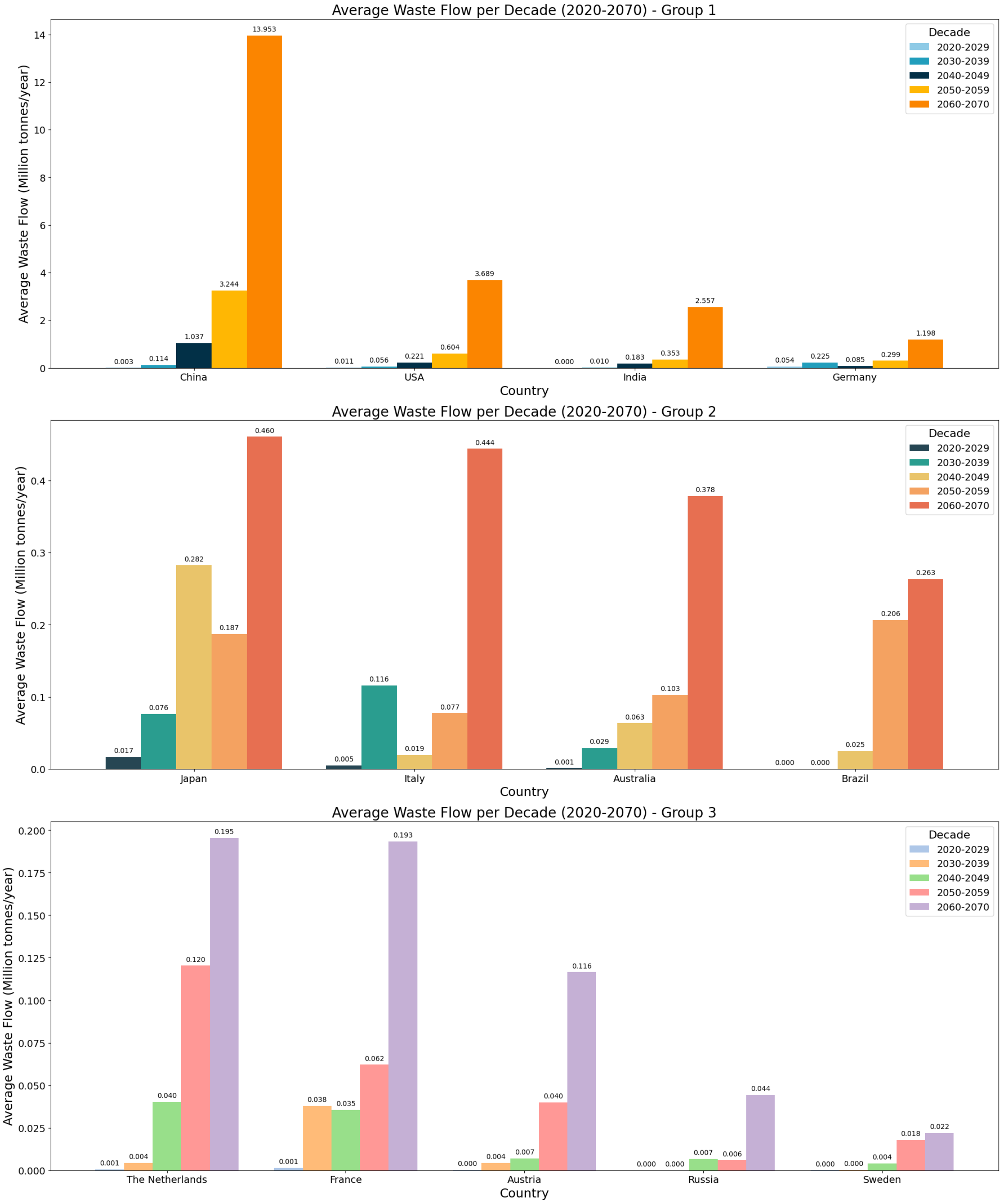

Figure 6.4: Country specific average EoL flows in the decades included in this projection. The three lines have different y-axiss to ensure the visibility of the smaller countries values

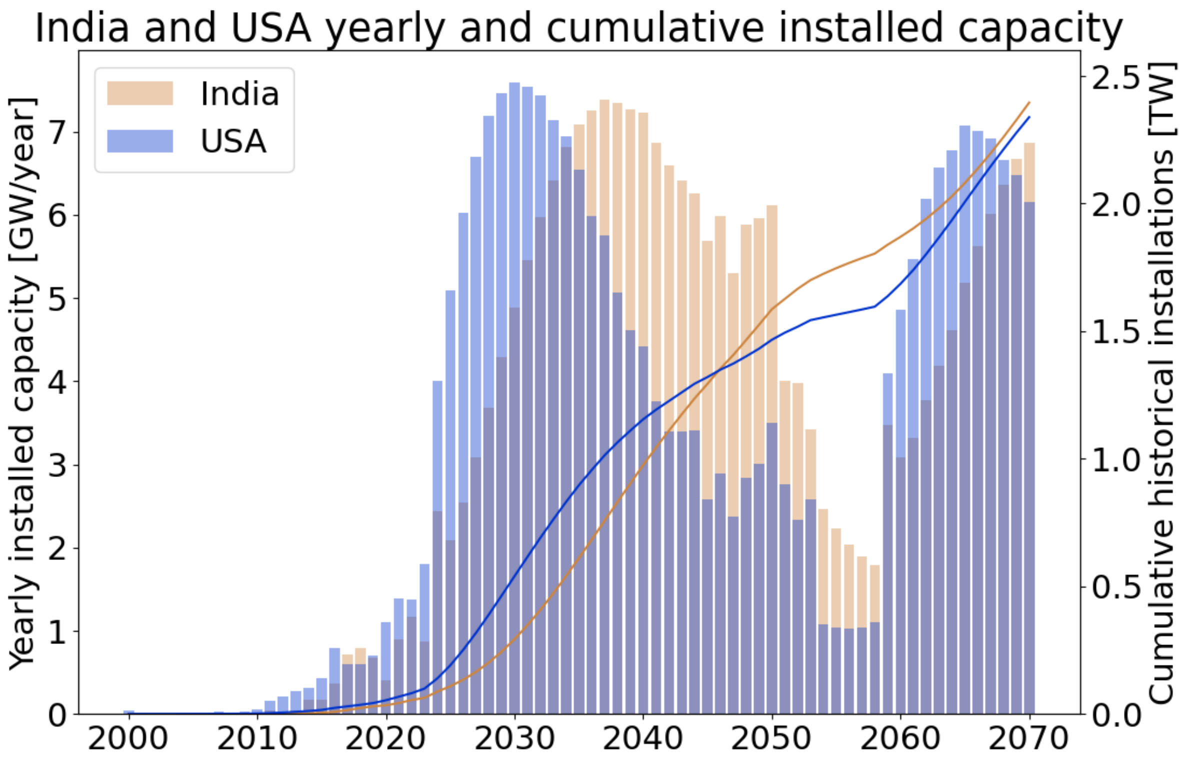

Figure 6.5: Comparison of new installed capacity (bars - left axis) and cumulative installations (line - right axis) in India and in the USA. The difference displayed in figure 6.2, where replacements were nit considered, does not appear anymore.

capacity. The table also shows to what percentage of the original expected demand this capacity corresponds. The increase differs significantly between the different countries. The lowest value of 27% in Australia and the highest of 110% in Japan can be explained according to the same phenomenon, the timeline of PV installations. In particular, countries where a significant portion of total capacity was added in the years around 2030 will experience a higher share of replacements. To put into perspective the influence of replacements on total demand, figure 6.5 shows the comparison on new installations and cumulative installations of India and the USA when considering replacements. These figures were already explored in figure 6.2, the figure showed India significantly ahead of the United States without considering replacements, including lost capacity adjustments reveals that the two countries have a much closer cumulative installation total by 2070.

6.4. Economic feasibility of recycling

This section will explore the economic feasibility related to recycling, in the different countries explored in this section. The method, assumptions and results of Pv recycling in the different countries considered is shown, exploring the optimal timing for the different countries to start domestic recycling practices, and the economical impact of such operations.

6.4.1. Methodology and Assumptions of the Economics of recycling

This subsection provides a detailed breakdown of the methodology used to evaluate the financial viability of photovoltaic recycling projects. The analysis follows a sequence of computational steps, in order to determine the optimal year to commence recycling operations, where ”optimal” is defined as the start year that achieves the best possible economical conditions. For this analysis, PV recycling is treated as a state-owned enterprise, with all recycling plants operating under uniform conditions and sharing revenues and costs. Although in reality, recycling plants are likely to be privately owned, this simulation framework helps to assess the feasibility of recycling across different countries. Specifically, it helps

Data Preparation

1. **Data Import:** For each country, specific data on available EoL PV material are used. The data comes from the EoL simulations done in the previous chapter, and it is divided among the materials that make up a PV module: glass, silicon, silver, aluminum (frame), backsheet, encapsulant and copper.
2. **Collection Rate Adjustment:** The available quantity is adjusted to account for the collection rate. This collection rate was set, for every country, at the value set by the European Union of 85%. This means that for every 1000kg of PV EoL material, 850kg were made available for recycling in this economic analysis. From this point forward, every reference to available recyclable material will account for this collection rate already.

Material Recovery

Each material's recoverable amount is calculated by applying material-specific recycling rates to the collected quantities, reflecting the efficiency of the recycling process. These values come from literature [87] and are the following:

- Glass = 100%
- Silver = 94%
- Silicon = 95%
- Aluminium = 100%
- Copper = 100%

The encapsulant and backseat are considered byproducts of the recycling process, together with the recycling scraps, and sold as filling material.

Financial Calculations

Revenue Estimation

For each material, the potential revenue is computed by multiplying the recoverable quantity by its respective market price per kilogram. These values were obtained from a 2023 D'Adamo et al. paper [87], in the "baseline price scenario" proposed by them . These prices are subject to market volatility and should therefore be treated as the main point of uncertainty of this economic analysis.

- Glass = 0.125 €/kg
- Silver = 650 €/kg
- Silicon = 2.1 €/kg
- Aluminium = 2.3 €/kg
- Copper = 8.5 €/kg
- Filling material = 0.01 €/kg

To diminish the effects of spikes and droughts in material availability caused by the nature of the simulation used in this research, **the input data was dynamically averaged over a period of 10 years using a centered rolling average**. This means that the input value for material availability for year X was calculated as the average of the available materials between year X-4 and year X+5. This approach reduces the impact of extremes while keeping the cumulative volumes close to the actual cumulative volumes. The effects of averaging at the edges, where fewer points are available, lead to some minimal misalignment. Every reference to input data or material availability in the remainder of this section will reference this rolling average rather than the raw input data coming from the PV ICE simulations.

Costs estimation

The estimation of fixed and variable costs for recycling in the different countries was treated by following these considerations. When operating a recycling plant, two expenditures need to be considered: the **CAPEX** and the **OPEX**. The CAPEX is the initial investment required to set up the recycling plant, while the OPEX are the annual recurring costs; such as labor, recycling operations, maintenance etc. The values for opex and capex were obtained from a 2022 Granata et al. paper [1] for different sizes of recycling plants and can be seen in table A.13. The available data considers plants that can handle volumes from 3000 to 30000 tons per year, providing the financial characteristics of each size between the extremes with steps of 3000 tonnes per year of recyclable capacity.

Determining the recycling capacity of countries

In order to understand the costs related with recycling in teh different countries, the size and time of investment in recycling plants was a crucial factor. In order to determine the schedule at which the recycling capacity of different countries was built, the following process was followed:

1. **Initial capacity estimation**: The initial capacity is estimated based on the average demand for the first 5 years. The initial capacity is chosen to be the smallest available capacity in the provided capacity sizes (table A.13) that can meet this average demand. The specific size chosen is correlated with an initial CAPEX and a corresponding OPEX in the first five years of operation.
2. **Evolution of recycling capacity**: Every five years, the installed recycling capacity is evaluated to determine if it is sufficient to meet the average recycling demands for the upcoming 5 years. If the current capacity is adequate, no changes are made and the recycling fleet continues to operate as is; if it is not, capacity expansion is undertaken. The expansion can consist of the following operations:

   - The current plant is expanded to minimum available capacity that allows to process the average future demand. Plants can only be expanded until the maximum size shown in table A.13. The CAPEX of this expansion are accounted by taking the difference of the new size with the old size. This approssimation does not lead to major effects in the results given that CAPEX costs are significantly lower than OPEX costs.

   - If the plant is expanded to the maximum capacity, but this does not allow to satisfy demand, then a new plant in "installed". The capacity of the new plant is the minimum required to satisfy future demand. It is possible that multiple plants get installed at the beginning of every 5 year period. The capex is calculated by summing up the CAPEXs associated with building new plants with the one coming from plant's expansion. At the end of this operation a new OPEX is calculated by summing up all the operational costs of the various plants.

   This methodology allows to build up the recycling fleet dynamically, minimizing overall CAPEX and OPEX costs.

Once the full expected costs are found, the cash flow calculation can be undertaken. In the next section the calculations and assumptions made are shown.

Cash Flow and NPV Calculation

This section shows how the cash flow of the recycling system was calculated. A 5% discount rate was considered to include a dynamic economical consideration. This is the same rate considered in the D'Adamo et al. paper used for the input data on recovery rates and material prices, in order to have similar assumptions when comparing the results.

1. **Net Cash Flow:** For each year, net cash flow is calculated by subtracting the sum of CAPEX and OPEX from the total revenue of that year. The CAPEX value was different than zero only in the years when the recycling fleet was expanded.

$$\text{Net Cash Flow}_t = \text{Total Revenue}_t - (\text{CAPEX}_t + \text{OPEX}_t)$$

2. **Discounting Cash Flows:** Apply a discount rate (5%) to each year's net cash flow to account for the time value of money, summing these to calculate the project's NPV.

$$\text{NPV} = \sum_{t=0}^{T} \frac{\text{Net Cash Flow}_t}{(1+r)^t}$$

The results of these calculations led to the (expected) finding that recycling is not profitable on its own, given the low values of recovered materials and the high costs of recycling procedures. For these reasons, the next section will explore how much recycling plants should be aided with a recycling fee, a monetary compensation that whoever sends its modules to the recycling center needs to pay. In this research we will explore how much countries should ask as a recycling fee, indicated in this research as "PV fee", in order to make their recycling operations break even.

PV Fee Calculation

In order to calculate the average PV fee required in each country, the main assumption was that the Net Present Value at the end of the simulation process had to be zero. This would allow for the assurance of an economically sustainable investment. The PV fee is therefore calculated as following

.

$$\text{PV Fee} = \frac{\text{NPV}}{\text{Total Recycled Material}}$$

This formulation allows to calculate what is the overall exta fee (€/ton) needed to make sure that recycling breaks even during the years of operation. In the next section the results of the economical consideration will be shown, exploring when countries should start their recycling efforts and what PV fees are required to make it sustainable.

6.4.2. Economical consideration results

Given the model the possibility to choose the ideal starting year, based on the lowest possible PV fee. In the next paragraphs and sections, teh results of this economical model will be presented and analyzed.

Best starting year and recycling fee

Table 6.5 shows the results for the best starting year and the consequential PV fee in the countries considered. The model was set up so that recycling operations could have started anywhere between 2025 and 2070, to follow then the evolution and calculations explained above. The main consideration is that the majority of countries would benefit from starting recycling operations sooner rather than later. Increasing the recycling fleet from earlier years leads to lower PV fee requirements over the considered period. This result is influenced by how the PV fee was calculated; considering the cash flow as discounted least to the fact that an investment made today is cheaper than an investment made tomorrow, leading towards a bias for early investments. The model also show a clear correlation between higher waste volumes and lower PV fees, as expected. Running bigger plants leads to lower operational costs and therefore to lower PV fees. The lowest fee is found in Germany, at 10€/tonne of recycled material. The reason behind this value is that the waste increase of the country is expected to be quite regular, without the presence of a significant increase in average waste flows in the latest decades considered (figure 6.3). These spikes in waste flows, present in most other similar countries (like the USA or India), lead to late investments in newer plants.

To put these figures into perspective, the D'Adamo et al. paper already cited above proposes a fee between 6€/ton and 476€/ton, with the most probable result being indicated as 241€/ton in order to lead to a zero NPV. These figures are calculated in the optics of a 3000 tons/year recycling center, a capacity significantly lower than what countries are expected to have (figure 6.6) that is therefore correlated with higher fees. Nevertheless the results found with the methodology proposed in this section are within the paper's range. Other literature sources proposes fees in the range of 112$/tonne [88] or in a range of and 225–425 $/tonne [1]. Both these papers consider smaller recycling sizes. The Netherlands in 2023 highered its PV recycling fee from 6.5€/tonne to 40€/tonne [89], a value more in line with the results of this economical analysis. To give these figures a more practical connotation, in 2033 solar energy is expected to cost around 608€/KWp [28], considering the whole installation process and BoS; considering an average module of 420 Wp, this would make the average price of a module equal to 255€. A 420 Wp module by Trina solar (Trina Solar Vertex S all black 420wp) weights 21.8kg, making the price per kilogram of solar energy equal to 11.7 €/kg. A PV fee of 100 €/ton would therefore translate to an increase of 0.1€/kg, less than 1% of total costs. It is fundamental to underline once more that these values for PV fees are the minimal values that over the timespam of operations lead to a 0€ NPV, considering a 5% discount rate.
This paragraph underlined the optimal schedule for Pv recycling in the different countries considered. Those countries where recycling does not make economic sense until later years will need to send their local pv waste to closer recycling plants. This will introduce higher costs related with transportations. In future analis, the impact of having a central European recycling facility for the European area could be investigated, exploring the effects on PV fees that a central collection center could have on a potentially common PV fee.

Recycling capacity

In figure 6.6, the projected optima recycling capacity is shown for the countries considered. The results are in line with expectations and scale with the expected waste flows shown in figure 6.4. The values are slightly lower than the decade waste flows because the recycling size considers an 85% collection rate. As shown above, smaller countries begin recycling operations later than smaller ones. By 2070, China is projected to have the largest recycling capacity at 12 million tonnes, significantly surpassing the USA, which ranks second with 3 million

Table 6.5: Best Starting Year and PV Fee for Recycling

Country	Best Starting Year	PV Fee (€/tonne)
Germany	2025	10.4
Japan	2025	40.5
USA	2025	41.5
China	2025	44.3
India	2025	47.3
Australia	2027	48.0
Italy	2027	70.8
France	2025	78.0
Brazil	2027	98.8
The Netherlands	2029	104.1
Austria	2044	147.7
Russia	2059	339.0
Sweden	2065	305.1

tonnes. India, Germany, Japan, and Italy follow, with recycling capacities of 2.4 million, 1.0 million, 0.4 million, and 0.4 million tonnes, respectively.

6.5. Conclusion on National consideration

This chapter delved into the national projections for photovoltaic installations and the associated end-of-life waste across various countries. Despite initial data limitations from the IEA, we expanded our scope through valuable insights from IEA-PVPS Task 12 experts, enabling a broader and more detailed analysis. The findings highlight the critical role of key countries like China, the USA, and India in the future landscape of PV installations, waste management and recycling. China, in particular, stands out with its significant projected increase in both PV capacity and EoL volumes, underscoring its pivotal position in the global PV market.
The economic feasibility of recycling PV modules was another aspect explored in this chapter. The analysis showed that early investment in recycling infrastructure could prove key to economic sustainability, in countries with sufficient PV EoL flows. One of the main discoveries of the economics of recycling was that every country will have to introduce a PV recycling fee to offset for negative profits deriving from PV recycling, a process where costs are higher than revenues. Countries with larger PV markets, such as China and the USA, could benefit from economies of scale, leading to lower PV fees compared to smaller markets like Austria and Sweden, where higher fees would be necessary to ensure financial viability. These smaller countries will probably have to initially send their PV waste to other central recycling since investments in a domestic PV recycling plant would not be economically viable The growth in PV EoL material and the economic infeasibility in some countries to run recycling plants in the near future, will require coordinated efforts, innovative solutions, and substantial investments to manage the economical and environmental impact effectively.

Overall, the national projections presented in this chapter offer a comprehensive overview of the anticipated growth and challenges in the PV industry at the local level. They underscore the need for proactive measures in both capacity expansion and waste management to ensure a sustainable energy future and underline the challenges correlated with PV recycling, a practice that will require adequate economic considerations and international collaboration.

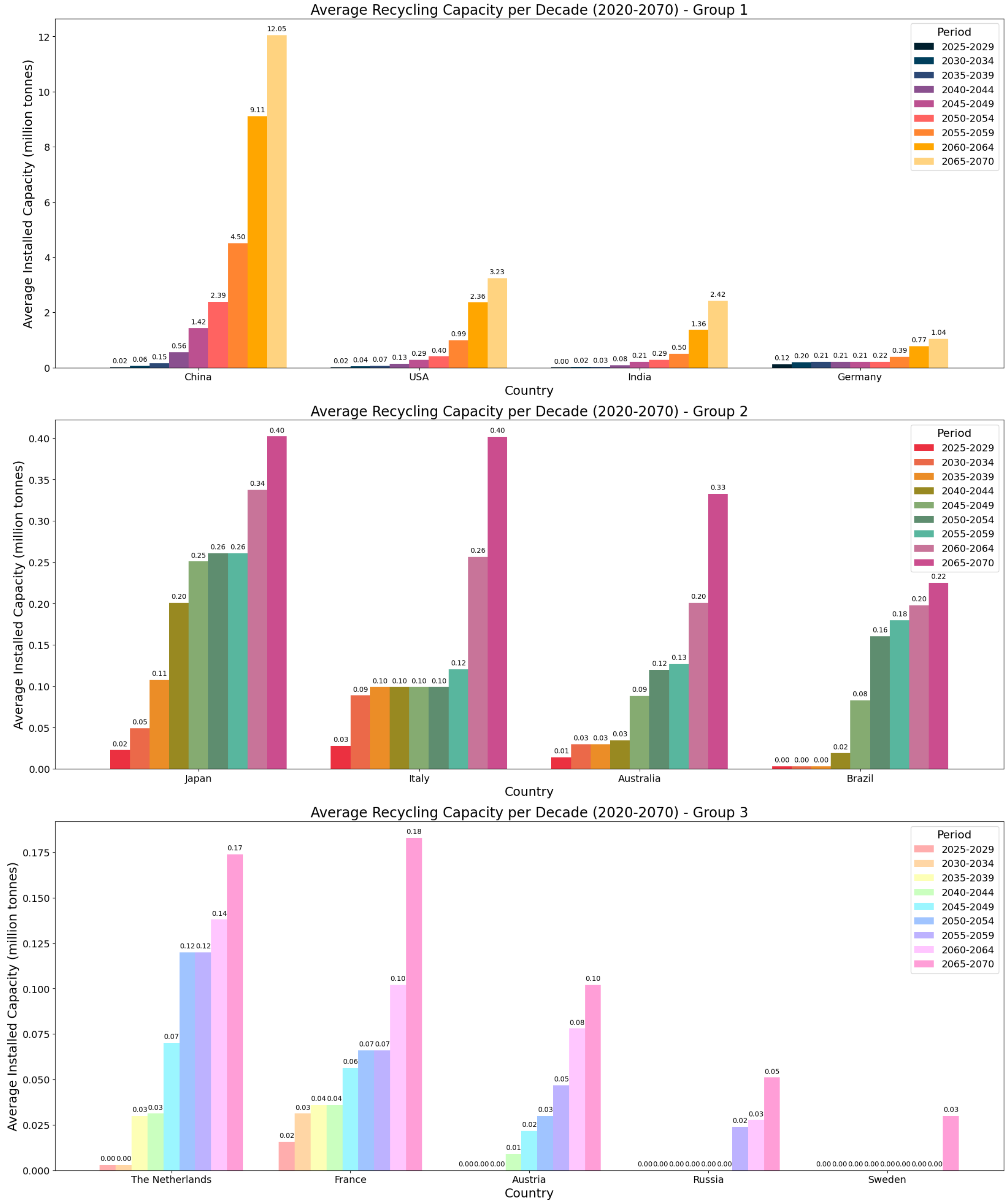

Figure 6.6: Economical model recycling capacity forecast every five years. The figure represents how much EoL Pv material can be handled in the country's recycling plants. The countries are divided into three groups to allow for better visualization of the results.

7
Conclusion

The objective of this research was to provide a projected estimation of photovoltaic (PV) End-of-Life (EoL) streams on three levels: global, continental (regional), and national. By analyzing the scale of module replacements and determining the amount of EoL materials available for recycling, this study offers critical insights into future PV waste management and recycling infrastructure needs.

Globally, the research forecasts a significant growth in PV EoL volumes, starting from 2040 and growing exponentially after 2060. By 2050, the projected cumulative EoL volumes are estimated at 42 million tons under both considered scenarios, significantly lower than the 60 to 78 million tons commonly cited in current literature. This difference comes from the different and updated methodology used in this research, which considers the temporal technological evolution of photovoltaics, in terms of reliability, performance, and material use. By 2070, global End of Life cumulative volumes are expected to surge to 432 million tons in the low scenario and 1 billion tons in the high scenario. This implies a 10 to 24 times higher cumulative volume than what was experienced in 2050, emphasizing the need for resilient and efficient plans of photovoltaic waste management. Modules that reach End of Life will need to be replaced, resulting in an expected increase in demand compared to the projections of cumulative installations proposed today. These increases were found to be equal to 62% in the low scenario (from 14.7 TW to 23.8 TW) and 28% in the high scenario (from 95.8 TW to 122.8 TW).

The peculiar shape of the installation forecast and the subsequent need for replacements will cause the demand for photovoltaic modules to experience periods of highs and lows, with peaks and draughts shifted of about 30 years (the average lifetime of a module) from the "original" valley (2000 to 2030) and peak, around 2050.

Two scenarios were also run on the global level, testing the effects on PV module installations and PV EOL volumes caused by different assumptions on degradation rates and on merchant tail. First, a scenario where degradation rates do not get better in the coming years (stagnating degradation) was tested, showing a clear increase in EoL volumes, +35% in the low installation scenario and 62% in the high one for cumulative 2070 volumes. A non - improving degradation would also lead to a significant increase in global module demand. The second scenario tested concerned the effects that merchant tail might have on modules. By merchant tail it is intended the possibility that modules are left on the field past the expiration of their economic lifetime. The effects are that higher merchant tail reduced both PV EOL volumes and module's demand.

Regionally, the distribution of potential EoL material will be predominantly concentrated in the Asia & Oceania region, with significant volumes also expected in North America and Europe. In the low scenario, Asia is projected to produce 274 million tons of EoL material, compared to 57 million tons in Europe and 65 million tons in North America. In the high scenario, these numbers rise to 539 million tons in Asia, 141 million tons in Europe, and 107 million tons in North America. In the high scenario, Africa is expected to play a fundamental role, becoming the secondary hub for both EoL material and PV demand. This research also investigated the impact that glass coming from photovoltaics in Europe might have on glass recycling volumes. In particular, given the trends on material use used in this research, it is forecasted that in case of a high installation scenario, glass waste coming from photovoltaics might account in 2070 to 10.5 million tons, a number that is equal to 67% of the total glass waste handled today in the European Union, signaling a clear need for sustainable glass policies, which might include finding alternative solutions for EoL glass, such as reusing or repurposing. The research also showed how countries more historically involved in photovoltaics, like Europe, will have around 70% of the installed capacity in 2070 being composed by modules installed in order to replace lost capacity. The research also investigated where the market for modules will be located, a market that considers new modules aimed at highering capacity and at substituting lost one. The results are that the region of Asia & Oceania will be, in both scenarios, responsible for around the same demand of the rest of the globe combined, with Africa being in both scenarios the second center of PV modules' demand.

Nationally, China is projected to accumulate the largest volume of EoL material, with 197 million tons by 2070. followed by India and the USA, with 33 million tons and 49 million tons, respectively. These results were obtained by assuming different shares of merchant tails in the countries considered, assumptions based on the cost of capital, and on the share of land that PV is expected to occupy over the total land of the respective country. With the results, a simple economic calculation on the possibility of PV recycling in the different countries was run, showing how all the countries considered will need to implement a PV recycling fee in order to allow for the economic sustainability of PV recycling. The value of this fee was found to be around 10 to 80 €/tonne for bigger countries, and around 100 to 340 €/tonne in smaller (in terms of PV installations) countries.

As solar energy continues to expand its role in the global energy mix, the need for robust end-of-life management becomes increasingly urgent. This study's projections underscore the necessity for investment in recycling technologies and the development of global standards and policies that encourage the reuse and recycling of materials. Such initiatives will be crucial to reducing the environmental footprint of solar energy and enhancing its sustainability over the long term, ensuring that the solar industry remains a cornerstone of the global transition to renewable energy, even when modules will stop producing.

Recommendations for future research

In order to make the results seen in this research more precise, some improvements are recommended

- **Using a non-fixed degradation rate for modules installed the same year**
  In this research, all modules installed in the same year were assigned identical characteristics in terms of material use and performance. This approach introduces a level of homogeneity in the photovoltaic fleet that is unrealistic, as each module produced may contain unique defects that could either reduce or enhance performance. This is particularly relevant for degradation rates. Measurements from real installations demonstrate that modules exhibit a wide distribution of degradation rates. To make End of Life simulations as realistic as possible, each installed module should be assigned a degradation rate within this distribution, rather than a standard median rate.

- **Economic lifetime subject to variability**
  As with degradation rates, the economic lifetime of photovoltaic systems should not be fixed based on the year of installation but should incorporate some degree of randomness, as the decisions regarding it largely depend on the operator. The combination of this and the previous recommendation would have reduced the "valley" in PV waste that this research forecasts in the years around 2050, introducing more realism.

- **Climate dependant degradation**
  Literature is consistent in saying that photovoltaic degradation is highly dependent on the installation location. Introducing a regional or country-specific degradation rate, related to the climate conditions of a certain country, would increase the accuracy of this forecast.

- **Introducing manufacturing waste**
  The results presented in this research do not account for manufacturing waste, which could significantly impact the overall footprint of photovoltaics. The effects of manufacturing waste should be approached and analyzed more deeply than was done in this study. Manufacturing waste carries important geographical connotations that cannot be ignored and are not related to the geographical distribution of photovoltaic modules. This waste is produced during the mining, refining, and assembly phases, which can occur in different locations and may have highly localized implications.
- **Understanding the impact of bifacial modules on installed capacity**
  This research only considered "traditional" monofacial modules, ignoring the potential impacts of bifacial modules on production capacity. The impact that bifacial modules might have given that their rating only

includes the electricity produced from the front side, leading to more unpredictable outputs and therefore more unpredictable needs for replacements of lost capacity

Bibliography

[1] G. Granata, P. Altimari, F. Pagnanelli, and J. De Greef, "Recycling of solar photovoltaic panels: Techno-economic assessment in waste management perspective," *Journal of Cleaner Production*, vol. 363, 8 2022.

[2] IEA, "World Energy Outlook 2023," Tech. Rep., 2023. [Online]. Available: www.iea.org/terms

[3] International Renewable Energy Agency, *World Energy Transitions Outlook 2023: 1.5°C Pathway*, 2023. [Online]. Available: www.irena.org

[4] B. M. Nancy Haegel, P. Verlinden, M. Victoria, P. Altermatt, H. Atwater, T. Barnes, C. Breyer, C. Case, S. De Wolf, C. Deline, M. Dharmrin, B. Dimmler, M. Gloeckler, J. Christoph Goldschmidt, B. Hallam, S. Haussener, B. Holder, U. Jaeger, A. Jaeger-Waldau, I. Kaizuka, H. Kikusato, B. Kroposki, S. Kurtz, K. Matsubara, S. Nowak, K. Ogimoto, C. Peter, I. Marius Peters, S. Philipps, M. Powalla, U. Rau, T. Reindl, M. Roumpani, K. Sakurai, C. Schorn, P. Schossig, R. Schlatmann, R. Sinton, A. Slaoui, B. L. Smith, P. Schneidewind, B. Stanbery, M. Topic, W. Tumas, J. Vasi, M. Vetter, E. Weber, A. W. Weeber, A. Weidlich, D. Weiss, and A. W. Bett, "SCIENCE science.org Photovoltaics at multi-terawatt scale: Waiting is not an option Annual electricity generation (TW-hour) Regional electricity demand supplied by solar PV," Tech. Rep., 2023. [Online]. Available: https://www.science.org

[5] D. Keiner, A. Gulagi, and C. Breyer, "Energy demand estimation using a pre-processing macro-economic modelling tool for 21st century transition analyses," *Energy*, vol. 272, 6 2023.

[6] D. Bogdanov, M. Ram, A. Aghahosseini, A. Gulagi, A. S. Oyewo, M. Child, U. Caldera, K. Sadovskaia, J. Farfan, L. De Souza Noel Simas Barbosa, M. Fasihi, S. Khalili, T. Traber, and C. Breyer, "Low-cost renewable electricity as the key driver of the global energy transition towards sustainability," *Energy*, vol. 227, 7 2021.

[7] M. Romel, G. Kabir, and K. T. W. Ng, "Analysis of barriers to photovoltaic waste management to achieve net-zero goal of Canada," *Environmental Science and Pollution Research*, vol. 30, no. 36, pp. 85 772–85 791, 8 2023.

[8] I. International Energy Agency, "Renewables 2023," Tech. Rep., 2023. [Online]. Available: www.iea.org

[9] N. M. Haegel and S. R. Kurtz, "Global Progress Toward Renewable Electricity: Tracking the Role of Solar (Version 3)," *IEEE Journal of Photovoltaics*, 11 2023.

[10] IEA, "Global Energy and Climate Model," 2023.

[11] M. G. Prina, G. Manzolini, D. Moser, B. Nastasi, and W. Sparber, "Classification and challenges of bottom-up energy system models - A review," 9 2020.

[12] M. Kittel and W.-P. Schill, "Renewable Energy Targets and Unintended Storage Cycling: Implications for Energy Modeling," 7 2021. [Online]. Available: http://arxiv.org/abs/2107.13380http://dx.doi.org/10.1016/j.isci.2022.104002

[13] C. Breyer, D. Bogdanov, M. Ram, S. Khalili, E. Vartiainen, D. Moser, E. Román Medina, G. Masson, A. Aghahosseini, T. N. Mensah, G. Lopez, M. Schmela, R. Rossi, W. Hemetsberger, and A. Jäger-Waldau, "Reflecting the energy transition from a European perspective and in the global context—Relevance of solar photovoltaics benchmarking two ambitious scenarios," *Progress in Photovoltaics: Research and Applications*, 12 2022.

[14] C. Breyer, D. Bogdanov, S. Khalili, and D. Keiner, "Solar Photovoltaics in 100% Renewable Energy Systems," in *Encyclopedia of Sustainability Science and Technology*. Springer New York, 2021, pp. 1–30.

[15] M. Jaxa-Rozen and E. Trutnevyte, "Sources of uncertainty in long-term global scenarios of solar photovoltaic technology," *Nature Climate Change*, vol. 11, no. 3, pp. 266–273, 3 2021.

[16] C. Breyer and M. Jefferson, “Use and abuse of energy and climate scenarios—a week of controversy on scenarios,” *Economics of Energy and Environmental Policy*, vol. 9, no. 1, pp. 7–19, 2020.

[17] C. Breyer, D. Bogdanov, A. Gulagi, A. Aghahosseini, L. S. Barbosa, O. Koskinen, M. Barasa, U. Caldera, S. Afanasyeva, M. Child, J. Farfan, and P. Vainikka, “On the role of solar photovoltaics in global energy transition scenarios,” *Progress in Photovoltaics: Research and Applications*, vol. 25, no. 8, pp. 727–745, 8 2017.

[18] F. Creutzig, P. Agoston, J. C. Goldschmidt, G. Luderer, G. Nemet, and R. C. Pietzcker, “The underestimated potential of solar energy to mitigate climate change,” *Nature Energy*, vol. 2, no. 9, p. 17140, 2017. [Online]. Available: https://doi.org/10.1038/nenergy.2017.140

[19] M. Xiao, T. Junne, J. Haas, and M. Klein, “Plummeting costs of renewables - Are energy scenarios lagging?” *Energy Strategy Reviews*, vol. 35, 5 2021.

[20] M. Victoria, N. Haegel, I. M. Peters, R. Sinton, A. Jäger-Waldau, C. del Cañizo, C. Breyer, M. Stocks, A. Blakers, I. Kaizuka, K. Komoto, and A. Smets, “Solar photovoltaics is ready to power a sustainable future,” pp. 1041–1056, 5 2021.

[21] *Working Group III contribution to the Sixth Assessment Report of the Intergovernmental Panel on Climate Change Mitigation of Climate Change*, 2022. [Online]. Available: www.ipcc.ch

[22] S. Ovaitt, H. Mirletz, S. Seetharaman, and T. Barnes, “PV in the circular economy, a dynamic framework analyzing technology evolution and reliability impacts,” *iScience*, vol. 25, no. 1, 1 2022.

[23] G. M. Wilson, M. Al-Jassim, W. K. Metzger, S. W. Glunz, P. Verlinden, G. Xiong, L. M. Mansfield, B. J. Stanbery, K. Zhu, Y. Yan, J. J. Berry, A. J. Ptak, F. Dimroth, B. M. Kayes, A. C. Tamboli, R. Peibst, K. Catchpole, M. O. Reese, C. S. Klinga, P. Denholm, M. Morjaria, M. G. Deceglie, J. M. Freeman, M. A. Mikofski, D. C. Jordan, G. Tamizhmani, and D. B. Sulas-Kern, “The 2020 photovoltaic technologies roadmap,” 12 2020.

[24] E. Christensen, “Electricity from photovoltaic solar cells. Flat-Plate Solar Array Project of the US Department of Energy’s National Photovoltaics Program: 10 years of progress,” Jet Propulsion Lab, Pasadena, CA (USA), Tech. Rep., 1985.

[25] Fraunhofer Institute, “International Technology
}Roadmap for Photovoltaics (ITRPV) 15th edition,” 5 2024.

[26] S. Philipps, F. Ise, W. Warmuth, and P. Projects GmbH, “Photovoltaics Report,” Tech. Rep. [Online]. Available: www.ise.fraunhofer.de

[27] B. Vicari Stefani, M. Kim, Y. Zhang, B. Hallam, M. A. Green, R. S. Bonilla, C. Fell, G. J. Wilson, and M. Wright, “Historical market projections and the future of silicon solar cells,” *Joule*, 12 2023. [Online]. Available: https://linkinghub.elsevier.com/retrieve/pii/S2542435123004804

[28] “Photovoltaic Equipment International Technology Roadmap for Photovoltaic (ITRPV) 2022 Results,” Tech. Rep., 2023.

[29] K. Medjoubi, A. M. Dubois, J. Castillon, T. Guillemot, J. Parra, M. Provost, J. B. Puel, J. Rousset, J. P. Medina Flechas, C. Bainier, D. Barrit, J. Badosa, and J. Posada, “Long Terms Stability and Metastable Behavior of Perovskite Solar Devices on Outdoor Conditions,” in *Conference Record of the IEEE Photovoltaic Specialists Conference*. Institute of Electrical and Electronics Engineers Inc., 2023.

[30] J. Lee, M. Bazilian, B. Sovacool, K. Hund, S. M. Jowitt, T. P. Nguyen, A. Månberger, M. Kah, S. Greene, C. Galeazzi, K. Awuah-Offei, M. Moats, J. Tilton, and S. Kukoda, “Reviewing the material and metal security of low-carbon energy transitions,” 5 2020.

[31] P. J. Verlinden, “Future challenges for photovoltaic manufacturing at the terawatt level,” *Journal of Renewable and Sustainable Energy*, vol. 12, no. 5, 9 2020.

[32] P. Newman and S. Tomlinson, “The Silver Institute 2023 INTERIM SILVER MARKET REVIEW,” Tech. Rep.

[33] B. Hallam, M. Kim, Y. Zhang, L. Wang, A. Lennon, P. Verlinden, P. P. Altermatt, and P. R. Dias, "The silver learning curve for photovoltaics and projected silver demand for net-zero emissions by 2050," *Progress in Photovoltaics: Research and Applications*, 2022.

[34] M. Kamran, M. Raugei, and A. Hutchinson, "Critical elements for a successful energy transition: A systematic review," *Renewable and Sustainable Energy Transition*, vol. 4, p. 100068, 8 2023.

[35] S. Davidsson and M. Höök, "Material requirements and availability for multi-terawatt deployment of photovoltaics," *Energy Policy*, vol. 108, pp. 574–582, 9 2017.

[36] "MINERAL COMMODITY SUMMARIES 2023," Tech. Rep., 2023.

[37] C. A. Miller, I. M. Peters, and S. Zaveri, "Thin Film CdTe Photovoltaics and the U.S. Energy Transition in 2020," 2020.

[38] G. A. Heath, D. Ravikumar, B. Hansen, and E. Kupets, "A critical review of the circular economy for lithium-ion batteries and photovoltaic modules–status, challenges, and opportunities," pp. 478–539, 2022.

[39] A. Sharma, S. Pandey, and M. Kolhe, "Global review of policies & guidelines for recycling of solar pv modules," pp. 597–610, 9 2019.

[40] IRENA and IEA-PVPS, "End-of-Life_Solar_PV_Panels_2016," 2016.

[41] Y. Zhang, M. Kim, L. Wang, P. Verlinden, and B. Hallam, "Design considerations for multi-terawatt scale manufacturing of existing and future photovoltaic technologies: Challenges and opportunities related to silver, indium and bismuth consumption," *Energy and Environmental Science*, vol. 14, no. 11, pp. 5587–5610, 11 2021.

[42] G. A. Heath, T. J. Silverman, M. Kempe, M. Deceglie, D. Ravikumar, T. Remo, H. Cui, P. Sinha, C. Libby, S. Shaw, K. Komoto, K. Wambach, E. Butler, T. Barnes, and A. Wade, "Research and development priorities for silicon photovoltaic module recycling to support a circular economy," *Nature Energy*, vol. 5, no. 7, pp. 502–510, 7 2020.

[43] N. J. Bartie, Y. L. Cobos-Becerra, M. Fröhling, R. Schlatmann, and M. A. Reuter, "The resources, exergetic and environmental footprint of the silicon photovoltaic circular economy: Assessment and opportunities," *Resources, Conservation and Recycling*, vol. 169, 6 2021.

[44] C. Liu, Q. Zhang, and L. Liu, "Estimation of photovoltaic waste spatio-temporal distribution by 2060 in the context of carbon neutrality," *Environmental Science and Pollution Research*, vol. 30, no. 12, pp. 34 840–34 855, 3 2023.

[45] I. D'Adamo, M. Miliacca, and P. Rosa, "Economic Feasibility for Recycling of Waste Crystalline Silicon Photovoltaic Modules," *International Journal of Photoenergy*, vol. 2017, 2017.

[46] W. L. Filho, M. Alzira, P. Dinis, S. Moggi, E. Price, and A. Hope, "SDGs in the European Region," Tech. Rep., 2023.

[47] H. K. Salim, R. A. Stewart, O. Sahin, and M. Dudley, "Drivers, barriers and enablers to end-of-life management of solar photovoltaic and battery energy storage systems: A systematic literature review," pp. 537–554, 2 2019.

[48] P.-H. Chen, W.-S. Chen, C.-H. Lee, and J.-Y. Wu, "Comprehensive Review of Crystalline Silicon Solar Panel Recycling: From Historical Context to Advanced Techniques," *Sustainability*, vol. 16, no. 1, p. 60, 12 2023.

[49] D. C. Jordan, N. Haegel, and T. M. Barnes, "Photovoltaics module reliability for the terawatt age," 4 2022.

[50] T. Rahman, A. A. Mansur, M. S. Hossain Lipu, M. S. Rahman, R. H. Ashique, M. A. Houran, R. M. Elavarasan, and E. Hossain, "Investigation of Degradation of Solar Photovoltaics: A Review of Aging Factors, Impacts, and Future Directions toward Sustainable Energy Management," 5 2023.

[51] O. A. Alimi, E. L. Meyer, and O. I. Olayiwola, "Solar Photovoltaic Modules' Performance Reliability and Degradation Analysis—A Review," 8 2022.

[52] D. C. Jordan, K. Anderson, K. Perry, M. Muller, M. Deceglie, R. White, and C. Deline, “Photovoltaic fleet degradation insights,” *Progress in Photovoltaics: Research and Applications*, vol. 30, no. 10, pp. 1166–1175, 10 2022.

[53] S. Lindig, J. Ascencio-Vasquez, J. Leloux, D. Moser, and A. Reinders, “Performance Analysis and Degradation of a Large Fleet of PV Systems,” *IEEE Journal of Photovoltaics*, vol. 11, no. 5, pp. 1312–1318, 9 2021.

[54] M. Halwachs, L. Neumaier, N. Vollert, L. Maul, S. Dimitriadis, Y. Voronko, G. C. Eder, A. Omazic, W. Mühleisen, C. Hirschl, M. Schwark, K. A. Berger, and R. Ebner, “Statistical evaluation of PV system performance and failure data among different climate zones,” *Renewable Energy*, vol. 139, pp. 1040–1060, 8 2019.

[55] L. Xia, Z. Wen, K. Liao, J. Chen, Q. Li, and X. Luo, “Unveiling the Failure Mechanism of Electrical Interconnection in Thermal-Aged PV Modules,” *IEEE Transactions on Device and Materials Reliability*, vol. 20, no. 1, pp. 24–32, 3 2020.

[56] N. Kyranaki, A. Smith, K. Yendall, D. A. Hutt, D. C. Whalley, R. Gottschalg, and T. R. Betts, “Damp-heat induced degradation in photovoltaic modules manufactured with passivated emitter and rear contact solar cells,” *Progress in Photovoltaics: Research and Applications*, vol. 30, no. 9, pp. 1061–1071, 9 2022.

[57] E. L. Meyer and E. E. Van Dyk, “Assessing the reliability and degradation of photovoltaic module performance parameters,” *IEEE Transactions on Reliability*, vol. 53, no. 1, pp. 83–92, 3 2004.

[58] P. Guerriero and S. Daliento, “Toward a Hot Spot Free PV Module,” *IEEE Journal of Photovoltaics*, vol. 9, no. 3, pp. 796–802, 5 2019.

[59] X. Jiang, F. Wang, A. Wang, H. Wang, J. Ding, J. Zhang, and J. Huang, *Study on Random Failure of Crystalline Silicon Solar Modules in the Field*, 2017.

[60] L. Zhang, S. Chang, Q. Wang, and D. Zhou, “Projection of Waste Photovoltaic Modules in China Considering Multiple Scenarios,” *Sustainable Production and Consumption*, vol. 33, pp. 412–424, 9 2022.

[61] A. Domínguez and R. Geyer, “Photovoltaic waste assessment of major photovoltaic installations in the United States of America,” *Renewable Energy*, pp. 1188–1200, 4 2019.

[62] C. C. Faircloth, K. H. Wagner, K. E. Woodward, P. Rakkwamsuk, and S. H. Gheewala, “The environmental and economic impacts of photovoltaic waste management in Thailand,” *Resources, Conservation and Recycling*, vol. 143, pp. 260–272, 4 2019.

[63] J. R. Peeters, D. Altamirano, W. Dewulf, and J. R. Duflou, “Forecasting the composition of emerging waste streams with sensitivity analysis: A case study for photovoltaic (PV) panels in Flanders,” *Resources, Conservation and Recycling*, vol. 120, pp. 14–26, 2017.

[64] J. D. Santos and M. C. Alonso-García, “Projection of the photovoltaic waste in Spain until 2050,” *Journal of Cleaner Production*, vol. 196, pp. 1613–1628, 9 2018.

[65] S. Mahmoudi, N. Huda, and M. Behnia, “Critical assessment of renewable energy waste generation in OECD countries: Decommissioned PV panels,” *Resources, Conservation and Recycling*, vol. 164, 1 2021.

[66] M. B. Nieto-Morone, M. C. Alonso-García, F. G. Rosillo, J. D. Santos, and M. A. Muñoz-García, “State and prospects of photovoltaic module waste generation in China, USA, and selected countries in Europe and South America,” *Sustainable Energy and Fuels*, vol. 7, no. 9, pp. 2163–2177, 3 2023.

[67] I. Renewable Energy Agency, *RENEWABLE CAPACITY STATISTICS 2024*, 2024. [Online]. Available: www.irena.org

[68] S. Ovaitt, H. Mirletz, and M. M. Ribo, “NREL/PV_ICE: v0.3.2 Release,” 2 2023. [Online]. Available: https://doi.org/10.5281/zenodo.7651576

[69] M. Bolinger, J. Seel, C. Warner, and D. Robson, “Utility-Scale Solar, 2022 Edition: Empirical Trends in Deployment, Technology, Cost, Performance, PPA Pricing, and Value in the United States,” Tech. Rep., 2022. [Online]. Available: https://escholarship.org/uc/item/7496x1pc

[70] A. Metz, M. Fischer, and J. Trube, "International Technology Roadmap for Photovoltaics (ITRPV) 8 th edition: Crystalline Silicon Technology Current Status and Outlook," Tech. Rep., 2017. [Online]. Available: www.siemens.com/presse

[71] P. Hülsmann and K. A. Weiss, "Simulation of water ingress into PV-modules: IEC-testing versus outdoor exposure," pp. 347–353, 5 2015.

[72] S. Chattopadhyay, R. Dubey, S. Bhaduri, S. Zachariah, H. K. Singh, C. S. Solanki, A. Kottantharayil, N. Shiradkar, B. M. Arora, K. L. Narasimhan, and J. Vasi, "Correlating infrared thermography with electrical degradation of PV modules inspected in all-india survey of photovoltaic module reliability 2016," *IEEE Journal of Photovoltaics*, vol. 8, no. 6, pp. 1800–1808, 11 2018.

[73] D. C. Jordan, C. Deline, M. Deceglie, T. J. Silverman, and W. Luo, *PV Degradation – Mounting & Temperature*. IEEE, 2019.

[74] D. o. E. United Nations and P. D. Social Affairs, "World Population Prospects 2022: Summary of Results. UN DESA/POP/2022/TR/NO. 3." 2022.

[75] P. Biermayr, S. Aigenbauer, C. Dißauer, M. Eberl, M. Enigl, H. Fechner, C. Fink, M. Fuhrmann, F. Hengel, M. Jaksch-Fliegenschnee, K. Leonhartsberger, D. Matschegg, S. Moidl, E. Prem, T. Riegler, S. Savic, C. Schmidl, C. Strasser, P. Wonisch, and E. Wopienka, "Innovative Energietechnologien
}in Österreich
}Marktentwicklung 2022," Tech. Rep., 2022. [Online]. Available: https://nachhaltigwirtschaften.at/de/publikationen/schriftenreihe-2023-36-

[76] V. Tan, R. Deng, and R. Egan, "Solar photovoltaic waste and resource potential projections in Australia, 2022–2050," *Resources, Conservation and Recycling*, vol. 202, 1 2024.

[77] Réseau de Transport d'Électricité (Rte), "Futurs énergétiques 2050 Rapport complet," Tech. Rep., 2022.

[78] M. Gaeta, C. N. Businge, F. Lanati, and A. Gelmini, "Scenari di neutralità climatica a supporto della Long Term Strategy," Tech. Rep., 2020.

[79] Energimyndigheten, *Scenarier över Sveriges energisystem 2023*, 2023. [Online]. Available: www.energimyndigheten.se

[80] M. Späth, S. Wieclawska, P. Sommeling, and F. Lenzmann, "BALANCING COSTS AND REVENUES FOR RECYCLING END-OF-LIFE PV PANELS IN THE NETHERLANDS," Tech. Rep., 2022.

[81] H. Wirth and F. Ise, "Aktuelle Fakten zur Photovoltaik in Deutschland," Tech. Rep., 2023. [Online]. Available: www.pv-fakten.de

[82] M. Motyka, J. Thomson, K. Hardin, and C. Amson, "2024 renewable energy industry outlook," 12 2023.

[83] T. D'Olier-Lees, G. Cantabrana Fernandez, A. Prabhu, L. Li, and P. Georges, "Renewable Energy Funding in 2023: A "Capital Transition" Unleashed," 9 2023.

[84] worldgovernamentbonds.com, "World governament bonds," 6 2024.

[85] A. Damodaran, "Country Default Spreads and Risk Premiums," 1 2024.

[86] Gestore dei Servizi Energetici GSE S.p.A., "INCENTIVA LA PRODUZIONE DI ENERGIA DA IMPIANTI FOTOVOLTAICI CONNESSI ALLA RETE," 2012.

[87] I. D'Adamo, F. Ferella, M. Gastaldi, N. M. Ippolito, and P. Rosa, "Circular solar: Evaluating the profitability of a photovoltaic panel recycling plant," *Waste Management and Research*, vol. 41, no. 6, pp. 1144–1154, 6 2023.

[88] A. Gautam, R. Shankar, and P. Vrat, "Managing end-of-life solar photovoltaic e-waste in India: A circular economy approach," *Journal of Business Research*, vol. 142, pp. 287–300, 3 2022.

[89] A. Skujins, "Netherlands raises solar panel recycling fee to 'absorb shocks' in market," 10 2023.

[90] M. Bolinger, J. Seel, J. M. Kemp, C. Warner, A. Katta, and D. Robson, "Utility-Scale Solar, 2023 Edition Utility-Scale Solar, 2023 Edition 2 Disclaimer," Tech. Rep. [Online]. Available: http://utilityscalesolar.lbl.gov

A

Appendix

chngcntr

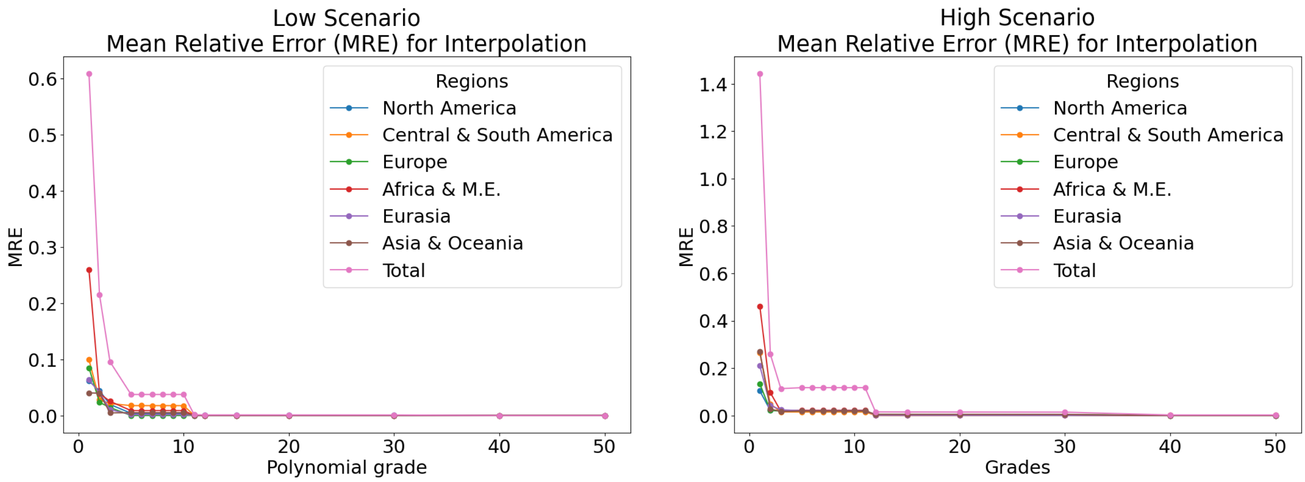

Figure A.1: MRE related to polynomial grade

Polynomial grade	North America	Central & South America	Europe	Africa & M.E.	Eurasia	Asia & Oceania	Total
1	6.15E-02	9.94E-02	8.51E-02	2.59E-01	6.34E-02	4.04E-02	1.02E-01
2	4.42E-02	2.79E-02	2.35E-02	3.92E-02	4.09E-02	3.96E-02	3.59E-02
3	1.98E-02	2.13E-02	1.42E-02	2.53E-02	1.04E-02	4.71E-03	1.60E-02
5	3.97E-03	1.77E-02	8.87E-05	8.72E-03	1.95E-03	5.06E-03	6.24E-03
6	3.96E-03	1.77E-02	9.63E-05	8.75E-03	1.95E-03	5.06E-03	6.24E-03
7	3.96E-03	1.76E-02	9.62E-05	8.77E-03	1.94E-03	5.08E-03	6.25E-03
8	3.96E-03	1.76E-02	9.12E-05	8.78E-03	1.94E-03	5.08E-03	6.25E-03
9	3.95E-03	1.76E-02	8.89E-05	8.80E-03	1.94E-03	5.09E-03	6.25E-03
10	3.95E-03	1.76E-02	8.62E-05	8.81E-03	1.94E-03	5.10E-03	6.25E-03
20	2.82E-04	1.89E-04	2.22E-04	1.08E-04	1.20E-04	1.09E-04	1.72E-04
30	2.82E-04	1.62E-04	2.16E-04	9.69E-05	1.15E-04	1.10E-04	1.64E-04
40	1.44E-05	5.10E-06	1.17E-05	4.83E-06	3.27E-06	5.32E-06	7.43E-06
50	1.42E-06	1.56E-06	2.65E-06	5.23E-07	1.00E-06	1.04E-06	1.37E-06

Table A.1: MRE with different polynomial grades, Low scenario

Polynomial grade	North America	Central & South America	Europe	Africa & M.E.	Eurasia	Asia & Oceania	Total
1	1.04E-01	2.64E-01	1.34E-01	4.61E-01	2.10E-01	2.70E-01	1.44E+00
2	2.15E-02	4.91E-02	2.16E-02	9.65E-02	4.21E-02	2.77E-02	2.59E-01
3	2.06E-02	1.52E-02	1.85E-02	1.81E-02	2.42E-02	1.70E-02	1.14E-01
5	2.10E-02	1.50E-02	1.96E-02	2.22E-02	2.06E-02	1.92E-02	1.18E-01
6	2.10E-02	1.50E-02	1.96E-02	2.22E-02	2.06E-02	1.92E-02	1.18E-01
7	2.10E-02	1.50E-02	1.96E-02	2.22E-02	2.06E-02	1.92E-02	1.18E-01
8	2.10E-02	1.50E-02	1.96E-02	2.22E-02	2.06E-02	1.92E-02	1.18E-01
9	2.10E-02	1.50E-02	1.96E-02	2.22E-02	2.06E-02	1.92E-02	1.18E-01
10	2.10E-02	1.50E-02	1.96E-02	2.22E-02	2.06E-02	1.92E-02	1.18E-01
20	9.09E-04	1.47E-03	4.31E-03	1.21E-03	1.80E-03	5.03E-03	1.47E-02
30	7.00E-04	1.62E-03	4.10E-03	1.43E-03	1.59E-03	4.82E-03	1.43E-02
40	4.56E-04	5.07E-04	1.65E-04	6.50E-04	5.05E-04	3.25E-05	2.32E-03
50	4.50E-04	4.98E-04	1.67E-04	6.41E-04	4.95E-04	2.38E-05	2.27E-03

Table A.2: MRE with different polynomial grades, high scenario

Region	Cumulative capacity = ax^6 + bx^5 + cx^4 + dx^3 + ex^2 + fx + g [MW]						
	a	b	c	d	e	f	g
North America	-2.1431E-11	1.7626E-07	-4.5419E-04	1.0058E-02	1.8834E+03	-3.1057E+06	1.5960E+09
Central & South America	1.7251E-11	-1.4068E-07	3.5873E-04	-2.0402E-03	-1.4835E+03	2.4211E+06	-1.2338E+09
Europe	3.9730E-11	-3.2284E-07	8.1967E-04	9.8384E-04	-3.3859E+03	5.5016E+06	-2.7939E+09
Africa & M.E.	3.0439E-11	-2.4741E-07	6.2836E-04	4.2595E-04	-2.5959E+03	4.2193E+06	-2.1433E+09
Eurasia	5.6046E-13	-4.5361E-09	1.1459E-05	1.0570E-04	-4.7273E+01	7.6415E+04	-3.8641E+07
Asia & Oceania	-2.0863E-10	1.6999E-06	-4.3307E-03	1.8239E-02	1.7905E+04	-2.9194E+07	1.4868E+10

Table A.3: Low scenario grade 6 polynomial polynomial coefficients

Region	Cumulative capacity = ax^6 + bx^5 + cx^4 + dx^3 + ex^2 + fx + g [MW]						
	a	b	c	d	e	f	g
North America	6.4316E-11	-5.2136E-07	1.3200E-03	5.8095E-03	-5.4412E+03	8.8160E+06	-4.4661E+09
Central & South America	4.1068E-11	-3.3310E-07	8.4395E-04	2.7063E-03	-3.4796E+03	5.6422E+06	-2.8601E+09
Europe	1.4103E-10	-1.1452E-06	2.9058E-03	2.7323E-03	-1.1985E+04	1.9461E+07	-9.8767E+09
Africa & M.E.	2.4222E-10	-1.9680E-06	4.9968E-03	-7.1071E-04	-2.0613E+04	3.3496E+07	-1.7009E+10
Eurasia	1.3793E-11	-1.1134E-07	2.8043E-04	3.5584E-03	-1.1544E+03	1.8605E+06	-9.3840E+08
Asia & Oceania	4.8091E-10	-3.9082E-06	9.9259E-03	-5.6690E-03	-4.0950E+04	6.6560E+07	-3.3806E+10

Table A.4: High scenario grade 6 polynomial polynomial coefficients

Region	Low scenario			High scenario		
	K optimal	b optimal	t0 optimal	K optimal	b optimal	t0 optimal
North America	1.863	0.203	2033.331	5.711	0.156	2040.378
Central & South America	0.596	0.148	2039.863	5.729	0.142	2047.043
Europe	1.262	0.183	2030.274	8.301	0.147	2041.901
Africa & M.E.	1.642	0.171	2042.137	22.432	0.151	2050.000
Eurasia	0.079	0.181	2037.019	2.316	0.150	2044.559
Asia & Oceania	8.997	0.186	2034.518	50.433	0.151	2045.315

Table A.5: Optimal values for the sigmoid extension functions, high and low scenario

	North America	Central & South America	Europe	Africa & M.E.	Eurasia	Asia & Oceania
Low scenario	0.0163	0.0164	0.0016	0.0858	0.0041	0.1295
High scenario	0.398	0.198	0.506	0.551	0.123	1.735

Table A.6: Delta of added capacity [TW], years 2051 - 2070

	2020	2025	2030	2035	2040	2045	2050
63 TWp scenario - Global Cumulative Capacity	1.10	3.53	10.21	18.27	30.53	43.49	63.38
Scaling factor	1.0000	1.0306	1.0611	1.0917	1.1222	1.1528	1.1833
75 TWp scenario - Global Cumulative Capacity	1.10	3.64	10.83	19.95	34.26	50.13	75.00

Table A.7: High scenario: scaling up the global forecast from 63 to 75 TWp

Country	Full PV capacity 2070 [GW]	Thin film share	Silicon PV Capacity 2070 [GW]	Source
USA	1926	30%	1348	[90]
China	7030	15%	5975	Assumption
India	1912	15%	1625	Assumption
Brazil	233	15%	198	Assumption
Russia	38	15%	32	Assumption
Japan	208	15%	177	Assumption
Austria	69	2%	68	[75]
Australia	704	15%	598	Assumption
France	138	5%	131	Assumption
Italy	294	5%	279	Assumption
Sweden	35	5%	33	Assumption
Netherlands	91	5%	86	Assumption
Germany	652	5%	619	Assumption

Table A.8: Share of thin film compared to silicon capacity used in this research and effect on cumulative 2070 number. The assumption unknown countriess of 15%, European countries were assumed to be at 5% to resemble the only real data available for Europe, Austria.

	Cumulative capacity = ax^6 + bx^5 + cx^4 + dx^3 + ex^2 + fx + g [MW]						
Country	**a**	**b**	**c**	**d**	**e**	**f**	**g**
Brazil	6.1220E-12	-4.9966E-08	1.2756E-04	-9.4866E-04	-5.2765E+02	8.6208E+05	-4.3974E+08
China	-2.2807E-10	1.8582E-06	-4.7335E-03	1.9177E-02	1.9570E+04	-3.1905E+07	1.6247E+10
India	7.3869E-11	-6.0150E-07	1.5311E-03	-4.3944E-03	-6.3290E+03	1.0310E+07	-5.2468E+09
Japan	-8.9786E-12	7.3303E-08	-1.8720E-04	1.4990E-03	7.7445E+02	-1.2658E+06	6.4583E+08
Russia	1.1553E-12	-9.4036E-09	2.3924E-05	-4.8342E-05	-9.8878E+01	1.6099E+05	-8.1891E+07
USA	-2.6656E-11	2.1856E-07	-5.6113E-04	9.1784E-03	2.3246E+03	-3.8194E+06	1.9571E+09
Austria	-8.8194E-13	7.1854E-09	-1.8303E-05	7.2670E-05	7.5670E+01	-1.2336E+05	6.2812E+07
France	5.6751E-12	-4.6223E-08	1.1772E-04	-5.7741E-04	-4.8600E+02	7.9212E+05	-4.0321E+08
Italy	-3.4435E-12	2.8097E-08	-7.1700E-05	4.9221E-04	2.9657E+02	-4.8436E+05	2.4700E+08
Sweden	5.4197E-12	-4.4118E-08	1.1226E-04	-2.5679E-04	-4.6398E+02	7.5558E+05	-3.8440E+08
The Netherlands	8.5494E-12	-6.9611E-08	1.7710E-04	1.3865E-04	-7.3429E+02	1.1956E+06	-6.0840E+08
Germany	-2.0768E-11	1.6924E-07	-4.3101E-04	3.4936E-04	1.7875E+03	-2.9134E+06	1.4837E+09
Australia	-	-	-	-	-	-	-

Table A.9: Nations PV installation forecasts grade 6 polynomial coefficients. The data for Australia was already provided for every year, therefore no interpolation was needed

Country	K_optimal	b_optimal	t0_optimal
Brazil	0.20098443031311036	0.1257274276459582	2037.3460029406724
China	5.874188770678936	0.1997742397566031	2033.3255098851512
India	1.6174624156951911	0.1823022554150431	2038.3992477906208
Japan	0.18113585800192666	0.19247288777241686	2024.5752532860201
Russia	0.031187188331826834	0.1706962044698027	2039.1115080769657
USA	1.349007377624512	0.20918513591724144	2032.7285272589927
Austria	0.06694630026817323	0.14642721655782312	2036.7737023635514
Australia	0.6552228205061961	0.11814716883035017	2049.9999999958986
France	0.13193206923697054	0.13111446421759193	2037.804494528876
Italy	0.248602161182453	0.1324030137887841	2037.8372503156377
Sweden	0.03221044298153059	0.11033772752322828	2046.053863950456
The Netherlands	0.08532295888548234	0.20342048223221545	2029.117750862055
Germany	0.6067982673645022	0.13715680917745376	2035.5929596979038
Australia	-	-	-

Table A.10: Optimal values for the sigmoid extension functions for the countries considered. The data for Australia was already provided for every year, therefore no interpolation was needed

Country	**Brazil**	**China**	**India**	**Japan**	**Russia**	**USA**	**Austria**
Delta [GW]	9.11	259.52	67.66	8.79	1.19	70.33	2.57
Country	**Australia**	**France**	**Italy**	**Sweden**	**Netherlands**	**Germany**	**Australia**
Delta [GW]	14.04	5.67	13.22	0.97	4.17	25.0	14.01

Table A.11: Added delta for the countries considered

Country	Cost of Debt	Cost of Equity	After-Tax Cost of Debt	WACC
China	0.0329	0.0906	0.0247	**0.0692**
United States	0.0479	0.0973	0.0378	**0.0795**
Japan	0.0136	0.0768	0.0095	**0.0564**
Italy	0.0539	0.1342	0.041	**0.1031**
India	0.0799	0.1637	0.0559	**0.1271**
Australia	0.0426	0.0952	0.0298	**0.0768**
Austria	0.0277	0.0872	0.0208	**0.0661**
Germany	0.0259	0.0782	0.0181	**0.0597**
The Netherlands	0.0274	0.0802	0.0206	**0.0645**
Sweden	0.0228	0.0752	0.0178	**0.0566**
France	0.0343	0.0938	0.0247	**0.0771**
Brazil	0.1369	0.221	0.0903	**0.1765**
Russia	0.2115	0.28566	0.158625	**0.24755**

Table A.12: Intermediate steps results for WACC calculation

Table A.13: CAPEX and OPEX for Various Recycling Capacities, [1]

Capacity (ton/year)	CAPEX ($)	OPEX ($/year)	Price per ton ($/ton)
3000	5 444 410	17 903 211	5977
6000	6 173 070	18 422 395	3070
9000	6 825 217	18 946 677	2105
12000	7 468 212	19 469 284	1622
15000	8 065 611	19 983 692	1332
18000	8 680 687	20 501 246	1138
21000	9 256 206	21 011 707	1000
24000	10 333 671	21 612 276	900
27000	10 897 224	22 120 593	819
30000	10 976 143	22 362 070	745

A.1. China

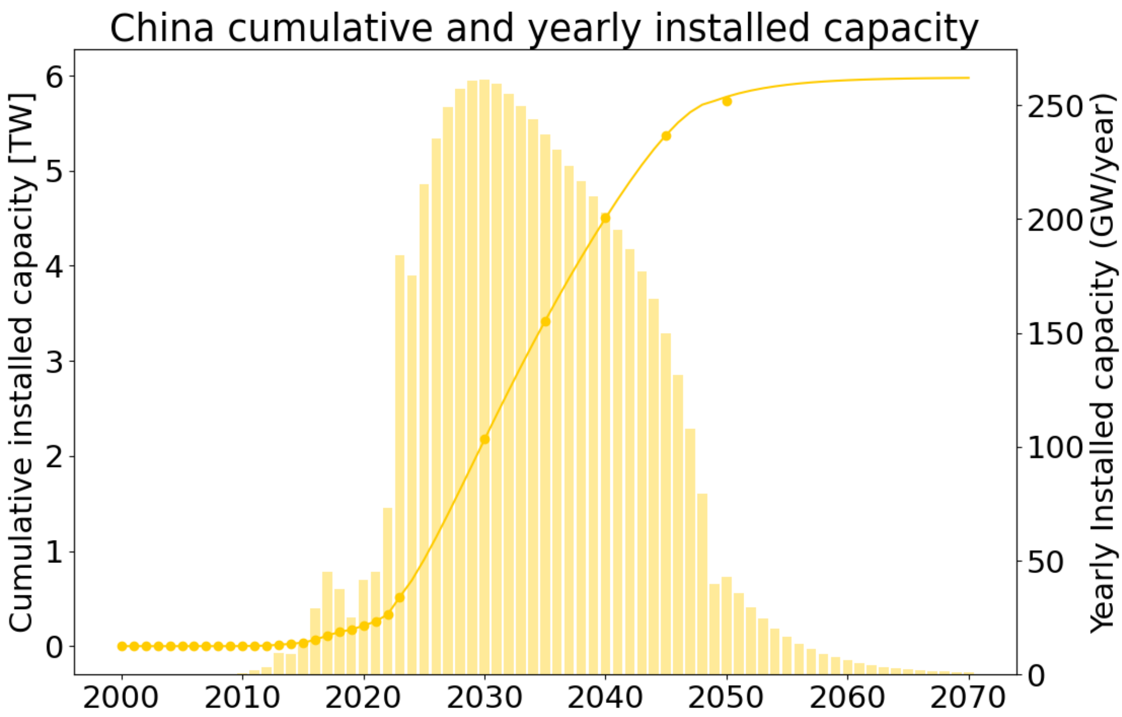

Figure A.2: Annual installation forecast for China. The dots represent forecasted points given from the source, the line is the interpolation and extension going through them.

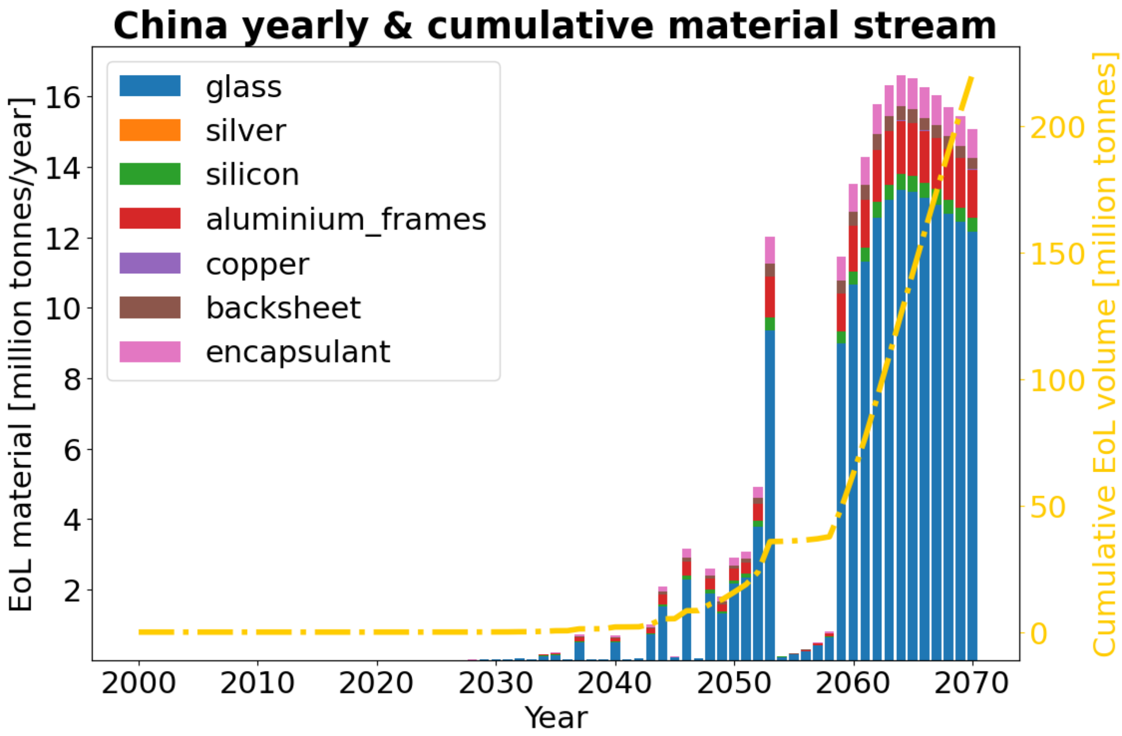

Figure A.3: Annual and cumulative expected End of Life flows for China. The dip in the years around 2060 has origins in the assumptions on degradation and lifetime; a more thorough explanation can be found in subsection 4.1.5

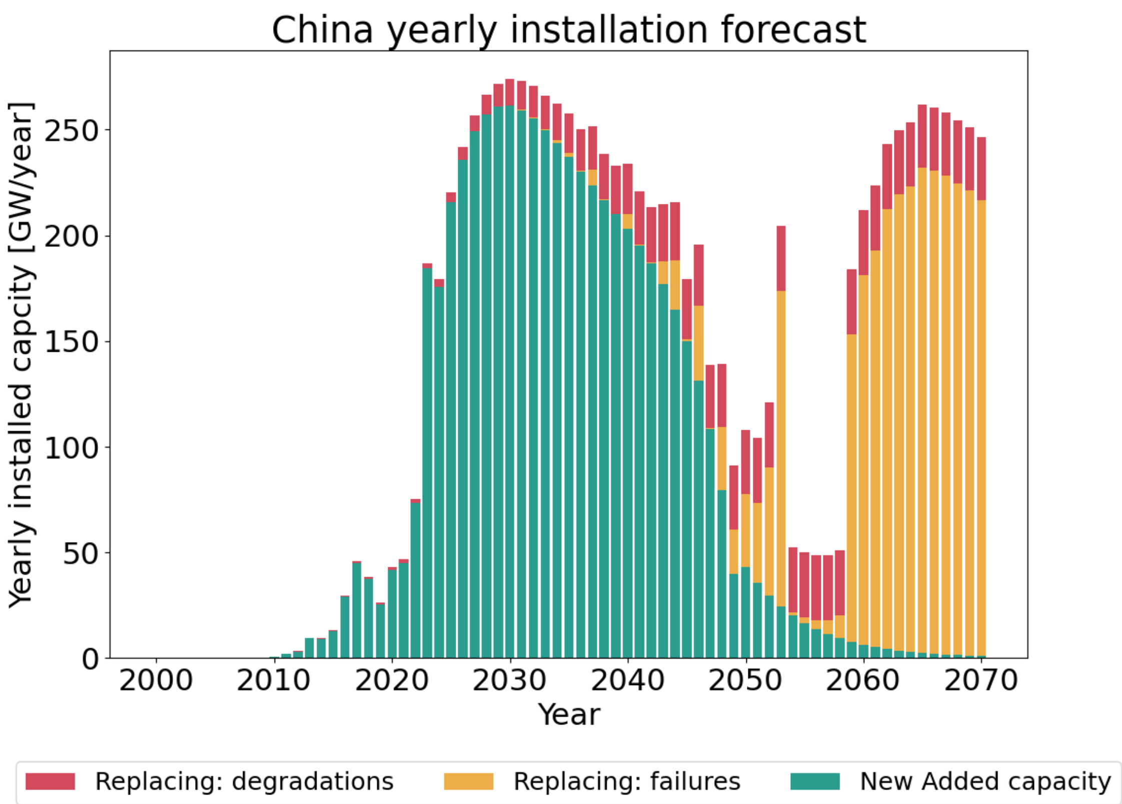

Figure A.4: Annual expected PV demand in China, divided among the three causes of new capacity demand: new installations (green bars), capacity failed (blue bars) and capacity degraded but still in operation (orange bars)

A.2. United States of America

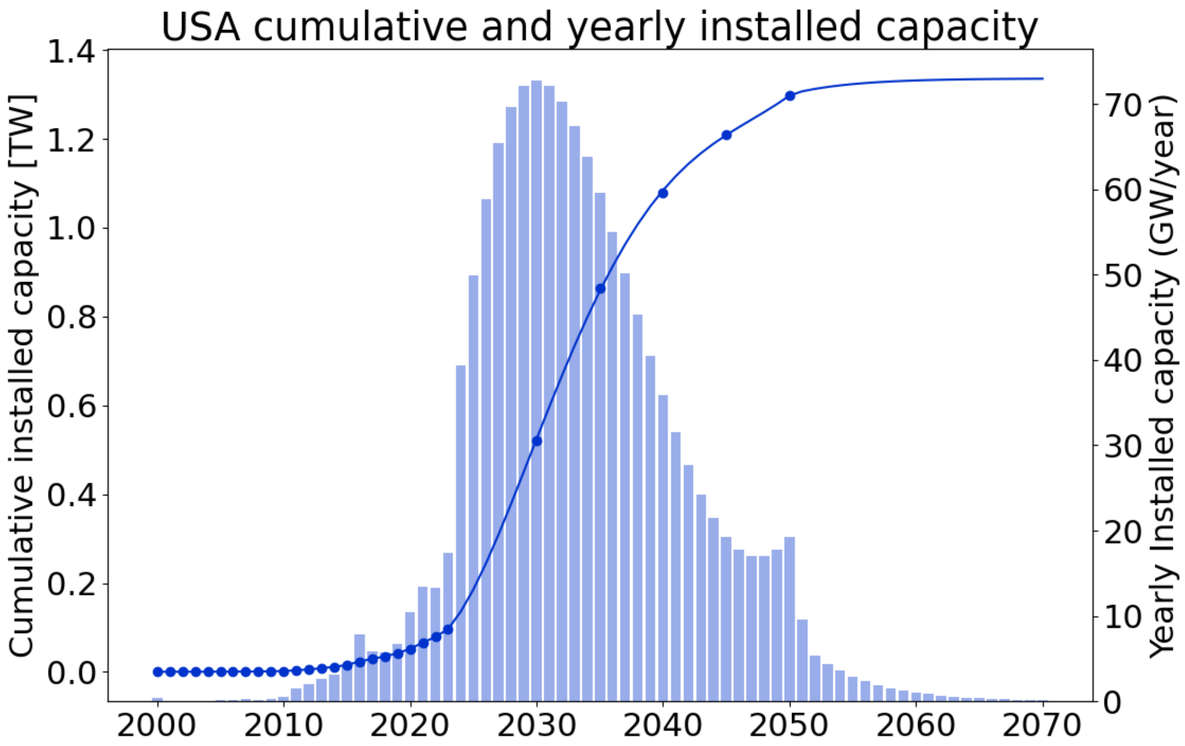

Figure A.5: Annual installation forecast for the United States of America. The dots represent forecasted points given from the source, the line is the interpolation and extension going through them.

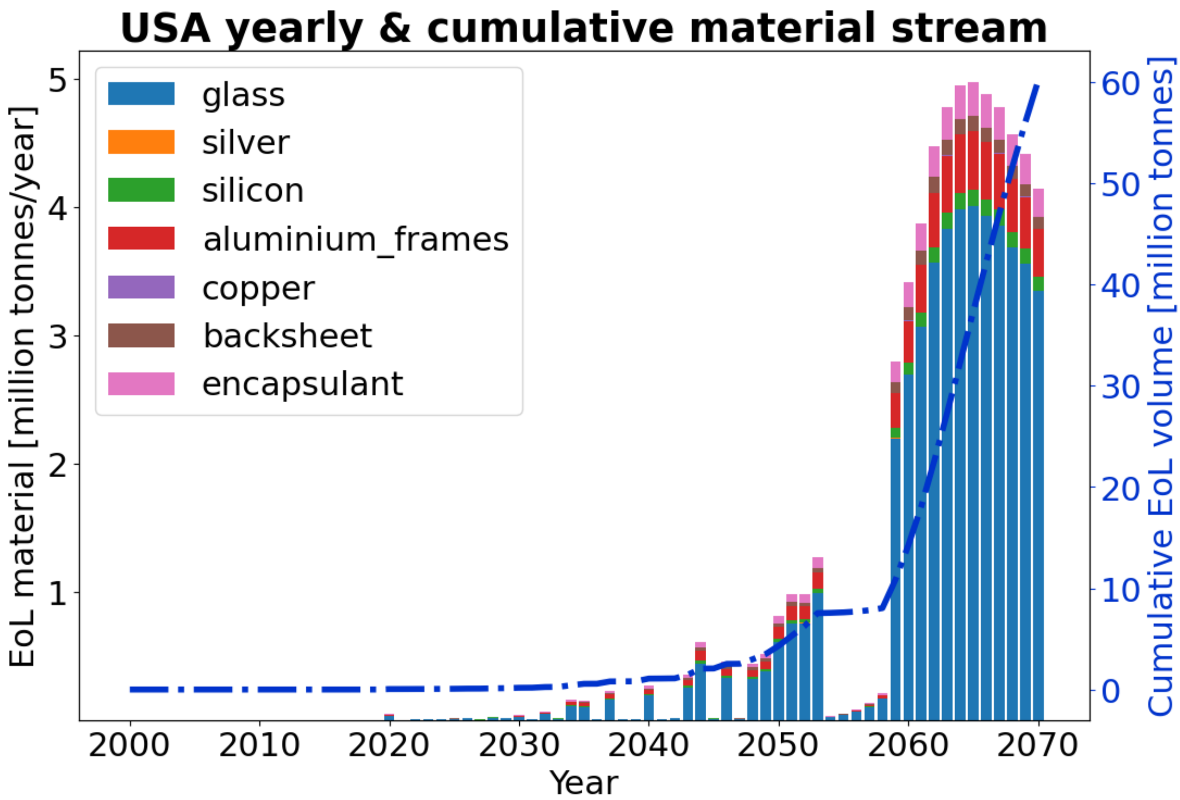

Figure A.6: Annual and cumulative expected End of Life flows for the United States of America. The dip in the years around 2060 has origins in the assumptions on degradation and lifetime; a more thorough explanation can be found in subsection 4.1.5

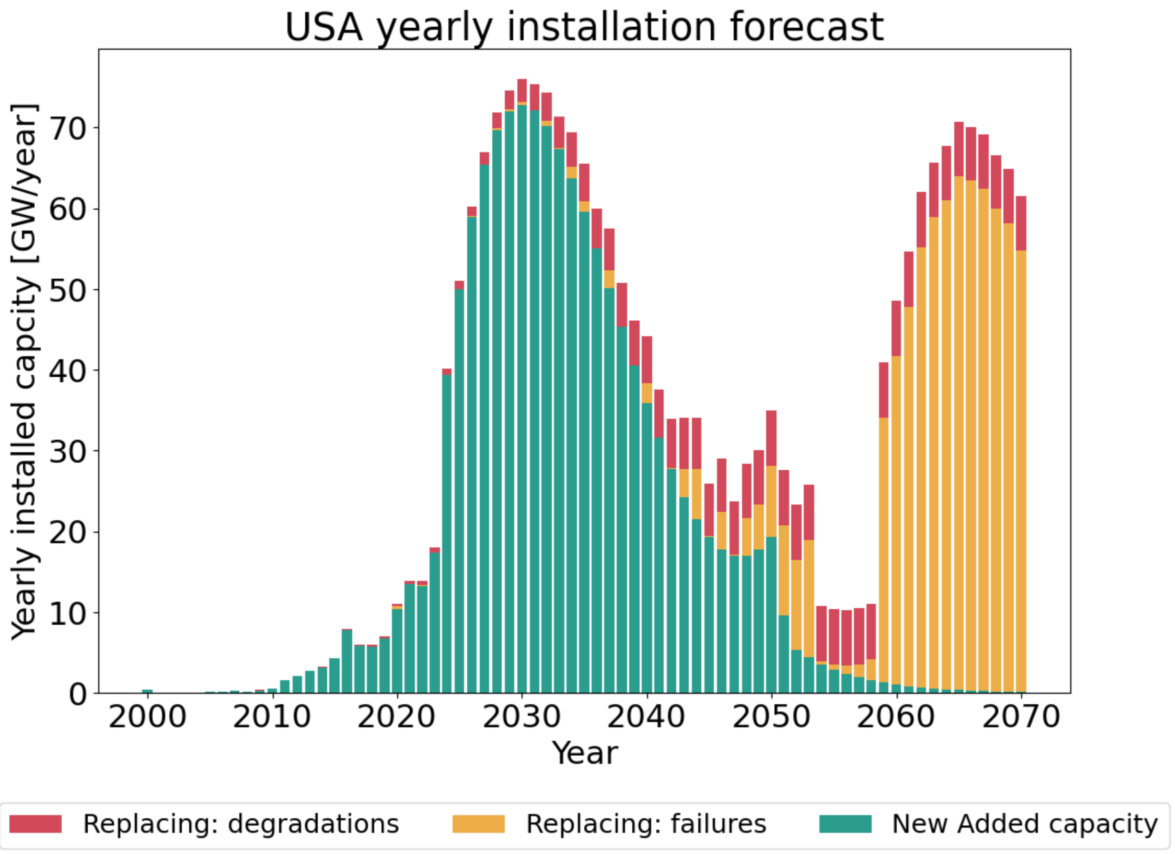

Figure A.7: Annual expected PV demand in the United States of America, divided among the three causes of new capacity demand: new installations (green bars), capacity failed (blue bars) and capacity degraded but still in operation (orange bars)

A.3. Japan

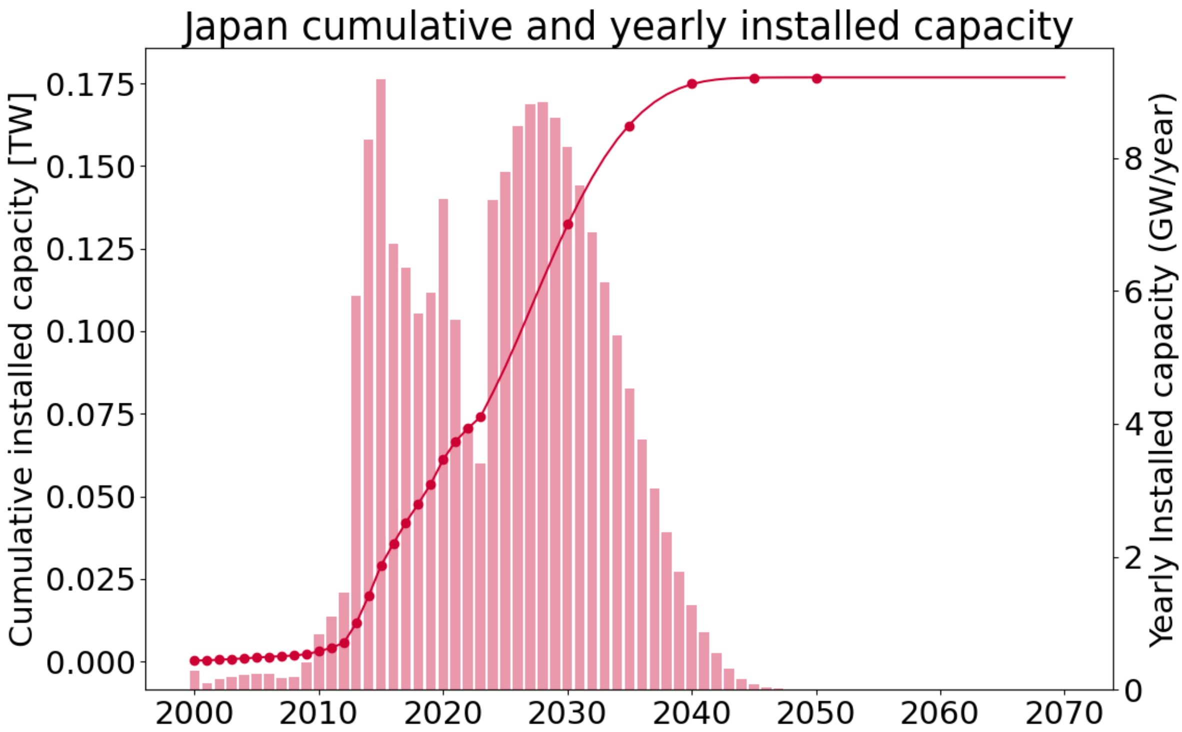

Figure A.8: Annual installation forecast for Japan. The dots represent forecasted points given from the source, the line is the interpolation and extension going through them.

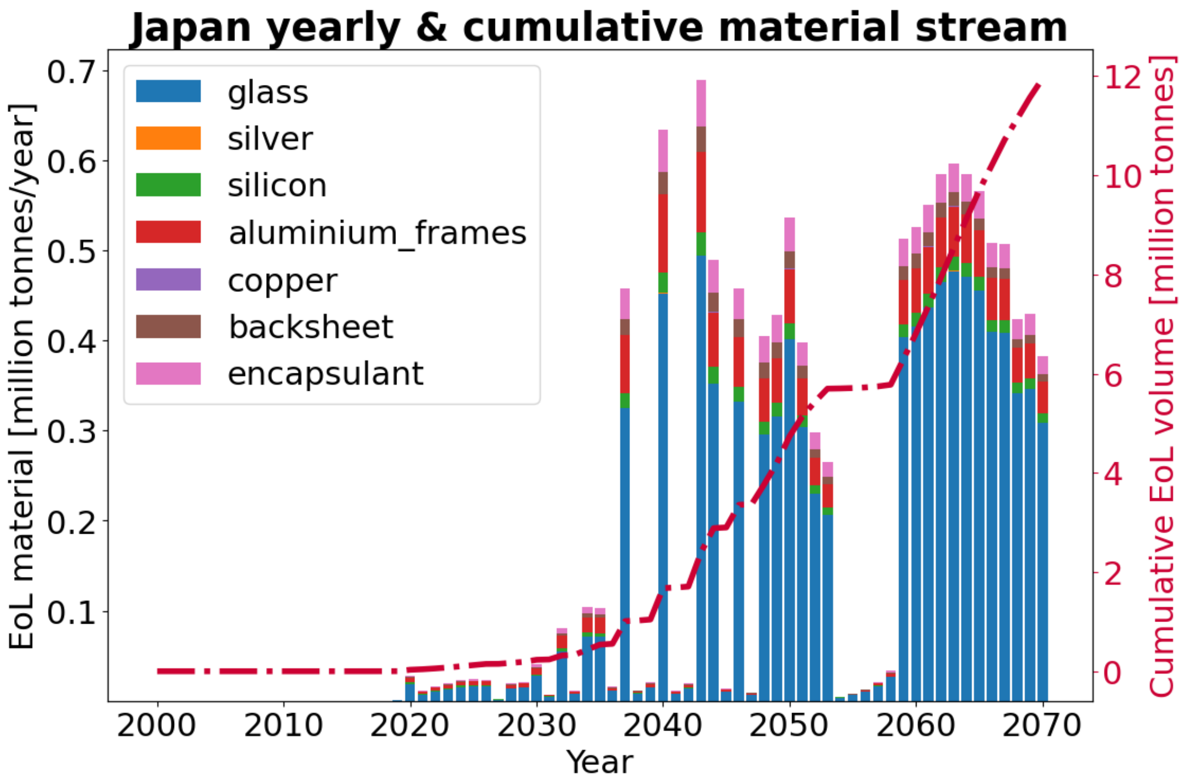

Figure A.9: Annual and cumulative expected End of Life flows for Japan. The dip in the years around 2060 has origins in the assumptions on degradation and lifetime; a more thorough explanation can be found in subsection 4.1.5

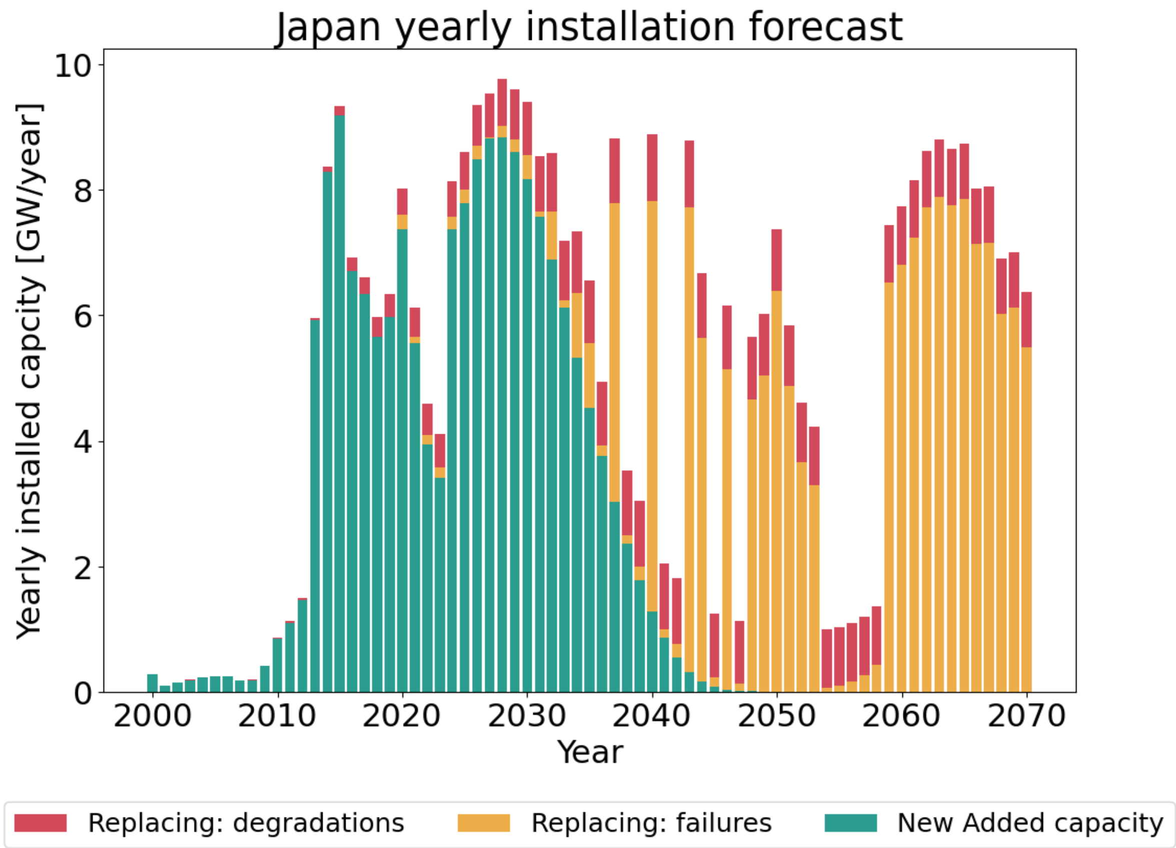

Figure A.10: Annual expected PV demand in Japan, divided among the three causes of new capacity demand: new installations (green bars), capacity failed (blue bars) and capacity degraded but still in operation (orange bars)

A.4. Italy

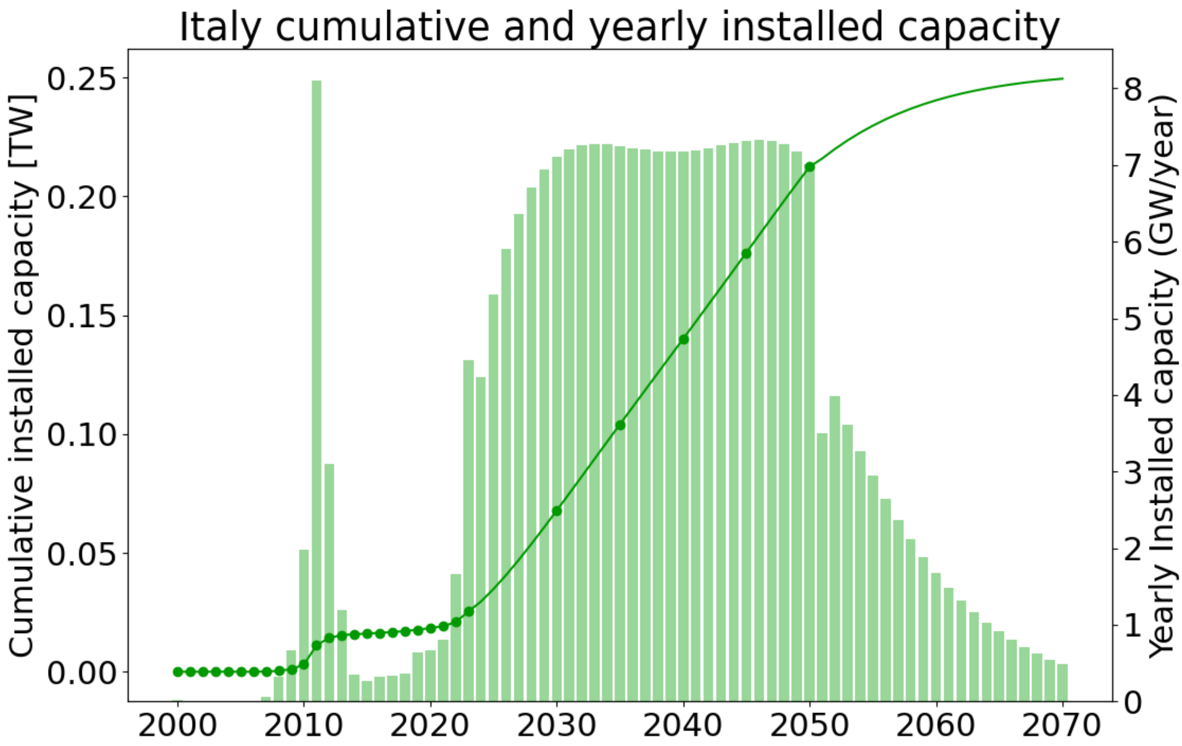

Figure A.11: Annual installation forecast for Italy. The dots represent forecasted points given from the source, the line is the interpolation and extension going through them.

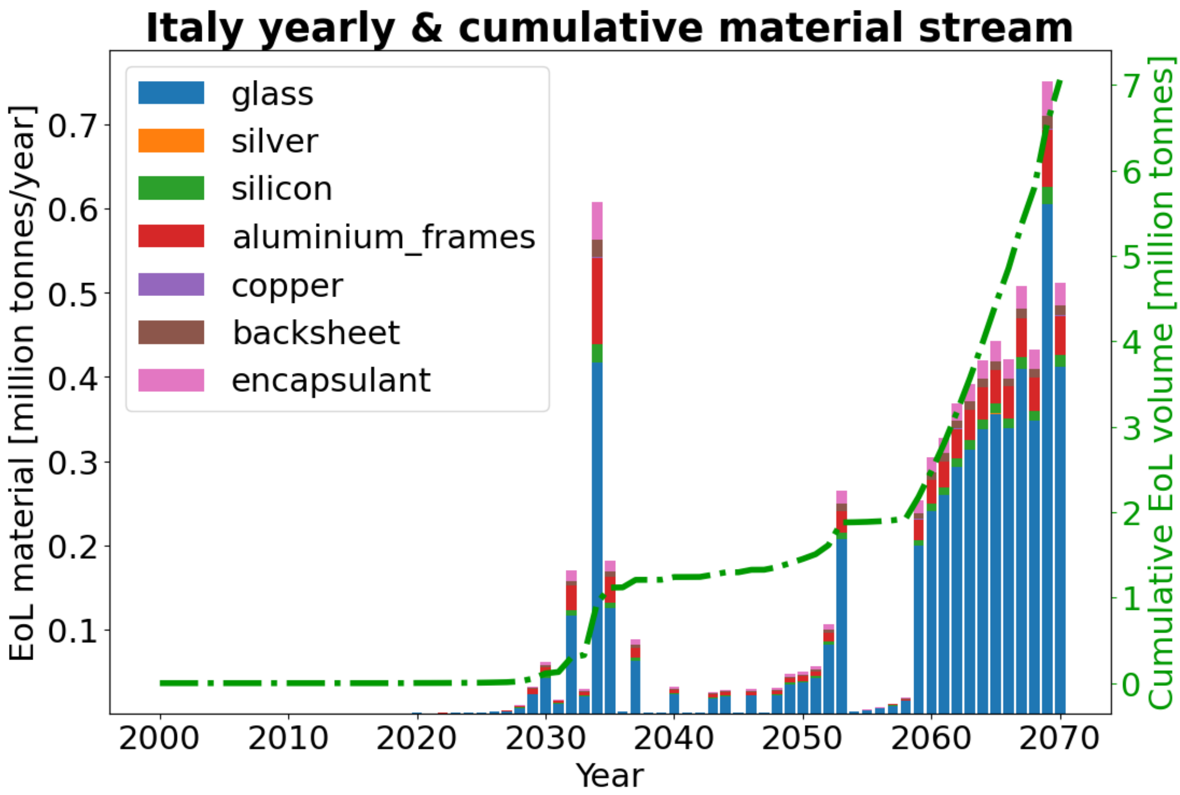

Figure A.12: Annual and cumulative expected End of Life flows for Italy. The dip in the years around 2060 has origins in the assumptions on degradation and lifetime; a more thorough explanation can be found in subsection 4.1.5

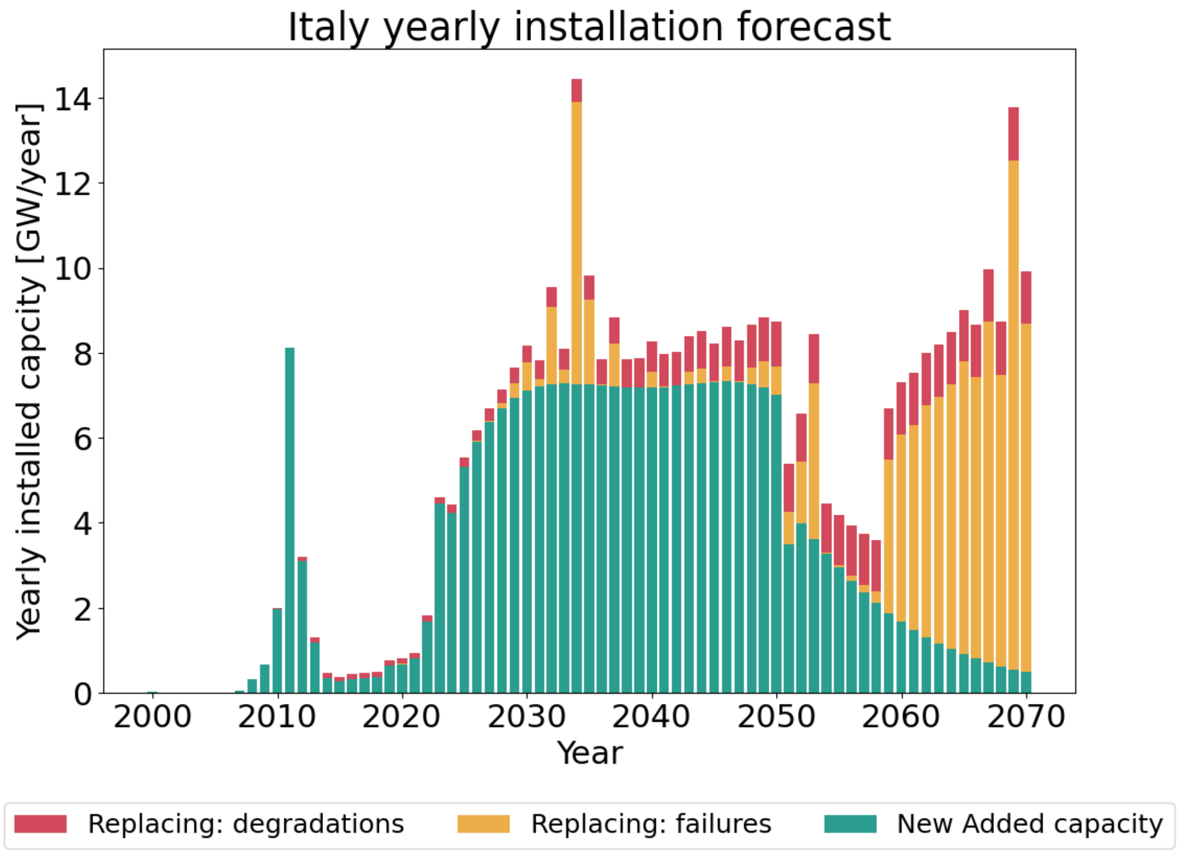

Figure A.13: Annual expected PV demand in Italy, divided among the three causes of new capacity demand: new installations (green bars), capacity failed (blue bars) and capacity degraded but still in operation (orange bars)

A.5. India

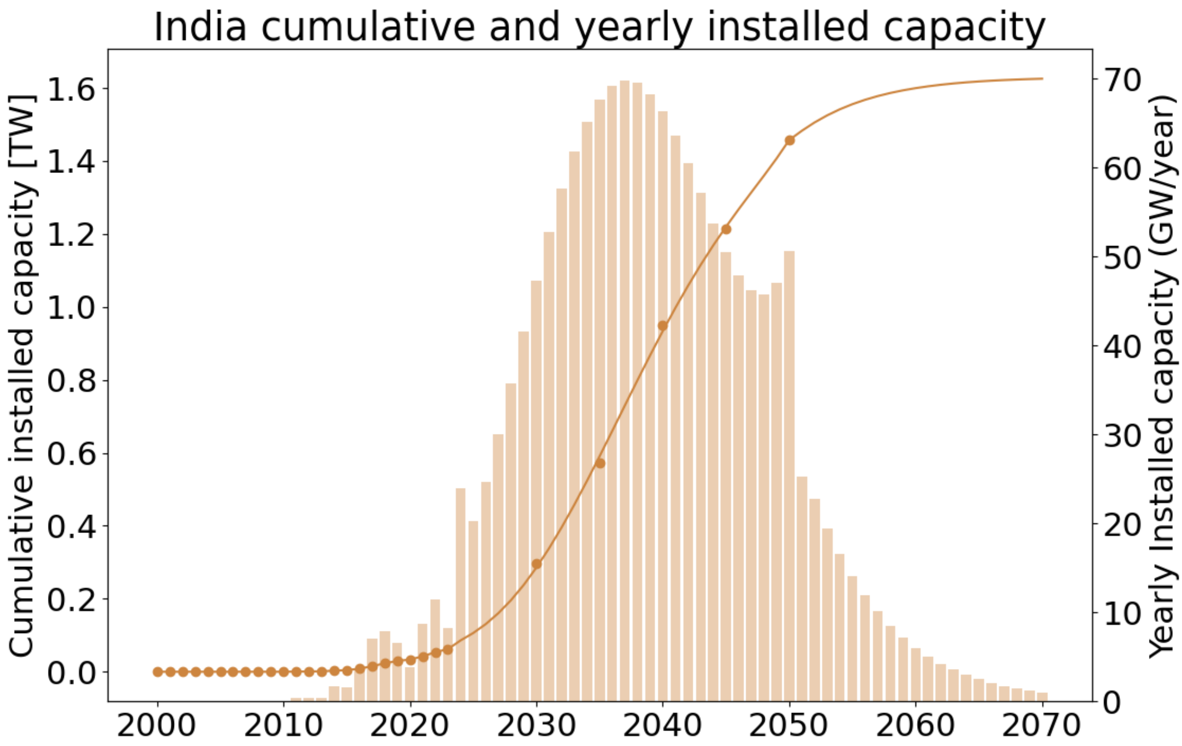

Figure A.14: Annual installation forecast for India. The dots represent forecasted points given from the source, the line is the interpolation and extension going through them.

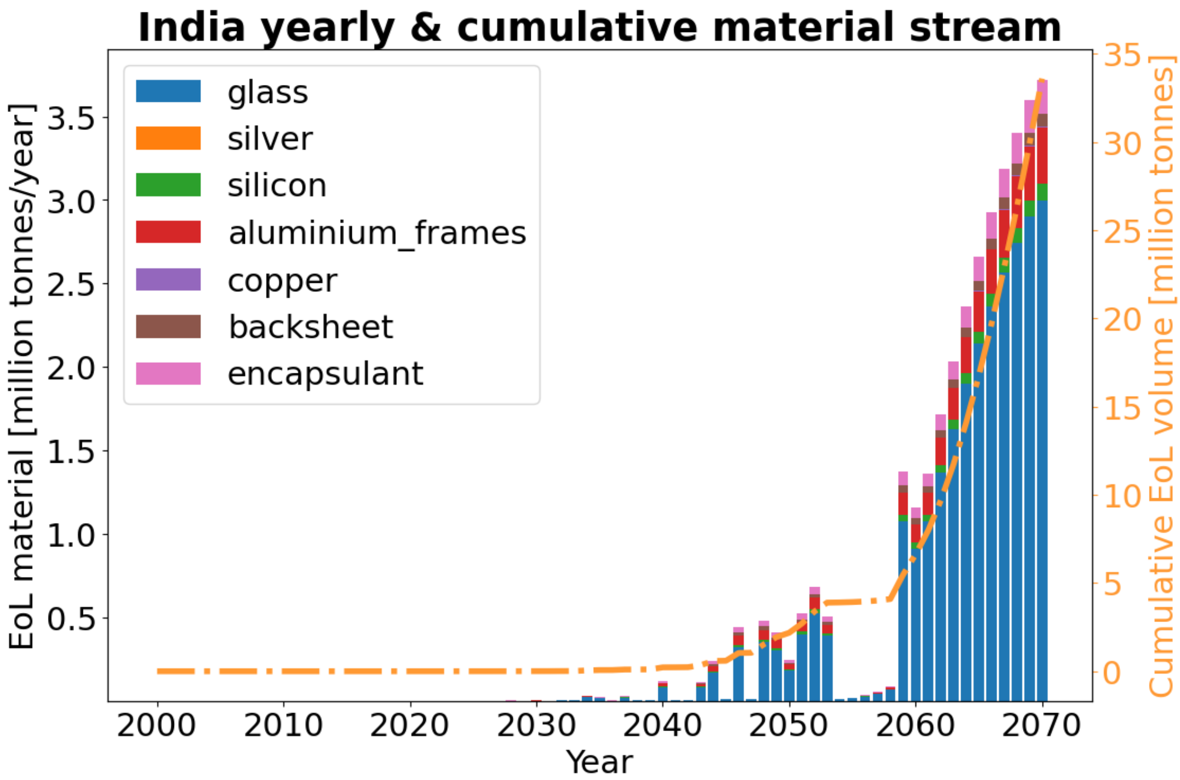

Figure A.15: Annual and cumulative expected End of Life flows for India. The dip in the years around 2060 has origins in the assumptions on degradation and lifetime; a more thorough explanation can be found in subsection 4.1.5

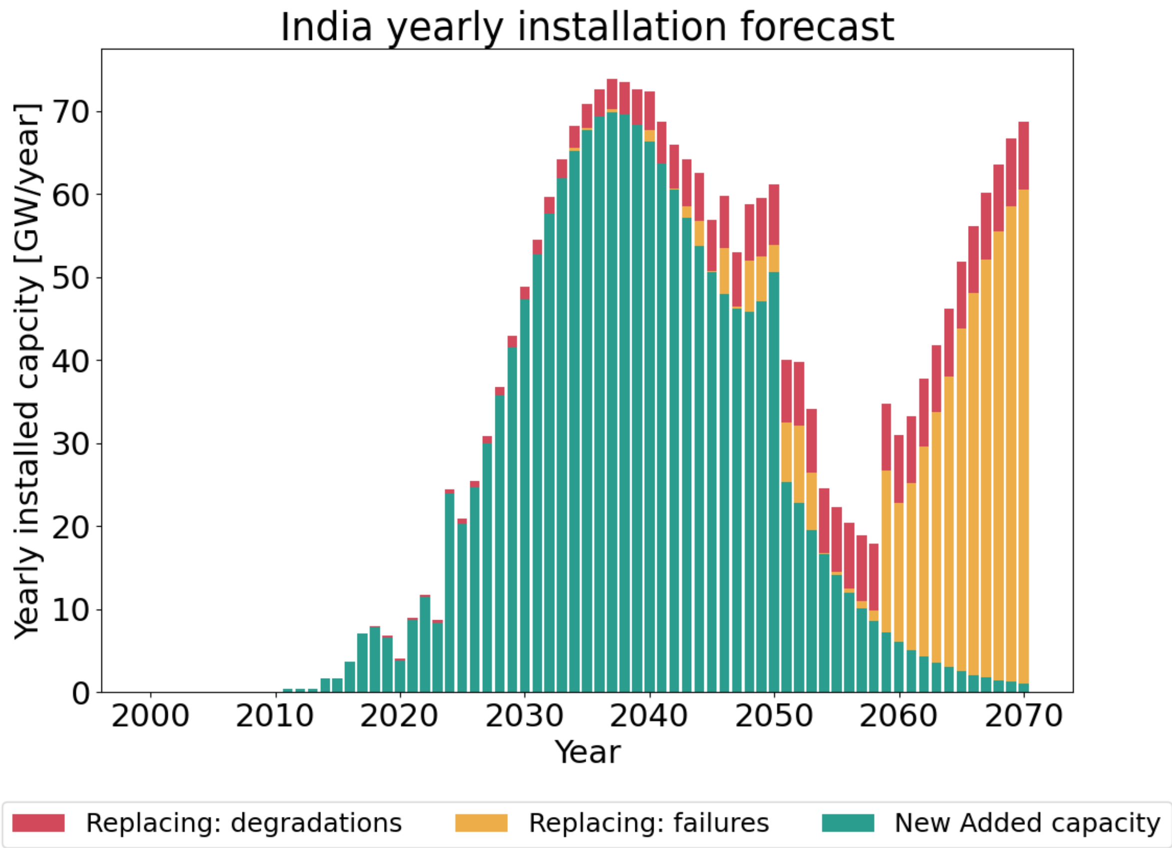

Figure A.16: Annual expected PV demand in India, divided among the three causes of new capacity demand: new installations (green bars), capacity failed (blue bars) and capacity degraded but still in operation (orange bars)

A.6. Russia

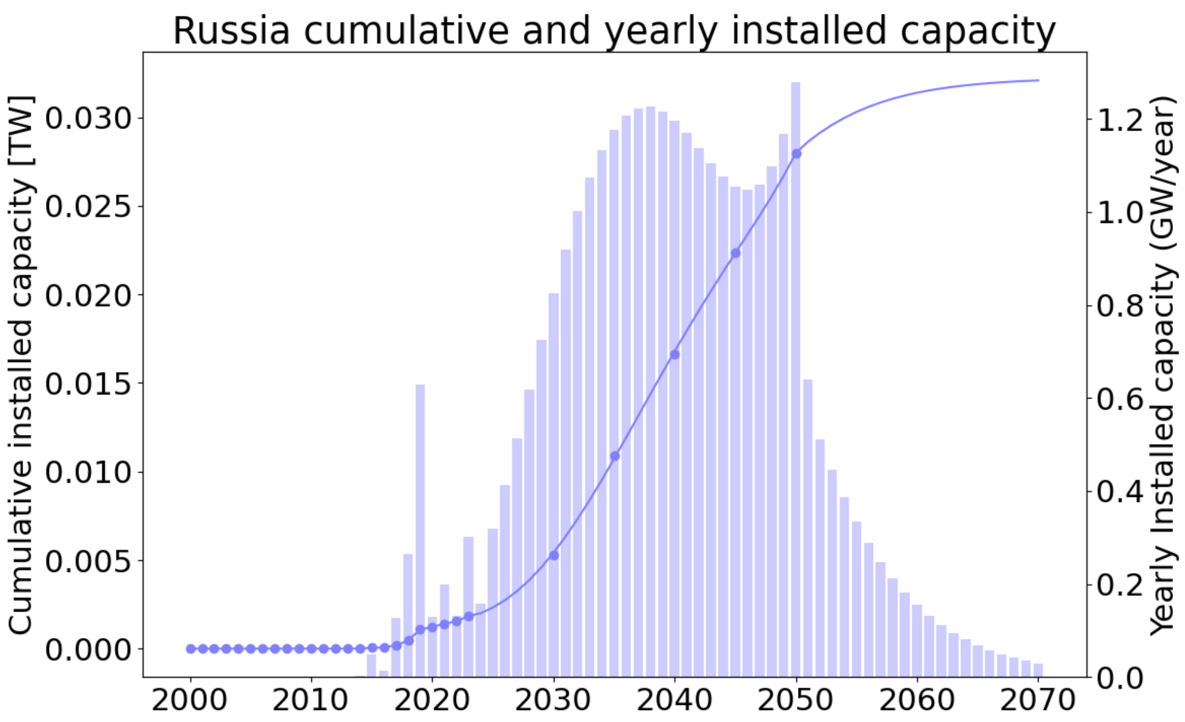

Figure A.17: Annual installation forecast for Russia. The dots represent forecasted points given from the source, the line is the interpolation and extension going through them.

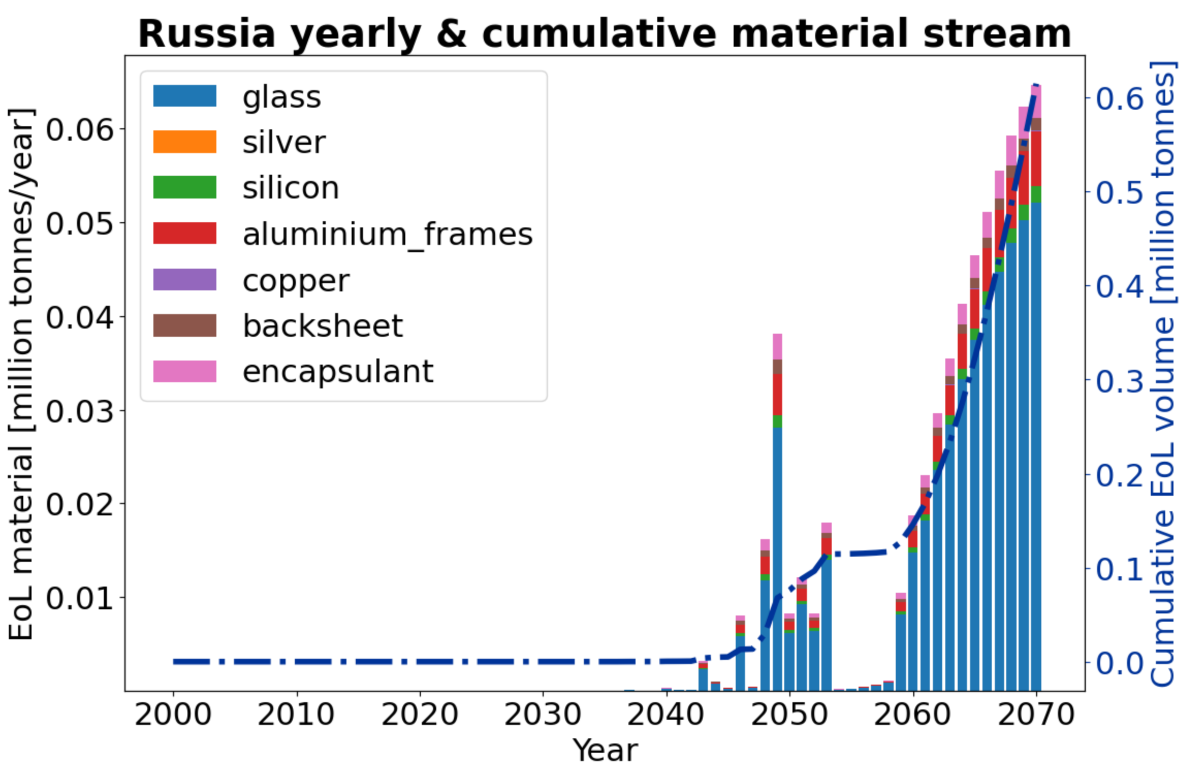

Figure A.18: Annual and cumulative expected End of Life flows for Russia. The dip in the years around 2060 has origins in the assumptions on degradation and lifetime; a more thorough explanation can be found in subsection 4.1.5

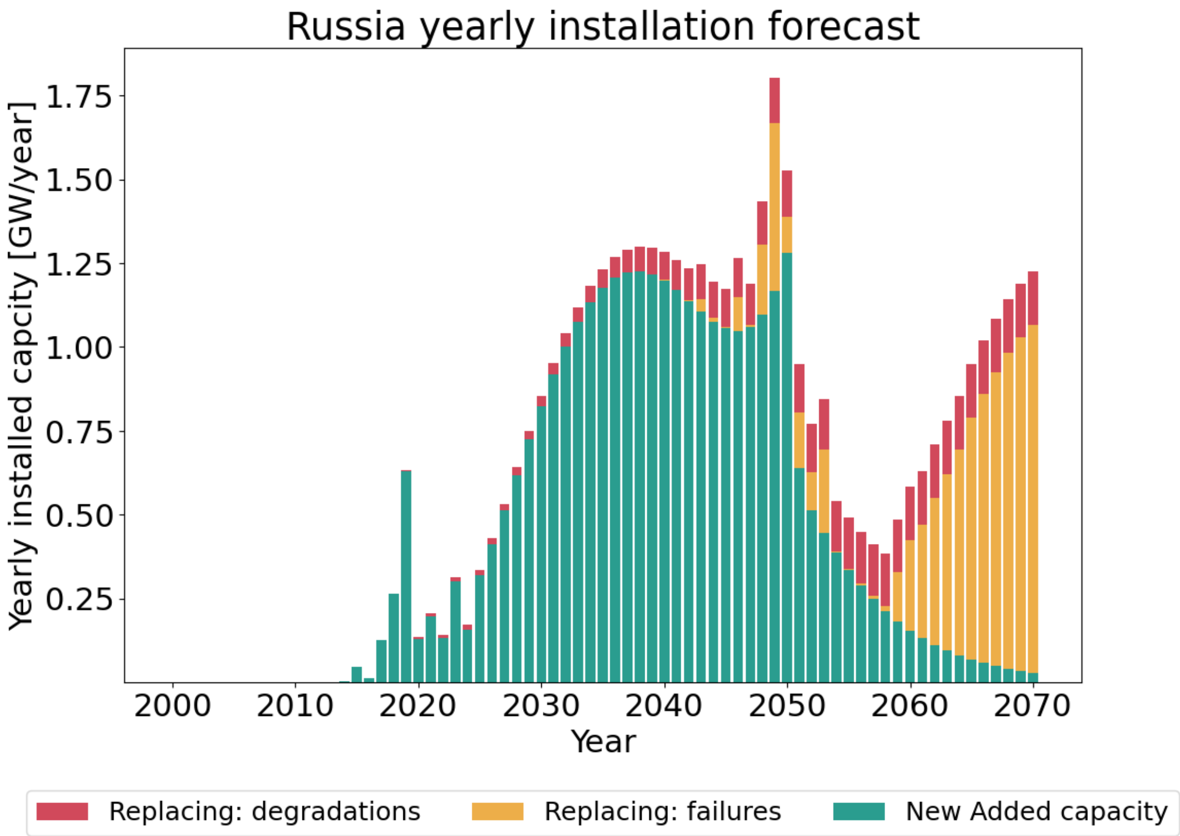

Figure A.19: Annual expected PV demand in Russia, divided among the three causes of new capacity demand: new installations (green bars), capacity failed (blue bars) and capacity degraded but still in operation (orange bars)

A.7. Australia

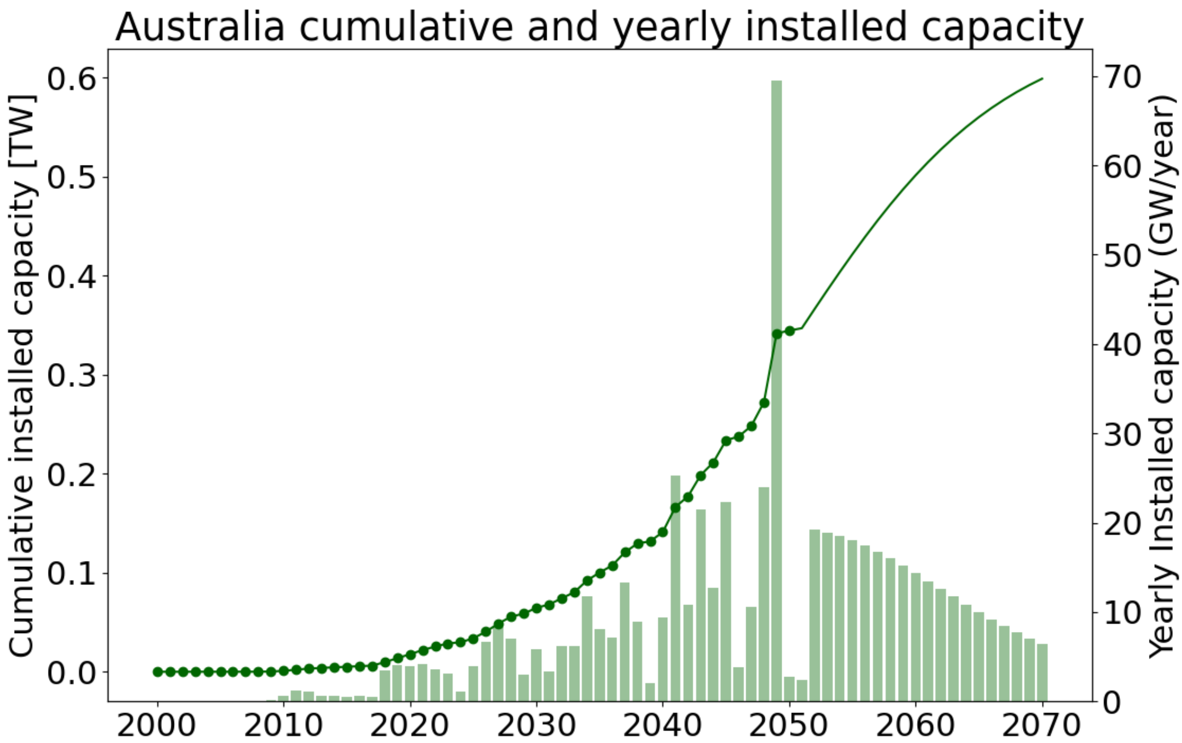

Figure A.20: Annual installation forecast for Australia. The dots represent forecasted points given from the source, the line is the interpolation and extension going through them.

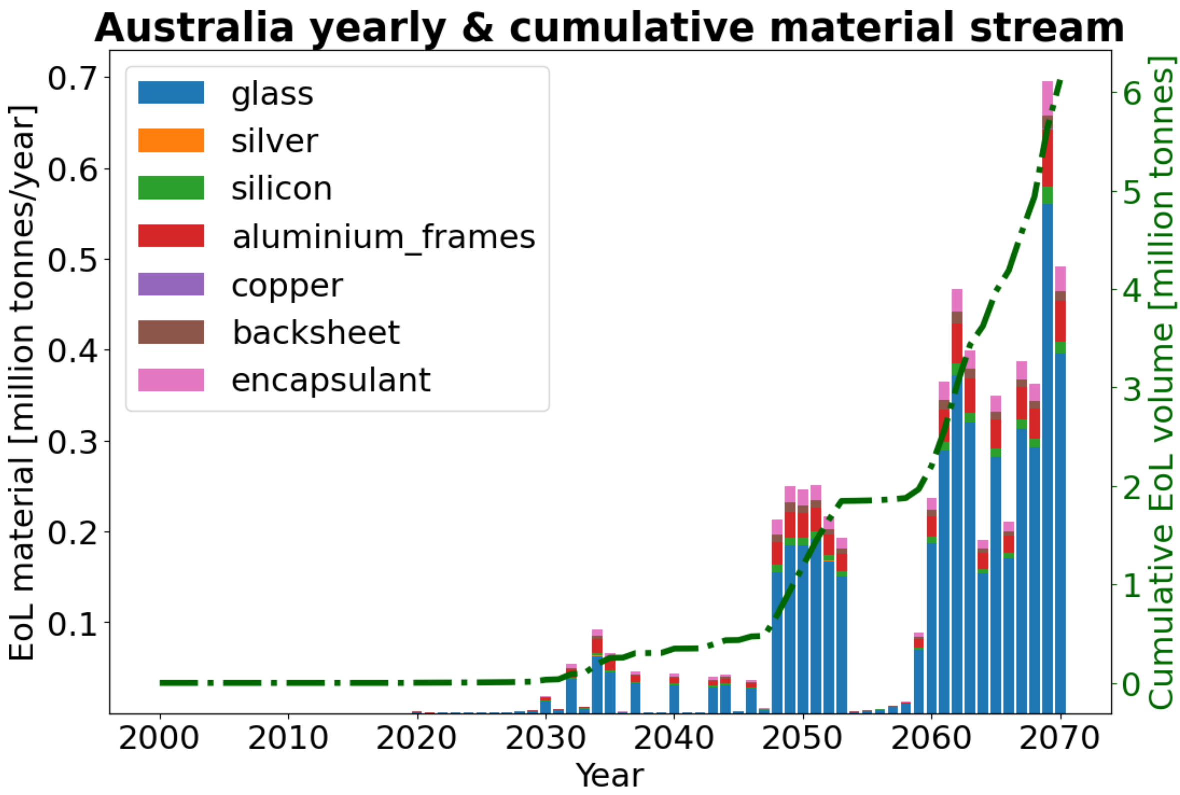

Figure A.21: Annual and cumulative expected End of Life flows for Australia. The dip in the years around 2060 has origins in the assumptions on degradation and lifetime; a more thorough explanation can be found in subsection 4.1.5

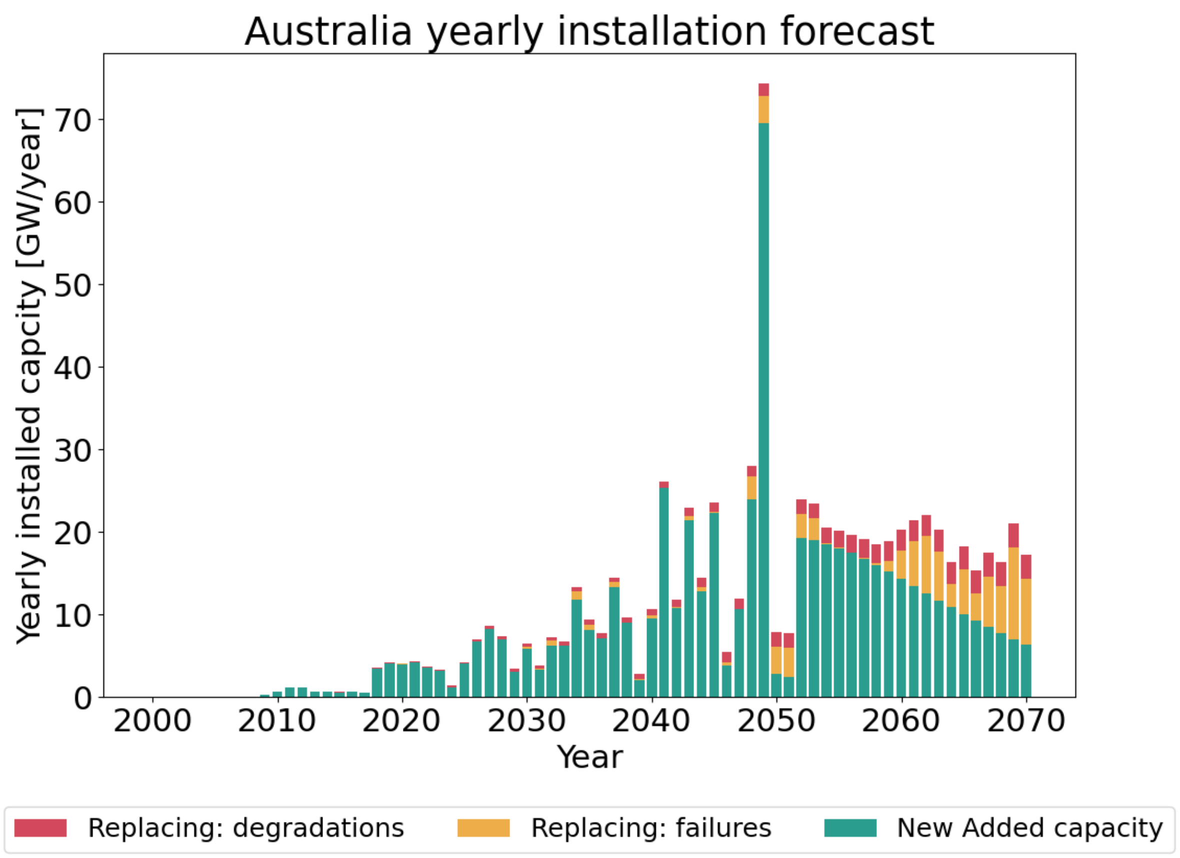

Figure A.22: Annual expected PV demand in Australia, divided among the three causes of new capacity demand: new installations (green bars), capacity failed (blue bars) and capacity degraded but still in operation (orange bars)

sectionAustria

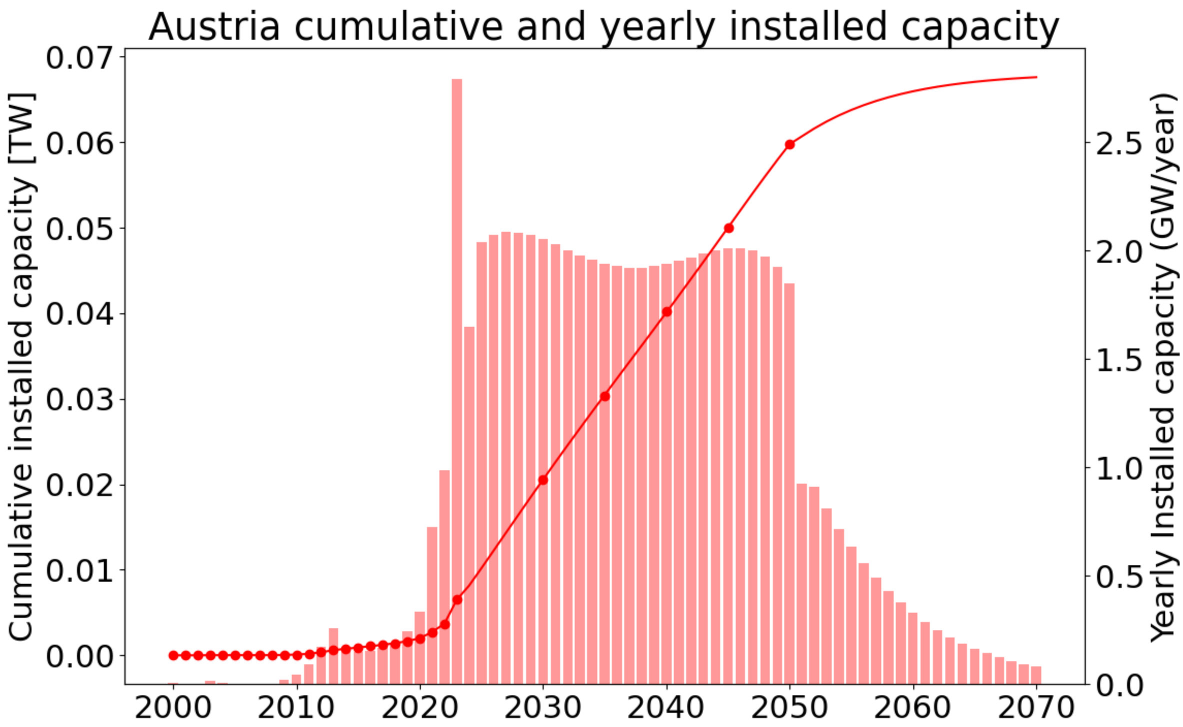

Figure A.23: Annual installation forecast for Austria. The dots represent forecasted points given from the source, the line is the interpolation and extension going through them.

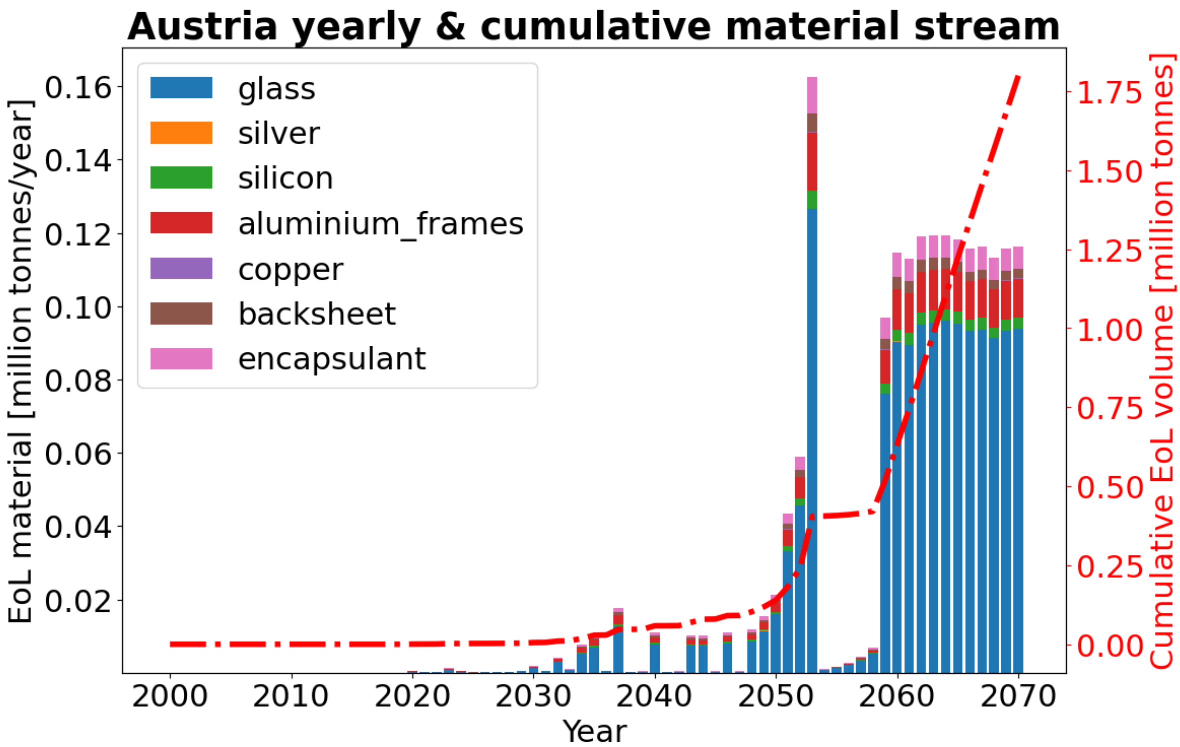

Figure A.24: Annual and cumulative expected End of Life flows for Austria. The dip in the years around 2060 has origins in the assumptions on degradation and lifetime; a more thorough explanation can be found in subsection 4.1.5

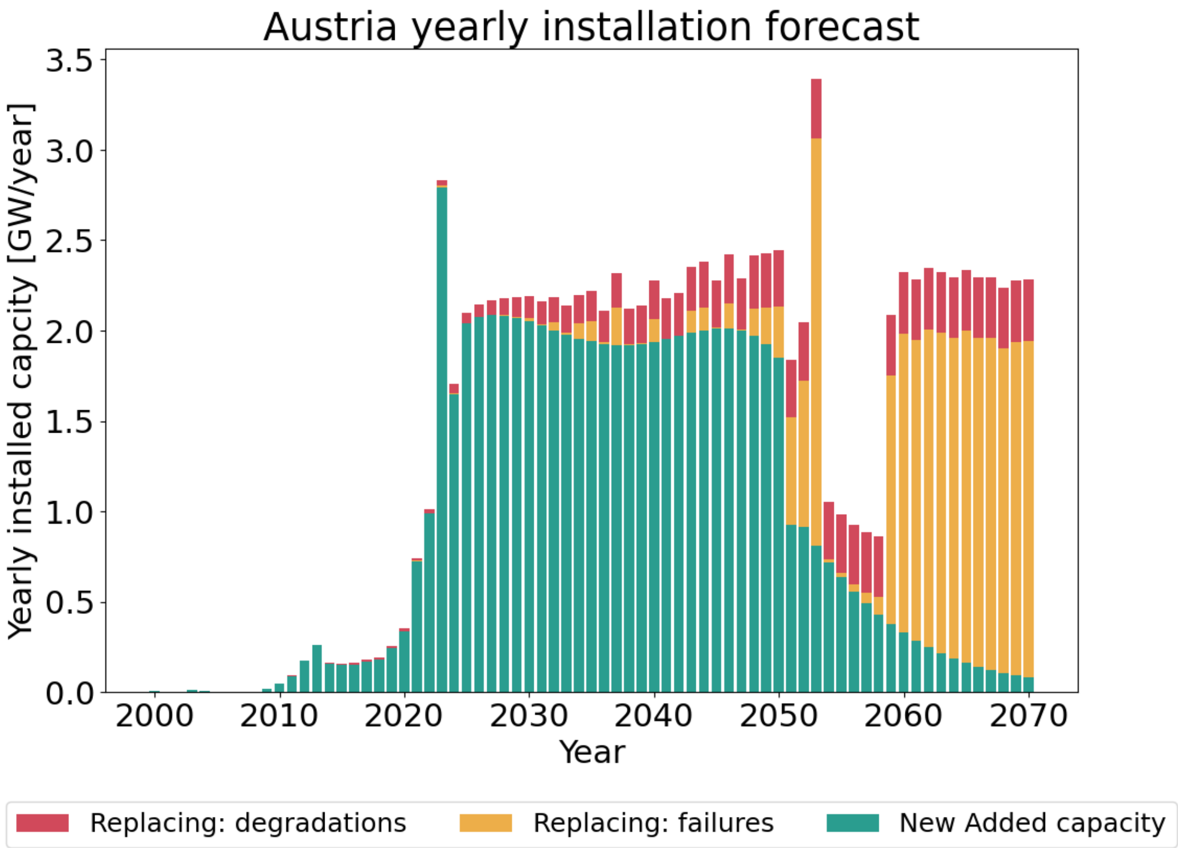

Figure A.25: Annual expected PV demand in Austria, divided among the three causes of new capacity demand: new installations (green bars), capacity failed (blue bars) and capacity degraded but still in operation (orange bars)

A.8. Brazil

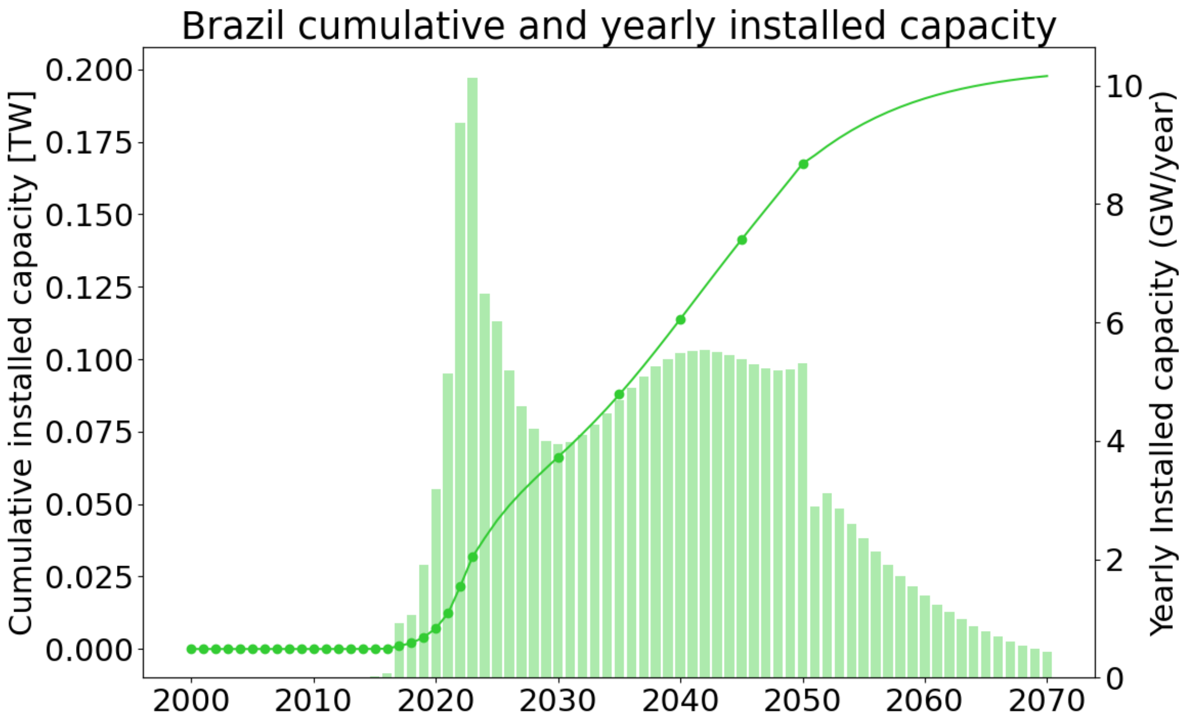

Figure A.26: Annual installation forecast for Brazil. The dots represent forecasted points given from the source, the line is the interpolation and extension going through them.

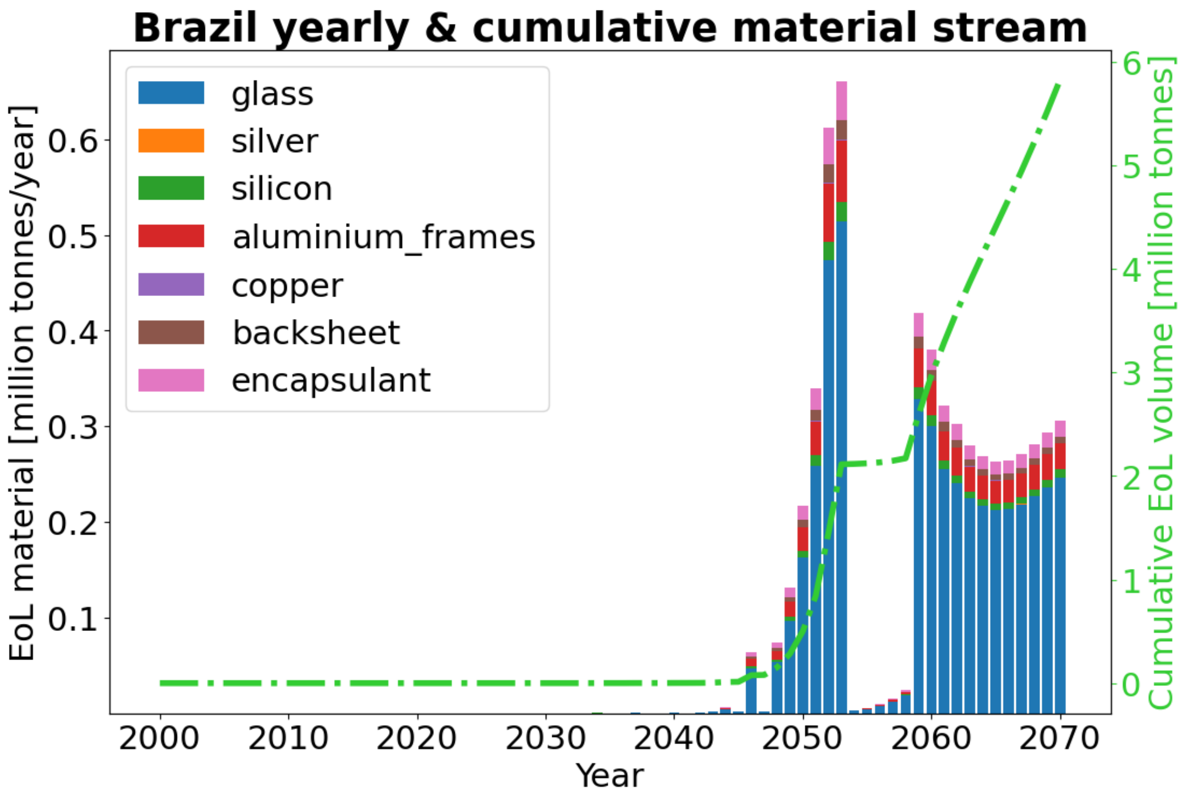

Figure A.27: Annual and cumulative expected End of Life flows for Brazil. The dip in the years around 2060 has origins in the assumptions on degradation and lifetime; a more thorough explanation can be found in subsection 4.1.5

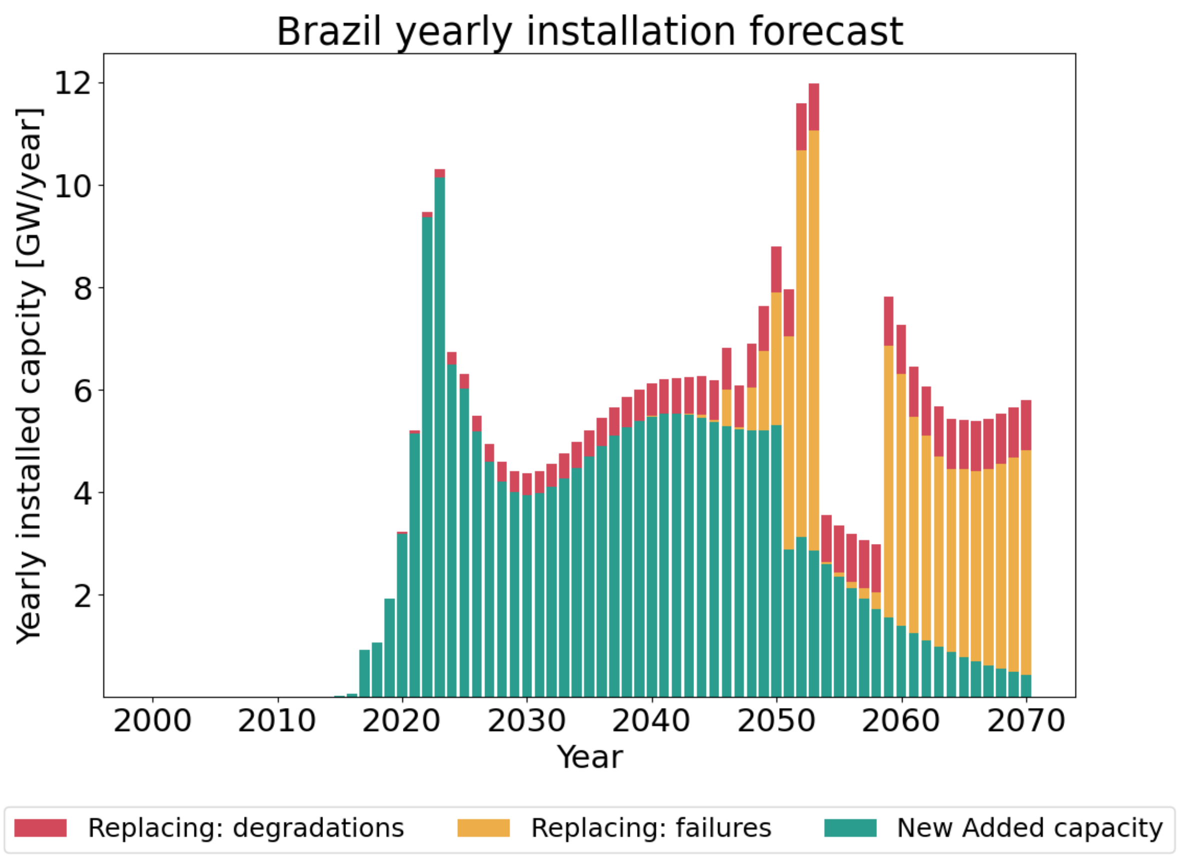

Figure A.28: Annual expected PV demand in Brazil, divided among the three causes of new capacity demand: new installations (green bars), capacity failed (blue bars) and capacity degraded but still in operation (orange bars)

A.9. Germany

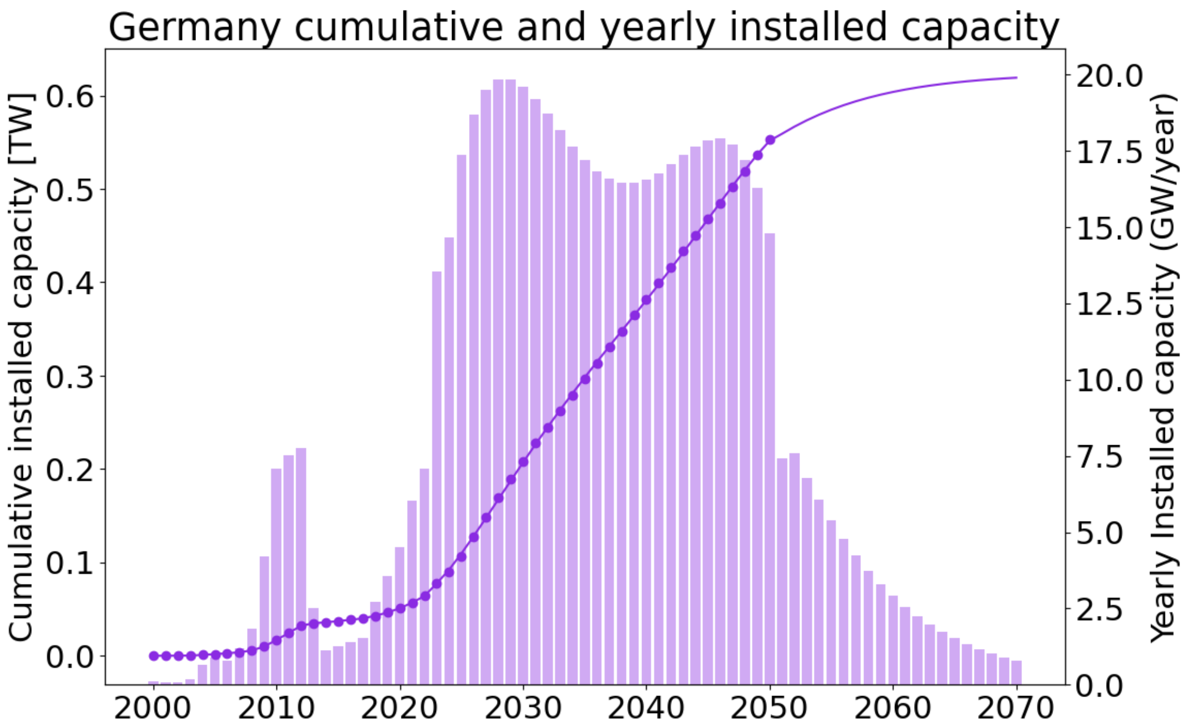

Figure A.29: Annual installation forecast for Germany. The dots represent forecasted points given from the source, the line is the interpolation and extension going through them.

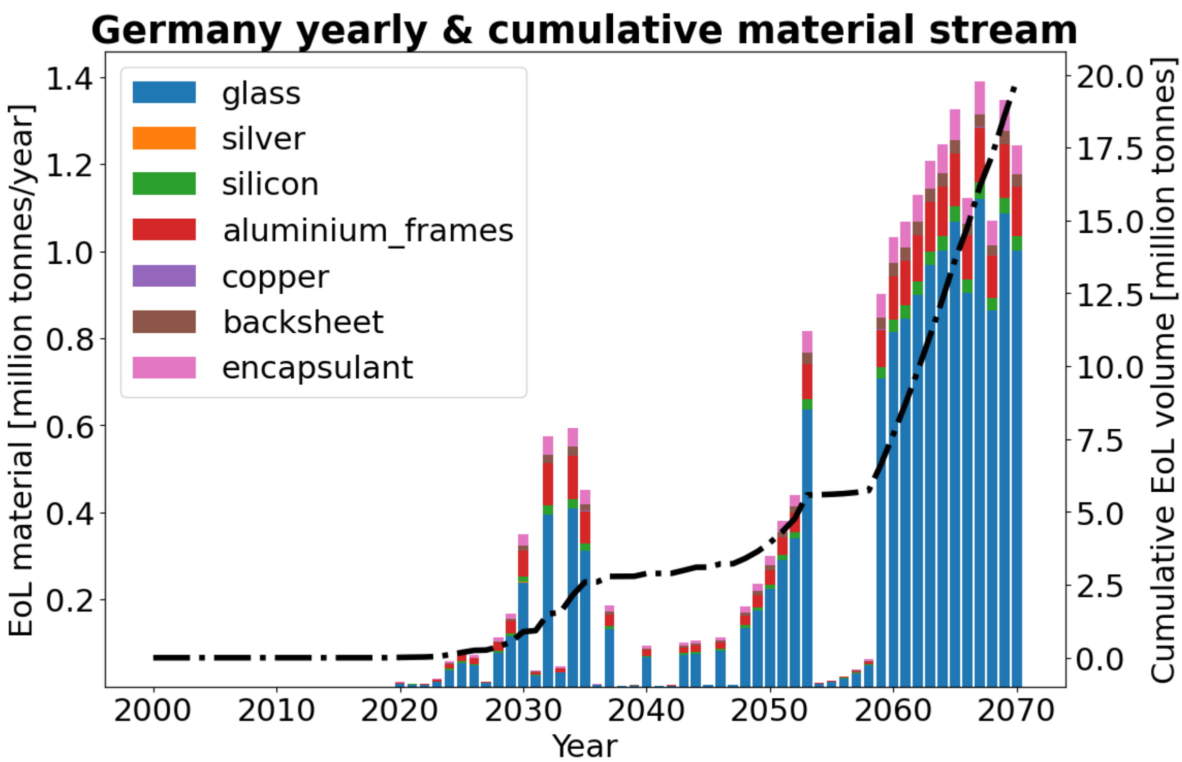

Figure A.30: Annual and cumulative expected End of Life flows for Germany. The dip in the years around 2060 has origins in the assumptions on degradation and lifetime; a more thorough explanation can be found in subsection 4.1.5

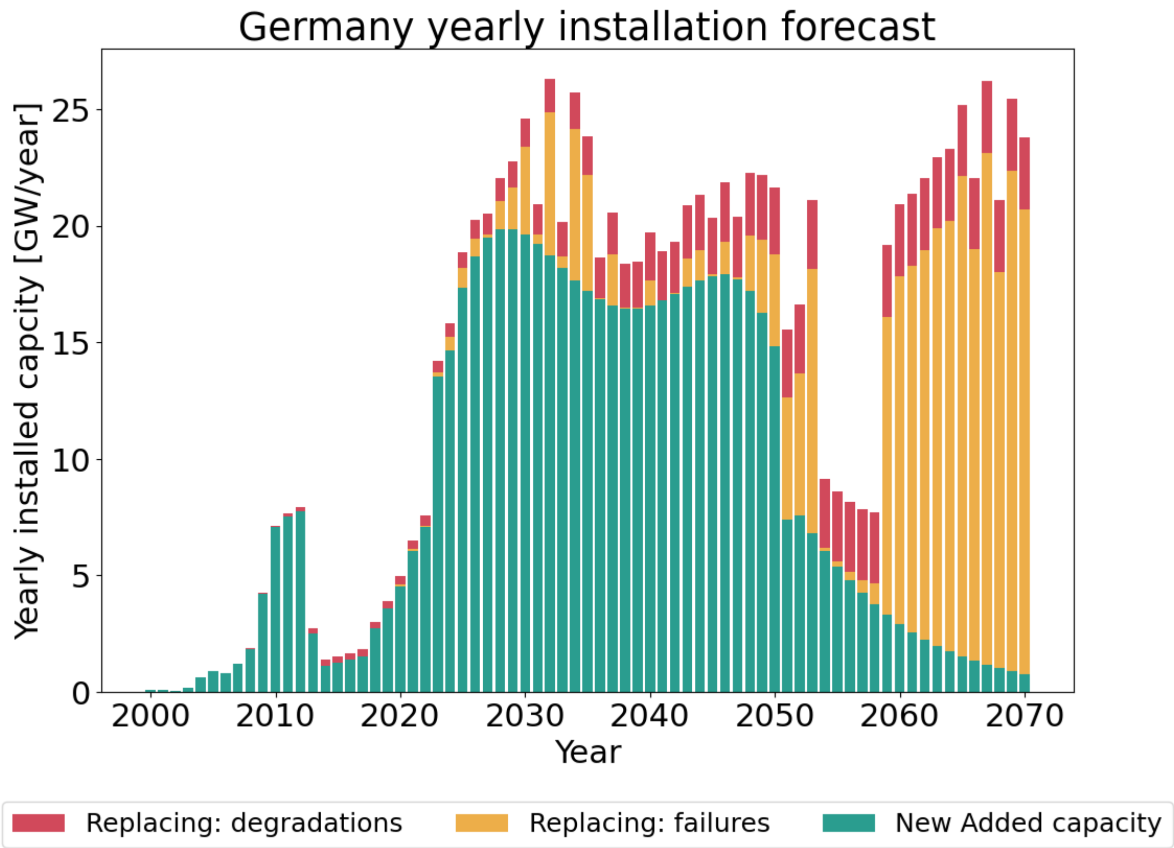

Figure A.31: Annual expected PV demand in Germany, divided among the three causes of new capacity demand: new installations (green bars), capacity failed (blue bars) and capacity degraded but still in operation (orange bars)

A.10. The Netherlands

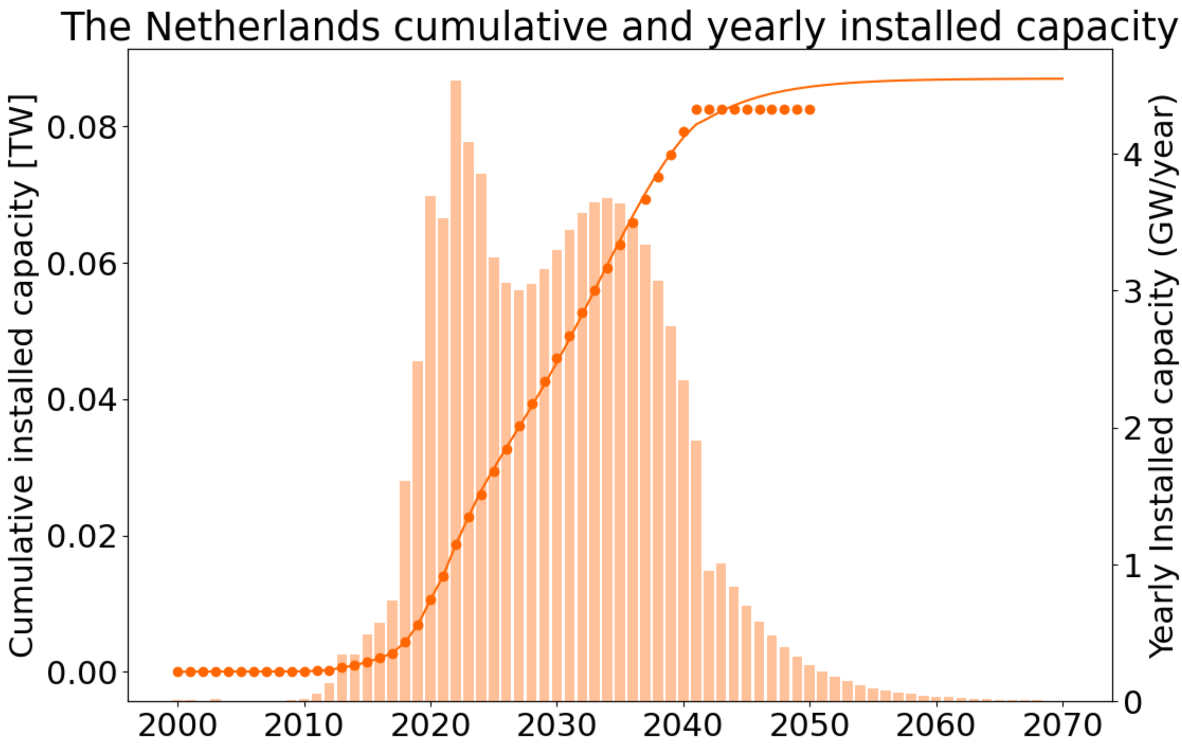

Figure A.32: Annual installation forecast for the Netherlands. The dots represent forecasted points given from the source, the line is the interpolation and extension going through them.

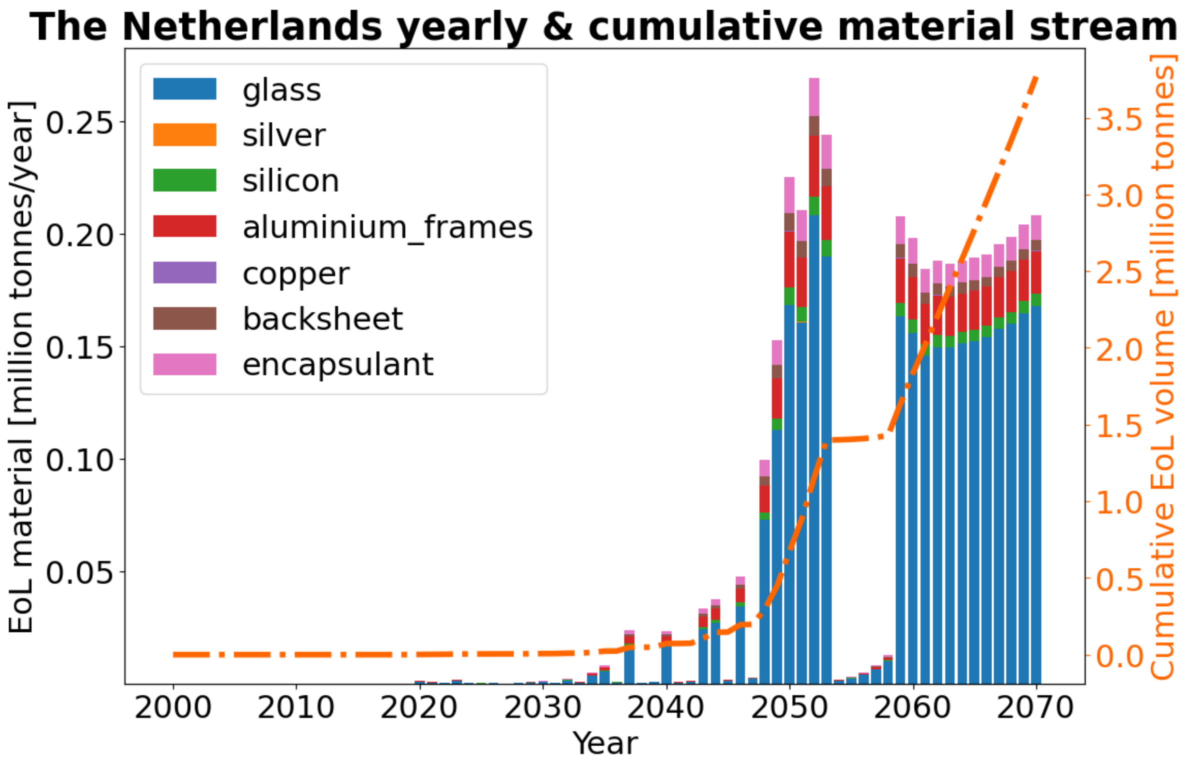

Figure A.33: Annual and cumulative expected End of Life flows for the Netherlands. The dip in the years around 2060 has origins in the assumptions on degradation and lifetime; a more thorough explanation can be found in subsection 4.1.5

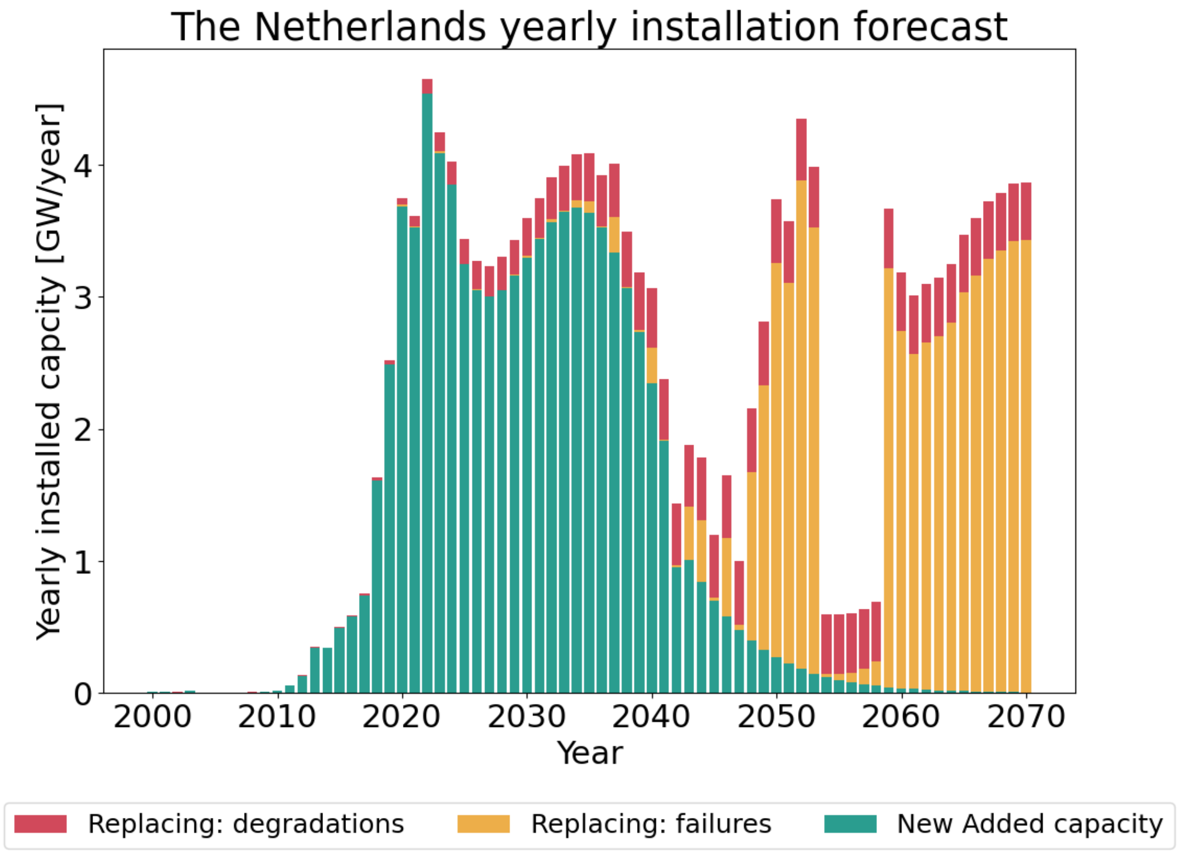

Figure A.34: Annual expected PV demand in the Netherlands, divided among the three causes of new capacity demand: new installations (green bars), capacity failed (blue bars) and capacity degraded but still in operation (orange bars)

A.11. Sweden

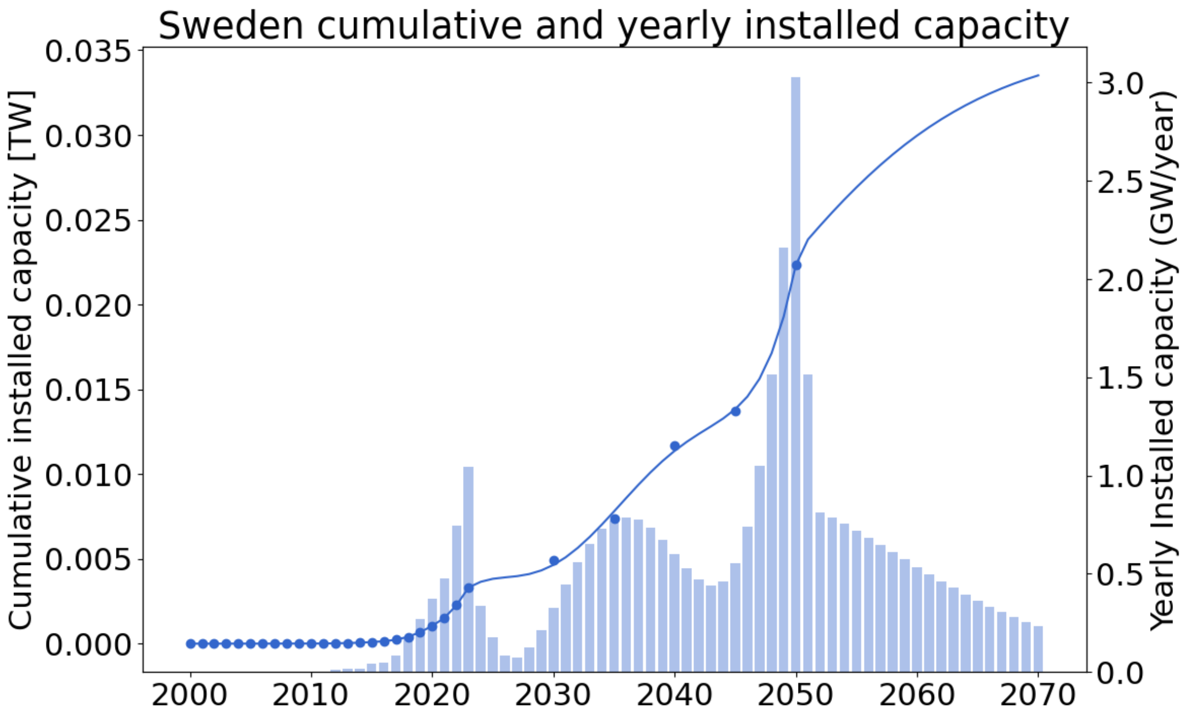

Figure A.35: Annual installation forecast for Sweden. The dots represent forecasted points given from the source, the line is the interpolation and extension going through them.

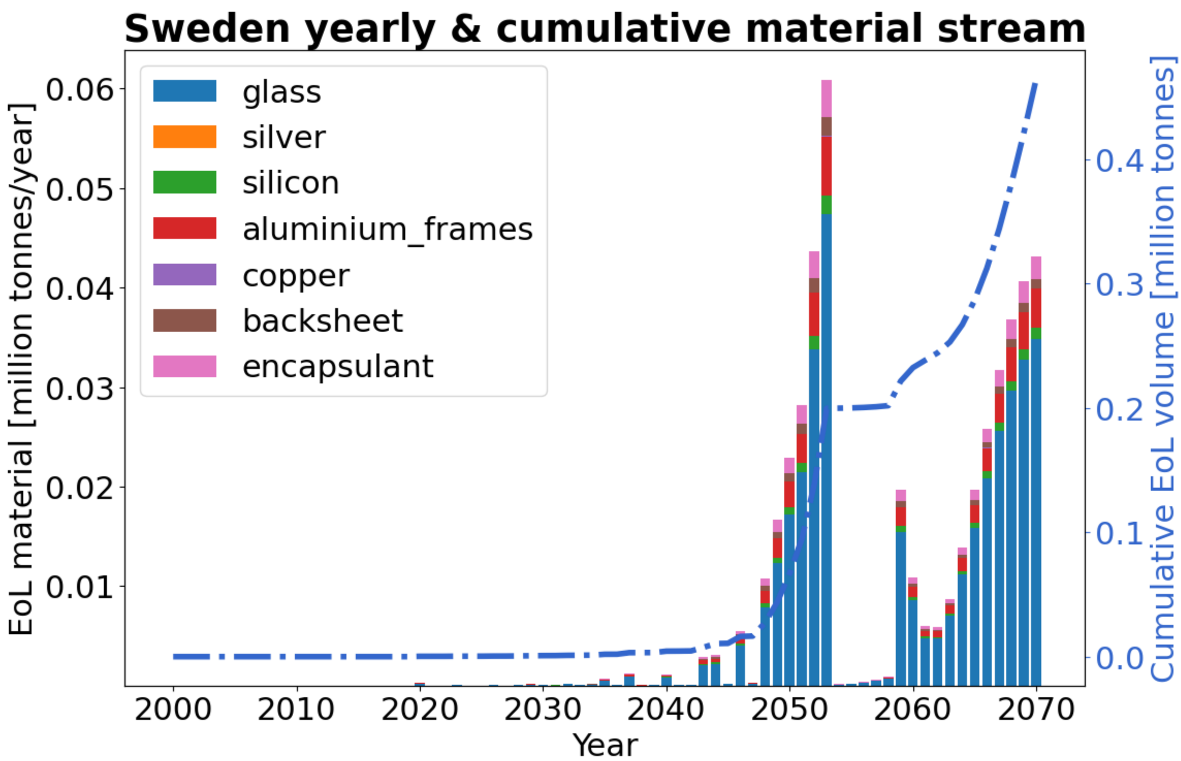

Figure A.36: Annual and cumulative expected End of Life flows for Sweden. The dip in the years around 2060 has origins in the assumptions on degradation and lifetime; a more thorough explanation can be found in subsection 4.1.5

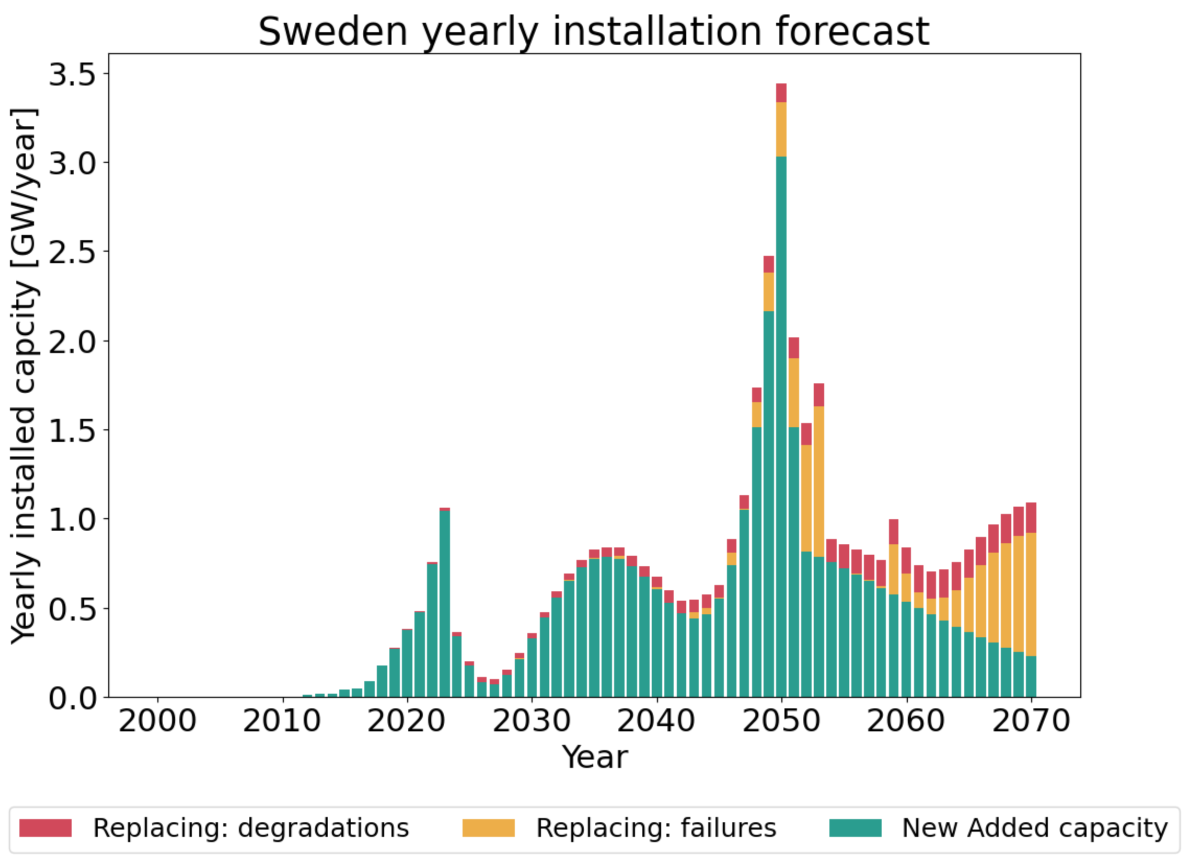

Figure A.37: Annual expected PV demand in Sweden, divided among the three causes of new capacity demand: new installations (green bars), capacity failed (blue bars) and capacity degraded but still in operation (orange bars)

A.12. France

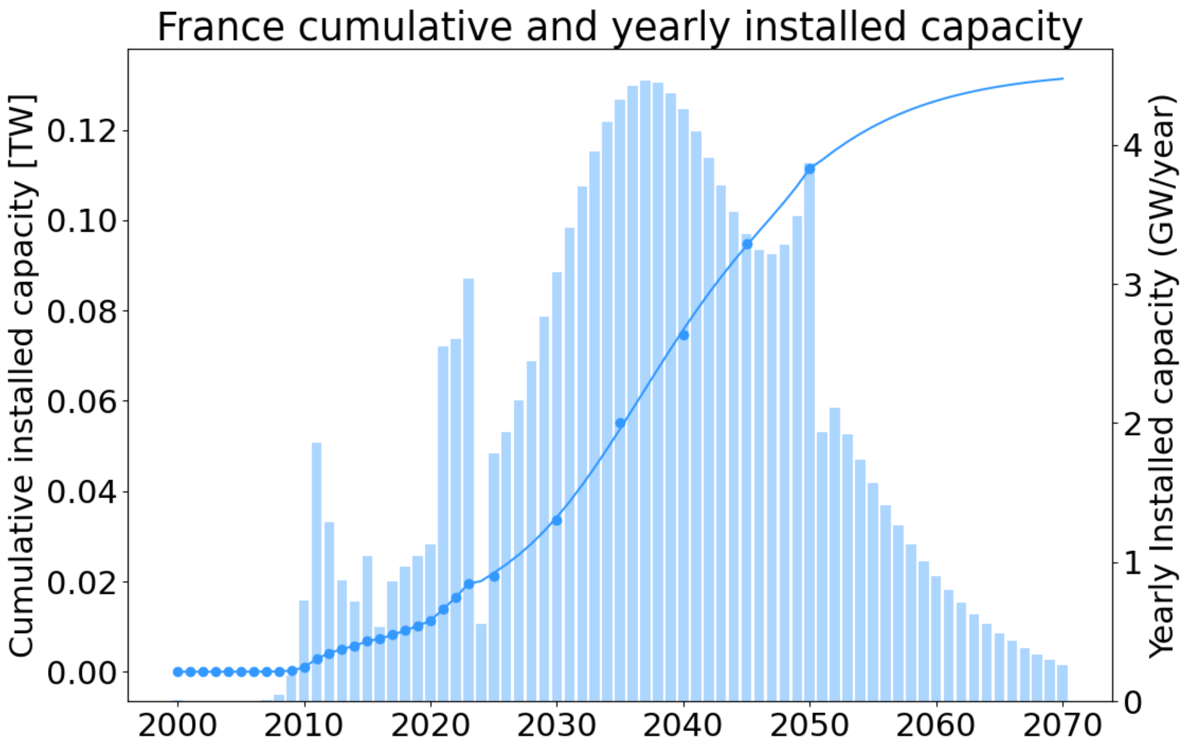

Figure A.38: Annual installation forecast for France. The dots represent forecasted points given from the source, the line is the interpolation and extension going through them.

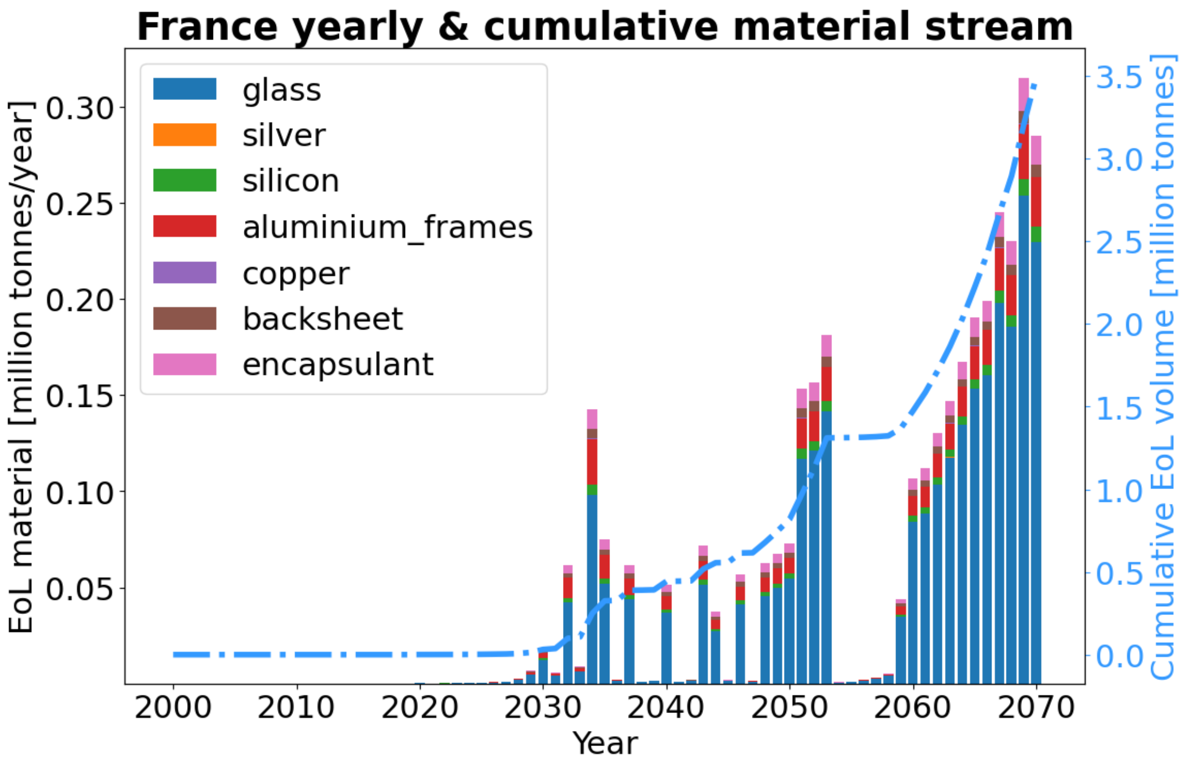

Figure A.39: Annual and cumulative expected End of Life flows for France. The dip in the years around 2060 has origins in the assumptions on degradation and lifetime; a more thorough explanation can be found in subsection 4.1.5

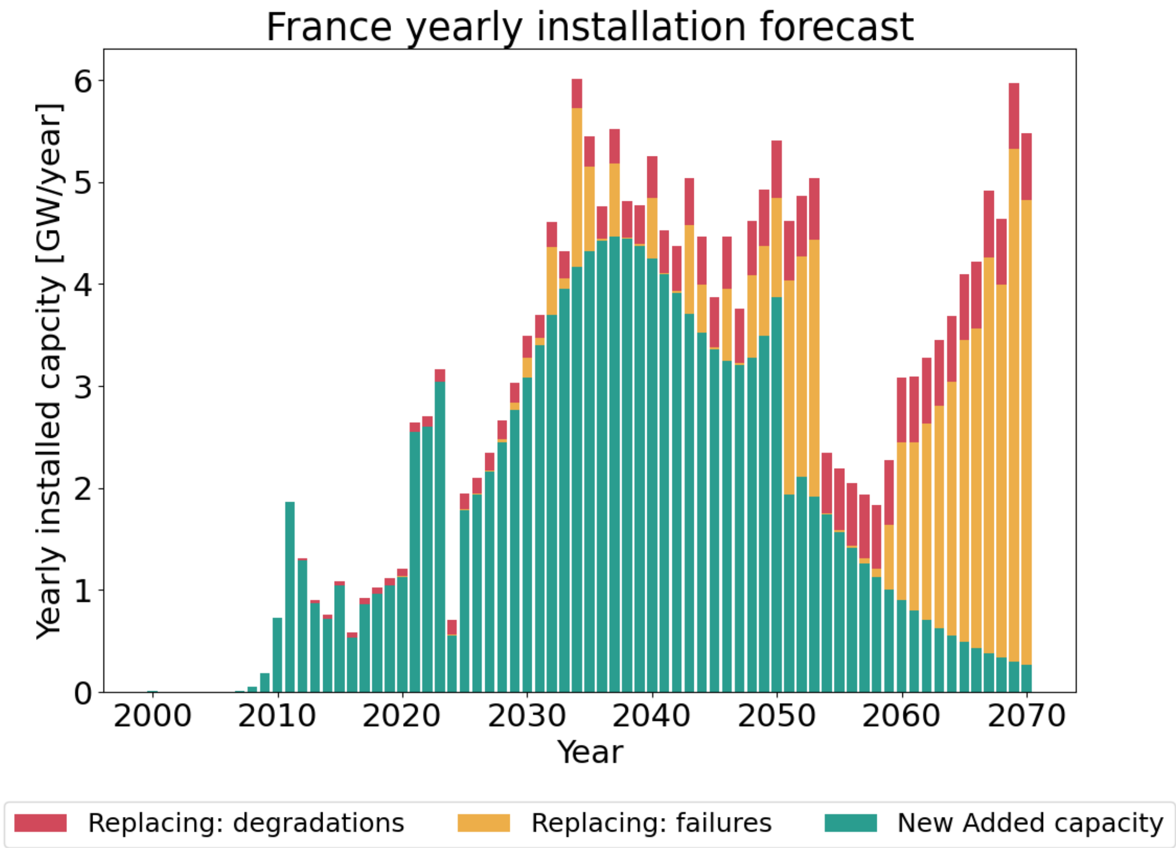

Figure A.40: Annual expected PV demand in France, divided among the three causes of new capacity demand: new installations (green bars), capacity failed (blue bars) and capacity degraded but still in operation (orange bars)

R